

Copyright © and Moral Rights for this thesis are retained by the author and/or other copyright owners. A copy can be downloaded for personal non-commercial research or study, without prior permission or charge. This thesis cannot be reproduced or quoted extensively from without first obtaining permission in writing from the copyright holder(s). The content must not be changed in any way or sold commercially in any format or medium without the formal permission of the copyright holders.

Note if anything has been removed from thesis.

P3-19, B1-B3, C4-C32 (illustrations and published paper)

When referring to this work, the full bibliographic details must be given as follows:

Ibicek, T. (2012). *Development of a Model to Predict Discomfort in a Vehicle due to Vibration*. PhD Thesis. Oxford Brookes University.

**Development of a Model to Predict Discomfort in a
Vehicle due to Vibration**

T Ibicek

PhD

2012

**Development of a Model to Predict Discomfort in a
Vehicle due to Vibration**

by

Tulay Ibicek

**Faculty of Technology, Design and Environment
Oxford Brookes University**

**A thesis submitted in partial fulfilment of the requirements of
Oxford Brookes University for the degree of**

Doctor of Philosophy

January 2012

ABSTRACT

Human exposure to vehicular vibration can cause sensations (e.g. physical discomfort or annoyance), health issues and safety problems. In industry, several measurement methods have been proposed to improve ride quality and increase the drivers' or passengers' expectations in terms of comfort. The measurement and evaluation methods of quantifying whole-body vibration exposure in relation to human comfort and vibration perception are defined by the International Standard ISO 2631-1. This is the most used standard which provides Health guidance caution zones for risk assessment. The human discomfort threshold limits are not given in this standard. Human discomfort, in general, is defined by measurements based on a shaker table and seat combination. These results when used for "in vehicle situations" may not accurately indicate the level of human discomfort in a vehicle.

In this thesis, a seated human's discomfort is quantified in heave, pitch and roll motions using a four-post rig simulator in order to determine a comfort metric. The quantifying and assessment of discomfort are studied in two categories, which are vehicle dynamics with road inputs, and the human response with human perception to vibration. Comfort/discomfort is a subjective variable; therefore the *in-situ* experiments were performed based on an objective measurement method with a subjective judgement method. The main novel contribution of this thesis is that subjective and dynamic responses of twenty-four seated subjects, in a car on the four post rig excitation, exposed to vertical sinusoidal vibration at five magnitudes in heave, pitch and roll motions were taken at Oxford Brookes University. The physical properties of participants such as age, height, and weight were recorded because human sensitivity, perception and threshold levels may be person dependent. The subjective assessment data was developed based on the response of twenty-four seated subjects to vibration in a car on the four post rig which makes this thesis unique in terms of quantifying of human feeling.

From the experimental data (RMS acceleration and subjective assessment), a discomfort metric was developed in terms of the cause-effect relations between the road and the human body. Based on the analysis and results, it was observed that the sensitivity to acceleration decreased with decreasing amplitude and increasing frequency. This discomfort metric was applied to a developed analytical model to predict the vibration response. A predictive integrated vehicle-seat-human model was developed to characterize the biodynamic response behaviour of a seated human subject and analyse the influence of vibration transmitted on the human body segments. The transmissibility results from an integrated model and *in-situ* discomfort curve measurements were combined to develop a human body discomfort model in a car. The discomfort index curves were predicted by combining the modelling study and the experimental results for heave, pitch and roll modes.

ACKNOWLEDGEMENTS

First I offer my sincere gratitude to my supervisor, Dr. Anand Thite, who supported me during my PhD study and writing of my thesis with his patience and knowledge. Also, I express my gratitude for his encouragement and effort during the course of this research work and writing of this thesis.

I would like to thank John Ward for helping me during the experimental study. I also thank Dr. Khaled Hayatley, Dr. Rob Beale and Jill Organ for their invaluable help.

I would like to thank my parents, my siblings, Prof. William Scott-Jackson and Dr. Julie Scott-Jackson for encouraging and supporting me. I also deeply thank Yusuf Bulut Ozturk and Oxford Brookes University who gave me this opportunity of research and supported my study. I would like to thank Oxford BMW Company.

Finally, I would like to thank my friends, Selina Dobson Gomez, Nevin Hurdogan and my colleagues who helped me.

CONTENTS

| | |
|--|------------|
| ABSTRACT | i |
| ACKNOWLEDGEMENTS | ii |
| TABLE OF CONTENTS | iii |
| LISTS OF FIGURES | ix |
| LIST OF TABLES | xix |
| LIST OF ABBREVIATIONS AND SYMBOLS | xxi |
| | |
| CHAPTER 1 INTRODUCTION | |
| 1.1 Introduction | 1-1 |
| 1.2 Aims of the Research | 1-2 |
| 1.3 Objectives of the Research | 1-2 |
| 1.4 Organization of the Thesis | 1-3 |
| | |
| CHAPTER 2 HUMAN RESPONSE TO VIBRATION LITERATURE REVIEW | |
| 2.1 Introduction | 2-1 |
| 2.2 Whole-Body Vibration in Relation to Discomfort/Comfort | 2-3 |
| 2.3 Methods for Measuring and Evaluating Whole-Body Vibration | 2-5 |
| 2.3.1 Human Vibration Comfort Rig- Shaker Table | 2-8 |
| 2.3.2 A Four-Post Rig Simulator | 2-9 |

| | | |
|-------|--|------|
| 2.3.3 | Standards for Whole-Body Vibration Measurement | 2-9 |
| 2.3.4 | Vibration Analysis for Ride Comfort Evaluation | 2-13 |
| 2.3.5 | Subjective Assessment of Vibration Effects | 2-16 |
| 2.3.6 | Discussion | 2-20 |
| 2.4 | Vehicle Ride Comfort Models | 2-20 |
| 2.4.1 | Quarter Vehicle Model | 2-21 |
| 2.4.2 | Four Degree-of-Freedom Vehicle Model | 2-22 |
| 2.4.3 | Full Vehicle Model | 2-23 |
| 2.4.4 | Discussion | 2-25 |
| 2.5 | Modelling of the Human Body | 2-26 |
| 2.5.1 | Single Degree-of-Freedom Model | 2-27 |
| 2.5.2 | Multi Degree-of-Freedom Lumped-Parameter and Other Complex Models | 2-30 |
| 2.5.3 | Integrated Human-Seat-Vehicle Biodynamical Model | 2-40 |
| 2.5.4 | Other Human Body-Vehicle Computer Models | 2-48 |
| 2.5.5 | Discussion | 2-49 |
| 2.6 | Summary | 2-50 |

CHAPTER 3 VEHICLE DYNAMICS AND THE INFLUENCE ON VEHICLE DISCOMFORT EXPERIMENTS

| | | |
|-----|--|------|
| 3.1 | Introduction | 3-1 |
| 3.2 | Cause-Effect Approach for Mechanism of Vibration Transfer and Vehicle Discomfort | 3-2 |
| 3.3 | Dynamic Characterization of the Car Motion | 3-4 |
| | 3.3.1 Dynamic Response of a Car | 3-4 |
| | 3.3.2 Dynamic Response of a Car Seat | 3-6 |
| 3.4 | Lumped Parameter Vehicle Dynamic Models Used to Analyse Vehicle Comfort | 3-7 |
| | 3.4.1 The Linear Half Vehicle Model | 3-8 |
| | 3.4.2 The Linear Full Vehicle Model | 3-11 |
| 3.5 | Experimental Characterization of Dynamics of the Test Vehicle | 3-16 |
| | 3.5.1 Four-Post Rig Road Simulator | 3-17 |
| | 3.5.2 Experimental Protocol | 3-22 |
| | 3.5.3 Results and Analysis for Resonance Behaviour of Car and Seat | 3-23 |
| 3.6 | Discussion | 3-37 |

CHAPTER 4 TEST PROCEDURE FOR *IN-SITU* MEASUREMENT OF VEHICLE DISCOMFORT

| | | |
|-------|--|------|
| 4.1 | Introduction | 4-1 |
| 4.2 | Vibration Limits for Human Discomfort | 4-3 |
| 4.3 | Defining of 'Effect' by Subjective Assessment | 4-7 |
| 4.4 | Dynamic Characterization of a Car Seat | 4-10 |
| 4.4.1 | The Vehicle Driver Seat Response to Vibration Input at Wheels | 4-10 |
| 4.5 | Test Procedure for <i>In-situ</i> Measurement of Car Comfort | 4-16 |
| 4.5.1 | The Scaling of Vibration Magnitudes for the Degree Level of Discomfort | 4-16 |
| 4.5.2 | Precautions to Avoid Risk of Injury | 4-18 |
| 4.5.3 | Participants | 4-19 |
| 4.5.4 | Procedure | 4-21 |
| 4.5.5 | Data Analysis | 4-22 |
| 4.6 | Discussion | 4-23 |

CHAPTER 5 EXPERIMENTAL QUANTIFICATION OF DISCOMFORT IN A CAR

| | | |
|-----|--|-----|
| 5.1 | Introduction | 5-1 |
| 5.2 | Analysis of Subjective Discomfort Assessment in Heave, Pitch and Roll Mode | 5-2 |

| | | |
|-------|--|------|
| 5.2.1 | Analysis of Subjective Discomfort Assessment in Heave Mode | 5-5 |
| 5.2.2 | Analysis of Subjective Discomfort Assessment in Pitch Mode | 5-13 |
| 5.2.3 | Analysis of Subjective Discomfort Assessment in Roll Mode | 5-19 |
| 5.2.4 | Variation of Discomfort Indices as Function of Frequency | 5-24 |
| 5.3 | Discussion | 5-28 |

CHAPTER 6 MODELLING OF BIODYNAMIC RESPONSE OF THE SEATED HUMAN BODY IN A CAR

| | | |
|-------|-------------------------------------|------|
| 6.1 | Introduction | 6-1 |
| 6.2 | Biomechanical Modelling | 6-3 |
| 6.2.1 | Single Degree of Freedom Model | 6-4 |
| 6.2.2 | Three Degree of Freedom Model | 6-11 |
| 6.2.3 | Summary | 6-17 |
| 6.3 | Integrated Human-Seat-Vehicle Model | 6-19 |
| 6.3.1 | Seven Degree of Freedom Model | 6-20 |
| 6.3.2 | Summary | 6-29 |
| 6.4 | Discussion | 6-30 |

**CHAPTER 7 PREDICTIVE MODEL OF HUMAN BODY COMFORT IN
A CAR**

| | | |
|-----|--|------|
| 7.1 | Introduction | 7-1 |
| 7.2 | Predictive Model of Human Body Discomfort in a Car | 7-1 |
| 7.3 | Validation of Predictive Model | 7-8 |
| | 7.3.1 Prediction of Discomfort Index | 7-11 |
| 7.4 | Discussion | 7-16 |

CHAPTER 8 CONCLUSIONS

| | | |
|-----|---------------------------------|-----|
| 8.1 | Conclusions | 8-1 |
| 8.2 | Recommendations for Future Work | 8-5 |

REFERENCES R-1

APPENDIX A A-1

APPENDIX B B-1

APPENDIX C C-1

APPENDIX D D-1

APPENDIX E E-1

LIST OF FIGURES

| | | |
|-------------|--|------|
| Figure 2.1 | Human Response to Vibration showing multi-disciplinary interaction [3]. | 2-1 |
| Figure 2.2 | Effects of vibration (motion sickness, whole-body vibration and hand-transmitted vibration) based on the typical frequency ranges and vibration magnitudes [3]. | 2-2 |
| Figure 2.3 | Whole-body vibration coordinate system for a seated human body [7] showing vibration perception mechanism. | 2-4 |
| Figure 2.4 | ISO 2631-1 Health Guidance Caution Zones. _ _ _ _ represents the upper threshold limit for feeling, represents the lower threshold limit for feeling [7]. | 2-11 |
| Figure 2.5 | a) One degree of freedom model (1-DOF) and b) Quarter vehicle model (2-DOF) [16, 40]. | 2-22 |
| Figure 2.6 | A four degree-of-freedom half body of vehicle suspension system model (4-DOF) in pitch mode [16, 43] | 2-23 |
| Figure 2.7 | Full vehicle model by Imine (2006) [49]. | 2-24 |
| Figure 2.8 | Integrated seat-full vehicle model (8-DOF) by Bouazara [50]. | 2-25 |
| Figure 2.9 | A human vibration model riding in an automobile vibration model [67]. | 2-44 |
| Figure 2.10 | Integrated human-vehicle model [77]. | 2-45 |
| Figure 3.1 | Vibration ‘cause-effect’ model for human perception of vibration. | 3-3 |
| Figure 3.2 | A relation between the road and seat which represents car characterization and transmissibility. | 3-5 |
| Figure 3.3 | The motion of a vehicle which interacts with the ground. | 3-6 |
| Figure 3.4 | Lumped parameter half (4-DOF) vehicle (front and rear left) model in the motion of pitch and heave. | 3-9 |
| Figure 3.5 | Lumped parameter full vehicle ride (7-DOF) model. | 3-12 |

| | | |
|-------------|--|------|
| Figure 3.6 | a) The four-post rig simulator (FR: Front-right; FL: Front-left; RR: Rear-right; RL: Rear-left actuators respectively). b) The four hydraulic actuators | 3-18 |
| Figure 3.7 | a) The four-post rig control panel (after Dynosoft MTCA, User Manual, 2009): 1 Rig Status; 2 Rig Enable; 3 Live Measurement; 4 Pressure Control; 5 Wave Control; 6 Acquisition Control. b) The four-post rig wave control panel (after Dynosoft MTCA, User Manual, 2009). | 3-19 |
| Figure 3.8 | A car (BMW Mini cooper <i>2.467 m wheel base, 1.465 m rear track, 1.455 m front track</i>) on the 4-post rig. The wheels are placed on the rig. | 3-20 |
| Figure 3.9 | a) The model 2210 accelerometers. b) Connector and Logical Channels. | 3-22 |
| Figure 3.10 | Installation of 2210 model accelerometers on the seat. | 3-23 |
| Figure 3.11 | The rig acceleration (rear-right (RR)) time history in heave mode at 5 Hz based on dependent constant velocity. | 3-24 |
| Figure 3.12 | The seat acceleration time history in heave mode at 5 Hz based on dependent constant velocity. | 3-25 |
| Figure 3.13 | The magnitude of transmissibility (floor to pad) with respect to the pad accelerations in heave mode with road input amplitude in the frequency range of 0.25 Hz- 20 Hz for 10 seconds durations. The four lines are for estimations based on four pad inputs respectively. | 3-27 |
| Figure 3.14 | Seat transmissibility (measured frequency response functions) with respect to the pad accelerations in heave mode with road input amplitude in the frequency range of 0.25 Hz -20 Hz. | 3-28 |
| Figure 3.15 | Seat transmissibility (measured frequency response functions) with respect to the floor accelerations in heave mode in the frequency range of 0.25 Hz -20 Hz. | 3-29 |
| Figure 3.16 | Linear floor transmissibility (measured frequency response function) with respect to the angular pad accelerations in pitch mode with road input amplitude in the frequency range of 1 Hz -20 Hz. | 3-30 |

| | | |
|-------------|--|------|
| Figure 3.17 | Linear seat transmissibility (measured frequency response function) with respect to the angular floor acceleration in pitch mode with road input amplitude in the frequency range of 1 Hz -20 Hz. | 3-31 |
| Figure 3.18 | Angular floor transmissibility (measured frequency response function) with respect to the angular pad accelerations in pitch mode with road input amplitude in the frequency range of 1 Hz -20 Hz. | 3-32 |
| Figure 3.19 | Angular seat transmissibility (measured frequency response function) with respect to the angular floor acceleration in pitch mode with road input amplitude in the frequency range of 1 Hz -20 Hz. | 3-32 |
| Figure 3.20 | Linear floor transmissibility (measured frequency response function) with respect to the angular pad accelerations in roll mode with road input amplitude in the frequency range of 1 Hz -20 Hz. | 3-33 |
| Figure 3.21 | Linear seat transmissibility (measured frequency response function) with respect to the angular floor acceleration in roll mode with road input amplitude in the frequency range of 1 Hz -20 Hz. | 3-34 |
| Figure 3.22 | Angular floor transmissibility (measured frequency response function) with respect to the angular pad accelerations in roll mode with road input amplitude in the frequency range of 1 Hz -20 Hz. | 3-35 |
| Figure 3.23 | Angular seat transmissibility (measured frequency response function) with respect to the floor acceleration in roll mode with road input amplitude in the frequency range of 1 Hz -20 Hz. | 3-36 |
| Figure 4.1 | Occupant comfort limit in the vertical vibration by Janeway [13]. | 4-5 |
| Figure 4.2 | Limits of whole-body vibration exposure criteria curves in vertical direction for equal fatigue-decreased proficiency boundaries [13]. | 4-6 |
| Figure 4.3 | Installation of 2210 model accelerometers in the car. The distances between the accelerometers are: a_4 - a_5 : 19 cm, a_5 - a_6 : 5.5 cm, a_1 - a_3 : 90.1 cm, a_2 - a_3 : 27.6 cm. | 4-11 |

| | | |
|------------|---|------|
| Figure 4.4 | Measured RMS (seat) acceleration in respect of the input displacement on the 4-Post Rig excitation at 1 Hz in heave mode. | 4-12 |
| Figure 4.5 | Measured RMS (seat) acceleration in respect of the input displacement on the 4-Post Rig excitation at 5 Hz in heave mode. | 4-13 |
| Figure 4.6 | Measured RMS (seat) acceleration in respect of the input displacement on the 4-Post Rig excitation at 10 Hz in heave mode. | 4-13 |
| Figure 4.7 | Measured RMS (seat) acceleration in respect of the input displacement on the 4-Post Rig excitation at 1 Hz in pitch mode (a) and roll mode (b) respectively. | 4-14 |
| Figure 4.8 | Measured output seat acceleration in respect of the input displacement on the 4-Post Rig excitation at 1.75 Hz in (a) pitch mode and (b) roll mode respectively. | 4-15 |
| Figure 4.9 | A seated human in a car on the 4-post rig excitation. | 4-22 |
| Figure 5.1 | Subjective discomfort index with respect to the measured seat RMS acceleration in heave mode at 5 Hz road input. | 5-4 |
| Figure 5.2 | Subjective discomfort index with respect to the measured seat RMS acceleration in pitch mode at 5 Hz road input. | 5-4 |
| Figure 5.3 | Subjective discomfort index with respect to the measured seat RMS acceleration in roll mode at 5 Hz road input. | 5-5 |
| Figure 5.4 | Subjective discomfort index with respect to the measured linear RMS acceleration on the seat in heave mode at 1 Hz for vertical vibration. _ _ _ lines represent the mean of the subjective ratings and measured seat RMS accelerations. | 5-6 |
| Figure 5.5 | Discomfort index variations for 24 participants as a function of seat RMS acceleration as measured during heave input to the vehicle at excitation frequency 1 Hz. — — — — mean discomfort index, _____ mean discomfort index $\pm 2\sigma$. | 5-7 |
| Figure 5.6 | Subjective discomfort index with respect to the measured linear RMS acceleration on the seat in heave mode at 5 Hz for vertical vibration. _ _ _ lines represent the mean of the subjective ratings and measured seat RMS accelerations. | 5-8 |
| Figure 5.7 | Discomfort index variation for 24 participants as a function of seat RMS acceleration as measured during heave input to the vehicle at excitation frequency 5 Hz. — — — — mean | 5-8 |

| | | |
|-------------|---|------|
| | discomfort index, _____ mean discomfort index $\pm 2\sigma$. | |
| Figure 5.8 | Subjective discomfort index with respect to the measured linear RMS acceleration on the seat in heave mode at 10 Hz for vertical vibration. _ _ _ lines represent the mean of the subjective ratings and measured seat RMS accelerations. | 5-9 |
| Figure 5.9 | Discomfort index variation for 24 participants as a function of seat RMS acceleration as measured during heave input to the vehicle at excitation frequency 10 Hz. — — — — mean discomfort index, _____ mean discomfort index $\pm 2\sigma$. | 5-10 |
| Figure 5.10 | Mean discomfort index variation for 24 participants as a function of mean seat RMS acceleration as measured during heave input to the vehicle at excitation frequency level between 1 Hz - 5 Hz. — 1 Hz, --⊖-- 2 Hz, 3 Hz, -.-.- 4 Hz, —+— 5 Hz. | 5-11 |
| Figure 5.11 | Mean discomfort index variation for 24 participants as a function of mean seat RMS acceleration as measured during heave input to the vehicle at excitation frequency level between 6 Hz - 10 Hz. — 6 Hz, --⊖-- 7 Hz, 8 Hz, -.-.- 4 Hz, —+— 10 Hz. | 5-11 |
| Figure 5.12 | Mean discomfort index variation for 24 participants as a function of mean seat RMS acceleration as measured during heave input to the vehicle at excitation frequency level between 11 Hz - 15 Hz. — 11 Hz, --⊖-- 12 Hz, -.-.- 13 Hz, -.-.- 14 Hz, —+— 15 Hz. | 5-12 |
| Figure 5.13 | Subjective discomfort index with respect to the measured linear RMS acceleration on the seat in pitch mode at 3 Hz for vertical vibration. _ _ _ lines represent the mean of the subjective ratings and measured seat RMS accelerations. | 5-14 |
| Figure 5.14 | Discomfort index variation for 24 participants as a function of seat RMS acceleration as measured during pitch input to the vehicle at excitation frequency 3 Hz. — — — — mean discomfort index, _____ mean discomfort index $\pm 2\sigma$. | 5-14 |
| Figure 5.15 | Subjective discomfort index with respect to the measured linear RMS acceleration on the seat in pitch mode at 5 Hz for vertical vibration. _ _ _ lines represent the mean of the subjective ratings and measured seat RMS accelerations. | 5-15 |

| | | |
|-------------|---|------|
| Figure 5.16 | Discomfort index variation for 24 participants as a function of seat RMS acceleration as measured during pitch input to the vehicle at excitation frequency 5 Hz. — — — — mean discomfort index, _____ mean discomfort index $\pm 2\sigma$. | 5-15 |
| Figure 5.17 | Subjective discomfort index with respect to the measured linear RMS acceleration on the seat in pitch mode at 10 Hz for vertical vibration. _ _ _ lines represent the mean of the subjective ratings and measured seat RMS accelerations. | 5-16 |
| Figure 5.18 | Discomfort index variation for 24 participants as a function of seat RMS acceleration as measured during pitch input to the vehicle at excitation frequency 10 Hz. — — — — mean discomfort index, _____ mean discomfort index $\pm 2\sigma$. | 5-16 |
| Figure 5.19 | Mean discomfort index variation for 24 participants as a function of mean seat RMS acceleration as measured during pitch input to the vehicle at excitation frequency level between 3 Hz - 5 Hz. 3 Hz, - - - - - 4 Hz, — + — 5 Hz. | 5-17 |
| Figure 5.20 | Mean discomfort index variation for 24 participants as a function of mean seat RMS acceleration as measured during pitch input to the vehicle at excitation frequency level between 6 Hz - 10 Hz. ——— 6 Hz, - - ⊕ - - 7 Hz, 8 Hz, - - - - - 9 Hz, — + — 10 Hz. | 5-18 |
| Figure 5.21 | Mean discomfort index variation for 24 participants as a function of mean seat RMS acceleration as measured during pitch input to the vehicle at excitation frequency level between 11 Hz - 15 Hz. ——— 11 Hz, - - ⊕ - - 12 Hz, 13 Hz, - - - - - 14 Hz, — + — 15 Hz. | 5-18 |
| Figure 5.22 | Subjective discomfort index with respect to the measured linear RMS acceleration on the seat in roll mode at 3 Hz for vertical vibration. _ _ _ lines represent the mean of the subjective ratings and measured seat RMS accelerations. | 5-19 |
| Figure 5.23 | Discomfort index variation for 24 participants as a function of seat RMS acceleration as measured on roll input to the vehicle at excitation frequency 3 Hz. — — — — mean discomfort index, _____ mean discomfort index $\pm 2\sigma$. | 5-20 |

| | | |
|-------------|---|------|
| Figure 5.24 | Subjective discomfort index with respect to the measured linear RMS acceleration on the seat in roll mode at 5 Hz for vertical vibration. lines represent the mean of the subjective ratings and measured seat RMS accelerations. | 5-20 |
| Figure 5.25 | Discomfort index variation for 24 participants as a function of seat RMS acceleration as measured during roll input to the vehicle at excitation frequency 5 Hz. mean discomfort index, mean discomfort index $\pm 2\sigma$. | 5-21 |
| Figure 5.26 | Mean discomfort index variation for 24 participants as a function of mean seat RMS acceleration as measured during roll input to the vehicle at excitation frequency level between 3 Hz - 5 Hz. 3 Hz, 4 Hz, 5 Hz. | 5-22 |
| Figure 5.27 | Mean discomfort index variation for 24 participants as a function of mean seat RMS acceleration as measured during roll input to the vehicle at excitation frequency level between 6 Hz - 10 Hz. 6 Hz, 7 Hz, 8 Hz, 9 Hz, 10 Hz. | 5-22 |
| Figure 5.28 | Mean discomfort index variation for 24 participants as a function of mean seat RMS acceleration as measured during roll input to the vehicle at excitation frequency level between 11 Hz - 15 Hz. 11 Hz, 12 Hz, 13 Hz, 14 Hz, 15 Hz. | 5-23 |
| Figure 5.29 | Discomfort index level (mean) versus to frequency range from 1 Hz to 15 Hz at 0.1 m/s ² measured seat RMS acceleration for 17 seconds. heave, pitch, and roll. | 5-25 |
| Figure 5.30 | Discomfort index level (mean) versus to frequency range from 1 Hz to 15 Hz at 0.16 m/s ² measured seat RMS acceleration for 17 seconds. pitch, and roll. | 5-25 |
| Figure 5.31 | Discomfort index level (mean) versus to frequency range from 1 Hz to 15 Hz at 0.25 m/s ² measured seat RMS acceleration for 17 seconds. heave, pitch, and roll. | 5-26 |

| | | |
|-------------|--|------|
| Figure 5.32 | Discomfort index level (mean) versus to frequency range from 1 Hz to 15 Hz at 0.4 m/s ² measured seat RMS acceleration for 17 seconds. — heave, - - + - pitch, and - - ⊕ - roll. | 5-26 |
| Figure 5.33 | Discomfort index level (mean) versus to frequency range from 1 Hz to 15 Hz at 0.63 m/s ² measured seat RMS acceleration for 17 seconds. — heave, - - + - pitch, and - - ⊕ - roll. | 5-27 |
| Figure 5.34 | Discomfort index level (mean) versus to frequency range from 1 Hz to 15 Hz in heave mode at 1 m/s ² measured seat RMS acceleration for 17 seconds. | 5-27 |
| Figure 6.1 | A SDOF biomechanical seated human model [28, 56]. | 6-5 |
| Figure 6.2 | The proposed equivalent SDOF model. | 6-5 |
| Figure 6.3 | Free body diagram for SDOF model. | 6-6 |
| Figure 6.4 | Magnitude of transmissibility for a seated human body response with respect to floor input. | 6-7 |
| Figure 6.5 | Effect of human body's mass for a SDOF model. Three total body masses: — 56.8 kg, - - - - 75 kg, - ···· 95 kg. | 6-8 |
| Figure 6.6 | Effect of stiffness coefficient for a 56.8 kg seated human body SDOF model. Three total stiffness coefficients: — 36932 N/m, - - - - 44130 N/m, - ···· 75500N/m. | 6-9 |
| Figure 6.7 | Effect of damping coefficient for a 56.8 kg seated human body SDOF model. Three total stiffness coefficients: — 326.63Ns/m, - - - - 1485 Ns/m, - ···· 3840 Ns/m. | 6-10 |
| Figure 6.8 | Biomechanical 6-DOF model for a seated human body subject. | 6-12 |

| | | |
|-------------|--|------|
| Figure 6.9 | The proposed 3-DOF model for a seated human body subject. | 6-13 |
| Figure 6.10 | The magnitude of transmissibilities in respect to the floor input for the 3-DOF model. ————— Head response, - - - - - Upper torso response, - · - · - · Lower torso response. | 6-16 |
| Figure 6.11 | The magnitude of transmissibility for head response in respect to the seat input for the 3-DOF model. | 6-17 |
| Figure 6.12 | A lumped parameter integrated human-seat-vehicle model (7-DOF) model without backrest support in the motion of heave and pitch modes at road input. | 6-21 |
| Figure 6.13 | The magnitude of transmissibility (vehicle/sprung mass) in heave mode with road input. | 6-25 |
| Figure 6.14 | The magnitude of transmissibility in heave mode with road input. ————— Head response, - - - - - Upper torso response, - · - · - · Lower torso response. | 6-26 |
| Figure 6.15 | The magnitude of transmissibility (vehicle/sprung mass) in pitch mode with road input. | 6-27 |
| Figure 6.16 | The magnitude of transmissibility for head response in respect to the seat input. | 6-28 |
| Figure 7.1 | A lumped parameter integrated human-seat-vehicle (10-DOF) model without backrest in the motion of heave, pitch and roll modes at road input. | 7-2 |
| Figure 7.2 | Comparison of road-to-seat transmissibility in heave mode. _____ Proposed model, - · - · - · measured vibration transmissibility for 24 participants at 0.1 m/s^2 vibration excitation. | 7-8 |
| Figure 7.3 | Comparison of road-to-floor transmissibility in heave mode. _____ Proposed model, - · - · - · measured vibration transmissibility for 24 participants at 0.1 m/s^2 vibration excitation. | 7-10 |

| | | |
|------------|--|------|
| Figure 7.4 | Predicted discomfort index for heave mode. | 7-14 |
| Figure 7.5 | Predicted discomfort index for pitch mode. | 7-14 |
| Figure 7.6 | Predicted discomfort index for roll mode. | 7-15 |

LIST OF TABLES

| | | |
|-----------|--|------|
| Table 2.1 | One degree-of-freedom (1-DOF) lumped parameter models of a seated human | 2-29 |
| Table 2.2 | Two degree-of-freedom (2-DOF) lumped parameter models of a seated human | 2-32 |
| Table 2.3 | Three degree-of-freedom (3-DOF) lumped parameter models of a seated human | 2-35 |
| Table 2.4 | Three degree-of-freedom (3-DOF) lumped parameter models of a seated human | 2-36 |
| Table 2.5 | Four degree-of-freedom (4-DOF) lumped parameter models of a seated human | 2-37 |
| Table 2.6 | Four degree-of-freedom (4-DOF) lumped parameter models of a seated human | 2-38 |
| Table 2.7 | Occupant-tractor (11-DOF) model with relaxation suspension to seat | 2-42 |
| Table 2.8 | Integrated human-vehicle (14-DOF) model | 2-46 |
| Table 2.9 | Seven-DOF quarter car and biodynamical model | 2-47 |
| Table 3.1 | Measured parameters of a BMW mini cooper car for 4-DOF model [83]. | 3-11 |
| Table 3.2 | Measured parameters of a BMW mini cooper car [83]. | 3-15 |
| Table 3.3 | Natural frequencies of lumped parameter full (7-DOF) vehicle model. | 3-16 |
| Table 3.4 | Resonance behaviour of BMW Mini Cooper. | 3-37 |
| Table 4.1 | Various degrees of comfort/discomfort scale and frequency-weighted acceleration. | 4-9 |
| Table 4.2 | Measured linear RMS (seat) acceleration in respect of the input amplitude at 1 Hz in heave mode. | 4-12 |
| Table 4.3 | Frequency-weighted acceleration level for a seated human in a car on the four-post rig excitation. | 4-17 |

| | | |
|-----------|---|------|
| Table 4.4 | Degree of discomfort scale for a seated human in a car on the four-post rig. | 4-17 |
| Table 4.5 | The physical parameters of the participants. | 4-20 |
| Table 5.1 | The measured and scaled discomfort assessment data from one participant (P20) are given for the frequency of 4Hz, 5Hz and 6 Hz. The physical parameters of P20 are: age 36; weight 75 kg; height 1.72 cm (see Chapter 4). *: Degree of comfort scale (see Chapter 4). | 5-3 |
| Table 6.1 | The parameters for a seated human body SDOF model from Cho and Yoon [28]. | 6-5 |
| Table 6.2 | The parameters for the proposed SDOF model. | 6-5 |
| Table 6.3 | The parameters for the 6-DOF model. | 6-13 |
| Table 6.4 | The parameters for the proposed 3-DOF model. | 6-15 |
| Table 6.5 | The parameters for the integrated human-seat-vehicle (7-DOF) model. | 6-24 |
| Table 7.1 | The parameters for the predictive 10-DOF model. | 7-9 |
| Table 7.2 | Predicted discomfort index with seat output acceleration up to 15 Hz in heave mode. | 7-12 |
| Table 7.3 | Predicted discomfort index with seat output acceleration up to 15 Hz in pitch mode. | 7-12 |
| Table 7.4 | Predicted discomfort index with seat output acceleration up to 15 Hz in roll mode. | 7-13 |

LIST OF ABBREVIATIONS AND SYMBOLS

| | |
|----------------------|---------------------------------------|
| 1-DOF | One degree-of-freedom |
| 2-DOF | Two degree-of-freedom |
| 3-DOF | Three degree-of-freedom |
| 4-DOF | Four degree-of-freedom |
| 4-Post Rig | Four-Post rig |
| 6-DOF | Five degree-of-freedom |
| 7-DOF | Seven degree-of-freedom |
| 9-DOF | Nine degree-of-freedom |
| 11-DOF | Eleven degree-of-freedom |
| a_i | r.m.s. acceleration |
| a_v | Vibration total value |
| $a_{wr.m.s.}$ | Frequency-weighted r.m.s acceleration |
| $a_w(t)$ | Frequency-weighted acceleration |
| c_i | Damper value |
| k_i | Spring value |
| k_x, k_y and k_z | Multiplying factors |
| m_i | Human body segment mass |
| r_i | Road input displacement |
| t | Time |
| t_0 | Time of observation |
| x, y, z | Translatory axes |
| x_i | Displacement, excitation input |
| y | Response displacement |

| | |
|-----------------|---|
| APP | Apparent mass |
| C.G. | Centre of gravity |
| DCI | Discomfort Index |
| DPMI | Driving-point mechanical impedance |
| F | Input force (forcing vector) |
| FL | Front left |
| FR | Front right |
| FTS | Floor-to-seat |
| HVC | Human vibration comfort |
| $I_{x,y,z}$ | Principle moments of inertia |
| L_f and L_r | Distances of the front and rear of the vehicle from its centre of gravity |
| MDOF | Multi degree-of-freedom |
| MTVV | Maximum transient vibration value |
| NDOF | Number of degrees of freedom |
| PSD | Power spectral density |
| RL | Rear left |
| RMS | Root-mean-square |
| RR | Rear right |
| SDOF | Single degree-of-freedom |
| STH | Seat-to-head |
| T | Duration |
| TR | Transmissibility |
| VDV | Vibration dose value |

| | |
|----------|--|
| W_c | Frequency weighting acceleration for seat-back measurements |
| W_d | Frequency weighting acceleration for x and y directions |
| W_e | Frequency weighting acceleration for measurement of rotational vibration |
| W_f | Motion sickness |
| W_i | Frequency weighting |
| W_j | Frequency weighting acceleration for measurement of vibration under the head of a recumbent person |
| W_k | Frequency weighting acceleration for z direction |
| WBV | Whole body vibration |
| XML | Extensible Mark-up Language |
| Y | Response vector |
| α | Angular roll displacement |
| ω | Natural frequency |
| θ | Angular pitch displacement |
| τ | Integration time for running averaging |

CHAPTER 1

INTRODUCTION

1.1 INTRODUCTION

Ever since people first started to make journeys in automobiles, the ride comfort offered for all the occupants has been an important design issue. The ride quality of a vehicle is one of the critical parameters determining competitiveness of the vehicle. It is vitally linked to discomfort. The discomfort in turn is influenced by the human dynamic response (vibration) and perception of the dynamic response. The vibration experienced by the human body depends on the vehicle dynamics and the road inputs. Currently, the discomfort in a vehicle due to vibration is assessed by correlation between the vibration response and the perception data from the standards. The perception data is, generally, based on standalone shaker table measurements and the discomfort produced is predicted by the vibration threshold. The available data from previous studies may not give consistency because of the different measurement techniques used.

There is continued interest in developing the vibration threshold levels of human perception to define discomfort/comfort. The human response to vibration has complex dependency on the frequency content and the amplitude levels. There seems to be no such thing as the perfect frequency response spectra from a comfort point of view. It does not help that threshold levels may be person dependent (age, sex, physique, etc. may play a role); there exists inherent variability. One way of improving ride comfort would be to reduce the perception of vibration in a vehicle. There are, however, conflicting requirements on suspension design; the optimization of setting for comfort (reduced vibration) invariably has detrimental effect on the performance of the vehicle. Depending on the end use there has to be compromise between giving best possible comfort and the performance.

In order to have a realistic view of discomfort, measurements may have to be performed on the vehicle. The measurement of discomfort in a vehicle requires an appropriate experimental method and assessment strategy to study the effect of bounce, pitch and roll motion on human sensitivity to vibration and its perception.

The definition of 'Comfort/Discomfort' has been an interesting research topic. In this study, based on the recent publications [1], discomfort is used throughout in relation to perception of vibration. There are many dynamic factors which influence discomfort. The aims and thesis plans are given below.

1.2 AIMS OF THE RESEARCH

The main aim of this research is to develop a discomfort metric in vertical and rotational directions for a seated human subject in a vehicle using a four-post rig simulator.

1.3 OBJECTIVES OF THE RESEARCH

- A new experimental protocol will be developed in order to understand the dynamic behaviour of vehicles.
- An objective vibration measurement on the occupants in a car will be studied to quantify the biodynamic response, human discomfort and perception.
- A discomfort index will be determined and a discomfort metric will be developed using subjective assessment of car passengers.
- A mathematical model will be developed to represent the dynamics of a vehicle-seat-occupant system to predict discomfort in a car.
- The discomfort indices will be predicted by combining the modelling study and experimental results for heave pitch and roll modes.

1.4 ORGANIZATION OF THE THESIS

Chapter 1 presents a general introduction of human comfort/discomfort. The aims of the present research are discussed.

Chapter 2 presents the literature review on the whole-body vibration (WBV), measurement and evaluation of WBV, vehicle ride models and the modelling of human body dynamics.

Chapter 3 presents in detail the cause-effect relation used to analyse vehicle comfort; an experimental design and characterization of the vehicle dynamics and the mathematical vehicle dynamic models.

Chapter 4 discusses the vibration limits for human comfort/discomfort with the aim of defining subjective assessment and rating. It also presents the dynamic characterization of a car seat and in detail the experimental procedure for *in-situ* measurement of car discomfort.

Chapter 5 discusses the experimental measurement results of twenty-four participants in terms of vibration stimuli and perception.

Chapter 6 presents a mathematical model that demonstrates the dynamic behaviour and characteristic of a seated human in a car and predicts the vibration response.

Chapter 7 presents a predictive discomfort model of a human body in a car using the results from Chapter 5 and 6.

Chapter 8 presents the conclusions of the study. The recommendations for future work are also outlined.

CHAPTER 2

HUMAN RESPONSE TO VIBRATION LITERATURE REVIEW

2.1 INTRODUCTION

‘Human Response to Vibration’ is a multi-disciplinary subject [2, 3, 4]; it involves disciplines in the field of biology, psychology, biomechanics, engineering, physics and physiology. These fields can be combined into three groups: a) human, b) response and c) vibration (Fig. 2.1). The interactions between the groups and their effects may vary, based on the vibration complexity, human subjectivity, and human anatomy.

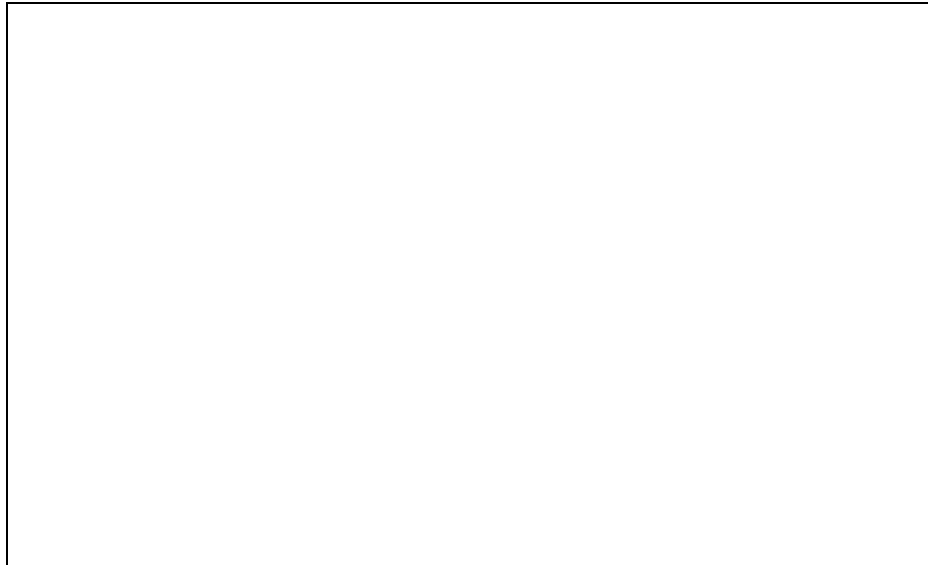


Figure 2.1: Human Response to Vibration showing multi-disciplinary interaction [3].

The vibration effects on a human body can be classified [3] into three zones based on the input frequency and vibration magnitude (Fig. 2.2). The vibration transmitted through a seat or feet is known as ‘*whole-body vibration*’ (WBV). It occurs for the frequencies between 1 and 30 Hz. People are most sensitive to

whole-body vibration in the frequency range of 1 to 20 Hz and seated subjects are most sensitive at 5 Hz and 16 Hz for vertical vibration. In the vertical vibration at 10 Hz frequency level, women are most sensitive to vibration than men. The responses of seated human body segments are given as; the lower abdomen at 4-5 Hz and head at 16 Hz [3, 4].

Whole-body vibration influences human health and performance. The vibration transmitted into the human body through hands is known as '*hand-transmitted vibration*'; the frequencies of interest range from 10 Hz to about 1000 Hz. '*Motion sickness*' can occur when a person is exposed to low frequency motion because below 1 Hz, sensory signals from the eyes and the organ of balance do not agree [5]. Hand-transmitted vibration and motion sickness are not within the scope of this study.

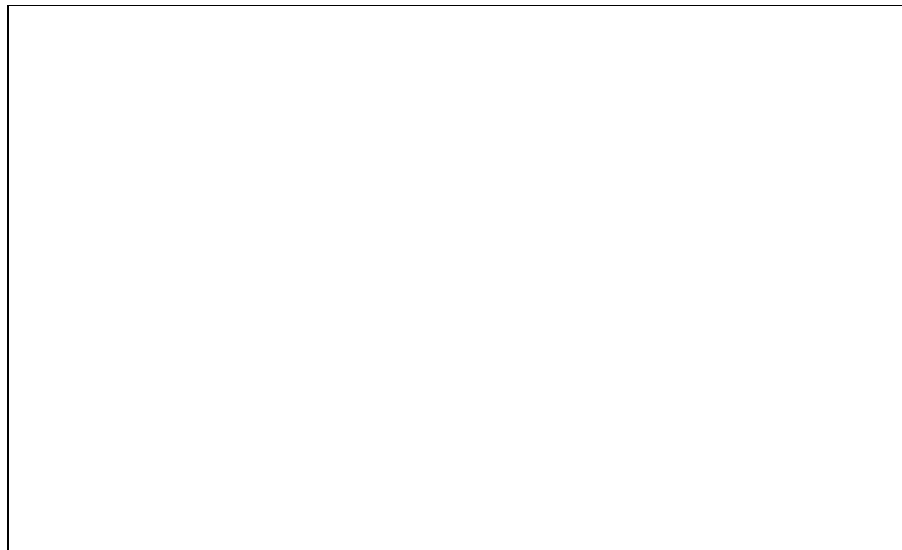


Figure 2.2: Effects of vibration (motion sickness, whole-body vibration and hand-transmitted vibration) based on the typical frequency ranges and vibration magnitudes [3].

The aim of this study is to evaluate ride discomfort for a seated human subject in a moving vehicle. This requires an understanding of the human body response to vibration, especially characteristics of the vibration transmitted and vibrational influences on the human body. There is a significant amount of published

literature in the related areas. Based on the emphasis of the thesis, a literature review can be grouped into four general themes which are discussed in subsequent sections of this chapter.

- a) Perception of vibration and sensitivity to vibration with emphasis on whole-body vibration,
- b) Measurement methods to find the relation between perception and the stimulus, and various measures currently used for comfort/discomfort rating,
- c) Vehicle vibration to various road inputs,
- d) Biodynamic modelling to understand and predict human dynamic response.

2.2 WHOLE-BODY VIBRATION IN RELATION TO DISCOMFORT/COMFORT

The human body is depicted as a complex and nonlinear dynamic system by Griffin [2] and Silva [4]; the influence of physiological and psychophysical factors makes the understanding of the human response to vibration a difficult task. The studies on whole-body vibration have become increasingly significant in understanding and evaluating human comfort/discomfort, health and motion sickness [2, 3, 4].

The vibration excitation is perceived by the brain through the sensory mechanism (Fig. 2.3), once signals are received via various parts of the human body (i.e., the feet, the buttocks, the back, and the head); the sensation may be direction dependent and hence multi-directional inputs considered [4, 6]. The axes system for whole-body vibrations has a six-degree-of-freedom coordinate system composed of three translatory axes (x , y , and z) and three rotational motions (roll, pitch, and yaw) [4].

The human response to vibration can be determined based on the understanding of the interactions between the human body and the vibrating contact surface. The influences of the vibration transmitted to the human body depend on the

extrinsic and intrinsic variables [2]. The extrinsic variables, which are the characteristics of the vibration excitation [2, 3, 4], consist of:

1. Spectral characteristics of the excitation
 - a) Specific frequency value
 - b) Frequency content of the vibration signal
 - c) Magnitude (level or amplitude) of vibration
2. Duration of exposure
3. Direction and location of application

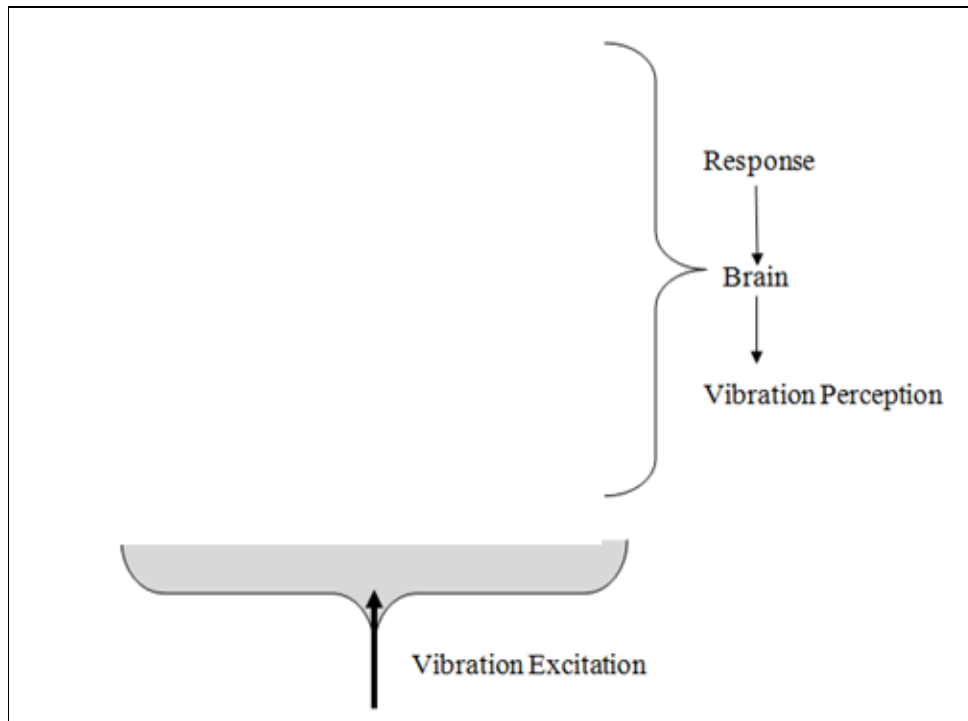


Figure 2.3: Whole-body vibration coordinate system for a seated human body [7] showing vibration perception mechanism.

The intrinsic or the physical characteristics are classified into two categories, 'Intra- and Inter-subject variability'. Intra-subject variabilities occur due to the human body posture, either in a sitting position or standing, which changes in a person over time. Inter-subject variabilities are due to the weight, dynamic response, and age, which can be completely different for each person, and as well

as the effects of gender. Several studies [2, 3, 8, 9] have researched the effect of vibration on the *health* and *well-being* of the human body, in particular, comfort/discomfort due to the extrinsic and intrinsic variables.

Many dictionaries as well as research publications on human response to vibration provide a definition of comfort as ‘a state of well-being or a feeling of well-being’ [2, 9, 10, 11]. There is widespread agreement, however, that being subjective the unique quantification of comfort is difficult. In some subjective assessments, comfort is defined in terms of feeling/sensation, such as ‘the opposite of discomfort [2]’ or ‘the absence of discomfort [3, 10]’ or ‘positive feeling [10]’. A more recent study [1] has established the difference between comfort and discomfort. Discomfort was found to depend more directly on stimulus (vibration input) than comfort does. Comfort was found to have influences from not only stimulus but many other aspects. Hence, it is appropriate in this study to use discomfort when quantifying the perception of vibration.

2.3 METHODS FOR MEASURING AND EVALUATING WHOLE-BODY VIBRATION

Comfort, as previously stated (section 2.2), has now become a higher priority for vehicle manufacturers due to the high-quality expectations of drivers and passengers. New designs and simulation methods have been developed with an aim to improve the ride comfort. However, these developments have not been enough to understand completely the characteristics of vibration interaction between a road surface, vehicle and drivers/passengers.

Ride discomfort levels or boundaries for drivers/passengers are difficult to identify; one needs complete understanding of stimulus and its perception. Understanding of the dynamic behaviour of the vehicle to vibration input, the human response to vehicle vibration and the dynamic interaction between the seat and driver is essential to evaluate discomfort. A variety of experimental methods

[12, 13] have been developed in the past in order to assess and evaluate the vehicle vibration and human response. The following contributions are reviewed in this section.

1. The road roughness measuring systems
2. Subjective ride comfort/discomfort measurements
3. Human vibration comfort/discomfort rating rig - shake table tests
4. Ride simulator tests
5. Ride comfort/discomfort measurement in vehicles

The characteristic of vibration excitation is an important aspect influencing human response; specifically frequency value, magnitude (level or amplitude) of vibration, and duration are important [2, 14]. All these factors are stated in International Standard ISO 2631-1 [7] or British Standard BS-6841 [15]. The road surface/roughness and road irregularities are the primary sources of vibration that affect the vehicle dynamics and ride comfort [12, 16]. The variability in road conditions in which the vehicles are expected to operate is huge. In the aim to improve design and experimental methods there has been a significant effort in compiling the statistical nature of the road input. The road roughness measurement systems consist of an instrumented vehicle with a road meter, driven or towed along a road [12].

Road testing is often used to assess ride comfort/discomfort; the tests involve rating of influence of vibration by subjective assessment on different types of road surfaces [2, 13]. Using this method, the researchers determine the ride comfort/discomfort by collated perception of drivers. For example, the participants drove a car for up to 15 minutes in a study [9] conducted to define comfort/discomfort ratings for car seats. In this approach, however, the difference between the ride discomfort levels for different road surfaces may not be quantitatively assessed. The method is also expensive. Further, the subjective rating tests on a vehicle, however, may have significant uncertainties, as: a) the inputs may not be repeatable and statistics not consistent, and b) the uncertainties in human perception may be difficult to quantify.

Alternatively, laboratory tests are used to quantify subjective ratings; the rig used is commonly known as the 'Human Vibration Comfort (HVC) Rig'. Most of the rigs used differ slightly in detail but the concept is similar [2, 17, 18, 19]. The HVC rig consists mainly of a shaker apparatus (i.e. shaker table). The main aims of these shaker table based studies are to assess the subjective human response to vibration in terms of 'feeling', quantify the human response to vibration and determine the human discomfort/comfort levels to vibration in a specific frequency range [13, 17].

Ride simulator is a powerful setup tool that simulates the different road conditions or surfaces on tyres of a road vehicle to repeat/reproduce the vehicle vibration while travelling [13]. On some of the ride simulators, the actual vehicle body is mounted on the hydraulic actuators to replicate the vehicle motion in pitch, roll and bounce (heave) modes. The simulators (typically four-post rigs [20]) have been used to characterize vehicles to improve their handling performance and general dynamic behaviour.

In the next few sections further details of the Human Vibration Comfort Rig simulator (shaker table), a Four-Post Rig Road simulator and the evaluation methods of the measuring human response to vibration are described briefly. Furthermore, various forms of representing input and output are discussed in terms of time histories, response spectrum and power spectral density (PSD).

2.3.1 Human Vibration Comfort Rig – Shaker Table

The HVC rig based methods used to identify the comfort/discomfort zones and predict the vibration levels in the presence of vibration are varied. The methods, however, invariably use some form of shaker table. These shaker table rigs are often known as motion simulators; which consist of a motion platform and a multi-axis shaker table with a seat combination [13, 17, 19]. This set-up is a mechanism to generate vibration and produce the effect on the seated human subjects in a moving vehicle in terms of feeling. There are many published studies on measurement of comfort/discomfort by making use of the shaker table tests.

An electro-hydraulic motion simulator was used by many researchers as listed below:

- 18 male participants [19] to quantify comfort;
- A group of 60 subjects participated in the test using a hydraulic vibrator platform [21];
- 30 men and 30 women participants were exposed to 8 second vibratory input in an experimental study with unrestrained sitting position on the vibrator plate [22];
- 16 subjects and 6 different automotive seat combinations were attached to a shaker to conduct experiments to express the comfort label of seat as good, bad or worst [23].

Although this area of research has been explored extensively, the test setups may not capture the complexity of vibration input required and, furthermore, they do not include the effects of real road/surroundings seen in a vehicle. And also, these types of motion simulator systems with combined seat may not represent the real dynamic behaviour of the vehicle body in vertical and rotational motions.

2.3.2 A Four-Post Rig Road Simulator

The four-post rig is a dynamic test setup simulating the effect of the road surfaces on vehicles used primarily to test suspension systems and the handling of vehicles [20, 24]. Four-post rigs comprise four road input electro-hydraulic actuators, one supporting each wheel. It is fully computer controlled and the actuators can be independently moved allowing varied motions to be generated. The wheels are placed on the pads, which are adjustable [20]. The position of each actuator can be controlled independently. Four-post rigs are a common feature in the industry to characterize and optimize vehicle dynamic performance.

One can use four-post rigs to perform detailed human response studies. A vital contribution from the use of the four-post rig would be to provide the same vibration environment for seated people like driving on the road. Namely, the system allows judgement of the driver's feeling to vibration when the vehicle travels in a straight line, takes a turn and changes lane, i.e. predictable inputs can be used.

2.3.3 Standards for Whole-Body Vibration Measurement

Standards define measurement methods of vibration and guidelines for the evaluation of whole-body vibration (WBV) in terms of human well-being. ISO 2631-1 [7] or BS 6841 [15] are the standards used for measurement and evaluation of human exposure to WBV. In this study a few details of ISO 2631-1 are discussed. One more standard, ISO 5982 [25] defines the vibration effects on seated human body subjects.

- **ISO 2631: Mechanical Vibration and Shock-Evaluation of Human Exposure to Whole-body Vibration-Part I: General Requirements**

In ISO 2631-1 [7], the methods for quantifying whole-body vibration are defined in connection with

- Human health and comfort;
- The probability of vibration perception;
- The incidence of motion sickness.

ISO 2631-1 defines the important frequency ranges of 0.5 Hz to 80 Hz for health, comfort and perception; and 0.1 Hz to 0.5 Hz for motion sickness. The location, direction and duration of vibration measurement are stated for the sitting position of a human body in the coordinate system, as shown in Figure 2.3. The human vibration exposures are measured at the contact interfaces between a seated human body and vibrating surface based on the occurred vibration levels [2]. Vibration can be analyzed in terms of displacement, velocity or acceleration parameters; acceleration is the most common response variable used to characterize the vibration. ISO 2631-1 provides guidelines for locations of transducers to measure the vibration of seat surface, seat back, and feet which are in contact with the floor.

Frequency weightings of measured acceleration are determined by ISO 2631-1 based on the human health, comfort and perception for the different axes of vibration. Two principal frequency weightings for whole-body vibration are W_k for the z direction, and W_d for the x and y directions. Also, one principal frequency weighting, W_f , is given for motion sickness. Furthermore, additional frequency weightings are given in ISO 2631-1 for the special cases of

- seat-back measurements (W_c)
- measurement of rotational vibration (W_e)
- measurement of vibration under the head of a recumbent person (W_j)

ISO 2631-1 provides a guide for the effects of vibration on human health. In this guide, vibration assessment is explained based on ‘Health guidance caution zones’ (Fig. 2.4) which represents the duration of exposure and weighted RMS acceleration. Figure 2.4 provides the threshold limits for human feeling to vibration.



Figure 2.4: ISO 2631-1 Health Guidance Caution Zones. _ _ _ _ _ represents the upper threshold limit for feeling, represents the lower threshold limit for feeling [7]. Figure 2.4 shows a health guidance caution zone by dashed lines. The standard (ISO 2631-1) [7] states that: “*For exposures below the zone, health effects have not been clearly documented and/or objectively observed; in the zone, caution with respect to potential health risks is indicated and above the zone health risks are likely*”. The lines represent two different daily exposures based on the human response which is related to energy. Equation 2.1 and 2.2 represent B1 and B2 respectively in Fig. 2.4.

$$a_{w1} \cdot T_1^{1/2} = a_{w2} \cdot T_2^{1/2} \quad (2.1)$$

$$a_{w1} \cdot T_1^{1/4} = a_{w2} \cdot T_2^{1/4} \quad (2.2)$$

Where a_{w1} and a_{w2} are the weighted RMS acceleration values for the first and second exposures, respectively; T_1 and T_2 are the corresponding durations for the first and second exposures.

In the health and caution zone (Fig. 2.4), health effects are not explained clearly below the lower boundary zone. Above the boundary zone health risks are indicated. Between the upper and lower boundary zones, a concern for health risk problems is raised [26]. This recommendation is underlined for exposures in the range of 4 h and 8 h by the shading in Fig. 2.4.

- **ISO 5982 Mechanical Vibration and Shock - Range of Idealized Values to Characterize Seated-Body Biodynamic Response under Vibration**

In ISO 5982 [25] alternative approaches to quantify measures that affect seated subjects' comfort/discomfort are given; the guidelines for measurement of driving-point impedance, apparent mass and seat-to-head transmissibility are provided. It also states the effect of the back support, posture, and feet while measuring biodynamic response. The standard values are given only for seated individuals, exposed to sinusoidal or broad-band random vertical vibration with unweighted RMS (root-mean-square) acceleration, between 1 m/s^2 and 5 m/s^2 , on the vibrating platform for 49 kg and 93 kg body masses. The seat-to-head transmissibility is defined as a ratio between the acceleration transmitted to the head and the acceleration measured at the buttocks in the frequency range of 0.5 Hz to 20 Hz while seated on a rigid surface with the back being unsupported.

2.3.4 Vibration Analysis for Ride Comfort Evaluation

The measurement of vibration is a complex and difficult study; simple methods and measures are required in order to control vibration limit on the human body [3]. Root-mean-square (RMS) method, vibration dose value (VDV) method, and power spectral density method, etc. are defined in WBV standards as some measures. They are used to calculate the statistical measure for analyzing vibration and assessing human health, comfort and safety. Additionally, these methods are also used to assess the acceleration and transmissibility of vibration transferred to the seat and the human body.

a) Spectral Analysis Techniques

The human body is a complex dynamic mechanism; the dynamics can be assessed as a function of frequency to account for the sensitivity to the low frequency vibration [26]. Vibrations can be analyzed in both the time and frequency domain. The signals in the time domain can be converted to the frequency domain. For random inputs power spectral density is used. The power spectral density (PSD) (also called spectral density or power spectrum) is the distribution of the mean square value of a time history over frequency [2, 26, 27] and the units are $(\text{m/s}^2)^2/\text{Hz}$ for acceleration measurement.

WBV standards define the specific metrics [26] for evaluating the human exposure in relation to health, safety and comfort. The most common metric used is the frequency-weighted RMS acceleration, and it is defined by ISO 2631-1 [6] as;

$$a_{wr.m.s.} = \sqrt{\frac{1}{T} \int_0^T a_w^2(t) dt} \quad (2.3)$$

Where a_{wrms} is the frequency-weighted RMS acceleration, T is the measurement duration, and $a_w(t)$ is the frequency-weighted acceleration at time t . It is defined based on the peak or peak-to-peak value. The units used are (m/s^2) for

translational vibration and (rad/s²) for rotational vibration. If the acceleration is not unidirectional, the following formula is used.

$$a_v = (k_x^2 a_{wx}^2 + k_y^2 a_{wy}^2 + k_z^2 a_{wz}^2)^{\frac{1}{2}} \quad (2.4)$$

Where a_{wx} , a_{wy} and a_{wz} are the weighted RMS accelerations with respect to the orthogonal axes x , y , z ; k_x , k_y and k_z are multiplying factors respectively. The exact value of the multiplying factors depends on the selected frequency weighting. The frequency weighting and multiplying factors for a seated human are specified in ISO 2631-1 [7].

b) Frequency Weighting

The human body is more sensitive to low frequency vibration; the level of sensitivity may vary with frequency and may also depend on the seated subject. The frequency dependence is analyzed and modelled using frequency weightings [2]. The human body is expected to have a resonance frequency of between 4 Hz to 6 Hz at the low level of vibration [2, 3, 22]; sensitivity increases around these frequencies. The measured acceleration can be weighted in the time or frequency domain [26]. The weighted acceleration used in earlier Equation 2.3 can be calculated by the expression as given below.

$$a_w = \left[\sum_i (W_i a_i)^2 \right]^{\frac{1}{2}} \quad (2.5)$$

Where W_i is the frequency weightings, a_i is the acceleration.

c) Transfer Functions

The transfer function characterizes the vibration transmission between the vibration source and the excitation system. It is defined as the ratio between the cross spectral density of the output and input and the auto spectral density of the input. For analyzing the transmission characteristics and human body resonance, two transfer functions are used. These are the driving-point mechanical impedance and transmissibility. Driving-point mechanical impedance (DPMI) is the ratio between the measured transmitted force and the input velocity of a vibrating system occurring in the same direction and at the same location.

The apparent mass, which is a transfer function, is used to describe biodynamic characteristics by many researchers [2, 3, 28]. It is the ratio between the transmitted force and the input acceleration [26]. Apparent mass is affected by the isolation properties. Transmissibility is the ratio between input and output measurements according to the vibration surface and at the locations where the vibration enters the body such as seat surface, human body parts and floor [3, 26, 27, 29].

d) The running RMS method

Another vibration evaluation method given by ISO 2631-1 [7] is called the running RMS evaluation; it takes into account occasional shocks and transient vibration by using running RMS with a short integration time constant. This method is used to characterize the vibration. The vibration magnitude is defined as a maximum transient vibration value (MTVV), i.e. the maximum of $a_w(t_0)$, which in turn is given by:

$$a_w(t_0) = \left\{ \frac{1}{\tau} \int_{t_0-\tau}^{t_0} [a_w(t)]^2 dt \right\}^{\frac{1}{2}} \quad (2.6)$$

where,

$a_w(t)$ is the instantaneous frequency-weighted acceleration;

τ is the integration time for running averaging;

t is the time;

t_0 is the time of observation.

Therefore, the maximum transient vibration value is given by:

$$\text{MTVV} = \max[a_w(t_0)] \quad (2.7)$$

e) The fourth power vibration dose method

The vibration dose value (VDV) defined in ISO 2631-1 [7] is more sensitive to peaks (large amplitudes) and represents exposure. It is a good measure where the vibration amplitude varies significantly. The vibration dose value (VDV) is measured in metres per second to the power 1.75 ($\text{m/s}^{1.75}$), or in radians per second to the power 1.75 ($\text{rad/s}^{1.75}$). VDV is defined as:

$$\text{VDV} = \left\{ \int_0^T [a_w(t)]^4 dt \right\}^{\frac{1}{2}} \quad (2.8)$$

where,

$[a_w(t)]$ is the instantaneous frequency-weighted acceleration;

T is the duration of measurement.

2.3.5 Subjective Assessment of Vibration Effects

Many researchers have been investigating the human response to whole-body vibration. The human body [2] produces different responses under varying vibration conditions based on the sensitivity of the human body to the environment. The published studies show that the limits of human vibration perception cannot be evaluated using an absolute standard defined by measurable parameters such as displacement amplitude or acceleration at a given frequency.

Alternatively, a subjective judgement method (assessment) can be incorporated into an objective measurement to determine a criterion of comfort/discomfort for drivers/passengers. The measured numerical data is assessed by perception ranges (i.e. painful, perceptible, and annoyance, etc.) which is given by the seated test subjects. In the field of subjective assessment experimental studies are carried out to predict the vibration effects on the human body in terms of the vibration stimuli, and the relation between the stimuli and comfort/discomfort is sought. Sinusoidal vibration exposures have been used to assess the subjective response in terms of comfort/discomfort. Most studies [2, 22, 30, 31] have aimed to produce curves describing ‘Comfort Level, Equal Comfort Contours and Threshold Limit Values’ in order to evaluate the sensitivity level to vibration input in multi-directional axes for a seated human.

a) Assessing Comfort Level:

A large number of expressions (i.e., comfort, discomfort, intensity, unpleasantness, annoyance, disturbance, intolerable, perceptible, etc.) are used in describing the comfort/discomfort based on the human response to vibration for varying frequencies [2, 22, 30]. To assess the vibration perceptions, investigative questionnaire methods (laboratory based studies) have been developed [2, 30]. The branch of study that deals with these aspects is psychophysics. Three methods are commonly used in psychophysical rating experiments.

- **Method of Ascending Limits:** There are different stimuli of different frequency and intensity. After each increasing amplitude stimulus, a seated subject is expected to give a number which is specified in the comfort labels (e.g. pleasing, comfortable) [30]. The experiments based on this method are very easy to perform and commonly used. There may, however, be some bias in the perception in a few cases.
- **Method of Constant Stimuli:** The stimuli of varying frequency and intensity occur randomly and the perception rating is sought from the participants after each stimulus. This method is time intensive.

- **Method of Adjustment:** In the experiments based on this method [2, 22, 30, 32], at the beginning the subjects are applied/introduced to a ‘reference’ motion. This motion is a constant quality and quantify stimulus from fixed frequency and magnitude. And then the subjects are exposed to ‘test’ stimuli. The participants are asked to adjust the intensity until ‘reference’ sensation is reached. In this method, the adjustment level is dependent on the human response limit and duration.

In this study for the reason of simplicity and shorter period time requirements, the first method, where increasing intensity stimulus occurs, is used.

The perception description can be a difficult matter to make precise. Based on the data available, the overall RMS value of the frequency-weighted acceleration can be compared with the following guidance:

- Less than 0.315 m/s^2 not uncomfortable
- 0.315 to 0.63 m/s^2 a little uncomfortable
- 0.5 to 1 m/s^2 fairly uncomfortable
- 0.8 to 1.6 m/s^2 uncomfortable
- 1.25 to 2.5 m/s^2 very uncomfortable
- Greater than 2 m/s^2 extremely uncomfortable

Depending on their particular interest, many researchers have focused their study on different frequency ranges to assess comfort level, for example: vertical and rotational vibration under random signal in the frequency range 1-50 Hz [33]; sinusoidal and random excitations in the vertical direction at frequencies up to 20 Hz [34]; under vertical vibration at 4.2 Hz and 7.7 Hz [28]; 0.5-50.5 Hz analysed based on 15s exposure [14]; during the exposure time of 60 s in the frequency range between 0.25 to 30 Hz [35].

b) Equal Sensation Contour/ Equivalent Comfort Contour:

Equivalent comfort/equal sensation contours demonstrate how the vibration magnitude produces similar comfort or discomfort levels at the different frequency, axis and input position. It indicates the equivalence in sensation between two stimuli. Comfort label studies (absolute and relative method) are used to determine equivalent comfort contours [2, 22, 30] to understand the relation between subjective judgement and objective intensity measurement at different frequency levels. The expression of 'equal sensation contour' signifies that for instance, 'a' m/s^2 at 5 Hz is equal in sensation to 'b' m/s^2 at 7 Hz which is equivalent to 'k' m/s^2 at 8 Hz etc. [32]. The main aim of the equal sensation contours is to evaluate the differences between the comfort labels (scaling levels) of vibration, such as 'comfortable level' and 'uncomfortable level'.

c) Duration of exposure:

Human sensitivity to vibration and human perception of vibration have been studied by many researchers [2, 3, 36] to determine vibration threshold levels for human body and perceived degree of comfort. The exposure duration is a critical parameter which may affect the well-being of people. The European Union directive (2002/44/EC) has stated an absolute maximum exposure limit of 1.15 m/s^2 or a vibration dose value of $21 \text{ m/s}^{1.75}$ during an eight-hour drive [37] for the whole-body vibration. The International Standards Organization [7] has proposed duration limits for vibration levels to reduce the discomfort level. Threshold limit values for daily limits of exposure to acceleration are given in Figure 2.4 which is specified by ISO 2631-1 [7].

2.3.6 Discussion

People are exposed to vibration because of the dynamic interaction between the vehicle and the road. This interaction may result in different levels of vibration which influence the human body in a variety of ways; the human perception may vary in terms of the sensitivity and tolerance eventually affecting the human comfort/discomfort. In order to understand the human response to vibration and qualify the human sensitivity limits in terms of comfort/discomfort, different measurement methods have been applied by many researchers.

2.4 VEHICLE RIDE COMFORT MODELS

The dynamics of the body of a vehicle is the primary factor influencing the ride comfort; the vibration transmitted is dependent on a variety of factors, including surface irregularities, road profile, and tyre behaviour, etc. [16, 38, 39]. It is essential to understand characteristics of the road surface, vibration and vehicle dynamic modelling in order to minimize the effects of vibration on the driver/passenger [16, 39].

Various vehicle ride comfort mathematical models of increasing degree of complexity have been developed and formed [16]. These models provide guiding principles for understanding vehicle behaviour. The mathematical models can be classified into two categories as distributed models (i.e., governed by partial differential equations) and lumped parameter models (i.e., governed by ordinary differential equations). Lumped parameter models are used for vehicle dynamic analysis (ride and handling) and control studies.

A vehicle can be represented as a sprung mass (the vehicle body) and unsprung masses (wheels, axles, and linkages) which are connected with suspensions components and tyres that are in interaction with the road surface. The motion of a vehicle [16] has six degrees of freedom classified as follows:

- longitudinal translation (forward and backward motion)
- lateral translation (side slip)
- vertical translation (bounce or heave)
- rotation around the longitudinal axis (roll)
- rotation around the transverse axis (pitch)
- rotation around the vertical axis (yaw)

In general, vehicle ride comfort models are restricted to modelling bounce (heave), pitch and roll motions. The main purpose of the modelling is to understand and characterize the vehicle performance for assessing the ride comfort. In this section, the vehicle mathematical models of varying degree of complexity are reviewed; in particular, the quarter vehicle model, 4-DOF vehicle model and full vehicle model are discussed.

2.4.1 Quarter Vehicle Model

The simplest representation of a vehicle suspension has one degree-of-freedom (1-DOF). This simple model (Fig. 2.5a) represents the chassis (body) by a mass (m_1) and the suspension unit by a spring (k_s) and a damper (c_s). Tyre mass and stiffness are neglected. The road input is x_0 , and the vehicle body displacement is x_1 . By incorporating a wheel into the model (1-DOF), a more accurate representation having 2-DOF (called a quarter car model) can be developed (Fig. 2.5b). The model then consists of the sprung mass m_1 and the unsprung mass m_2 . The tyre is modelled as a linear spring with stiffness k_t .

The 1-DOF model and 2-DOF quarter vehicle model are still popular models in automotive engineering suspension research because of their simplicity and effectiveness. A quarter vehicle (2-DOF) model can be used to find suspension characteristics based on different road/speed/handling conditions, tyre dynamic, the ground roughness, and the tyre-road interface [16, 40]. Using this model a great deal of progress has been made by many researchers in understanding the tyre, a good suspension design to improve the ride control of road vehicles [41], and passenger comfort [40, 42].

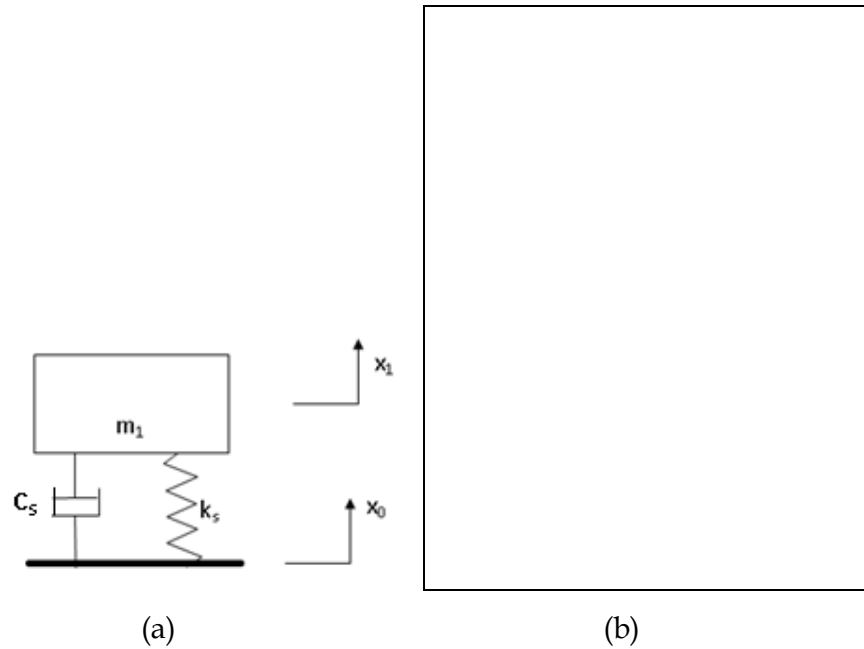


Figure 2.5: a) One degree of freedom model (1-DOF) and b) Quarter vehicle model (2-DOF) [16, 40].

2.4.2 Four Degree-of-Freedom Vehicle Model

A four degree-of-freedom (4-DOF) model is an extension of the 2-DOF model and it has a translational degrees-of-freedom and a rotational degree of freedom to describe, respectively, bounce (the vertical movement of the body centre of gravity and wheels) and pitch motions or, bounce and roll motions [16, 43]. Figure 2.6 shows a four degree-of-freedom vehicle suspension system model which includes the effect of tyre-hub masses and elasticity. The parameters of the model are: $m_{vehicle}$ is the sprung mass (vehicle body), m_f and m_r the front and rear unsprung masses (wheels), I_{zz} the pitch inertia, L_f and L_r the distances between the front and rear of the vehicle respectively from its centre of gravity. The 4-DOF model can also be used to analyse the roll motion by replacing the pitch motion parameters from that of roll motion.



Figure 2.6: A four degree-of-freedom vehicle suspension system model (4-DOF) in pitch mode [16, 43].

The 4-DOF vehicle model has been investigated by many researchers [43-45] in order to improve roll stiffness and the ride performance in heave and pitch modes. Lin and Huang (2004) [43] describe a linear four degree-of-freedom (4-DOF) vehicle suspension model for developing a nonlinear back stepping design to improve the inherent trade-off between the ride comfort of passenger and suspension travel utility. This model can be applied in the analysis of vehicle behaviour in the motion of either roll or pitch. Guglielmino [16] underlines the limitations of 4-DOF model; the model cannot take into account the cross-couplings between the front and rear/the right- and left-hand side of the car. These interactions can be taken into account only by using a full 7-DOF vehicle model.

2.4.3 Full Vehicle Model

A quarter vehicle model or a 4-DOF vehicle model is not enough in practical applications as explained previously. Because of the reduced number of degrees-of-freedom certain information is unobtainable from these models. In the case of the 4-DOF vehicle model, both roll and pitch information cannot be included. The full vehicle (7-DOF) model [46, 47] uses: 3-DOFs to represent the motion of the

vehicle body (bounce, roll and pitch), 4-DOFs to represent wheel motion (1-DOF for each tyre-hub combination), as shown in Figure 2.7. More complex full vehicle models have been also used by many researchers [46, 48, 49] to analyse the behaviour of the vehicle and suspension in heave, pitch and roll motions (see Appendix A, Figure A.1 and A.2).

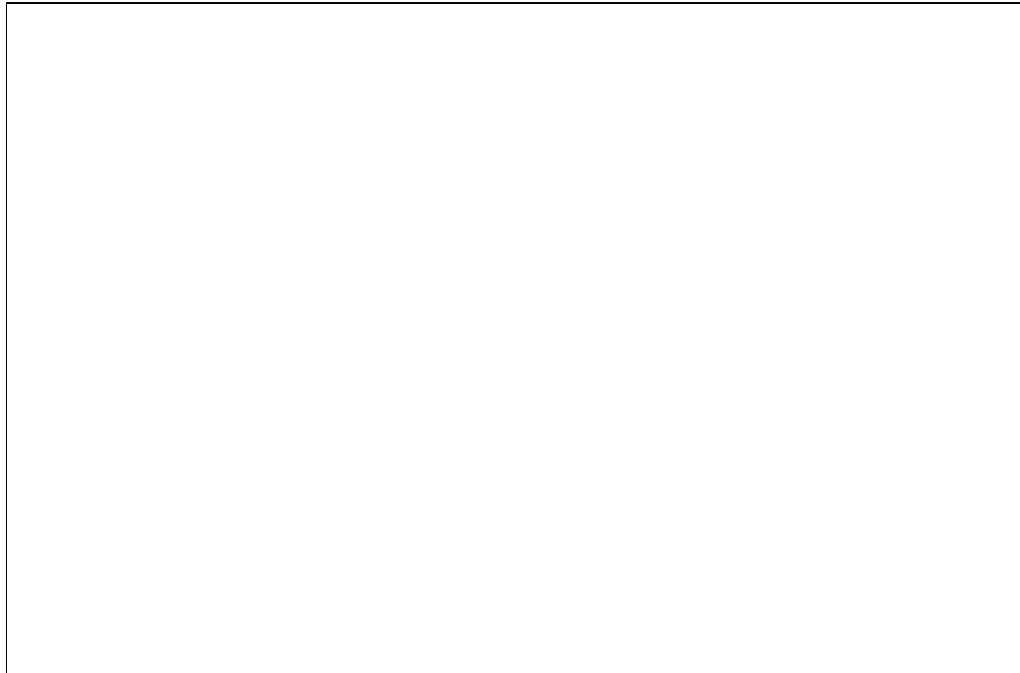


Figure 2.7: Full vehicle model by Imine [49].

Bouazara (2006) [48] analysed the effects of vibration and seat positions on comfort and road holding capabilities (See Appendix A, Fig. A.2); the parametric studies on suspension coefficients, road disturbances and the seat position are also reported. Imine (2006) [49] proposed a new method to estimate the effect of road profile input variability on vertical acceleration displacement of the wheels and vertical and rotational movement of the vehicle body by using a full vehicle simulation model (see Appendix A, Fig. A.1).

The 4-DOF and full vehicle models can be made more complex by ‘adding in the’ driver seat and driver/passenger, which can describe the effect of a seat and passenger. Addition of a 1-DOF seat model to the full vehicle (7-DOF) model results in an integrated 8-DOF model. The purpose of 8-DOF models (Fig. 2.8) is

to analyse the vehicle and seat response to vibration in the lateral and rotational motion [50, 51] (see Appendix A, Fig. A.3 and Fig. A.4).

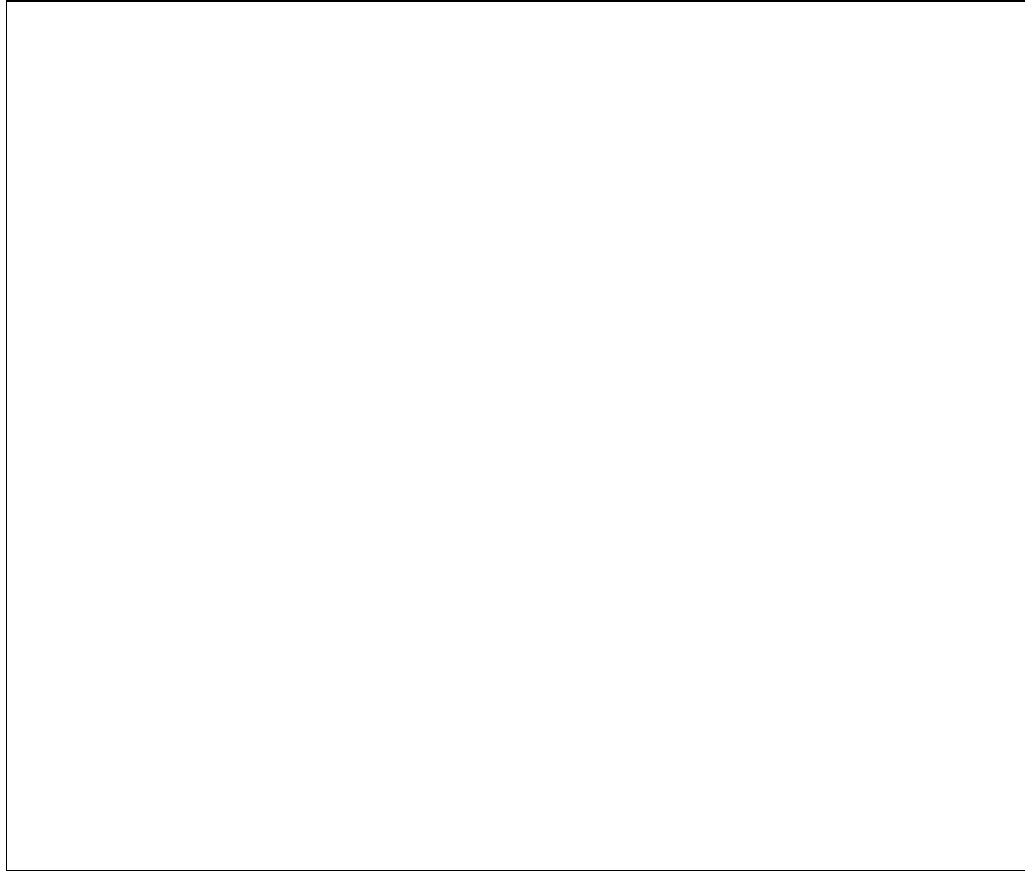


Figure 2.8: Integrated seat-full vehicle model (8-DOF) by Bouazara [50].

2.4.4 Discussion

Various complex vehicle ride mathematical models have been developed for ride comfort/discomfort assessment and the analysis of vehicle performance. For simulation or modelling of test subjects and vehicle behaviour/performance, lumped parameter models are used. The given models in this section are classical ride models. Higher DOF ride models can be developed including further degrees of freedom, such as seat and driver, when there is a need to accurately investigate the interaction between road-vehicle-seat-driver/occupants.

2.5 MODELLING OF THE HUMAN BODY

Human vibratory response to a given input is generally obtained experimentally. Ideally, industries would like to have mathematical models to analyse the dynamic response so that the designs can be refined to provide good ride results. There has been significant development in this area. Biodynamical/mechanical models have been developed and designed [2, 28, 52, 53] to quantify and understand the characteristics of the biodynamic response to a given input.

Various biomechanical models analyse the seated human response in vertical vibration because the vertical motions are found to be a dominant source of discomfort. The vibration behaviour has been studied in the horizontal direction as well [2]. In most linear biomechanical modelling the effects of legs are neglected as the influence of the legs is irrelevant when the overall whole-body is exposed to vibrations through the seat and the backrest. In experimental work, in most case, the hand is positioned on the steering wheel; Rakheja [54] showed that the hand has a significant effect on the whole-body response. In general, however, the legs and the hands are usually omitted in the linear biomechanical modelling.

The human body can be modelled as a vibrating system exposed to the vibrations from contact points. The human body parts are modelled as equivalent lumped parameters to represent distributed properties of mass, elasticity and damping [2, 28, 52, 53]. Several biomechanical models have been studied to characterize the behaviour of the human body parts or structures starting with a simple single degree-of-freedom (SDOF) system to complex multi degree-of-freedom (MDOF) systems under various stimulus conditions [2, 3, 28, 52, 55].

Based on the Coermann's (1962) [56] approach, "the human body is considered as very complicated system of masses, elasticities, and viscous dampers, each connected to the other". The biomechanical models can be lumped-parameter models or multi-body models or finite element models [28]. In general lumped-parameter models are used. These models reproduce the human body in a sitting posture using a mechanical system composed of several rigid body masses and

linear translational/rotational springs and dampers to describe the response of the person [2, 3, 28]. The biodynamic response characteristic of a seated human body subject to vibration can be described in terms of driving-point mechanical impedance, apparent mass and seat-to-head transmissibility.

A single-degree-of-freedom system is the simplest form of lumped-parameter model which was first used by Coermann [56]. Later, several biomechanical models higher degrees-of-freedom (DOFs) have been used in order to obtain driving point impedance, apparent mass, body movements in multi-axis vibrations; transmissibility and human behaviour in vertical and horizontal vibrations [28]. Multi-body models define the human body with body segments and joint parts of the body such as upper body, lower body, feet etc by using computer simulation programs [57].

The parameters of the biomechanical models have been mainly obtained through the driving-point mechanical impedance, transmissibility (seat-to-head) data of specific body segments reported, or a combination of these methods [28]. Driving-point mechanical impedance (DPMI), the apparent mass (APMS) and transmissibility (TR) have been calculated based on the measured acceleration on the seat-human interface. In this research, lumped-parameter models are reviewed.

2.5.1 Single Degree-of-Freedom Model

The single degree-of-freedom (SDOF) model is the most simple and convenient lumped-parameter model [2]. The SDOF model is easy to analyse and validate. However, it generally implies, as such, that there is only one important resonance frequency on the body and is limited to one-directional analysis, such as vertical direction. This model was firstly studied by Coermann [56] in order to define the physical and physiological effects of vibrations, to obtain the parameters of the mechanical body system, to define mechanical impedance measurements in sitting and standing position at low frequencies and to calculate the dynamic mechanical response to different types of force application. Later it was adopted

by Wei & Griffin [58] and Cho & Yoon [28] to study comfort/discomfort. The details of the model are shown in Table 2.1.

For a seated human body there is a connection between buttock & legs and seat cushion so there are two segments [55, 58], i.e. body and buttock & legs are interconnected with a spring and a damper in the human-seat system. The SDOF model is used to calculate the transmissibility between the seat and the human body in the vertical direction. Cho and Yoon's model [28] includes the seat spring and damper which are connected to the human hip spring and damper (see Table 2.1). The seat mass is neglected for both models in Table 2.1.

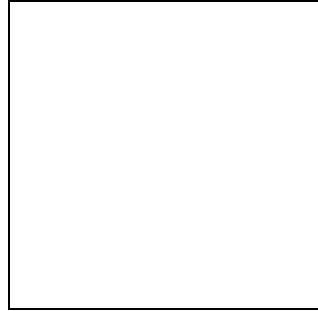
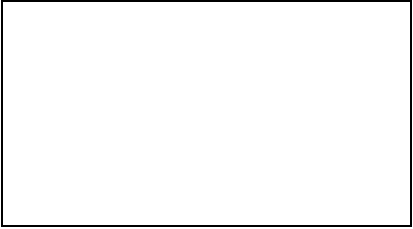
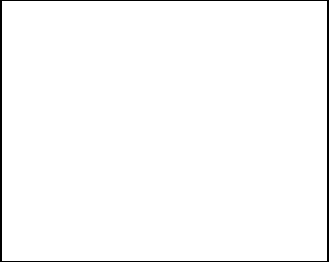
| Authors & Remarks | Biodynamic parameters | | | Schematic of Model |
|--|--|--|---|--|
| | Mass (kg) | Damping (Ns/m) | Stiffness (N/m) | |
| Coermann's simplest linear 1-DOF model of the human body is a one-mass-spring system with damping in the vertical direction [55, 56]. | $m = 56.8 \pm 9.4$ Mtotal: 56.8 | $c = 3840.0 \pm 1007.0$ | $k = 75500.0 \pm 28300.00$ |  |
| Wei and Griffin's linear 1-DOF model in the vertical direction. Buttocks & legs connected with seat surface [55, 58]. | $m_1 = 43.4$ $m_0 = 7.8$ Mtotal: 51.2 | $c_1 = 1485.0$ | $k_1 = 44130.0$ |  |
| Cho and Yoon's linear 1-DOF model in the vertical direction. The seat spring and damper serially connected to the hip spring and damper [28]. | $m_1 = 56.8 \pm 9.4$ Mtotal: 56.8 | $c_{sv1} = 3840 \pm 1007$ $c_{sv1} = 357$ | $k_{sv1} = 75500 \pm 28.3$ $k_{sv1} = 72300$ |  |

Table 2.1: One degree-of-freedom (1-DOF) lumped parameter models of a seated human.

2.5.2 Multi Degree-of-Freedom Lumped-Parameter and Other Complex Models

A moving vehicle is exposed to vibration in multi-directions based on the road conditions. This shows that the vibrations may be applied at one or more locations of the seated human body and in one or more directions [4]. Therefore, the SDOF model is not sufficient to predict the behaviour and response of the segments of a seated human body in a moving vehicle to vibration in multi-directional movement, such as pitch and roll mode. In order to define ride comfort/discomfort in translational and rotational motion, the human body segments are required to be represented (i.e. head, upper torso, and lower torso, etc.) in the biodynamic modelling studies. The development in robotic technology has indicated the requirement of increased DOFs for human models to understand the nature of body movements [2]. In the literature various lumped-parameter models have been developed to increase the number of moving masses to predict the movement adequately.

The apparent mass and mechanical impedance can be calculated using lumped-parameter models incorporating experimental data [33, 58]. The lumped parameter values used in biodynamic modelling are difficult to estimate [3]. Some published studies used a prototype anthropodynamic dummy in order to measure mechanical impedance and correlate the modelling with experimental studies. However, the dummy used cannot give the same response as much as a seated human body gives, and also a human stomach is an important segment influencing comfort/discomfort.

The aim of the increased degree of freedom models is to find the characteristics of the human body. However, many models have been proposed with complexity without clearly indicating the behaviour of the body [2]. For instance, it is neither useful nor adequate to predict seat-to-head (STH) transmissibility without identifying that the head will move in pitch and it will have large influence on variations in body posture. The torso (the body except head) does not move as much as the head moves, therefore the movement of the head is,

generally, analyzed separately in the multi degree-of-freedom models. Recently many published studies have achieved a degree of sophistication in modelling STH transmissibility using multi-degree-of-freedom model. Some of these models are reviewed below.

a) Two Degree-of-Freedom (2-DOF) Model

The two degree of freedom (2-DOF) model incorporates additional information compared with the SDOF model [28]. These types of models, shown in Table 2.2, assume the human body is composed of two rigid bodies, which are the head and the torso (legs, lower torso, upper torso & arms). Coermann [56] concluded that a two degree of freedom system was required to approximate the dynamic response of the human body at low frequencies [59]. The development of this model was based on correlating the model parameters to the results of experimental investigations of the mechanical impedance of the human body.

Suggs [59] developed a seated human model (Table 2.2), which consists of two uncoupled masses (lower and upper body), to understand dynamic characteristics of a seated human body. This model represents two independent SDOF systems rather than a 2-DOF system. There is no connection between the two masses, so it suggests that the vibration of the human head and the upper torso is independent of the vibration of the rest of the body. So the uncoupled masses may not give accurate results for interaction between the body segments with respect to transmitted/entered vibration from floor and seat surface.

A clearer model was proposed by Cho and Yoon [28] in order to evaluate the seat-to-head transmissibility in the vertical direction with seat backrest and without seat backrest. The analysis of the 2-DOF model gives an opportunity to evaluate the seat-to-head transmissibility. However, when considering human response to vibration, this model has limited practical value because the model does not include multi-directional movement. It allows only one-directional analysis such as vertical direction.

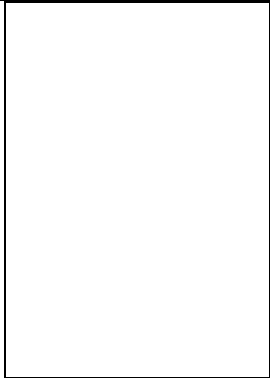
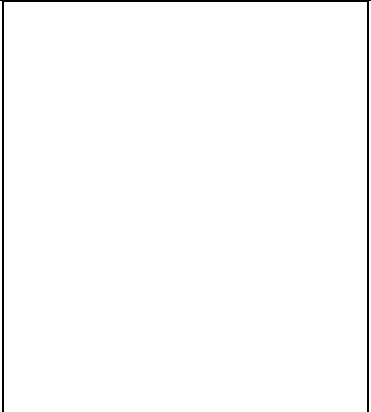
| Authors & Remarks | Biodynamic parameters | | | Schematic of Model |
|--|--|---|---|--|
| | Mass (kg) | Damping (Ns/m) | Stiffness (N/m) | |
| Sugg's linear 2-DOF model in the vertical direction consists of two uncoupled masses [59]. | $m_1=36.29$ $m_2= 18.60$ Mtotal: 54.89 | $c_1: 484.515$ $c_2: 882.926$ | $k_1: 25904.05$ $k_2: 441446.48$ |  |
| Cho and Yoon's linear 2-DOF model in the vertical direction. The seat spring and damper serially connected to the hip spring and damper [28]. | $m_1 =51.3 \pm 8.5$ $m_2 =5.5 \pm 0.9$ Mtotal: 56.8 | $c_{v1}=2807 \pm 98$ $c_2=318 \pm 161$ $c_{sv1}= 357$ | $k_{v1}= 74300 \pm 17.4$ $k_2= 41000 \pm 24.1$ $k_{sv1}= 72300$ |  |

Table 2.2: Two degree-of-freedom (2-DOF) lumped parameter models of a seated human.

b) Three and Four Degree-of-Freedom (3-DOF and 4-DOF) Models

The 3-DOF models are the most commonly used models in the literature for a human body in sitting position to obtain the seat-to-head and seat-to-upper body transmissibilities. The 3-DOF model consists of three body parts (i.e. lower body, upper body and head) for evaluating the vehicle ride comfort/discomfort. An anatomical description of a seated human body 3-DOF lumped-parameter model was proposed by Muksian and Nash [60, 61] in order to estimate the damping coefficient parameters of the human body connections (see Table 2.3). The coefficient parameters are determined using the head-to-seat or body-to-seat acceleration ratio.

Another 3-DOF seated human model was proposed by Cho and Yoon [28] by refining Suggs' [59] model with and without backrest for evaluating the vehicle ride comfort/discomfort (see Table 2.3). The biomechanical model parameters were measured for a human body and seat; however, there is no information on the calculation of the parameters. The seated human body has an interface with a seat surface/cushion, which is important for lower body transmissibility. Tewari and Prasad [62] developed an analytical model (see Table 2.4) of a tractor seat suspension system, which was investigated by using a computer simulation. The optimized suspension seats and cushion parameters were obtained from experimental results. It was found that the subject mass influences the ride comfort/discomfort.

Wan and Schimmels suggested a slightly complex 4-DOF model [63] (see Table 2.5) and parametric calculations were also performed. The 4-DOF models are a refinement of 3-DOF models with the addition of a seat suspension system. In Wan and Schimmles's model, the seated human body was constructed with four separate mass segments interconnected by five sets of springs and dampers. This model was compared with experimental data to analyse seat-to-head transmissibility and driving point impedance at higher frequencies in the vertical direction. The aim was to simplify the design of seat suspension.

Another frequently cited model (see Table 2.5) was proposed by Boileau and Rakheja [64] to understand the human body responses without backrest under vertical vibration. The parameter estimation was done based on the measured driving point impedance and seat-to-head transmissibility. This linear model was also selected by Srdjevic and Cveticanin [65] for describing response function in the frequency domain. As mentioned previously, the vibration may enter the human body in multi-directions. For horizontal direction, the human back and the head are the important segments of influence. The seated occupant with backrest model (see Table 2.6) was developed by Rakheja [54] for characterizing the apparent mass responses in the vertical and horizontal directions.

| Authors & Remarks | Biodynamic parameters | | | Schematic of Model |
|--|---|--|--|--------------------|
| | Mass (kg) | Damping (Ns/m) | Stiffness (N/m) | |
| Muksian and Nash's linear 3-DOF model in the vertical direction [61]. | $m_1 = 5.44$ $m_2 = 47.17$ $m_3 = 27.22 \text{ kg}$ Mtotal: 79.38 | $c_{p1} = 1780$ $c_{p2} = 686$ $c_{p3} = 467$ | $k_{p1} = 27158$ $k_{p2} = 0$ $k_{p3} = 63318$ | |
| Cho and Yoon's linear 3-DOF model in the vertical direction. The seat spring and damper are serially connected to the hip spring and damper [28]. | $m_1 = 15.25 \pm 2.5$ $m_2 = 36.0 \pm 6.0$ $m_3 = 5.5 \pm 0.9$ Mtotal: 56.8 | $c_{v1} = 2806 \pm 1000$ $c_2 = \infty$ $c_3 = 318 \pm 142$ $c_{sv1} = 357$ | $k_{v1} = 74300 \pm 17.4$ $k_2 = \infty$ $k_3 = 40900 \pm 22.7$ $k_{sv1} = 72300$ | |

Table 2.3: Three degree-of-freedom (3-DOF) lumped parameter models of a seated human.

| Authors & Remarks | Biodynamic parameters | | | Schematic of Model |
|--|--|--|---|--------------------|
| | Mass (kg) | Damping (Ns/m) | Stiffness (N/m) | |
| Tewari and Prasad's 3-DOF tractor seat suspension model in the vertical direction [62]. | 45.4 <math>m</math> <math>< 80</math> m is the total subject mass | $c_3=500$ $c_2=750$ $c_1=1000$ Seat damping is between 0.665 and 1.099 kNs/m | $k_3=15000$ $k_2=20000$ $k_1=25000$ Seat spring is between 10.726 and 18.957 kN/m | |
| ISO 5982 [25]. | $m_0=2$ $m_1=6$ $m_2=2$ $m_3=45$ Mtotal: 75 | $c_1=387$ $c_2=234$ $c_3=1.39 \times 10^3$ | $k_1=9.99 \times 10^3$ $k_2=3.44 \times 10^4$ $k_3=3.62 \times 10^4$ | |

Table 2.4: Three degree-of-freedom (3-DOF) lumped parameter models of a seated human.

| Authors & Remarks | Biodynamic parameters | | | Schematic of Model |
|---|---|--|--|--------------------|
| | Mass (kg) | Damping (Ns/m) | Stiffness (N/m) | |
| Wan and Schimmles's 4-DOF linear model in the vertical direction [63]. | $m_1=36$ $m_2=5.5$ $m_3=15$ $m_4=4.17$ Mtotal: 60.67 | $c_1=2475$ $c_2=330$ $c_3=200$ $c_4=250$ $c'_2=909.09$ | $k_1=49341.6$ $k_2=20000$ $k_3=10000$ $k_4=134400$ $k'_2=192000$ | |
| Boileau and Rakheja's 4-DOF linear model in the vertical direction [64]. | $m_1=5.31$ $m_2=28.49$ $m_3=8.62$ $m_4=12.78$ Mtotal: 55.2 | $c_1=400$ $c_2=4750$ $c_3=4585$ $c_4=2064$ | $k_1= 310000$ $k_2=183000$ $k_3=162800$ $k_4=90000$ | |

Table 2.5: Four degree-of-freedom (4-DOF) lumped parameter models of a seated human.

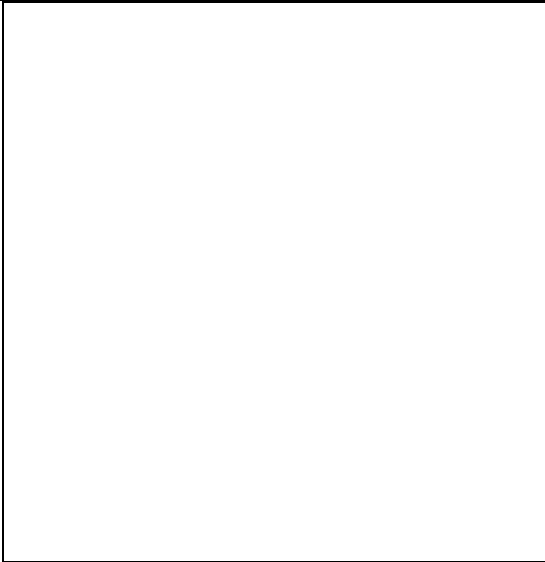
| Authors & Remarks | Biodynamic parameters | | | Schematic of Model |
|--|-----------------------|----------------|------------------|---|
| | Mass (kg) | Damping (Ns/m) | Stiffness (N/m) | |
| Rakheja's 4-DOF linear model in the vertical and horizontal direction [54]. | $m_2= 3.56$ | $c_1=1764$ | $k_1=299000$ |  |
| | $m_1=29.9$ | $c_2=1047$ | $k_2=42700$ | |
| | $m_0=19.94$ | $c_{b1}=859$ | $k_{b1}=77100$ | |
| | Mtotal: 53.40 | $c_{b2}=1006$ | $k_{b2}=1430500$ | |

Table 2.6: Four degree-of-freedom (4-DOF) lumped parameter models of a seated human.

c) Other Complex Models

The simple mass-spring-damper model (SDOF) is the basic and fundamental model for vibration analysis. It allows the mass to move only up and down. As given above, the published studies show that 2-DOF, 3-DOF and 4-DOF models are used to predict the seat-to-head (STH) transmissibility in the vertical direction. The mathematical models of increasing degree of complexity progress to include more human body masses, such as five, six, seven, etc. The main aim of the complex models is to depict human motion in respect of whole body vibration characteristics.

In an early study, Mertens [66] studied nonlinear behaviour of seated humans under increased gravity and analysed the resonant frequency with regard to the increased gravity in the vertical direction. The 5-DOF mathematical model is shown in Appendix A. Table A.1 gives the damping coefficients used which range between 500-4000 Ns/m. A slightly refined model, from an anatomical description of a seated human body, a 6-DOF nonlinear model (see Appendix A, Table A.2) was formulated to analyse the pelvis-to-head transmissibility in the vertical direction by Muksian and Nash [60].

A 9-DOF model [28, 67], 10-DOF model [33], 11-DOF model [68-70] and 14-DOF model [71] were developed to evaluate the relationship between the physical and physiological reactions of a seated human body in the translational and rotational directions (see Appendix A.2). These models were obtained by theoretical and experimental studies to predict the transmissibility, apparent mass or mechanical impedance. However, only Liang and Chiang, [71] specified the evaluation of ride comfort by investigating a seated human body linear model with backrest and without backrest. Moreover, it was recommended that the influences of a different mass and the influence of the hands may need to be investigated to understand the source of the vibration on the human body in a vehicle.

2.5.3 Integrated Human-Seat-Vehicle Biodynamical Model

When driving a ground vehicle, the driver's body is subjected to motions of the vehicle, usually transferred through a seat. Vehicle motion plays an important role in influencing response of the driver/human subject. It can be simulated using vehicle dynamic models; the parameter calculation and interactions may be difficult to identify. In order to understand and evaluate the vibration response of the subject, increased number of degrees of freedom (N-DOF) biodynamical human models were developed to investigate integrated behaviour; these models are known as occupant-vehicle models. There are not many published studies on the 'Integrated human-seat-vehicle model'.

An 11-DOF occupant-tractor lumped parameter nonlinear model was proposed by Patil [72, 73] to analyse the vertical and rotational (pitch) vibration response to ground reactions and suspension parameters. This 11-DOF model consists of an 8-DOF human lumped parameter model and a 3-DOF half tractor lumped parameter model. The masses of head (M_h), back (M_b), torso (M_t), thorax (M_{th}), diaphragm (M_d), abdomen (M_a) and pelvis (M_p) were connected by springs and dampers. The spring and damper values were obtained based on the publication by Muksian [60]. The half tractor model captures the influence of seat, chassis body and tyre-hub masses which were interconnected by linear vertical springs and with velocity dependent dampers. The main aim of this study was to isolate the rotational pitch vibration being transmitted to the driver of the tractor. The response of the human model was evaluated based on the road conditions.

In 1980 a new (13-DOF) model was proposed by Patil based on the refinement to earlier (11-DOF) model with the inclusion of suspensions for the front and rear wheels of the system to improve the ride comfort. This model was further extended to a 19 DOF model in a translational and rotational (pitch, roll, yaw) axes by Kumar and Mahajan [74]. The results of the linear model in the frequency domain were correlated with objective measurement results to understand the backache problems of the drivers based on the road surface.

The model parameters and schematic diagram are given in Table 2.7.

| Authors & Remarks | Biodynamic parameters | | | Schematic of Model |
|---|---|--|---|--------------------|
| | Mass (kg) | Damping (Ns/m) | Stiffness (N/m) | |
| <p>Patil's 11-DOF occupant-tractor model [72].</p> <p>The tractor occupant is a lumped parameter nonlinear model. The tractor was idealized by seat, chassis body and tyre masses interconnected by springs and dampers of the seat suspension system.</p> <p>*The units of damping constants, giving rise to linear and nonlinear forces respectively are: kgf/cm/sec and kgf/(cm/sec)³. + The units of spring constants, giving rise to linear and nonlinear forces respectively are kgf/cm and kgf/cm³.</p> | <p>$m_7=0.00555$</p> <p>$m_6=0.00694$</p> <p>$m_5=0.03333$</p> <p>$m_4=0.001389$</p> <p>$m_3=0.0004629$</p> <p>$m_2=0.00602$</p> <p>$m_1=0.0277$</p> | <p>$c_7=3.651$</p> <p>$c_6=3.651$</p> <p>$c_5^*=0.298$</p> <p>$c_{56}^*=3.651$</p> <p>$c_4^*=0.298$</p> <p>$c_3^*=0.298$</p> <p>$c_2^*=0.298$</p> <p>$c_1=0.378$</p> | <p>$k_7=53.64$</p> <p>$k_6=53.64$</p> <p>$k_5^+=0.8941$</p> <p>$k_{56}^+=53.64$</p> <p>$k_4^+=0.8941$</p> <p>$k_3^+=0.8941$</p> <p>$k_2^+=0.8941$</p> <p>$k_1=25.5$</p> | |

Table 2.7: Occupant-tractor (11-DOF) model with relaxation suspension to seat.

A quarter vehicle-driver (4-DOF) model was proposed by Gundogdu [75] to minimize the transmitted acceleration to the lower back, head and upper body. The system was assumed to move in the vertical direction only. The parameters used in this model (Table 2.8) were from the previous published studies. Another quarter vehicle-driver (7-DOF) model (Table 2.9) was developed to analyze the motion in vertical direction by Papalukopoulos and Natsiavas [76]; dynamic response and the vibration behaviour were determined in order to quantify ride comfort for drivers and passengers. A two-dimensional automobile and a seated human vibration model were recommended [67] to simulate the vibration behaviour of a human body riding in an automobile (Fig. 2.9). Kubo [67] predicted the physiological and physical reaction of a person riding the two-dimensional automobile. However, there is no information on the calculation method of the parameters on Kubo's model. It only deals with mechanical vibration system design.

In order to analyse the response of a seated pregnant woman in a vehicle in translational and rotational movements, a 14-DOF model was developed by Liang [77]. The seated non-pregnant and pregnant human body models were developed using the information from: Muksian's non linear model (6 DOF); Patil's non-linear model (7 DOF) (see Appendix A, Table A.2); Merten's non-linear (5-DOF) model; and Qassem's 11-DOF model (see Appendix A, Table A.1 and A.6).

A 7-DOF vehicle model was assumed allowing for pitch, roll and bounce motion. Muksian's modified model was integrated to the 7-DOF full vehicle model with seat spring and damper; the resulting model has 14-DOFs, which are shown in Figure 2.10. The model results were validated using measured seat-to-head transmissibility, driving point impedance and apparent mass.



Figure 2.9: A human vibration model riding in an automobile vibration model [67].

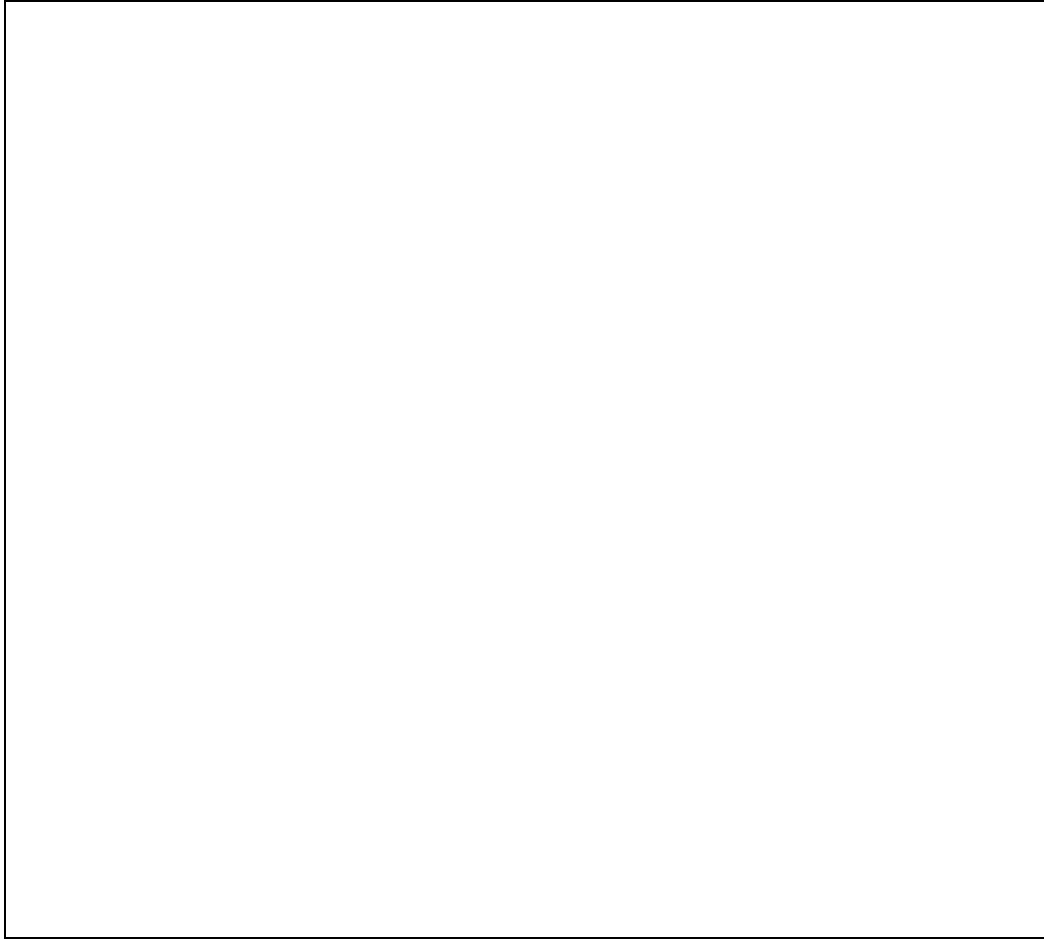


Figure 2.10: Integrated human-vehicle model [77].

| Authors & Remarks | Biomechanical parameters | | | Schematic of Model |
|---|--|-----------------------------|--|--------------------|
| | Mass (kg) | Damping (Ns/m) | Stiffness (N/m) | |
| A Quarter vehicle model with driver (4-DOF) [75]. | m (The mass of driver) $m_t=2m/7$ $m_p=5m/7$ $m_s=240$ $m_u=36$ | $c_s=980$ $c_t=1360$ | $k_s=16000$ $k_y=160000$ $k_t=45005.3$ | |

Table 2.8: Integrated human-vehicle (14-DOF) model.

| Authors & Remarks | Biomechanical parameters | | | Schematic of Model |
|---|---|---|---|--------------------|
| | Mass (kg) | Damping (Ns/m) | Stiffness (N/m) | |
| <p>Papalukopoulos and Natsiavas's 7-DOF model [76].</p> <p>(a) Quarter car model (b) Biodynamical model</p> | <p>$m_{\text{wheel}}=60$</p> <p>$m_{\text{vehicle body}}=375$</p> <p>$m_{\text{seat}}=8$</p> <p>$m_{\text{pelvis}}=29$</p> <p>$m_{\text{upper torso}}=21.8$</p> <p>$m_{\text{viscera}}=6.8$</p> <p>$m_{\text{head}}=5.5$</p> | <p>$k_1=200000$</p> <p>$k_2=15000$</p> <p>$k_3=500000$</p> <p>$k_6=2831.8$</p> <p>$k_7=202286$</p> | <p>$c_1=7$</p> <p>$c_2=475$</p> | |

Table 2.9: Seven-DOF quarter car and biodynamical model.

2.5.4 Other Human Body-Vehicle Computer Models

The number of people injured in automotive traffic accidents is required further safety improvements and vehicle safety measurement methods. Therefore, vehicle companies have developed human body models to quantify injury parameters and predict injuries to the human body. For this type of studies, it is difficult to use volunteers because of health and safety. The crash test dummy may be used; however, a dummy structurally is different from the human body due to impact response.

In recent years, human body simulation models have been developed using computers. For analysis of injury mechanism and evaluation of vehicle crash safety, human body simulation models are used by automotive manufactures [78, 79]. The most used models are:

- Total Human Model for Safety (THUMS) is a family of human models
- Human Model for Safety (HUMOS) is full human body model
- Mathematical Dynamic Model (MADYMO) provides a series of multi-body models
- LS DYNA is a finite element program and used to analyze vehicle designs.

These models are not within the scope of this study.

2.5.5 Discussion

The human body is a complex dynamic system. This complex system has been modelled by many researchers to identify the characteristics of humans subjected to vibration. The transmission of vibration to the body and the transmissibility of vibration through the body and the factors which influence the vibration in the body are still under investigation. Lumped-parameter models of human beings are the most common mathematical model used for simulating and predicting human vibration response. More complex multi-degree of freedom models are required to specify the body posture and seating conditions (with backrest and without backrest). Based on the published studies various lumped-parameter models have been developed to increase the number of moving masses to predict the movement adequately.

The majority of the models proposed in the literature are lumped-parameter models, where the parameters are mostly identified from measured biodynamic response data. The model parameters are mostly identified from either measured driving-point mechanical impedance or vibration transmissibility characteristics of the human subjects. However, there are no universally accepted parameters of human body biodynamics models. The main problems in modelling the response of the body are the differences that occur both between and within subjects.

There are a great many published studies regarding human body modelling; however, the method of the calculation and measurement of parameter values of the human body segment springs and dampers are not clear. On their own, the seated human lumped parameter models are not adequate to predict the ride comfort based on real environmental conditions; a vehicle model cannot be used to define ride comfort without a seated subject in a car. In order to understand the interaction between the vehicle vibration and the seated human, integrated-human-seat-vehicle models are required. Based on the published occupant-vehicle models, there is not enough information on parametric studies.

2.6 SUMMARY

Human comfort response to whole-body vibration is difficult to determine due to subject sensitivity. Many published studies provide the definition of discomfort/comfort in terms of feeling and sensations. However, the difference between these two terms (comfort and discomfort) has been indicated by De Looze (2010) [1] as discomfort depends on vibration input and comfort has influences from vibration input and other aspects. Therefore, in this study discomfort was used for quantification of vibration perception.

A review of the available published studies indicated the following;

- Determining human comfort boundaries is difficult due to quantification of human sensitivity.
- Comfort and discomfort have differences between each other based on vibration input.
- Road conditions and vehicle dynamics have influences on human comfort and health.
- The measurement of road surface may not be enough to quantify ride comfort without subjective assessment.
- The subjective ride measurement tests on a vehicle, however, may have significant uncertainties such as a) the inputs may not be repeatable and statistics not consistent and b) the uncertainties in human perception may be difficult to quantify.
- The shaker table test setups may not capture the complexity of vibration input required and furthermore they do not include the effects of surroundings seen in a vehicle.
- The human sensitivity to vibration is determined by subjective feeling rating in terms of the sensation of discomfort.
- Under laboratory conditions, for measuring of a full vehicle, a road simulator (e.g. four-post rig) is required to produce real vehicle motions to provide a subjective assessment.

- For analysis of the multi-directional motion of the human body postures, multi-degree of freedom models are required rather than studying only single degree-of-freedom models.
- There are no universally accepted parameters of human body biodynamics models. The main problems in modelling the response of the body are the differences that occur both between and within subjects. There are many published studies regarding modelling; however, the method of calculation and measurement of the parameter values of the human body segment springs and dampers is not clear.
- In order to understand the influence between vehicle vibration and seated humans, integrated-human-seat-vehicle models are required. Based on the published occupant-vehicle models, there is not enough information on parametric studies.
- Human body-vehicle computers models (HUMOS, THUMS, LS-DYNA, and MADYMO) have been developed to understand the injury mechanism and vehicle safety. This models give an opportunity to make detailed models of the human body structurally and of its mechanical properties.

CHAPTER 3

VEHICLE DYNAMICS AND THE INFLUENCE ON VEHICLE DISCOMFORT EXPERIMENTS

3.1 INTRODUCTION

A vehicle's dynamic behaviour has a large influence on the vibrations that affect the human perception of vibration. In this study, the vehicle discomfort is analysed in two phases: *the vibration transmitted from the road through the seat* and *the dynamic behaviour occupant and its perception*. These two categories “through-to-the-seat” and “to-the-occupant” are treated as “cause” and “effect” in the discussion of the discomfort analysis in the vehicle. When considering “cause”, the transmission of the vibration is influenced by the dynamic parameters of the vehicle system. The transmitted vibration through to the seat is determined by the resonant behaviour. When we study “effect”, we explore the transmitted vibration to the human body and response.

The aim of this Chapter is to understand the dynamic behaviour of vehicles within a newly developed experimental protocol which differs from other published studies. Firstly, in this experimental study, the concept of the ‘cause-effect’ relation is described. Then these relations are analyzed in terms of the vehicle resonant modes. In the following study, in order to develop a predictive mathematical model for the ‘cause-effect’ relations, the lumped parameter models are reviewed in detail. These simplified and reviewed models help to analyze and interpret the results of the experimental measurements on the four-post rig.

3.2 CAUSE-EFFECT APPROACH MECHANISM OF VIBRATION TRANSFER AND VEHICLE DISCOMFORT

Ride discomfort is a subjectively perceived vibration for a seated human body in a moving car on different road conditions. The interaction between the road surface and vehicle influence the seated human body subjects (who are in contact with the vehicle seat). This interaction provides the information about the relation between the vibration output and input; the interface between driver and vehicle is the system output variable and the road surface is the vibration input.

A moving car (Figure 3.1) is exposed to a mechanical vibration due to the interaction between the vehicle and the road surface. This mechanical vibration is transmitted through to the vehicle, vehicle floor and seat based on both characteristics of the vehicle and the road conditions. The vehicle floor and the seat are the surfaces that support the seated human subjects. Therefore, the vibration entry points are classified as the feet, buttocks, back, and the head [2-4].

The relation between perception and response can be addressed by a 'cause-effect model'; Figure 3.1 shows the seated human body in contact with a vibrating surface. The vibration excitation can be expressed as a 'cause' which is 'a motion input from the road surface resulting in vibration at the seat'. The human response to vibration is defined as 'effect'. The effect may be expressed [4] using vibration sensation, perception, annoyance, discomfort, comfort, various biomechanical effects and health consequences.

The vibration input and output relation are quantified by the excitation-response relations (Fig. 3.1). From the vibration input and output relations, the human response to vibration is assessed by either a threshold curve (as a function of frequency) or an excitation curve (as a function of frequency). The threshold curve represents the boundary level of perception; excitation curves are used to determine either the transmissibility function or frequency transfer function [4].

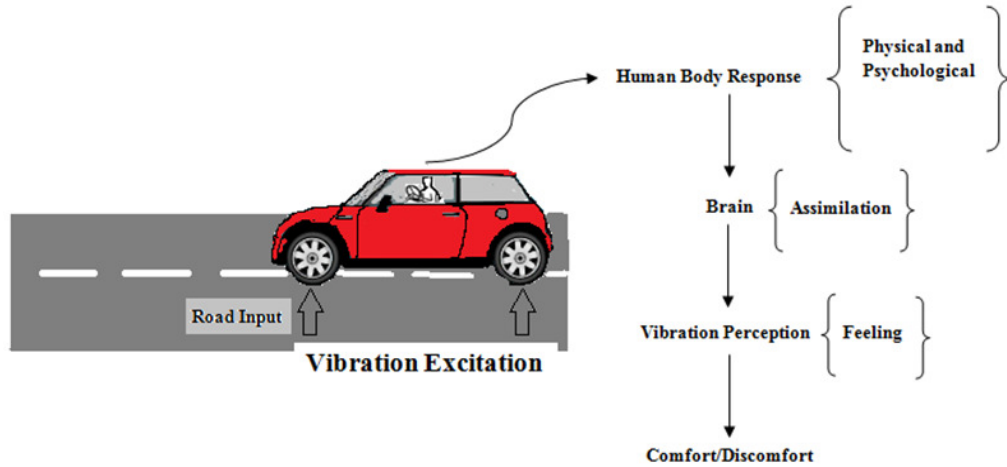


Figure 3.1: Vibration ‘cause-effect’ model of human perception of vibration.

The response is categorized by Silva [4] based on its intensity as:

1. Sense and feel,
2. Distraction and annoyance,
3. Discomfort (e.g., poor ride quality),
4. Minor, moderate, or major health consequences.

Distraction, annoyance, discomfort, and health consequences influence human performance. Below 1 Hz vibration may cause motion sickness but low levels of vibration may not directly cause discomfort. The effects of sensation and feeling are determined based on the vibration at low frequency. The human body is most sensitive to the vertical vibration around 5 Hz – 6 Hz [2, 4]. The characteristics of human sensitivity are quantified and evaluated by a subjective assessment method which is the judgement method of ride comfort/discomfort by the seated human body subjects. The characteristics and behaviour of the human response to vibration are quantified by an objective measurement method.

The method of ‘the cause-effect model’ can also be used to predict the excitation-response relations between the seated human body and the vibrating surface (i.e. seat). The vibration input to the seat is strongly affected by the dynamic characteristics of the vehicle system (i.e., tyre and suspension), which influence the seated human body. In this research, the measurements were performed on the

four-post rig and the data eventually used to quantify the ‘cause’ part of the model.

3.3 DYNAMIC CHARACTERIZATION OF THE CAR MOTION

The ride discomfort depends on the dynamic behaviour of a vehicle. For accurate representation the vehicle behaviour needs to be found using experimental techniques; the dynamic characteristic of the car needs to be measured. The dynamic behaviour can be quantified by vibration transmissibility measurements. In this section, the dynamic characterization of a car and seat is studied to analyze and specify the vibration transmissibility (vibration transmitted) from the road to the vehicle.

3.3.1 Dynamic Response of a Car

The natural frequencies and mode shapes of the vehicle are important factors determining the vibration behaviour of a vehicle [80]. The frequency range of interest for ride discomfort studies can be restricted to 0-25 Hz. Above 25 Hz is considered a noise and vibration issue (the noise is not within the scope of this study). 20 Hz frequency is the lower frequency threshold of hearing.

During driving (Fig. 3.2), the external forces act on a vehicle through the wheels due to the road surface input. Due to complex transfer paths, the spectra of vibrations contain dynamic contributions from tyre, suspension, engine, chassis stiffness and body mass etc. The vibration is transmitted through the wheels and suspension to the vehicle body including the vehicle floor, seat and occupants [13, 80, 81].

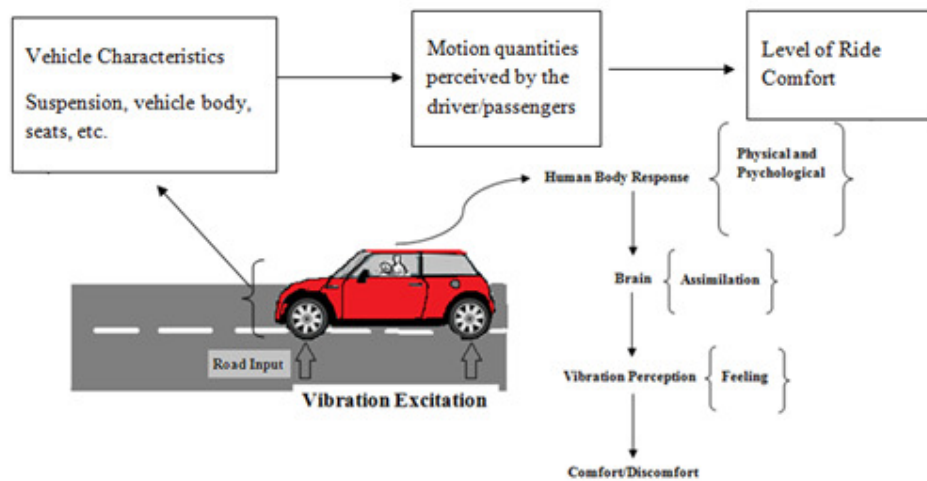


Figure 3.2: A relation between the road and seat which represents car characterization and transmissibility.

The vehicle (Fig. 3.3) goes through various types of movements based on the input; bump (upwards) and droop (negative bump) are the wheel displacements relative to the car body. Heave, which is known as bounce, is a vertical motion of the car body where pitch or roll motion are absent. The vertical motion is a symmetrical upward displacement, so it is also called double bump. The 6-DOF vehicle motion is given in Chapter 2.4. In this study, the vehicle dynamics was analyzed in heave, pitch and roll modes (Fig. 3.3). The pitch motion can occur during acceleration, deceleration and when the input to the rear wheels is delayed relative to the front wheels. The roll motion becomes important while vehicles take a turn. The combination of motion occurs if a wheel or two go over a bump.

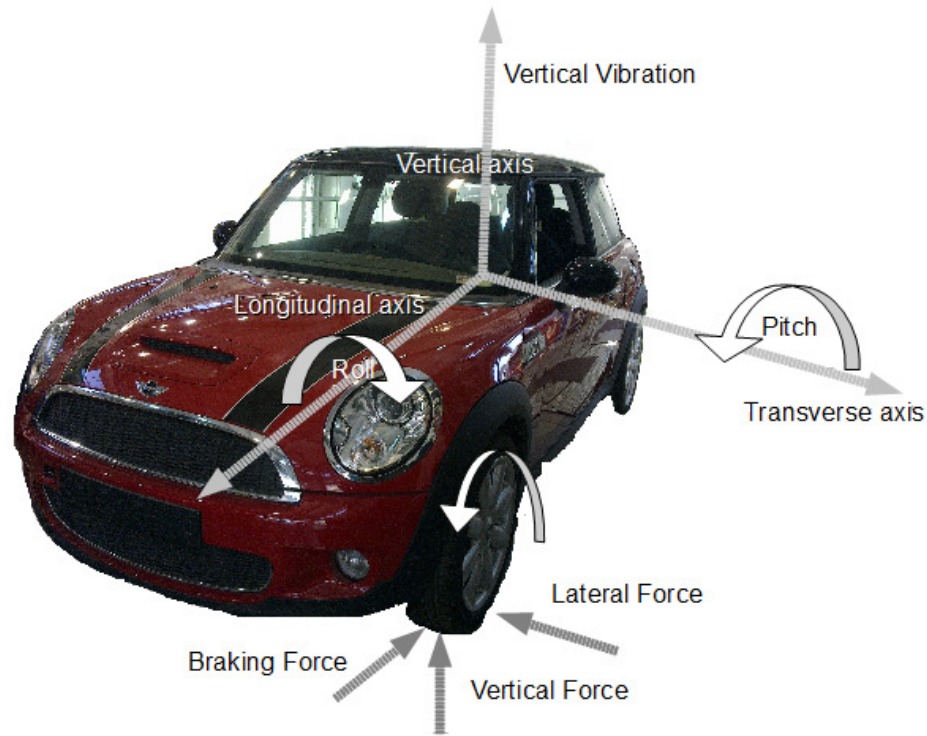


Figure 3.3: The motion of a vehicle which interacts with the ground.

3.3.2 Dynamic Response of a Car Seat

The study of seat dynamics is one of the most important in affecting the human vibration characteristics and eventually ride comfort/discomfort. The seats are designed and developed with the aim of reducing the vibration transmissibility to occupants. So this requires an understanding of vibration characteristics in terms of transmissibility, for example, how the vibration enters the human body through the seat. The input to a seated human body can come from various contact points (seat surface, seat back and the seat headrest) between the seat and occupant and the input can be multidirectional.

Different measurements, i.e. static and dynamic methods have been used to characterize the seat performance. Many published papers [2, 18, 23, 82] have focused on both methods to determine the seated human comfort/discomfort by using a seat mounted on a shaker platform. The response measurements are taken

at the seat and the floor in order to estimate the magnitude of vibration transmitted and then predict the human discomfort.

As previously stated in Chapter 2, the vertical seat dynamics are characterized by the transmissibility; which is the ratio between input (seat surface, vehicle floor) and output (human body parts) response measurements (a frequency-response function) [3, 27, 29]. The shaker table measurements are used to estimate the seat-to-head (STH) and the floor-to-seat (FTS) transmissibilities. From the published papers [2, 3, 19, 21, 23], it is shown that vibrations in the vertical direction are the most important for discomfort rating. This area of research has been explored extensively; the shaker table test setups may not capture the complexity of vibration input as required for an occupant in a vehicle.

3.4 LUMPED PARAMETER VEHICLE DYNAMIC MODELS USED TO ANALYSE VEHICLE COMFORT

The behaviour of vehicle body to vibration can be analysed using various vehicle dynamic mathematical models of varying degrees of complexity. These models can be used to determine the vehicle response, characterize the vehicle vibration behaviour and eventually ride comfort/discomfort [12, 16, 80, 81, 83]. In the vehicle dynamic mathematical models, a car is considered as consisting of a sprung mass (chassis) and unsprung masses (wheels, axles and linkages), which are interconnected with a number of springs and dampers. These masses may be exposed to external forces. The motion of a vehicle body (Fig. 3.3) can be represented with a six-degree-of-freedom coordinate system (translatory and rotational motions) (See Section 2.2). Vehicle ride mathematical models contain a set of simultaneous ordinary differential equation coefficients which have inertia, stiffness and damping coefficient values.

In this study, to characterize and predict the vehicle dynamic behaviour in heave, pitch and roll modes, *a lumped parameter 4-DOF vehicle model* and *a lumped parameter full vehicle-seat (7-DOF) model* have been studied. A short theoretical background of the modelling is given below. The natural frequencies found are

discussed for a 4-DOF vehicle model and a full-vehicle model. The parameters used are typical for a BMW Mini Cooper, which is the car used in this research study.

3.4.1 The Linear 4-DOF Vehicle Model

The 4-DOF vehicle mathematical model (Fig. 3.4) represents the vehicle body connected via springs and dampers to unsprung masses allowing motion heave and pitch modes. Namely, in this model the main body consists of a mass that is free to rotate and heave vertically. The aim of this model is to analyze the frequency response functions and transmissibilities. The parameters of the model are: masses for the vehicle body m_v and two unsprung masses m_{11} and m_{21} ; damping coefficients c_{s11} and c_{s21} ; stiffness coefficients of the vehicle suspension k_{s11} , and k_{s21} ; tyre stiffness k_{t11} and k_{t21} ; pitch moment of inertia I_{zz} .

If y_3 and θ represent the bounce displacement and angular pitch displacement of the sprung mass, respectively, then $y'_1 = y_3 + \theta l_f$ and $y'_2 = y_3 - \theta l_r$ will be the sprung mass displacements at the front and rear suspension connections. l_f is the distance from the vehicle's centre of gravity (C.G.) to the front suspension and l_r is the distance from the vehicle C.G. to the rear suspension. The left and right stiffness of the tyre are connected to the ground; the road inputs are represented as r_{11} and r_{21} in the model. Rear input is the same as the front for purely 'heave' response. For 'pitch' response, front and rear inputs are out of phase. For calculating natural frequencies, the values of these are set to zero.

The equations of motion for dynamic behaviour of the 4-DOF model can be obtained using Newton's second law (Eq. 3.1).

$$\mathbf{M}\ddot{\mathbf{Y}} + \mathbf{C}\dot{\mathbf{Y}} + \mathbf{K}\mathbf{Y} = \mathbf{F} \quad (3.1)$$

By considering a free-body diagram, the following differential equations of motion (Eq. 3.2) are obtained for the motion of sprung and unsprung masses.

$$\begin{aligned}
m_v \ddot{y}_2 + k_{t11}(y_2) - k_{s11}(y'_2 - y_2) - c_{s11}(\dot{y}'_2 - \dot{y}_2) &= k_{t11}(r_{11}) \\
m_{21} \ddot{y}_1 + k_{t21}(y_1) - k_{s21}(y'_1 - y_1) - c_{s21}(\dot{y}'_1 - \dot{y}_1) &= k_{t21}(r_{21}) \\
m_v \ddot{y}_3 + k_{s11}(y'_2 - y_2) + c_{s11}(\dot{y}'_2 - \dot{y}_2) + k_{s21}(y'_1 - y_1) + c_{s21}(\dot{y}'_1 - \dot{y}_1) &= 0 \\
J \ddot{\theta} + \{k_{s21}(y'_1 - y_1) + c_{s21}(\dot{y}'_1 - \dot{y}_1)\} l_r - \{k_{s11}(y'_2 - y_2) + c_{s11}(\dot{y}'_2 - \dot{y}_2)\} l_f &= 0
\end{aligned} \quad (3.2)$$

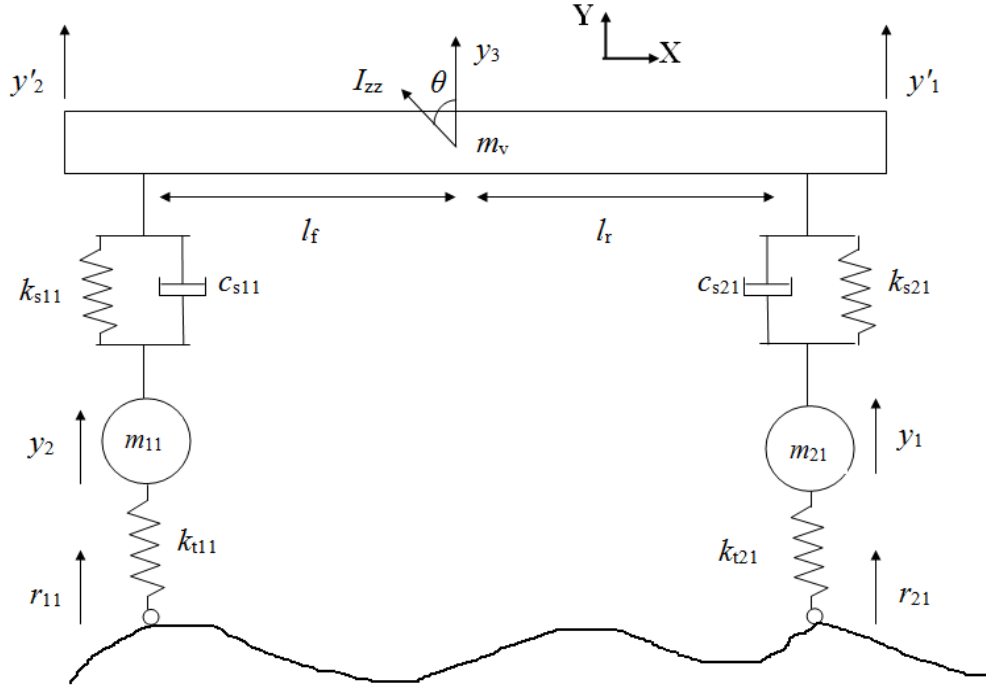


Figure 3.4: Lumped parameter 4-DOF vehicle (front and rear left) model in the motion of pitch and heave.

From Eq. 3.2, matrices for mass (**M**), damping (**C**), stiffness (**K**) and input (**F**) are given below.

Mass matrix:

$$\mathbf{M} = \begin{bmatrix} m_{11} & 0 & 0 & 0 \\ 0 & m_{21} & 0 & 0 \\ 0 & 0 & m_v & 0 \\ 0 & 0 & 0 & I_{zz} \end{bmatrix} \quad (3.3)$$

Stiffness matrix:

$$\mathbf{K} = \begin{bmatrix} k_{t11} + k_{s11} & 0 & -k_{s11} & k_{s11}l_f \\ 0 & k_{t21} + k_{s21} & -k_{s21} & -k_{s21}l_r \\ -k_{s11} & -k_{s21} & k_{s11} + k_{s21} & -k_{s11}l_f + k_{s21}l_r \\ ks_{11}l_f & -k_{s21}l_r & k_{s21}l_r - k_{s11}l_f & k_{s21}l_r^2 + k_{s11}l_f^2 \end{bmatrix} \quad (3.6)$$

Damping matrix:

$$\mathbf{C} = \begin{bmatrix} c_{s11} & 0 & -c_{s11} & c_{s11}l_f \\ 0 & c_{s21} & -c_{s21} & -c_{s21}l_r \\ -c_{s11} & -c_{s21} & c_{s11} + c_{s21} & -c_{s11}l_f + c_{s21}l_r \\ c_{s11}l_f & -c_{s21}l_r & c_{s21}l_r - c_{s11}l_f & c_{s21}l_r^2 + c_{s11}l_f^2 \end{bmatrix} \quad (3.7)$$

Response vector:

$$\mathbf{Y} = [y_2, y_1, y_3, \theta]^T \quad (3.4)$$

Excitation vector:

$$\mathbf{F} = [k_{t11}r_{11}, k_{t21}r_{21}, 0, 0]^T \quad (3.5)$$

For free vibration analysis, neglecting the damping and assuming a sinusoidal response of the form $\mathbf{y} = \mathbf{Y}e^{j\omega t}$ eigenvalue problem results.

$$\det[\omega^2\mathbf{M} - \mathbf{K}] = 0 \quad (3.11)$$

The resulting characteristic equation can be solved to obtain natural frequencies and mode shapes. For an N-DOF system, \mathbf{M} and \mathbf{K} are both $n \times n$ matrices. It follows that the characteristic equation has n roots of ω^2 . For physically realizable

systems these n roots are all non-negative and they yield the n natural frequencies $\omega_1, \omega_2, \omega_3, \dots, \omega_n$ of the system.

Undamped natural frequencies calculated for 4-DOF vehicle model of a BMW mini cooper car are: Pitch, 1.87 Hz; Heave, 2.21 Hz, Front Left-Hub, 19.22 Hz and Rear Left-Hub, 17.65 Hz respectively. The parameters of a BMW mini for 4-DOF model are given in Table 3.1.

| Parameter | Value |
|---------------------------------|------------------------|
| Sprung mass | 534 kg |
| Front axle to centre of gravity | 0.871 m |
| Rear axle to centre of gravity | 1.596 m |
| Front unsprung mass | 33 kg |
| Rear unsprung mass | 36 kg |
| Pitch inertia | 1170 kg m ² |
| Front suspension stiffness | 48000 N/m |
| Rear suspension stiffness | 32200 N/m |
| Front damping coefficient | 4500 Ns/m |
| Rear damping coefficient | 1660 Ns/m |
| Front tyre stiffness | 433000 N/m |
| Rear tyre stiffness | 410000 N/m |

Table 3.1: Measured parameters for a BMW mini cooper car for a 4-DOF model [84].

3.4.2 The Linear Full Vehicle Model

The information of pitch and roll motion is essential in understanding the complete dynamics. In this study, the lumped parameter full vehicle ride (7-DOF) model is studied to analyze the vehicle and seat vibrations with input excitations. The full vehicle 7-DOF ride model consists of the 3-DOF model for heave, pitch, and roll modes of the sprung masses; and 4-DOF vertical dynamic model for the unsprung masses with a 1-DOF model for each tyre-hub model.

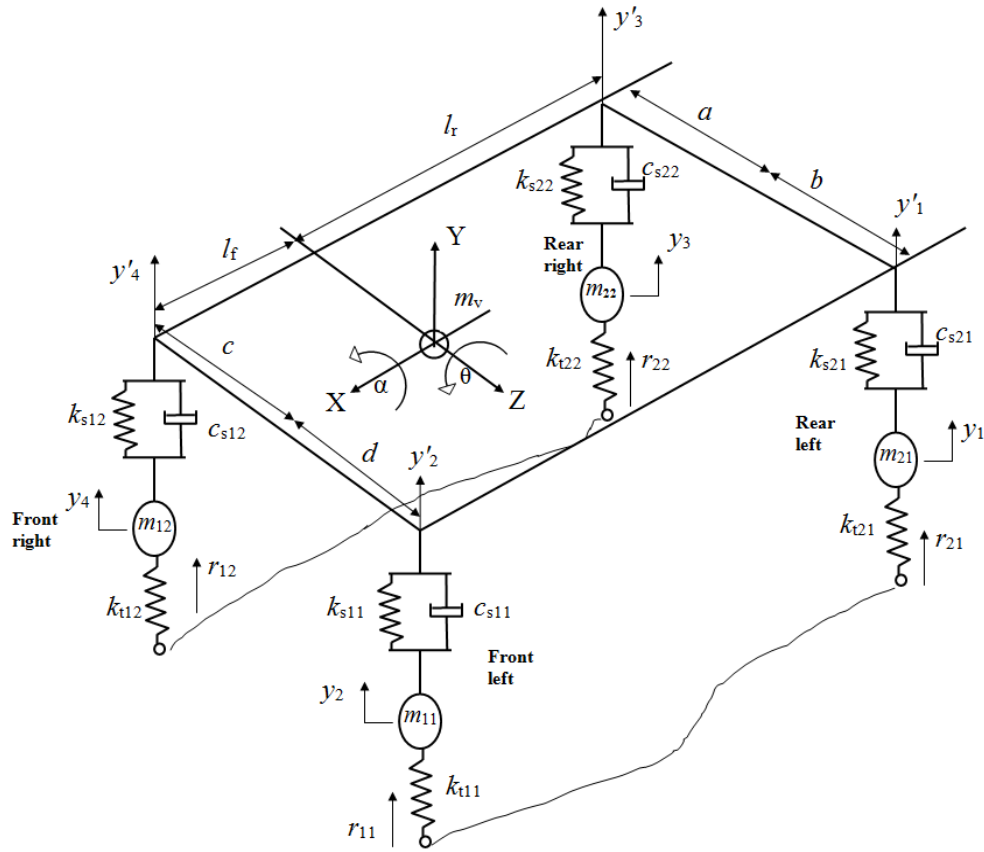


Figure 3.5: Lumped parameter full vehicle ride (7-DOF) model

Figure 3.5 shows the linear full vehicle (7-DOF) model for the motion in the vertical direction of the sprung mass (car body), which is connected to four unsprung masses (front-left, front-right, rear-left, and rear-right), considering heave, pitch and roll modes. The displacements of unsprung masses in the vertical direction are y_1 , y_2 , y_3 , and y_4 for left rear, left front, right rear and right front respectively. The vertical displacement, pitch angle, and roll angle are y , θ and α respectively. The other parameters of the model are: a and b are distances along Z axis of centre of gravity and the rear wheels; c and d are distances along Z axis of centre of gravity and the rear wheels; L_f and L_r are the distances from the centre of gravity and front and rear wheels; m_{11} , m_{21} , m_{22} , and m_{12} are the unsprung masses of the left front, left rear, right rear and right front respectively; m_v is the vehicle body (sprung) mass; I_{zz} is the sprung mass pitch moment of inertia; I_{xx} is the sprung mass roll moment of inertia; k_{tr} is the roll stiffness.

For the small angles θ and α , the linearized governing equations for this system are obtained directly as:

$$\begin{aligned}
y'_2 &= y - l_f \theta + d\alpha \\
y'_1 &= y - l_r \theta + b\alpha \\
y'_3 &= y + l_r \theta - a\alpha \\
y'_4 &= y - l_f \theta - c\alpha
\end{aligned} \tag{3.12}$$

$$\begin{aligned}
m_{11}\ddot{y}_2 + k_{t11}(y_2) - k_{s11}(y'_2 - y_2) - c_{s11}(\dot{y}'_2 - \dot{y}_2) &= k_{t11}(r_{11}) \\
m_{21}\ddot{y}_1 + k_{t21}(y_1) - k_{s21}(y'_1 - y_1) - c_{s21}(\dot{y}'_1 - \dot{y}_1) + \left\{ \frac{k_{trr}}{2}(y_1 - y_3) \right\} &= k_{t21}(r_{21}) \\
m_{12}\ddot{y}_4 + k_{t12}(y_4) - k_{s12}(y'_4 - y_4) - c_{s12}(\dot{y}'_4 - \dot{y}_4) &= k_{t12}(r_{12}) \\
m_{22}\ddot{y}_3 + k_{t22}(y_3) - k_{s22}(y'_3 - y_3) - c_{s22}(\dot{y}'_3 - \dot{y}_3) - \left\{ \frac{k_{trr}}{2}(y_1 - y_3) \right\} &= k_{t22}(r_{22}) \\
m_v \ddot{y} + k_{s11}(y'_2 - y_2) + c_{s11}(\dot{y}'_2 - \dot{y}_2) + k_{s21}(y'_1 - y_1) + c_{s21}(\dot{y}'_1 - \dot{y}_1) \\
+ k_{s12}(y'_4 - y_4) + c_{s12}(\dot{y}'_4 - \dot{y}_4) + k_{s22}(y'_3 - y_3) + c_{s22}(\dot{y}'_3 - \dot{y}_3) &= 0 \\
I_{zz} \ddot{\theta} - \{k_{s11}(y'_2 - y_2) + c_{s11}(\dot{y}'_2 - \dot{y}_2)\} l_f - \{k_{s12}(y'_4 - y_4) + c_{s12}(\dot{y}'_4 - \dot{y}_4)\} l_f \\
+ \{k_{s21}(y'_1 - y_1) + c_{s21}(\dot{y}'_1 - \dot{y}_1)\} l_r + \{k_{s22}(y'_3 - y_3) + c_{s22}(\dot{y}'_3 - \dot{y}_3)\} l_r &= 0 \\
I_{xx} \ddot{\alpha} - \{k_{s12}(y'_4 - y_4) + c_{s12}(\dot{y}'_4 - \dot{y}_4)\} c + \{k_{s11}(y'_2 - y_2) + c_{s11}(\dot{y}'_2 - \dot{y}_2)\} d \\
+ \{k_{s21}(y'_1 - y_1) + c_{s21}(\dot{y}'_1 - \dot{y}_1)\} b - \{k_{s22}(y'_3 - y_3) + c_{s22}(\dot{y}'_3 - \dot{y}_3)\} a &= 0
\end{aligned} \tag{3.13}$$

Mass matrix:

$$\mathbf{M} = \begin{bmatrix} m_{11} & 0 & 0 & 0 & 0 & 0 & 0 \\ 0 & m_{21} & 0 & 0 & 0 & 0 & 0 \\ 0 & 0 & m_{12} & 0 & 0 & 0 & 0 \\ 0 & 0 & 0 & m_{22} & 0 & 0 & 0 \\ 0 & 0 & 0 & 0 & m_v & 0 & 0 \\ 0 & 0 & 0 & 0 & 0 & I_{zz} & 0 \\ 0 & 0 & 0 & 0 & 0 & 0 & I_{xx} \end{bmatrix} \tag{3.14}$$

Stiffness matrix:

$$\mathbf{K} = \begin{bmatrix} +k_{t11} + k_{s11} & 0 & 0 & 0 & -k_{s11} & +k_{s11}l_f & -k_{s11}d \\ 0 & k_{t21} + k_{s21} + \frac{k_{trr}}{2} & 0 & -\frac{k_{trr}}{2} & -k_{s21} & -k_{s21}l_r & -k_{s21}b \\ 0 & 0 & k_{t12} + k_{s12} & 0 & -k_{s12} & +k_{s12}l_f & k_{s12}c \\ 0 & -\frac{k_{trr}}{2} & 0 & k_{t22} + k_{s22} + \frac{k_{trr}}{2} & -k_{s22} & -k_{s22}l_r & k_{s22}a \\ -k_{s11} & -k_{s21} & -k_{s12} & -k_{s22} & +k_{s11} + k_{s21} + k_{s12} + k_{s22} & -k_{s11}l_f + k_{s21}l_r - k_{s12}l_f + k_{s22}l_r & k_{s11}d + k_{s21}b - k_{s12}c - k_{s22}a \\ +k_{s11}l_f & -k_{s21}l_r & +k_{s12}l_f & -k_{s22}l_r & -k_{s11}l_f - k_{s12}l_f + k_{s21}l_r + k_{s22}l_r & +k_{s11}l_f^2 + k_{s12}l_f^2 + k_{s21}l_r^2 + k_{s22}l_r^2 & -k_{s11}ld + k_{s12}lc + k_{s21}lb - k_{s22}la \\ -k_{s11}d & -k_{s21}b & +k_{s12}c & +k_{s22}a & -k_{s12}c + k_{s11}d + k_{s21}b - k_{s22}a & +k_{s12}lc - k_{s11}ld + k_{s21}lb - k_{s22}la & k_{s12}c^2 + k_{s11}d^2 + k_{s21}b^2 + k_{s22}a^2 \end{bmatrix} \quad (3.15)$$

Response vector:

$$\mathbf{Y} = [y_2, y_1, y_4, y_3, y, \theta, \alpha]^T \quad (3.16)$$

Force vector:

$$\mathbf{F} = [k_{t11}r_{11}, k_{t21}r_{21}, k_{t12}r_{12}, k_{t22}r_{22}, 0, 0, 0]^T \quad (3.17)$$

For the full vehicle ride (7-DOF) model, the parameters of a BMW mini are given in Table 3.2.

| Parameter | Value |
|---------------------------------|------------------------|
| Sprung mass | 1068 kg |
| Front axle to centre of gravity | 0.871 m |
| Rear axle to centre of gravity | 1.596 m |
| Front unsprung mass | 33 kg |
| Rear unsprung mass | 36 kg |
| Pitch inertia | 1170 kg m ² |
| Front suspension stiffness | 48000 N/m |
| Rear suspension stiffness | 32200 N/m |
| Front damping coefficient | 4500 Ns/m |
| Rear damping coefficient | 1660 Ns/m |
| Front tyre stiffness | 433000 N/m |
| Rear tyre stiffness | 410000 N/m |
| Rear roll stiffness | 19600 N/m |
| Rear track | 1.465 m |
| Front track | 1.455 m |
| Wheelbase | 2.467 m |

Table 3.2: Measured parameters of a BMW mini cooper car [84].

From Eq. 3.11, the undamped natural frequencies are calculated for the 7-DOF vehicle model (Table 3.3). For the motion in the vertical direction the natural frequency of pitch, roll and heave occur at 1.76 Hz, 2.41 Hz, and 2.19 Hz respectively. The natural frequencies for each unsprung mass are 19.21 Hz (front left), 19.22 Hz (front right), 17.69 Hz (rear left), and 17.67 Hz (rear right). These results are listed below in Table 3.3.

| Vibration Mode | Natural Frequency (Hz) |
|---------------------------|-------------------------------|
| Pitch | 1.76 |
| Roll | 2.41 |
| Heave | 2.19 |
| Front-Left unsprung mass | 19.21 |
| Front-Right unsprung mass | 19.22 |
| Rear-Left unsprung mass | 17.69 |
| Rear-Right unsprung mass | 17.67 |

Table 3.3: Natural frequencies of lumped parameter full (7-DOF) vehicle model.

In summary, there are a range of different modes with varying complexities influencing dynamics of vehicles. The full vehicle model is modelled by including roll stiffness in order to understand vehicle natural frequencies. The results of this section will be compared with the measured results in the following study.

3.5 EXPERIMENTAL CHARACTERIZATION OF DYNAMICS OF THE TEST VEHICLE

In this experimental study, the resonance behaviour of a car and seat were measured without a seated human subject in a car on a four-post rig. This study focused on maintaining constant velocity by controlling input values for each frequency in a vertical direction for heave, pitch, roll and pitch and roll motion. The measured results are evaluated in the frequency domain to quantify transmissibility vibration from road-to-floor; road-to-seat and floor-to-seat in order to define the inputs required for specific motion of the seat.

3.5.1 Four-Post Rig Road Simulator

The four post rig, at Oxford Brookes University, used in this work (Fig 3.6a) is an experimental piece of equipment used for simulating the effect of road surfaces on vehicles to test suspension systems and vehicle handling [20, 85]. In general, four-post rigs (a road simulator system) have been used [86] to develop standard test procedures to characterise vehicle suspension systems in laboratory conditions by objective measurement methods.

Based on published studies four-post rig simulators have not been used either in the measurement of human comfort or quantification of vehicle ride comfort/discomfort. The idea of the measurement of comfort/discomfort by this test was given by Vanhees and Maes [86]; however, there is not enough explanation or information provided for quantification of human comfort/discomfort. The proposed study is the first to address the quantification of ride comfort/discomfort by using the four-post rig road simulator in this way.

The four-post rig comprises of four road input electro-hydraulic actuators (Fig 3.6b), one supporting each wheel. It is fully computer controlled and the actuators can be independently moved allowing varied motions to be generated. The wheels are placed on the pads (Fig 3.7 and Fig. 3.8) which are height adjustable. The four pads can be positioned based on the wheel base and track width for setup of the vehicle as required. The four corner pads (Fig 3.6a) are called Front Left (FL), Front Right (FR), Rear Left (RL), and Rear Right (RR). The motion of each corner can be lagged relative to the other corners to simulate events.

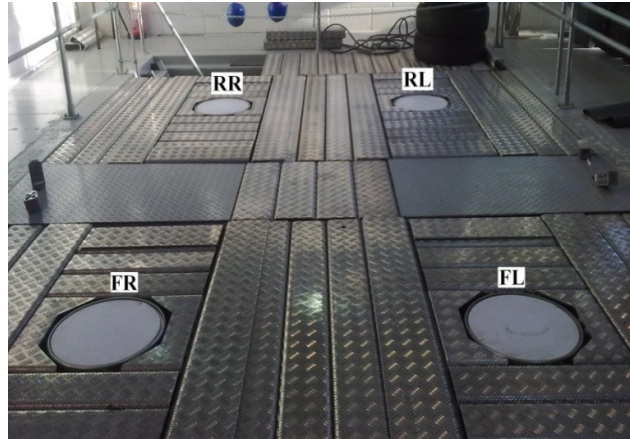


Figure 3.6a: The four-post rig simulator, Oxford Brookes University (FR: Front-right; FL: Front-left; RR: Rear-right; RL: Rear-left actuators respectively)



Figure 3.6b: The four hydraulic actuators, Oxford Brookes University

The four-post rig road simulator is controlled by the *Dynosoft MX* (Dynosoft MTCA, User Manual) [20, 85] software, the component rig control and analysis software. The setup and the measurement data are recorded; the output file from Dynosoft is in the XML (Extensible Mark-up Language) format. This data can be directly imported into Matlab for analyses.

The software has four separate modules, which are:

1. Rig Control and Database Entry Module: to set up and run (Fig 3.7a) the test and record it.
2. Data Retrieval Module: to retrieve saved data.
3. Data Display and Analysis Module: to display measured data in graphs.

4. Model Modules: to apply models allowing the user to display performance curves, such as damper test data.

Figure 3.7a: The four-post rig control panel (after Dynosoft MTCA, User Manual, 2009): 1 Rig Status; 2 Rig Enable; 3 Live Measurement; 4 Pressure Control; 5 Wave Control; 6 Acquisition Control.

Figure 3.7b: The four-post rig wave control panel (after Dynosoft MTCA, User Manual).



Figure 3.8: A car (BMW Mini cooper 2.467 m wheel base, 1.465 m rear track, 1.455 m front track) on the four-post rig. The wheels are placed on the rig.

On the rig, the different road conditions are created using a control panel. The input wave forms can be created and uploaded to the controller. There are 12 standard wave types available as inputs: sine wave, sine step, square wave, square step, square pulse, triangle wave, triangle step, triangle pulse, swept sine fixed amplitude, swept sine fixed velocity, fade and track data. Figure 3.7b shows the wave control panel. On this panel, the frequency, time, amplitude and wave type can be chosen according to required position, velocity and acceleration level.

The rig can run with maximum absolute velocity of 180 mm/s in heave mode, and 160 mm/s in pitch and roll mode. The wave forms used can be the same on all actuators or different for each actuator in order to control the actuators independently based on the generated motions. The default motion set is heave; the mode of operation can be modified (all actuator synchronised) to obtain pitch, roll or warp.

In this project it is proposed to impose prescribed conditions in order to measure the vehicle responses and vibration transmissibility. From the objective and subjective measurement data, the occupants' sensitivity and effectiveness can be judged on the four-post rig when the vehicle travels in a straight line or takes a turn.

On the four-post rig, each pad has an inbuilt sensor to measure the input acceleration. For vibration measurements, SD Silicon Design 2210 model (Fig 3.9a) accelerometers (Appendix B, Figure B.1) are used on the four-post rig. The accelerometer is tailored for zero to medium frequency instrumentation applications. The performance specification of the accelerometers is (Appendix B, Figure B.1): input range $\pm 10g$, frequency response (nominal, 3dB) 0-600 Hz and sensitivity 400 mV/g.

An experimental run will typically record the values of physical (sensor) measurements taken at time intervals, or 'Time Series data'. Each physical measurement series is called a channel [20]. The sensor accelerometers are connected to logical channels (Fig 3.9b) according to their standard name (Fig 3.9). The measured data is acquired using a custom-built data acquisition system controlled by Dynosoft MX multi-axis test control and acquisition software at the rate of 200 Hz. Frequencies of up to 50 Hz can be used in the experiments; however, the full range will not be used in this investigation. Although random inputs could be used in the experiments to replicate the road profile, the sinusoidal inputs were preferred so as to understand the effect of input frequencies and levels. This allows us: a) to develop input frequency and a level

based comfort metric, and b) to assess the effect of combined resonant behaviour of a vehicle and human subject dynamic system.

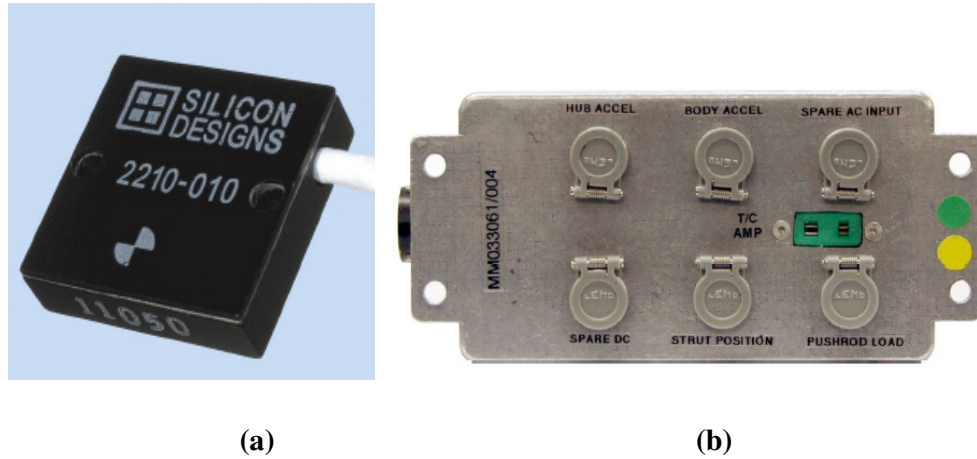


Figure 3.9: a) The model 2210 accelerometers b) Connector and Logical Channels

3.5.2 Experimental Protocol

The experiments were performed on a BMW Mini Cooper car to measure response at locations where the driver is exposed to vibrations. These locations are the driver's seat cushion and the seat base. From the measured data the seat and floor response to vibration, and transmissibility between them in heave, pitch, roll and pitch-roll motions are analysed. The driver seat has a backrest and seat surface inclined at 13° to the horizontal. A total of ten channels of acceleration (three ' a_4 , a_5 and a_6 ' on the seat surface and seat base ' a_1 , a_2 and a_3 ' (Fig. 3.10); four FL (front left), FR (front right), RL (rear left) and RR (rear right) pad accelerations) was recorded. Accelerometers were mounted on the driver seat surface and the driver seat base respectively in the triangular position shown in Figure 3.10. A bag weighing 51 kg was placed on the seat for the equivalent weight of the occupant.

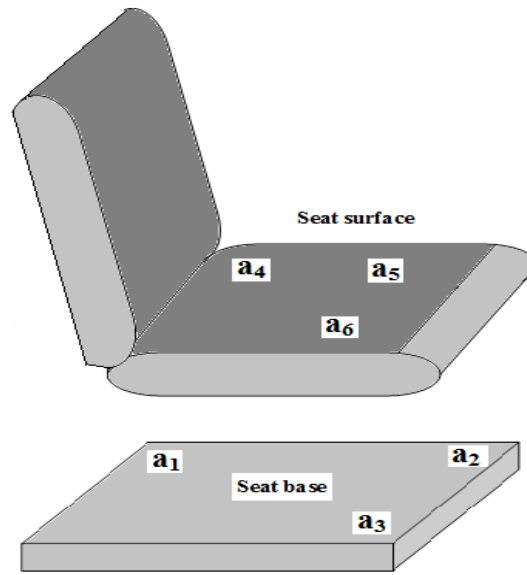


Figure 3.10: Installation of 2210 model accelerometers on the seat.

3.5.3 Results and Analysis for Resonance Behaviour of Car and Seat

In this experimental study, the transmission of vibration in the motions of heave, pitch and roll modes from the road-to-seat base; from the road to the seat surface; from the seat base to the seat surface were measured for given input amplitudes. The input amplitudes were calculated by keeping the velocity constant (80 mm/s) for each frequency level.

The experiments were carried out at 0.25 Hz steps, from 0.25 Hz up to 20 Hz with a constant sine wave for 10 seconds duration without a seated human in a car. The four-post rig pads were positioned 75 mm from the ground level. The input amplitude of the pad varied between 50 mm and 0.65 mm. In the excitations for particular car motion, the rig started from the standstill position. Therefore, transients and frequency contamination may occur. To overcome anticipated difficulties, the frequency and amplitude were gradually increased from zero to the required values so that no transients were experienced.

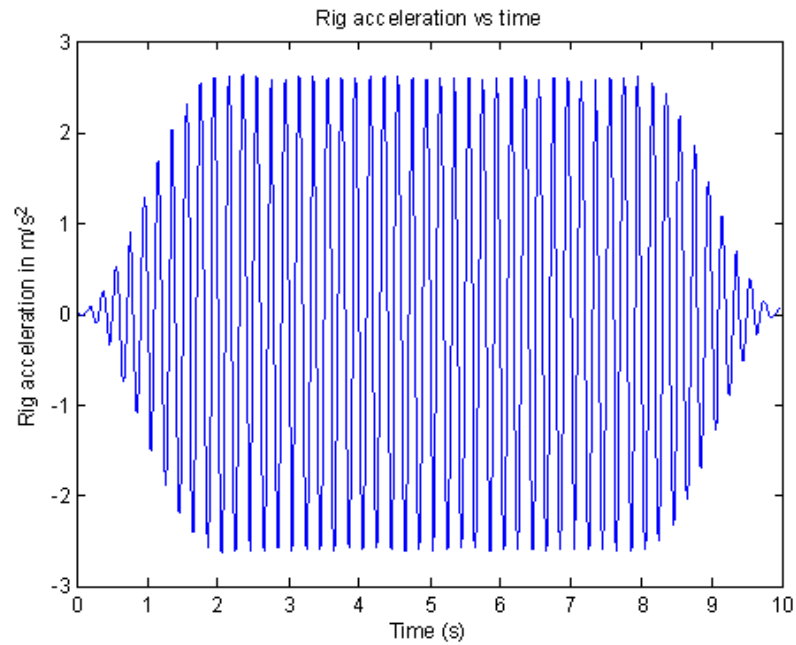


Figure 3.11: The rig acceleration (rear-right (RR)) time history in heave mode at 5 Hz based on dependent constant velocity.

Figure 3.11 shows one such input i.e. pad acceleration at 5 Hz frequency for 10 seconds duration in heave mode based on 80 mm/s constant velocity; it is clear that by 2 seconds the input reaches required value and it stays constant until 8 seconds is reached and after that gradually reduces to zero amplitude. Figure 3.12 shows the seat acceleration at one of the locations. As expected, no transient build-up is seen in the plot.

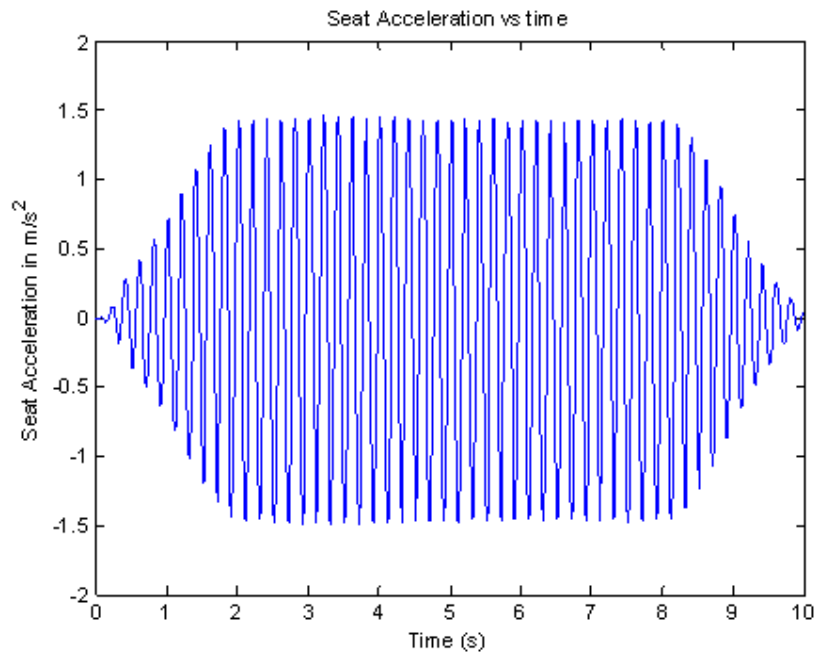


Figure 3.12: The seat acceleration time history in heave mode at 5 Hz based on dependent constant velocity.

The test results recorded by the Dynosoft MX software were analysed in Matlab using the RMS (root-mean-square) method and Transfer Function Estimate method (see Chapter 2). The time history, for the 6 second duration between 2 seconds and 8 seconds, is analyzed. Using the transmissibility equation repeatedly at all the excitation frequencies, frequency response functions can be constructed. In this study, the resonance behaviour of the car and seat are characterized. The transmission of vertical and angular vibration through the seat base and seat surface is considered.

a) Heave Mode of input

The floor response (i.e. eventual input for seat vibration studies) with respect to the pads (pad motion is the source of vibration that simulates the road and the tyre contact) is shown in Figure 3.13. The transmissibility (measured frequency response functions) variables are given in Appendix B, Table B.1. Resonant behaviour is clearly seen in the plot. The first dominant peak occurs at 1.75 Hz

where the transmissibility is 1.5. The peak corresponds to the car body bounce or heave mode of vibration. The second peak, which represents the dominant motion of wheels (hub mode) of the car, occurs at 13.25 Hz where the transmissibility is 0.4. Small variations are also seen around 8 Hz. In all there are four curves in the plot; these correspond to four inputs. As seen, all four transmissibilities are almost identical which gives confidence in the rig inputs; therefore, a mean of pad accelerations is used to evaluate the seat and floor responses. The characteristics discussed above influence the inputs to the seat. This behaviour cannot be replicated completely when shaker table tests are used.

Figure 3.14 shows the seat response with respect to the pad acceleration. The first dominant peak occurs at 1.75 Hz where the transmissibility is 1.5. It corresponds to the car body bounce mode of vibration as seen in Figure 3.13. Due to the transmitted vibration from the wheels (hub mode) the influence of vibration on the floor and seat are seen between 7.25 Hz and 13 Hz. There are three small peaks, at 8.75 Hz, 11.5 Hz and 12.75 Hz, where the transmissibilities are 0.51, 0.46, and 0.47 respectively.

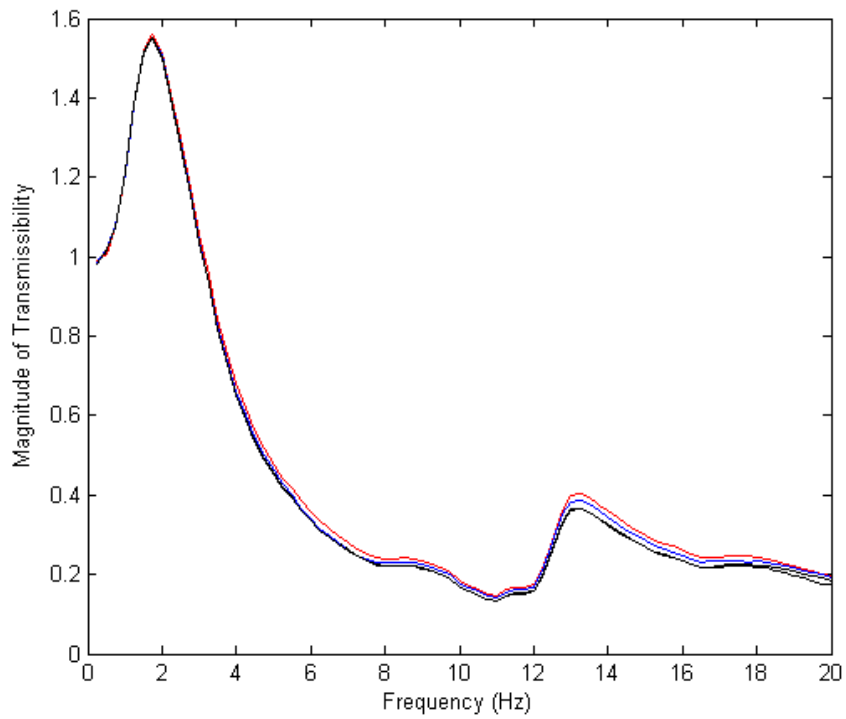


Figure 3.13: The magnitude of transmissibility (floor to pad) with respect to the pad accelerations in heave mode with road input amplitude in the frequency range of 0.25 Hz- 20 Hz for 10 seconds durations. The four lines are for estimations based on four pad inputs respectively.

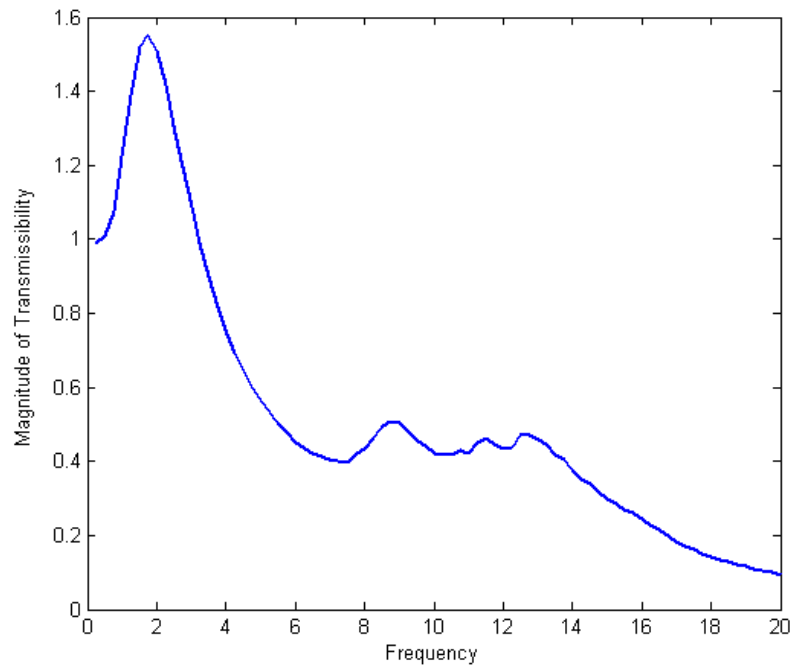


Figure 3.14: Seat transmissibility (measured frequency response functions) with respect to the pad accelerations in heave mode with road input amplitude in the frequency range of 0.25 Hz -20 Hz.

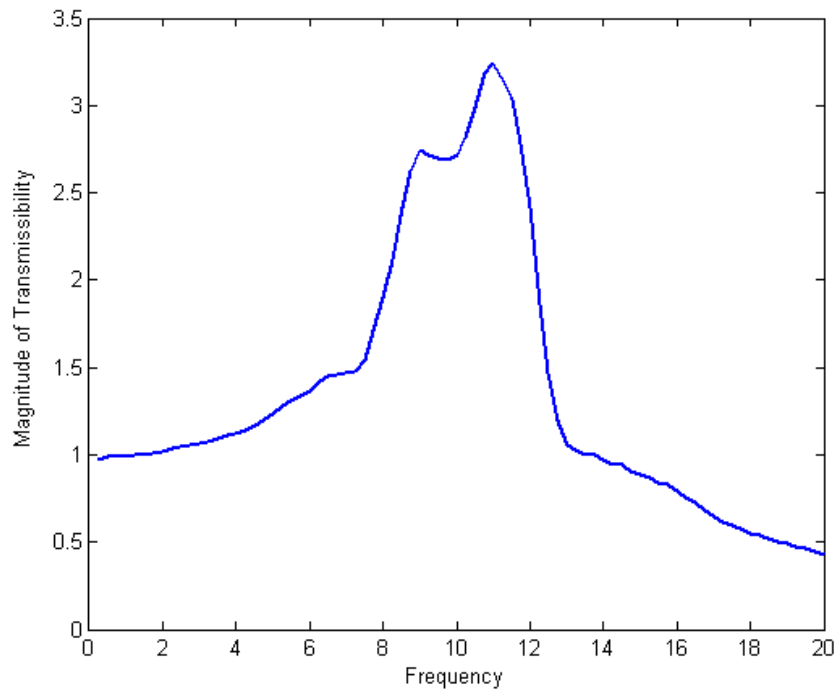


Figure 3.15: Seat transmissibility (measured frequency response functions) with respect to the floor accelerations in heave mode in the frequency range of 0.25 Hz -20 Hz.

Figure 3.15 shows the seat transmissibility with respect to the floor acceleration. The first small peak occurs at around 9 Hz, where the transmissibility is 2.74. This peak corresponds to the seat heave response. The second dominant peak occurs at 11 Hz, where the transmissibility is 3.24. This peak corresponds to the seat backrest response.

b) Pitch Mode of input

i) Angular Input to Linear Output

Figures 3.16 and Figure 3.17 show the responses relating angular input to linear output measurement results in pitch mode. In Figure 3.16 the floor response with respect to the pad inputs is given. The first and second sharp peaks occur at around 2 Hz and 12.75 Hz respectively. These two peaks correspond to the car body pitch mode and the hub mode of vibration. Small variations are seen at around 4.75 Hz and 6.5 Hz.

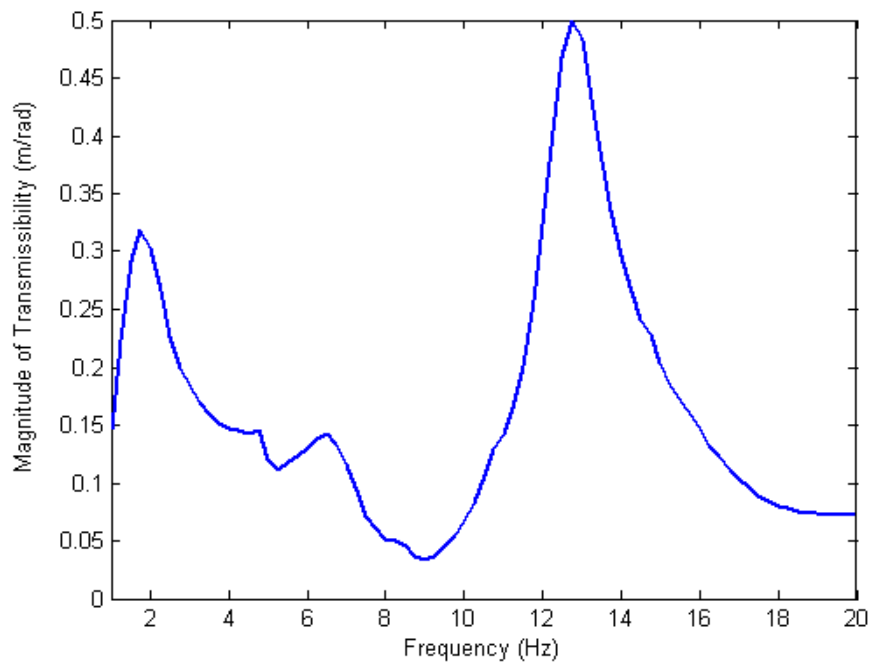


Figure 3.16: Linear floor transmissibility (measured frequency response function) with respect to the angular pad accelerations in pitch mode with road input amplitude in the frequency range of 1 Hz -20 Hz.

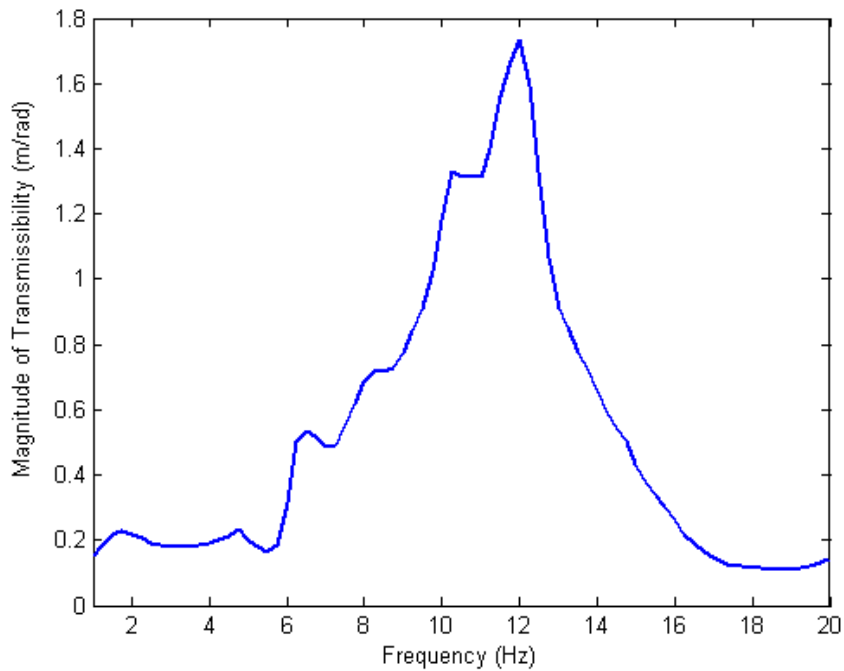


Figure 3.17: Linear seat transmissibility (measured frequency response function) with respect to the angular floor acceleration in pitch mode with road input amplitude in the frequency range of 1 Hz -20 Hz.

Figure 3.17 shows the seat response with respect to floor accelerations. The sharp dominant peak occurs at 12 Hz, where the transmissibility is 1.73. This peak corresponds to the seat backrest response in pitch mode. As can be seen in the plot, small peaks and variations occur at around 4.75 Hz, 6.5 Hz, 8.25 Hz and 10.5 Hz.

ii) Angular Input to Angular Output

Figures 3.18 and 3.19 show the angular input to angular output results of car characterization measurement in pitch mode. The floor response with respect to the pad inputs is shown in Figure 3.23. Resonant behaviour is clearly seen in the plot. The first dominant peak occurs at 2 Hz where the transmissibility is 1.57. The peak corresponds to the car body in pitch mode. The second peak occurs at 13 Hz where the transmissibility is 0.55. This peak corresponds to the wheel motion in pitch mode of input.

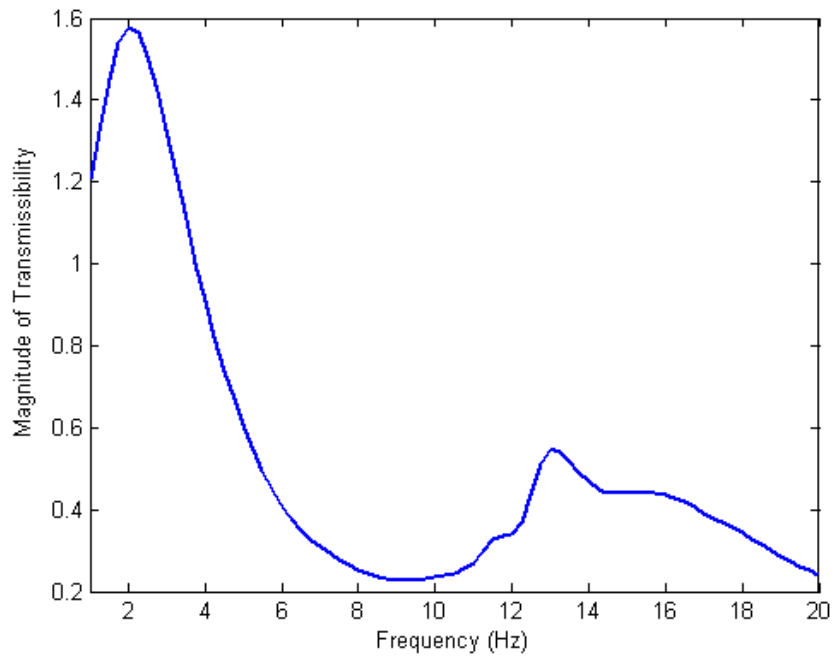


Figure 3.18: Angular floor transmissibility (measured frequency response function) with respect to the angular pad accelerations in pitch mode with road input amplitude in the frequency range of 1 Hz -20 Hz.

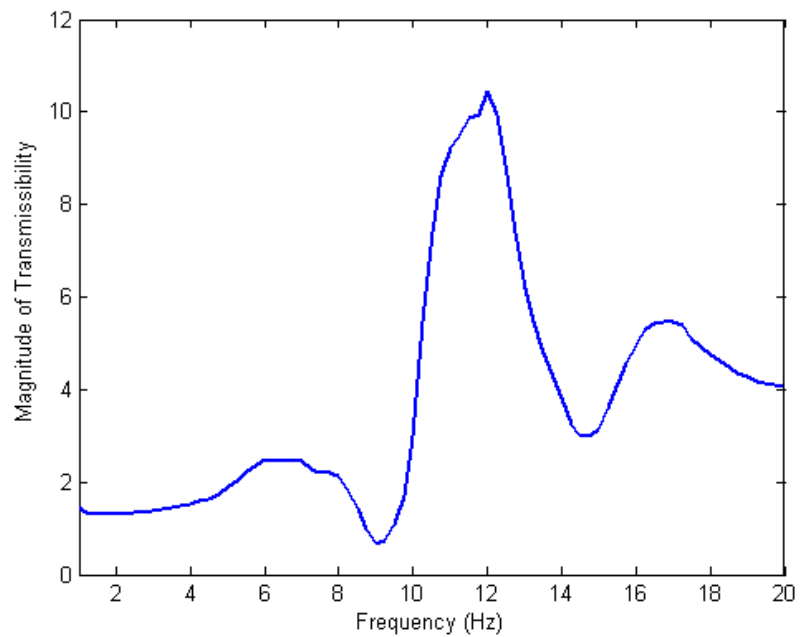


Figure 3.19: Angular seat transmissibility (measured frequency response function) with respect to the angular floor acceleration in pitch mode with road input amplitude in the frequency range of 1 Hz -20 Hz.

Figure 3.19 shows the seat response with respect to the floor acceleration. The sharp dominant peak occurs around 12 Hz, where the transmissibility is 10.44. This peak corresponds to seat backrest motion.

c) Roll Mode of input

i) Angular Input to Linear Output

Figures 3.20 and 3.21 show the angular input to linear output measurement results for roll input. Figure 3.20 shows the linear floor transmissibility with respect to the pad input accelerations. The first dominant peak occurs at 2.25 Hz, where the transmissibility is 0.81. This peak corresponds to the car body movement in roll mode. The second peak occurs at 13.75 Hz where the transmissibility is 0.22. This peak corresponds to the hub mode (wheel motion) contribution. Small variations at 4.5 Hz and two small peaks occur at around 6.5 Hz and 7.75 Hz are seen in the plot.

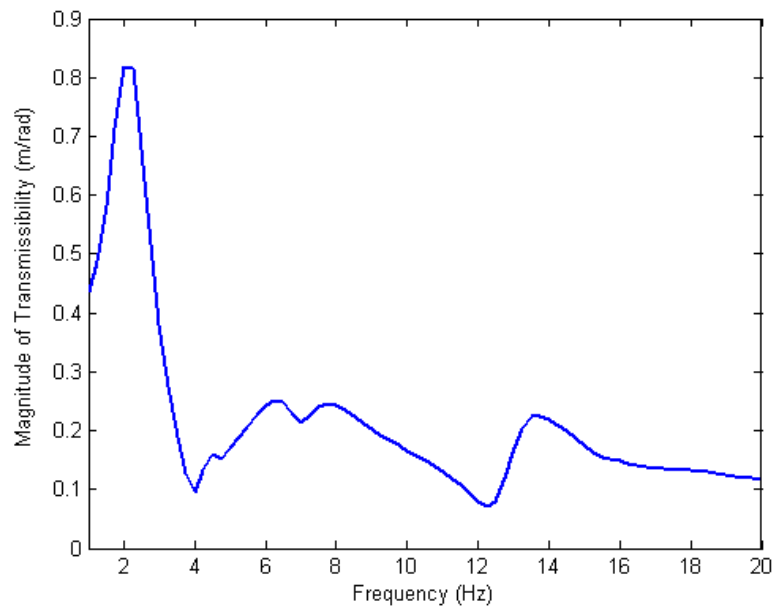


Figure 3.20: Linear floor transmissibility (measured frequency response function) with respect to the angular pad accelerations in roll mode with road input amplitude in the frequency range of 1 Hz -20 Hz.

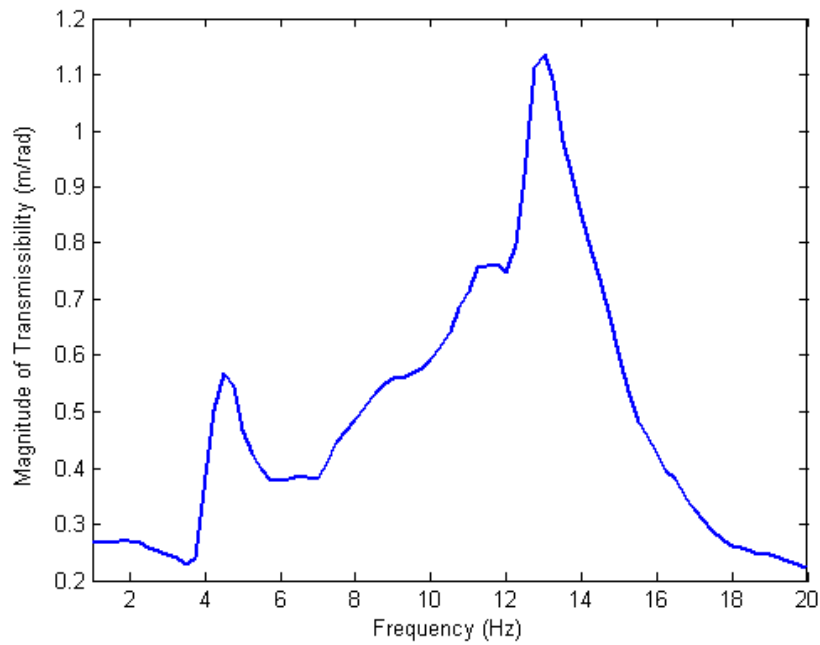


Figure 3.21: Linear seat transmissibility (measured frequency response function) with respect to the angular floor acceleration in roll mode with road input amplitude in the frequency range of 1 Hz -20 Hz.

Figure 3.21 shows the seat response with respect to the floor acceleration. The sharp and dominant peak occurs at 13 Hz, where the transmissibility is 1.13. This peak corresponds to the seat backrest response for the roll input. A small peak and small variations are seen in the plot at 4.45 Hz, 8.75 Hz and 11.25 Hz respectively.

ii) Angular Input to Angular Output

Figures 3.22 and Figure 3.23 show the angular input to angular output measurement results. Figure 3.22 shows the floor response with respect to the pad input accelerations. The first dominant and sharp peak occurs at 2 Hz, where the transmissibility is 2.35. This peak corresponds to the car body motion in roll mode and small variations and peaks are seen in the plot at around 4.75 Hz, 6.25 Hz and 8 Hz, of which one of the peaks corresponds to seat heave motion. The hub mode is not clearly seen in the plot.

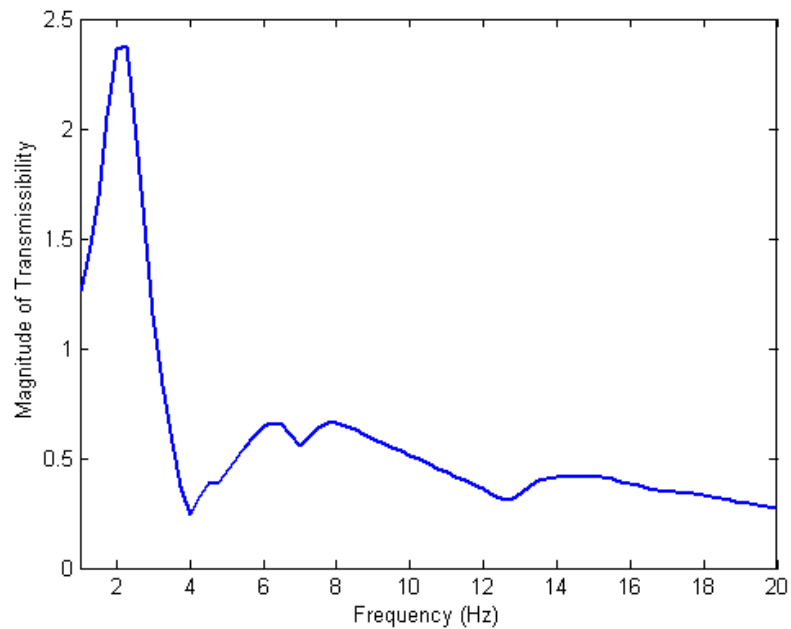


Figure 3.22: Angular floor transmissibility (measured frequency response function) with respect to the angular pad accelerations in roll mode with road input amplitude in the frequency range of 1 Hz -20 Hz.

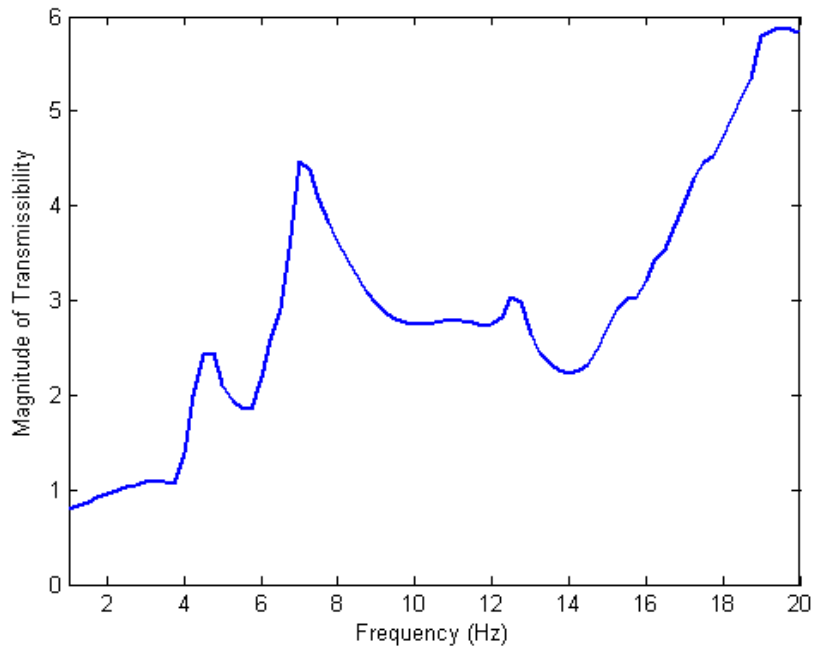


Figure 3.23: Angular seat transmissibility (measured frequency response function) with respect to the floor acceleration in roll mode with road input amplitude in the frequency range of 1 Hz -20 Hz.

Figure 3.23 shows the seat response with respect to the floor accelerations. The first small peak occurs at 4.5 Hz (the effect of yaw motions as observed during the tests), where the transmissibility is 2.44. The second peak occurs at 7 Hz, where the transmissibility is 4.46; this peak corresponds to the seat response in roll mode. A third small peak occurs at 12.5 Hz, where the transmissibility is 3.03. This peak corresponds to the seat backrest response. The transmissibility is increasing rapidly after 15.5 Hz, which shows sensitivity to roll input at higher frequencies.

3.6 DISCUSSION

In this chapter, the resonance behaviour of a car and seat was analyzed on the four-post rig with respect to the ‘cause-effect’ relations. The experiments were carried out at 0.25 Hz steps, from 0.25 Hz up to 20 Hz with constant sine wave input for 10 second durations. The measurement results were evaluated in reference to the transmissibility for the road to the car, floor and seat. The resonant frequencies observed in this analysis are listed in Table 3.4. The backrest responds well for frequencies between 11 and 12.5 Hz. This behaviour might change significantly when the seat is occupied as the interaction between the human body and the backrest is expected to change the dynamics.

| Resonance behaviour | Heave Mode | Pitch Mode | Roll Mode | Yaw Mode | Input-Output |
|--------------------------|------------|------------|-----------|----------|--------------------|
| The car body | 1.75 Hz | 2 Hz | 2.25 Hz | - | Angular to Linear |
| | | 2 Hz | 2 Hz | - | Angular to Angular |
| Hub mode (Wheel motions) | 13.25 Hz | 12.75 Hz | 13.75 Hz | - | Angular to Linear |
| | | 13 Hz | - | - | Angular to Angular |
| Seat response | 9 Hz | 10.5 Hz | 11.25 Hz | - | Angular to Linear |
| | | 11.5 Hz | 7 Hz | 4.5 Hz | Angular to Angular |
| Seat backrest response | 11 Hz | 12 Hz | 13 Hz | - | Angular to Linear |
| | | 12 Hz | 12.5 Hz | - | Angular to Angular |

Table 3.4: Resonance behaviour of a BMW Mini Cooper.

CHAPTER 4

TEST PROCEDURE FOR *IN-SITU* MEASUREMENT OF VEHICLE DISCOMFORT

4.1 INTRODUCTION

Understanding human response to vibration is one of the most important contributing factors in improving ride quality [38] and driver-passenger expectations in terms of comfort or discomfort [21]. Achieving a high performance and quality of ride comfort requires a method of measurement, evaluation and assessment of bounce, pitch and roll motions with consideration of human sensitivity and perception. There is no universally [10] accepted measurement method for quantification of comfort. However, subjective assessment and objective measurement [30, 87-89] are the main approaches to the understanding of the relationship between the vibration stimuli and the level of comfort/discomfort in terms of the sensitivity level of a seated human exposed to vibration. The characterization and quantification will help improve understanding the design requirements of a vibration control strategy to achieve good comfort under the influence of multi-direction inputs.

Many researchers have been performing studies involving objective measurements with questionnaires [2] to measure comfort. These lab based studies use ‘a driver seat’ placed on a motion platform to assess the ride comfort/discomfort by the response of a seated person [2, 19]. These methods, however, invariably use some form of shaker table. Although this area of research has been explored extensively, there are gaps in the information, viz:

- a) The discomfort curves produced for heave motion are at a limited number of frequencies which will restrict development of detailed predictive models.

- b) Although experiments have been conducted to assess discomfort due to pitch and roll motion the variety of excitations used is limited.
- c) The test setups may not capture the complexity of vibration input required and further they do not include the effects of the surroundings seen inside a vehicle. The road inputs to any car can result in a complex form of vibration consisting of vertical motion (bounce) superimposed by rotational motion (pitch, roll and yaw).
- d) The weighting to be attached to rotational acceleration, i.e. pitch and roll motions, is not clear because a seat in a vehicle has limited movement (i.e. the seat does not move as much as a body of vehicle moves on the road).

The standard ISO 2631-1 [7] gives more quantitative guidance on the effects of vibration on health and comfort as well as on perception for vertical, horizontal and rotational frequency-weighted acceleration for seated and standing persons. However, this standard does not give any details regarding ‘the type and specification of seat, vehicle model, road conditions,’ etc. The current standards do not provide any guidance concerned with the seated human in a car in pitch and roll mode; nevertheless, a limited amount of information is available from research publications.

The main aim of this Chapter is to assess the dynamic behaviour of a vehicle driver seat in the vertical and rotational motions in order to develop input specification to obtain discomfort curves at several frequencies in an *in-situ* experimental study. In arriving at the experimental procedure three aspects need to be considered.

- a) The magnitude of vibration and duration of exposure to limit injury and pain so that experiments capture only discomfort,
- b) The scaling used to relate objective seat vibration to subjective rating,
- c) Input requirements at four-post rig shakers to achieve seat vibrations for discomfort experimental study. This will remove the vehicle resonant influence and allow the set-up be used as a simulator of heave, pitch and roll motion.

In the next three sections the above requirements are explored using the research database leading to a test procedure that will help achieve the following objectives.

- a) To determine the minimum and maximum RMS (root-mean-square) acceleration of the driver-seat combination for the experiments; to find corresponding pad inputs for the 4-post rig excitation in heave, pitch and roll mode,
- b) To identify the comfort/discomfort scale to be used in the experiments,
- c) To develop an experimental procedure for *in-situ* experimental study.

4.2 VIBRATION LIMITS FOR HUMAN DISCOMFORT

Human response to vibration has been studied by many researchers [2, 3, 13, 30] in order to define ride discomfort/comfort. The determination of ride discomfort/comfort requires subjective judgement. To relate to the easily measurable performance parameters, objective measurement methods have been developed to assist subjective assessment methods. The objective measurement is a way to quantify the vibration in a vehicle, the subjective assessment is the way to judge and define the vibration perception. Ride comfort/discomfort has dependency on the sensation of a seated human subject in a moving vehicle. An important criterion is the human tolerance to vibration which does not exceed a certain level of vibration [13].

The vibration sensation is expressed subjectively in terms of discomfort by the feeling of seated human body subjects. The expression of 'feeling' is a description of the 'effect' of the vibration on the human body. The level of this effect/feeling may be termed using expressions; however the boundaries (level of cause) of the human ride comfort/discomfort are difficult to determine objectively due to the variations in human sensitivity to vibration.

To achieve objective measures for evaluating comfort in the vertical vibrations, it is essential to have an understanding of the human tolerance limits to vibration. The sensation threshold limit of the human body can be affected to a varying degree by the frequency, magnitude, axes and duration. The human body parts can be influenced differently by these factors; the human body segments may have different threshold levels to vibration. Human feeling threshold limit and human sensitivity limit are subjective, i.e. it may change from person to person.

The vibration limit for human comfort is a function of the displacement amplitude, frequency, duration time and acceleration. Comfort criteria were described for vertical vibration by Janeway [13] for passengers. Figure 4.1 shows the comfort criteria curve which covers a specific frequency range in respect of the input vibration amplitude (displacement, acceleration and velocity). The recommended limits which define the acceptable amplitude of vibration are a function of frequency. In the frequency range of 1-6 Hz the jerk value determines the threshold line, where the line represents constant jerk. In this range the product of the amplitude and the cube of the circular frequency should not exceed 12.6 m/s^3 .

For example, at 1 Hz ($2\pi \text{ rad/s}$), the recommended limit of amplitude is 50.8 mm (Eq. 4.1).

$$\frac{12.6 \text{ m/s}^3}{(2\pi \text{ s}^{-1})^3} = 0.0508 \text{ m (2in.)} \quad (4.1)$$

For the frequency of 6-20 Hz range the threshold limit is based on a peak value acceleration of 0.33 m/s^2 . The product of the amplitude and the circular frequency, which is the peak velocity value, should not exceed 2.7 mm/s in the frequency range of 20-60 Hz.



Figure 4.1: Occupant comfort limit in the vertical vibration by Janeway [13].

Janeway's comfort criterion relates the comfort to vertical sinusoidal vibration of a single frequency. This data may not evaluate the resultant effect of vibration where the combinations of different frequencies exist. The data used to establish the ride comfort boundaries were obtained with test subjects standing or sitting on a hard seat. Janeway's comfort criterion study is not sufficient to define human ride comfort boundaries and human tolerance to vibration in heave, pitch and roll motions, i.e. multi-axis vibration.

A general guide of "human fatigue limits to varying modes of vibration" is given in ISO 2631-1 [7] (see Chapter 2) for the frequency range of 1 to 80 Hz. Figure 4.2 shows human tolerance limits to vertical vibrations as a function of both time and frequency. The threshold root-mean-square values (RMS) of acceleration,

which is a function of frequency, are given for the fatigue or decreased proficiency for the exposure to vertical vibration. As expected, for an increase in the average daily exposure time, the threshold decreases.

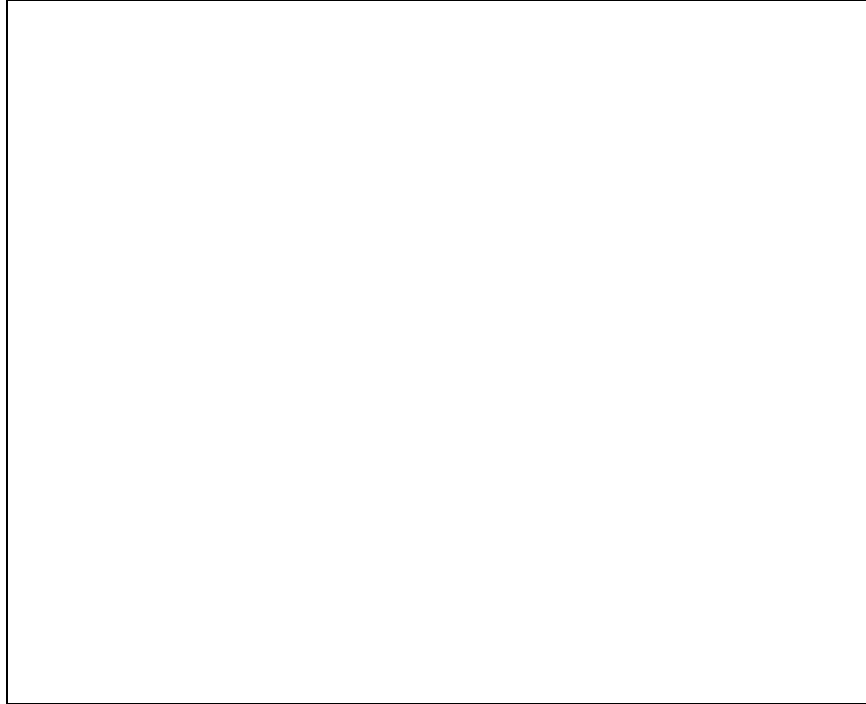


Figure 4.2: Limits of whole-body vibration exposure criteria curves in vertical direction for equal fatigue-decreased proficiency boundaries [13].

The human body is most sensitive below 10 Hz due to the lower threshold of human perception, mainly in the frequency range of 4 Hz and 8 Hz [2, 13] influenced by human body dynamics. Human beings' ability to perceive is the single most difficult element when quantifying vibration threshold. Another factor to consider for human exposure to vibration is the duration and time exposure to vibration. There are exposure limits for safety (health) reasons; ISO 2631-1 [7] recommends a 'health guidance caution zone', which is shown in Fig. 2.4 (see Chapter 2). The dependence of comfort/discomfort on response frequency content and exposure time is of continued interest to researchers.

The human response to vibration excitation depends directly on the characteristic of vibration excitation. The specific frequency value, the magnitude of vibration

and the exposure duration are the main factors used to characterize the excitation [14]. All these effects are captured in some average sense by frequency-weighting and time duration as published in ISO 2631-1 [7].

Due to exposure to vibration there is a risk of injury. This can come from the duration of exposure, frequency content of vibration input and breaching of threshold of pain. The decreased level of vibration input may reduce this risk. In performing experiments to understand and rate comfort/discomfort this risk has to be considered. In this research, the risk of injury will be minimized by restricting: a) the duration of exposure and b) combination of frequency and amplitude in accordance with Fig. 2.4.

In order to define the weighted RMS acceleration limits and exposure duration for each frequency level, Figure 2.4 was referenced in this study. The maximum RMS acceleration was chosen as 1 m/s^2 for heave mode, and as 0.63 m/s^2 for the pitch and roll modes with a 15 sec exposure duration. The quantification of the human response to vibration on these vibration thresholds limits the risk of injury and pain. The RMS acceleration can be controlled by the form of input to the tyres. Several experiments were performed on an empty car to achieve a robust set of input parameters delivering the required accelerations. Ethical approval by Oxford Brookes University was obtained for this experimental study.

4.3 DEFINING OF ‘EFFECT’ BY SUBJECTIVE ASSESSMENT

There is a significant amount of published studies which deal with the relation between objective measurements and subjective ratings in respect of vibration exposure. In this section, the subjective scaling methods and categories available are reviewed in order to develop the relevant scale range for planned *in-situ* experimental study. A seated human responding to vehicle vibration is rated based on the judgement of perceived vibration. These subjective judgements may indicate the level of vehicle seat acceleration. Eventually, the ride discomfort is

assessed by relating objective measurement of vibration and corresponding subjective perception (see Chapter 2).

The most used rating scale methods (Table 4.1) relate subjective perception and vibration exposure [36, 90, 91]. The judgement of the received stimulus is expressed using various terms [30, 89] such as “perceptible, comfortable, uncomfortable, intensity, unpleasantness, annoyance, disturbance and intolerable, etc”.

Various scales of comfort/discomfort are given in Table 4.1 from the published literature. These judgement methods are for only a single frequency and vertical sinusoidal vibration input. The scales evaluated the relationship between the level of vibration acceleration and the respective subjectively perceived values. The vibration input acceleration varies in the range of 0.2 and 3.7 m/s². These types of experimental measurements may not pinpoint accurately the human comfort/discomfort scale in the presence of different frequency spectrums in the vertical and rotational motion exposure. Moreover, the comfort/discomfort scales were determined using the tests on the shaker table or platform. This may not indicate the real vehicle vibration environment. The ratings, however, can be used as a guideline to arrive at the experimental process of this project. The scaling used in this study, showing the subjective rating and the vibration levels, at the seat will be given later in this chapter.

| Source (Year) | Scale (Category) | Frequency-weighted RMS acceleration (m/s^2) |
|---|-----------------------------------|---|
| Fothergill, 1972 [90] | Very unpleasant | 2.5 |
| | Unpleasant | 1.7 |
| | Mildly unpleasant | 1.1 |
| | Not unpleasant | 0.7 |
| | Noticeable | 0.3 |
| Jones & Saunders, 1974 [90] | Very unpleasant | 3.7 |
| | Very uncomfortable | 2.2 |
| | Uncomfortable | 1.2 |
| | Mean threshold of discomfort | 0.7 |
| Oborne & Clarke, 1974 [90] | Not uncomfortable | 0.33 |
| | Very uncomfortable | >2.3 |
| | Uncomfortable | 1.2-2.3 |
| | Fairly uncomfortable | 0.5-1.2 |
| | Fairly comfortable | 0.23-0.5 |
| Fothergill & Griffin, 1977 [90] | Very comfortable | <0.23 |
| | Very uncomfortable | 2.7 |
| | Uncomfortable | 1.8 |
| | Mildly uncomfortable | 1.1 |
| | Noticeable, but not uncomfortable | 0.4 |
| ISO 2631-1, 1997 [7] | Extremely uncomfortable | Greater than 2 |
| | Very uncomfortable | 1.25-2.5 |
| | Uncomfortable | 0.8-1.6 |
| | Fairly uncomfortable | 0.5-1 |
| | A little uncomfortable | 0.315-0.63 |
| Maeda, Mansfield and Shibata, 2008 [91] | Not uncomfortable | Less than 0.315 |
| | Not uncomfortable | >0.56 |
| | A little uncomfortable | 0.56-0.87 |
| | Fairly uncomfortable | 0.87-1.26 |
| | Uncomfortable | 1.26-1.96 |
| Kaneko, Hagiwara And Maeda, 2005, [36] | Very uncomfortable | <1.96 |
| | Not uncomfortable | |
| | A little uncomfortable | 0.2 |
| | Fairly uncomfortable | 0.4 |
| | Uncomfortable | 0.8 |
| | Very uncomfortable | 1.2 |
| | Extremely uncomfortable | 1.8 |

Table 4.1: Various degrees of subjective perception scales and frequency-weighted accelerations.

4.4 DYNAMIC CHARACTERIZATION OF A CAR SEAT

The use of four-post rig and vehicle combination as a simulator requires that the resonant behaviour of the vehicle is accounted for so that consistent vibration seat inputs can be obtained at every frequency and every level of vibration. Series of experiments were conducted with the aim to determine the shaker inputs to obtain particular vibration parameters on the driver seat in a car on the 4-post rig in heave, pitch and roll modes. The results of this experimental study will help create a procedure used in the following chapters regarding objective and subjective measurement of seated human subjects in a car.

4.4.1 The Vehicle Driver Seat Response to Vibration Input at Wheels

As previously mentioned in Chapter 3, the input amplitude can be controlled independently on the four-post rig to achieve a required displacement, velocity or acceleration. The rig can run with 180 mm/s maximum absolute velocity in heave and 160 mm/s for pitch and roll. In order to understand the vibration transfer, a BMW Mini Cooper was tested on the four-post rig with the given range of displacement values. The procedure for the BMW Mini Cooper car set up follows the same rules, as given in Chapter 3, without putting any mass on the driver seat. The measurement locations are the driver's seat cushion and the floor of the front passenger seat. 2210 model accelerometers are mounted as shown in Figure 4.3. The required inputs at the pads for a particular seat output depend on suspension parameters among other things. The experimental results were analyzed based on pad-input and seat-output relations for heave, pitch and roll motions.

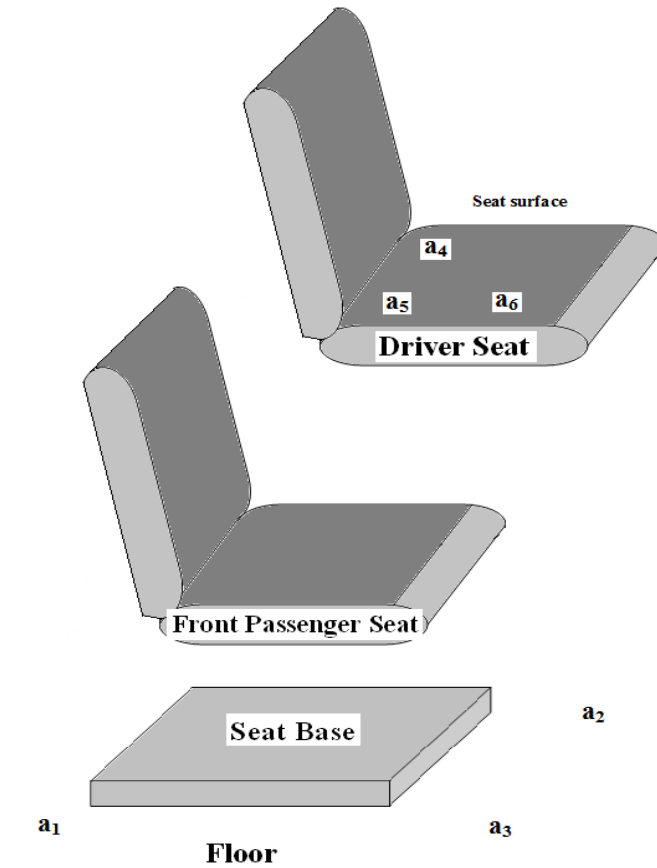


Figure 4.3: Installation of 2210 model accelerometers in the car. The distances between the accelerometers are: a_4 - a_5 : 19 cm, a_5 - a_6 : 5.5 cm, a_1 - a_3 : 90.1 cm, a_2 - a_3 : 27.6 cm.

The BMW Mini Cooper car and driver seat response are measured from 1 Hz up to 16 Hz with constant sine wave pad input for 30 seconds duration on the four-post rig. Table 4.2 lists the sample data for 1 Hz input frequency (the data of Fig. 4.4). The seat acceleration is measured for the ten different input amplitudes at 1 Hz in heave mode. From the measurement results, the seat output accelerations as a function of pad displacement can be plotted as shown in Fig. 4.4. The behaviour is almost linear.

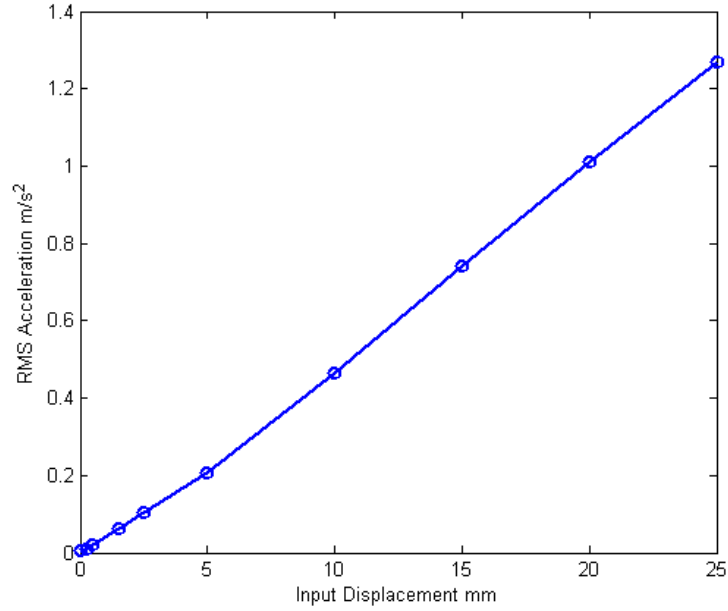


Figure 4.4: Measured RMS (seat) acceleration in respect of the input displacement on the 4-Post-Rig excitation at 1 Hz in heave mode.

| Input Amplitude (mm) | Linear RMS (m/s²) |
|-----------------------------|-------------------------------------|
| 0.05 | 0.0061 |
| 0.25 | 0.0108 |
| 0.5 | 0.0227 |
| 1.5 | 0.0624 |
| 2.5 | 0.1025 |
| 5 | 0.2074 |
| 10 | 0.4648 |
| 15 | 0.7401 |
| 20 | 1.0126 |
| 25 | 1.2702 |

Table 4.2: Measured linear RMS (seat) acceleration in respect of the input amplitude at 1 Hz in heave mode.

Figures 4.5 and 4.6 show that measured output seat acceleration with the input heave mode excitations on the four-post rig at 5 Hz and 10 Hz, respectively. The input amplitudes are decreasing with increased frequencies.

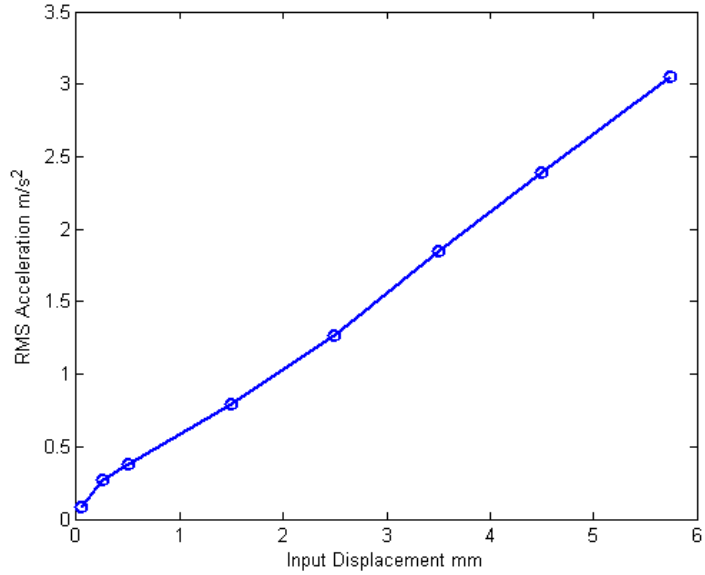


Figure 4.5: Measured RMS (seat) acceleration in respect of the input displacement on the 4-Post Rig excitation at 5 Hz in heave mode.

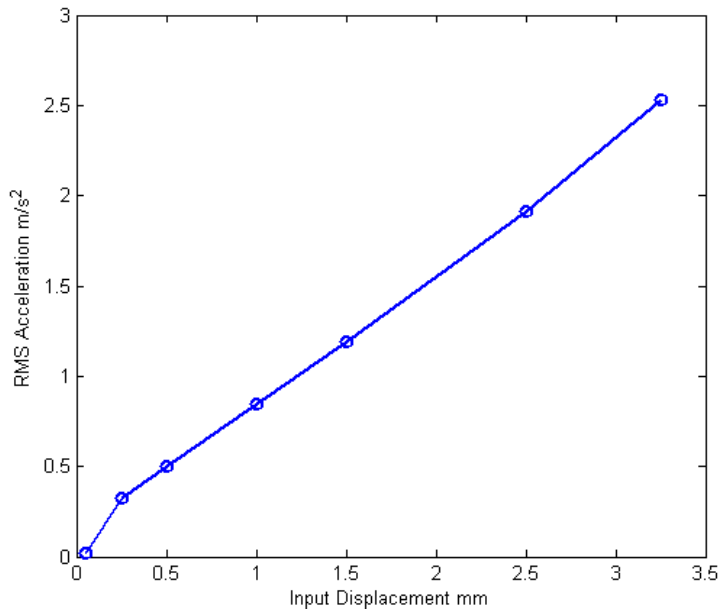
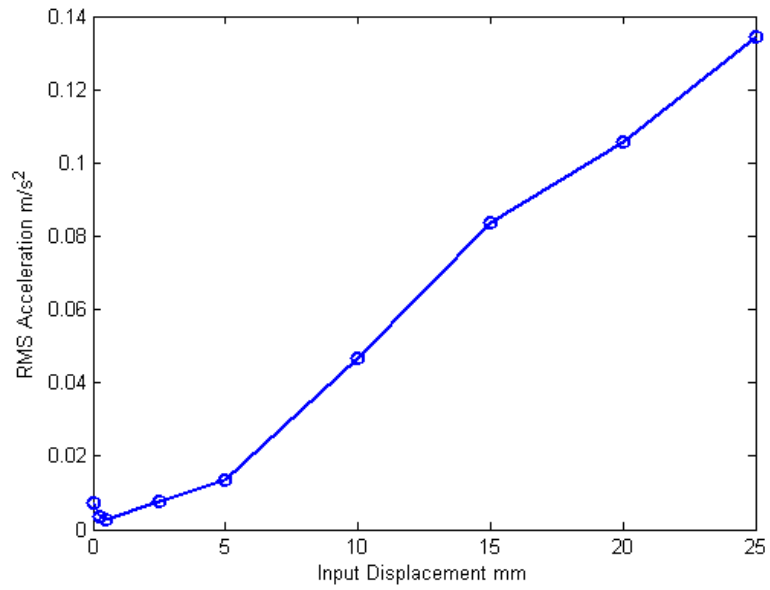
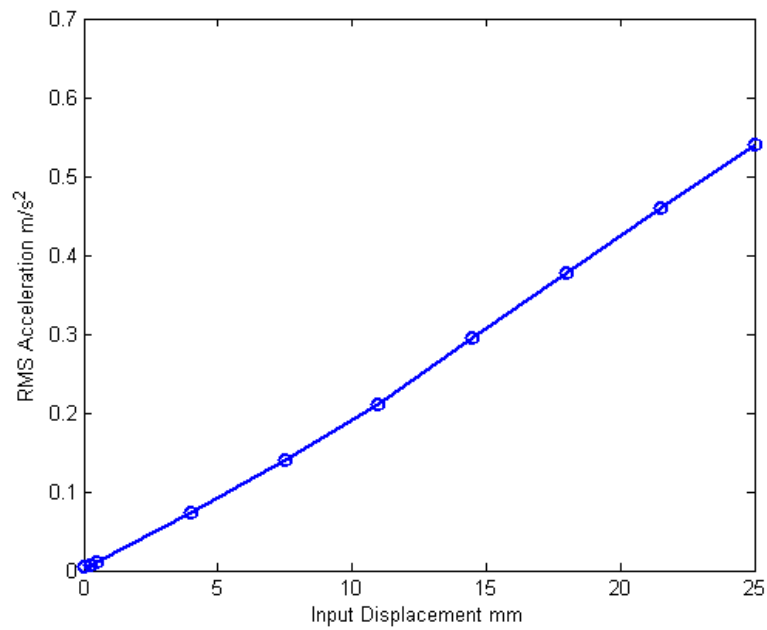


Figure 4.6: Measured RMS (seat) acceleration in respect of the input displacement on the 4-Post Rig excitation at 10 Hz in heave mode.

Similar results for pitch and roll input are shown in Figures 4.7 and 4.8. Due to dynamics and limitations of the test rig, the required maximum amplitude of seat motion cannot be reached in pitch and roll motion. Therefore, the vehicle was tested at 1.75 Hz (Fig. 4.8). The behaviour is highly non-linear.

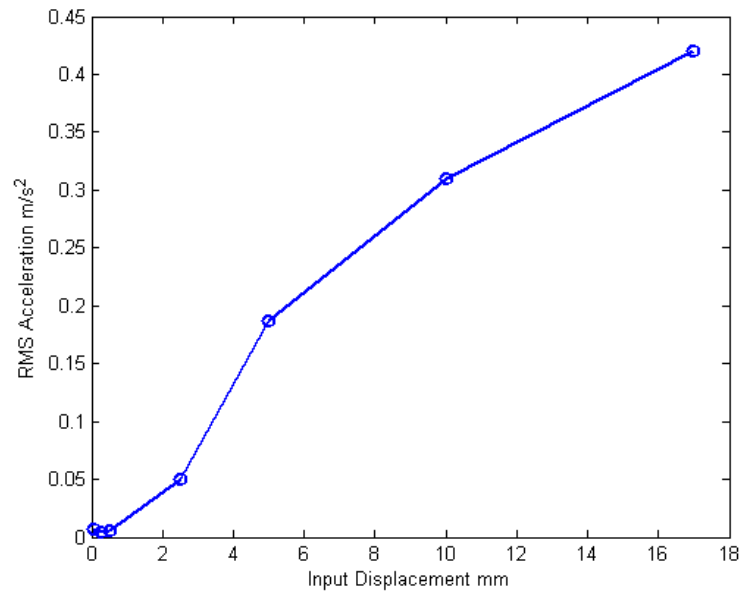


(a)

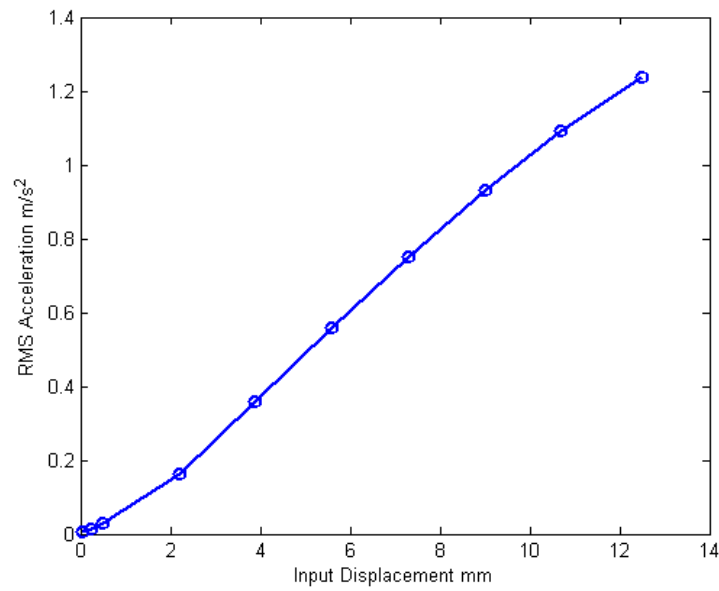


(b)

Figure 4.7: Measured RMS (seat) acceleration in respect of the input displacement on the 4-Post Rig excitation at 1 Hz in pitch mode (a) and roll mode (b) respectively.



(a)



(b)

Figure 4.8: Measured output seat acceleration in respect of the input displacement on the 4-Post Rig excitation at 1.75 Hz in (a) pitch mode and (b) roll mode respectively.

4.5 TEST PROCEDURE FOR *IN-SITU* MEASUREMENT OF CAR COMFORT

In this section, the test procedure is given in detail for *in-situ* measurement of car comfort/discomfort. The experimental procedure was written based on the results of a pilot study on the occupant-seat response to given vibration inputs [92] (see Appendix C). From the characteristics of the seat dynamics, the vibration transmitted to the driver seat and through the driver seat was determined. Participants' physical parameters were recorded. The *in-situ* experimental procedure was determined based on the principle of minimizing the risk.

4.5.1 The Scaling of Vibration Magnitudes for the Degree Level of Discomfort

The output-input relations were assessed in order to estimate the anticipated vibration magnitude on the seat. The weighted acceleration levels (human exposure) and the exposure duration time were determined based on ISO 2631-1 'Health guidance cautions zone' (Fig. 2.4) [7]. The vibration RMS acceleration levels on the seat to be used for discomfort assessment were chosen as 0.1, 0.25, 0.4, 0.63 and 1 m/s^2 for heave mode; 0.1, 0.16, 0.25, 0.4 and 0.63 m/s^2 for pitch and roll modes respectively with 17 seconds exposure time. These acceleration amplitudes are listed in Table 4.3. The aim is that the anticipated linear seat output acceleration will not exceed 1 m/s^2 in heave mode and 0.63 m/s^2 in pitch and roll modes. To provide these weighted acceleration levels on the driver seat, the input amplitudes are calculated from the graphs of input-output relation of vehicle seat response accounting for non-linearity.

The frequency range used is: a) 1 to 15 Hz in heave; b) 1.75 Hz to 15 Hz in pitch and c) 2 Hz to 15 Hz in roll. The stimuli with frequency of 1.75 Hz at 0.4 and 1 m/s^2 RMS, and stimuli with frequencies from 2 Hz to 15 Hz at 1 m/s^2 RMS were not presented in the pitch and roll motions due to a displacement limitation of the four-post rig.

| Weighted acceleration m/s² | | |
|--|--------------|-------------|
| Heave | Pitch | Roll |
| 0.1 | 0.1 | 0.1 |
| 0.25 | 0.16 | 0.16 |
| 0.4 | 0.25 | 0.25 |
| 0.63 | 0.4 | 0.4 |
| 1 | 0.63 | 0.63 |

Table 4.3: Frequency-weighted acceleration level for a seated human in a car on the four-post rig excitation.

Based on the literature review, the chosen discomfort scale is given in Table 4.4 for a seated human in a car on the four-post rig.

| Perception | Rating |
|----------------------------------|---------------|
| Not uncomfortable | 1 |
| Noticeable but not uncomfortable | 2 |
| Slightly uncomfortable | 3 |
| Uncomfortable | 4 |
| Highly uncomfortable | 5 |

Table 4.4: Degree of discomfort scale for a seated human in a car on the four-post rig.

4.5.2 Precautions to Avoid Risk of Injury

There is a risk of injury with respect to human discomfort and health due to exposure to vibration. This can come from the duration of exposure, frequency content of vibration input and breaching of threshold of pain. The decreased level of vibration input may reduce this risk. In this study, the risk will be minimized by restricting: a) the duration time of exposure and b) combination of frequency and amplitude in accordance with ISO 2631 recommendations. In addition, in the event of unforeseen input (failure of the test system), the suspension system restricts the vibration and in effect, along with the seat, acts as an isolator of vibration.

In experiments that will be performed, exposure duration will be of less than 10 min and weighted acceleration will be less than 1; these parameters are taken from ISO 2631-1 which has a figure (Figure 2.4) showing guidelines for threshold limits for human feeling to vibration (see Chapter 2). This measure should ensure injury free experimentation. In addition, the participant questionnaire on health should filter out potentially risky participants.

The weighted acceleration can be controlled by the form of input to the tyres. Several experiments have been performed on an empty car to achieve a robust set of input parameters delivering required accelerations. The setting is such that in the case of a failure of the simulator the vibration levels will be restricted by equipment setting as well as the suspension system of the car. In these unexpected circumstances, the four-post rig platform also has four emergency control buttons; one button controlled by the passenger, and in addition, there is an emergency control on the computer software. When someone is in the car, the system can be switched off by either the intervention of the researcher or the participant during an unexpected event. The car will not continue climbing; it will simply be dropped.

4.5.3 Participants

The experimental study was carried out with twenty-four healthy, trained (not in vibration perception but made aware of the objectives, the test setup and procedure of the experiment) university students (6 females, 18 males) of Oxford Brookes University in the automotive laboratory at the School of Technology. The age, height and weight of the volunteers (Listed in Table 4.5) were in the range 19-36 years, 1.57-1.99 m and 50-100 kg, respectively. With the participants' agreement, each part of the experiment was recorded by a camera. Age was not really part of this study so older occupants were not included.

| Participant Number | F/M | Weight (kg) | Height (m) | Age |
|---------------------------|------------|--------------------|-------------------|------------|
| P1 | M | 78 | 1.76 | 26 |
| P2 | M | 83 | 1.84 | 26 |
| P3 | M | 81 | 1.81 | 29 |
| P4 | M | 60 | 1.80 | 22 |
| P5 | M | 90 | 1.99 | 32 |
| P6 | M | 67 | 1.85 | 20 |
| P7 | M | 67 | 1.65 | 23 |
| P8 | M | 84 | 1.80 | 26 |
| P9 | M | 76 | 1.75 | 26 |
| P10 | M | 85 | 1.80 | 27 |
| P11 | M | 95 | 1.80 | 22 |
| P12 | M | 70 | 1.82 | 31 |
| P13 | M | 73 | 1.82 | 35 |
| P14 | F | 59 | 1.66 | 24 |
| P15 | M | 76 | 1.79 | 25 |
| P16 | M | 77 | 1.73 | 26 |
| P17 | F | 50 | 1.56 | 20 |
| P18 | F | 55 | 1.70 | 23 |
| P19 | M | 100 | 1.76 | 24 |
| P20 | M | 75 | 1.72 | 36 |
| P21 | F | 48 | 1.60 | 19 |
| P22 | M | 90 | 1.83 | 28 |
| P23 | F | 54 | 1.58 | 26 |
| P24 | F | 85 | 1.57 | 19 |

Table 4.5: The physical parameters of the participants.

4.5.4 Procedure

Participants were first given the information sheet explaining the procedure of the experiment. The subjects sat inside the car (Figure 4.12) in a comfortable driving sitting posture, looking straight ahead, with their hands on the steering wheel, wearing a seat belt and with backrest contact. The seated subjects were exposed to sinusoidal vertical vibration having frequencies of up to 15 Hz for 17 seconds duration. Five different magnitudes of vibration were used in the experiment at each frequency.

To prevent confusion, a defined discomfort scale sheet was taped onto the front of the window. It made easy for seated participants to read and assign a number or define verbally their perception. In order to quantify the responses and ride perceptions in the heave, pitch and roll mode frequency range, the discomfort scale included a 4-, 4+ or 5+ point scale. In the degree of discomfort scale, the range (i.e. 4- (3.5), 4+ (4.5), 5+ (5.+)) was added based on the feeling of occupants. This range of scale was determined by the participants in the pilot study. The seated subjects gave their judgements in terms of comfort/discomfort as 'between 3 and 4' or 'more than 3 and less than 4' which was recorded as 3+ or 3.5. This applied for each scale level for *in-situ* experimental study. At the end of each testing session, the subjects specified qualitatively the influence of vibration on different body parts such as back, neck, lower body, upper body and feet. Moreover, the subjects compared the influence of bounce, roll and pitch motion on their body at the end of the testing.



Figure 4.9: A seated human in a car on the four-post rig excitation.

4.5.5 Data Analysis

The measured data was recorded by Dynosoft MX. The rated comfort scale subjective data was recorded by a researcher at the end of each exposure duration time. The end of each testing session the comments of the subjects were recorded. The testing results were analysed in Matlab by using the transfer function, frequency weighted RMS acceleration and power spectral density.

4.6 DISCUSSION

Human sensitivity is an important factor to assess the ride comfort/discomfort in the objective and subjective measurement methods. In this chapter, a new method was developed and investigated for objective and subjective assessment based on the use of the four-post rig. The boundaries of the human tolerance in the Health Caution Zone were evaluated to estimate the test seat response magnitudes on the driver seat under risk assessment conditions. Degrees of discomfort/comfort and subjective assessment were analyzed to develop an experimental procedure for *in-situ* measurement.

CHAPTER 5

EXPERIMENTAL QUANTIFICATION OF DISCOMFORT IN A CAR

5.1 INTRODUCTION

In this chapter, the experimental data of the twenty-four participants will be analysed in order to assess the human discomfort and to develop a discomfort metric. The details of measurement methods, participants, and the procedure are given in Chapter 4. The characteristic of the human response to vibration is determined and evaluated based on the main distinguishing features which are the frequency of vibration, direction of the motion, magnitude of the vibration, duration, and the point of entry of the vibration.

The interaction between the vehicle-seat-road was described in Chapters 2 and 3 in terms of the transmitted vibration. The resonance behaviour of the vehicle was analysed and measurements were performed to obtain the pad input required for achieving appropriate seat vibration levels. Considering the available published literature on vibration perception, the input vibration parameters were determined. A discomfort scale of 1-5 was defined. Eventually complete procedure was developed with consideration of risk associated.

The experiments were performed on twenty-four participants in accordance with the procedure developed in the previous chapter. Each participant was exposed to the vibration five times (increasing excitation amplitudes) for 17 seconds at each frequency in heave, pitch and roll mode. The measured objective and subjective discomfort data are analyzed in this chapter in order to create a discomfort metric. A discomfort metric is developed by using relationships between frequency weighted acceleration and subjective assessment. The results show the varying significance of roll, pitch and heave in related discomfort assessment.

5.2 ANALYSIS OF SUBJECTIVE DISCOMFORT ASSESSMENT IN HEAVE, PITCH AND ROLL MODE

The measured data of the twenty-four people are analysed based on the output RMS acceleration and subjective judgement discomfort scale. According to these evaluated results, the discomfort index is developed for heave, pitch and roll motions. Each measured human subject data is analyzed separately at every frequency; the mean of the results is calculated from all measured human subjects' data at these frequencies. The objective measurement data and subjective assessment data are given in Table 5.1 for a seated human subject (one participant). The data is given only for excitation frequencies between 4 and 6 Hz.

Figures 5.1, 5.2 and 5.3 show the discomfort index of one participant for heave, pitch and roll respectively. The data for the figures is listed in Table 5.1. A fundamental feature of these plots is that they confirm a widely held view of increased stimuli resulting in increasing discomfort. The increase in discomfort is, however, not a linear function of stimuli. Based on the discomfort index the roll input at 5 Hz appears to result in higher discomfort than others, even at lower input amplitude levels. The detailed discussion of the results is given in rest of the chapter.

| | Heave | Heave | Pitch | Pitch | Roll | Roll |
|-----------|--------------------------|--------------|--------------------------|--------------|--------------------------|--------------|
| Frequency | Measured Seat RMS Acc | Subjective | Measured Seat RMS Acc | Subjective | Measured Seat RMS Acc | Subjective |
| Hz | m/s ² | Assessment * | m/s ² | Assessment * | m/s ² | Assessment * |
| 4 | 0.1034 | 1.5 | 0.1060 | 2 | 0.0928 | 3 |
| 4 | 0.2593 | 3 | 0.1703 | 3 | 0.1748 | 3.5 |
| 4 | 0.3945 | 4 | 0.2446 | 3.5 | 0.2494 | 4 |
| 4 | 0.6958 | 4.5 | 0.4424 | 5.5 | 0.4548 | 5 |
| 4 | 1.0727 | 5 | 0.7560 | 5.5 | 0.5483 | 5.5 |
| 5 | 0.1000 | 2 | 0.1103 | 2 | 0.1360 | 2 |
| 5 | 0.2706 | 4 | 0.1642 | 3 | 0.1842 | 3 |
| 5 | 0.4171 | 4.5 | 0.2894 | 4 | 0.2803 | 4 |
| 5 | 0.6843 | 5 | 0.4567 | 5 | 0.3780 | 5 |
| 5 | 1.0823 | 5 | 0.7453 | 5.5 | 0.5542 | 5 |
| 6 | 0.1178 | 2 | 0.1150 | 2 | 0.1179 | 2 |
| 6 | 0.2813 | 3 | 0.1857 | 3 | 0.1718 | 3 |
| 6 | 0.4707 | 4 | 0.2899 | 4 | 0.2792 | 3.5 |
| 6 | 0.7184 | 5 | 0.5143 | 5 | 0.4474 | 4 |
| 6 | 1.1344 | 5 | 0.6921 | 5.5 | 0.7511 | 5 |

Table 5.1: The measured and scaled discomfort assessment data from one participant (P20) are given for the frequency of 4Hz, 5 Hz and 6 Hz. The physical parameters of P20 are; age 36; weight 75 kg; height 1.72 cm (see Chapter 4). *: Degree of discomfort scale (see Chapter 4).

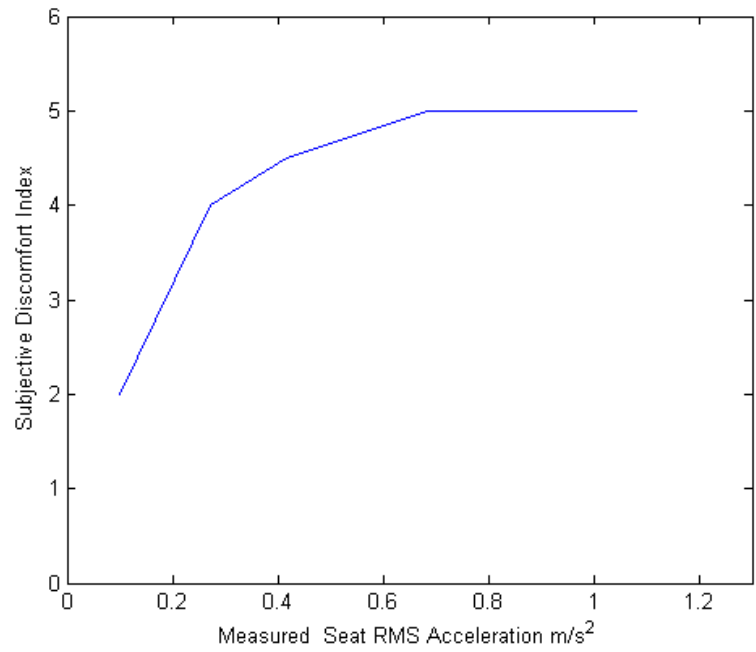


Figure 5.1: Subjective discomfort index with respect to the measured seat RMS acceleration in heave mode at 5 Hz road input.

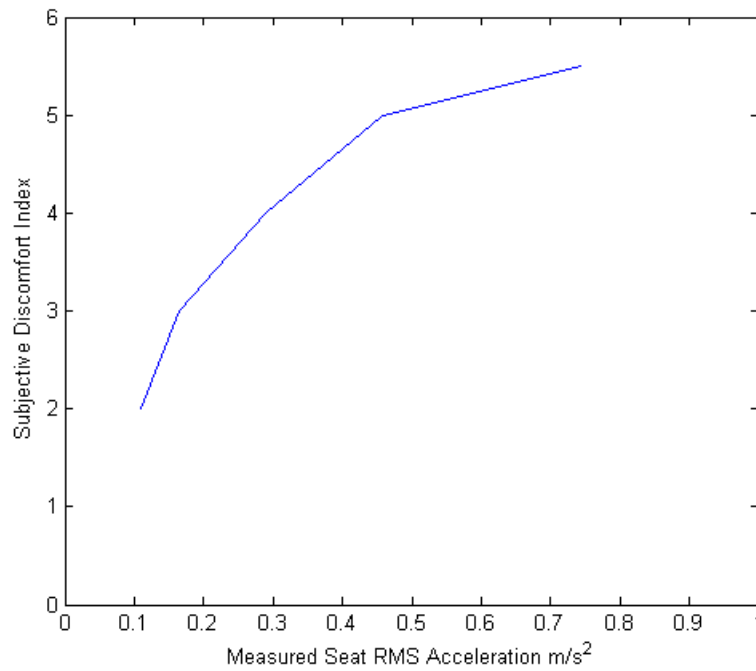


Figure 5.2: Subjective discomfort index with respect to the measured seat RMS acceleration in pitch mode at 5 Hz road input.

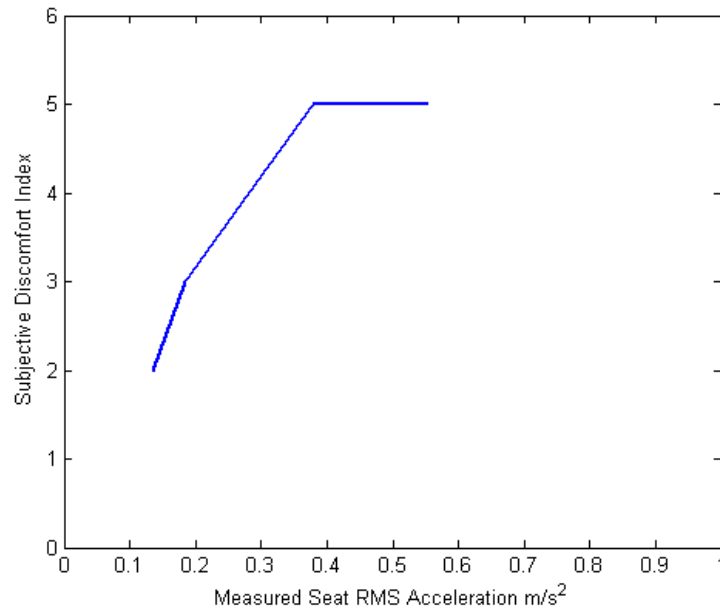


Figure 5.3: Subjective discomfort index with respect to the measured seat RMS acceleration in roll mode at 5 Hz road input.

5.2.1 Analysis of Subjective Discomfort Assessment in Heave Mode

The graphs of heave motion are given in Figures 5.4-5.12. The graphs for the subjective discomfort level varying as a function of the measured seat RMS acceleration at five vibration excitation magnitude 0.1 m/s², 0.25 m/s², 0.4 m/s², 0.63 m/s² and 1 m/s² are shown at 1 Hz, 5 Hz, 10 Hz. Figure 5.4 shows the measurement data for twenty-four subjects, who are marked with different symbols, are exposed to five different magnitudes of vibration for 17 seconds duration. Figure 5.5 show the discomfort index variations for 24 participants in heave mode at 1 Hz.

The spread of discomfort rating at 1 Hz (Fig. 5.4 and 5.5) shows a slight variation for increasing seat acceleration levels. In fact, it increases with acceleration levels. It can be concluded, however, that the sensitivity to magnitude of input acceleration is similar at 1 Hz. The mean of the discomfort index (DCI) is between the feeling of ‘*not uncomfortable and uncomfortable*’ at 1 Hz. Overall,

the mean discomfort rating curve shows a smooth variation. The highly discomfortable rating is never reached. The confidence interval of $\pm 2\sigma$ (Fig. 5.5, σ is standard deviation) also confirms the above finding.

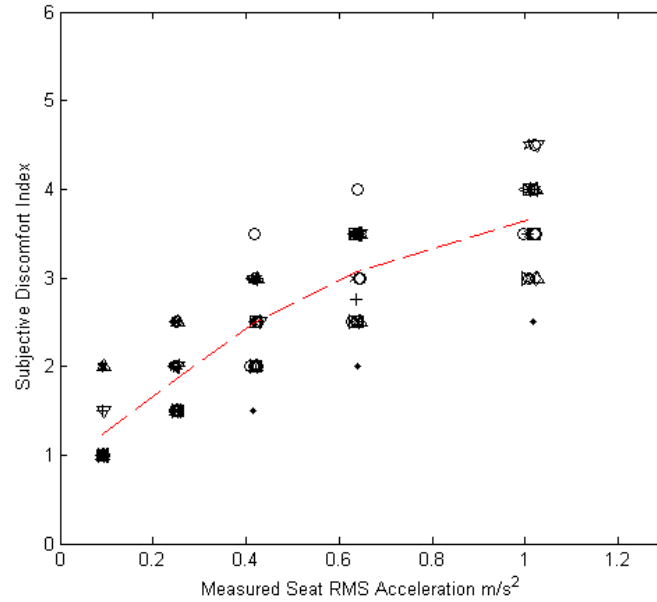


Figure 5.4: Subjective discomfort index with respect to the measured linear RMS acceleration on the seat in heave mode at 1 Hz for vertical vibration. _ _ _ lines represent the mean of the subjective ratings and measured seat RMS accelerations.

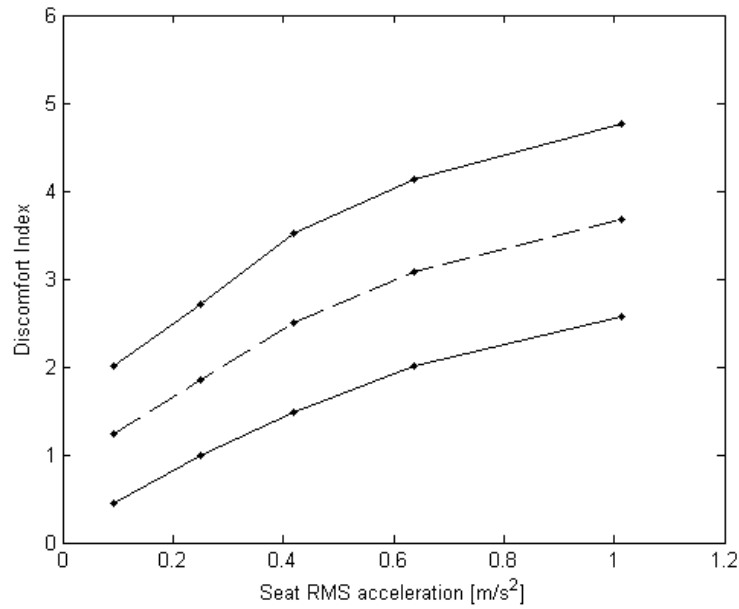


Figure 5.5: Discomfort index variations for 24 participants as a function of seat RMS acceleration as measured during heave input to the vehicle at excitation frequency 1 Hz. — — — — mean discomfort index, _____ mean discomfort index $\pm 2\sigma$.

Figures 5.6 and 5.7 show discomfort ratings for heave input at 5 Hz. Compared with 1 Hz rating, the discomfort level increases with frequency. The D.C.I. is now varying between the feeling of '*noticeable but not uncomfortable and highly uncomfortable*'. When the frequency results are compared, the human body perception is getting more sensitive for increased frequency. The variation in the perception of participants is also getting larger with the frequency (compare Fig. 5.5 and 5.7). The variation at 5 Hz goes up to almost 3 rating levels showing high level of person dependency. This frequency (5 Hz) happens to be in the region of the whole body of human resonance.

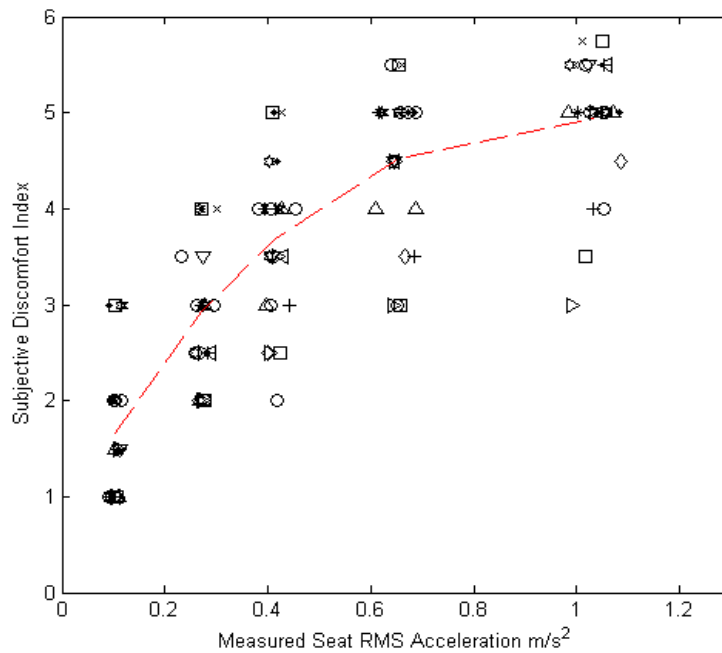


Figure 5.6: Subjective discomfort index with respect to the measured linear RMS acceleration on the seat in heave mode at 5 Hz for vertical vibration. --- lines represent the mean of the subjective ratings and measured seat RMS accelerations.

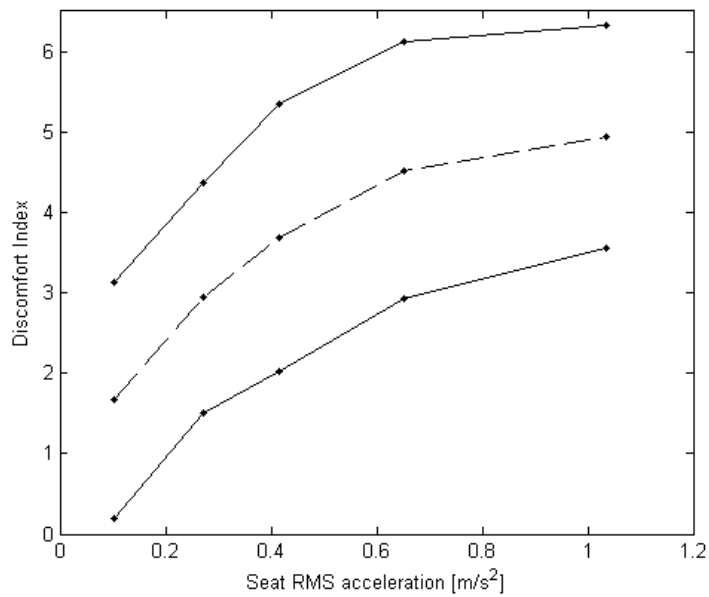


Figure 5.7: Discomfort index variation for 24 participants as a function of seat RMS acceleration as measured during heave input to the vehicle at excitation frequency 5 Hz. --- mean discomfort index, _____ mean discomfort index $\pm 2\sigma$.

Figure 5.8 and 5.9 show discomfort ratings for 10 Hz excitation in heave mode. Overall, the ratings are smaller than that for 5 Hz (compare Fig. 5.6 and 5.8), but the scatter of ratings is similar. The discomfort rating for increasing acceleration on an average varies between the feelings of ‘not uncomfortable to uncomfortable’. At lower amplitude of acceleration the perception variation between participants is slightly smaller than that for higher amplitude acceleration.

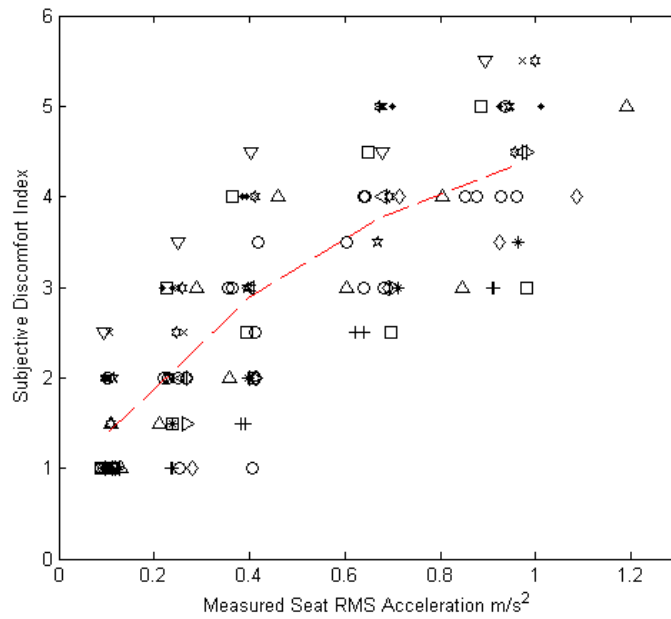


Figure 5.8: Subjective discomfort index with respect to the measured linear RMS acceleration on the seat in heave mode at 10 Hz for vertical vibration. _ _ _ lines represent the mean of the subjective ratings and measured seat RMS accelerations.

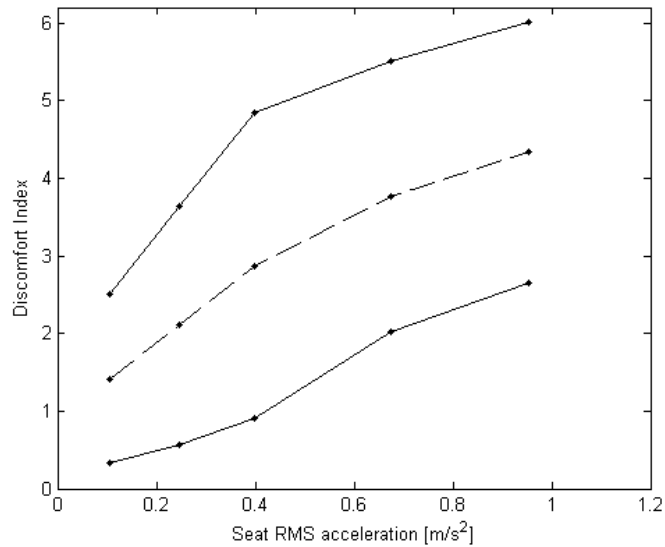


Figure 5.9: Discomfort index variation for 24 participants as a function of seat RMS acceleration as measured during heave input to the vehicle at excitation frequency 10 Hz. — — — — mean discomfort index, _____ mean discomfort index $\pm 2\sigma$.

Figures 5.10 to 5.12 show the mean of participant discomfort rating curves for frequencies varying from 1 to 15 Hz. The difference in ratings depends on the seat RMS acceleration values. For up to 5 Hz (Fig. 5.10), the difference in ratings is small for lowest of the seat acceleration i.e. the influence of frequency is minimal. At larger amplitudes the differences increase and the effect of frequencies is clear. The perception sensitivity is the highest for 5 Hz. The effect of frequency diminishes for higher frequencies (Fig. 5.11 and Fig. 5.12). The curves overlap for frequencies between 6 and 10 Hz. Similar behaviour is seen for frequencies 11 to 15 Hz.

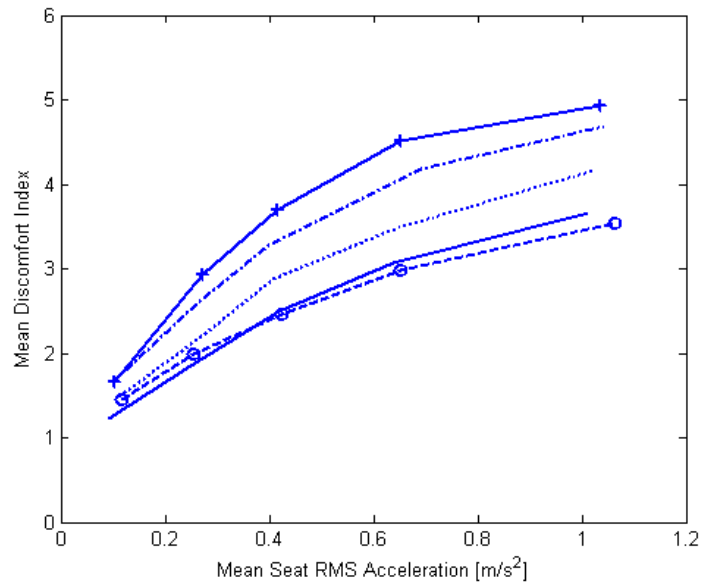


Figure 5.10: Mean discomfort index variation for 24 participants as a function of mean seat RMS acceleration as measured during heave input to the vehicle at excitation frequency level between 1 Hz - 5 Hz. — 1 Hz, —○— 2 Hz, 3 Hz, -.-.- 4 Hz, —+— 5 Hz.

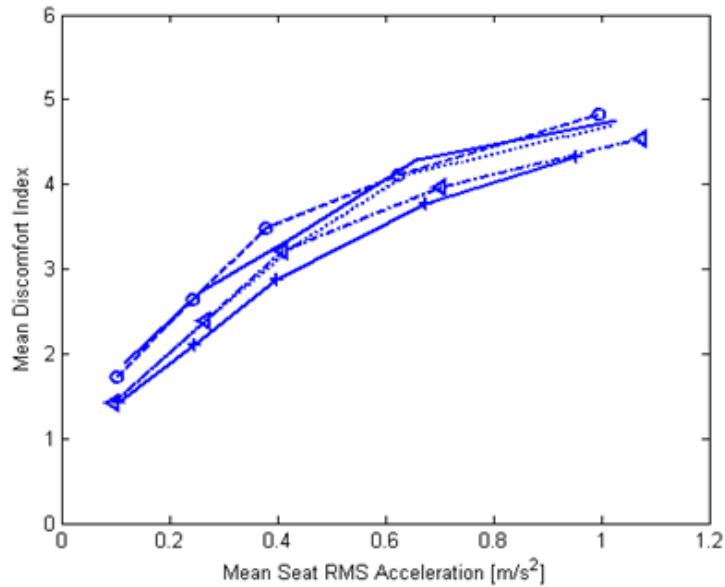


Figure 5.11: Mean discomfort index variation for 24 participants as a function of mean seat RMS acceleration as measured during heave input to the vehicle at excitation frequency level between 6 Hz - 10 Hz. — 6 Hz, —○— 7 Hz, 8 Hz, —◀— 4 Hz, —+— 10 Hz.

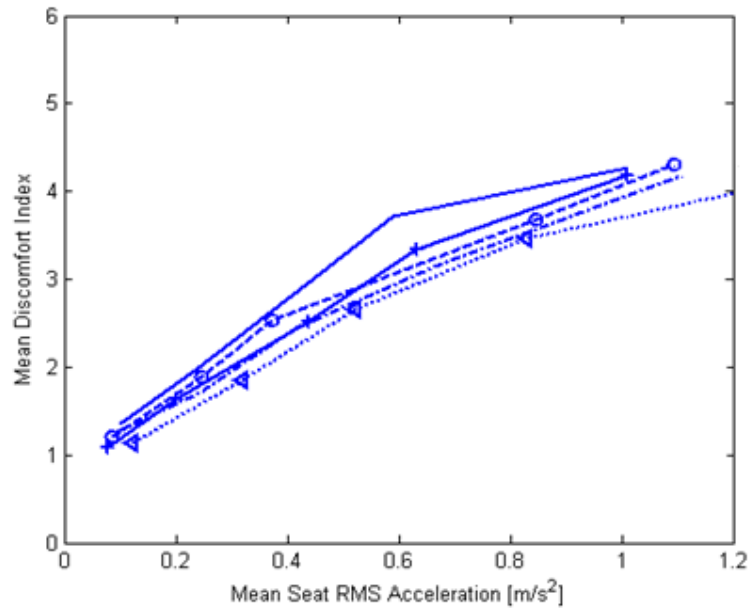


Figure 5.12: Mean discomfort index variation for 24 participants as a function of mean seat RMS acceleration as measured during heave input to the vehicle at excitation frequency level between 11 Hz - 15 Hz. — 11 Hz, -○- 12 Hz, ···◀··· 13 Hz, -·-·- 14 Hz, —+— 15 Hz.

5.2.2 Analysis of Subjective Discomfort Assessment in Pitch Mode

Figures 5.13 and 5.14 show discomfort curves for 3 Hz pitch mode of input. The X axis is shown in terms of equivalent rectilinear motion rather than angular motion. The plots show increased sensitivity to vibration in pitch mode as compared with heave mode input for both low and high accelerations; overall, the mean value curve appears to have shifted up compared to, for example, Figure 5.4. The feeling of high discomfort is reached at much smaller values of seat accelerations. The scatter (Fig. 5.14) is of similar level at low and high seat accelerations.

Figures 5.15 and 5.16 show results for 5 Hz pitch mode input. Relatively, the sensitivity is higher at this frequency compared with 3 Hz. The discomfort ratings range from noticeable but not uncomfortable to highly uncomfortable. The scatter is of similar range throughout the acceleration changes. Figures 5.17 and 5.18 show discomfort curves for 10 Hz pitch input. The results range from feeling of not uncomfortable to uncomfortable. The scatter appears relatively large at larger seat accelerations.

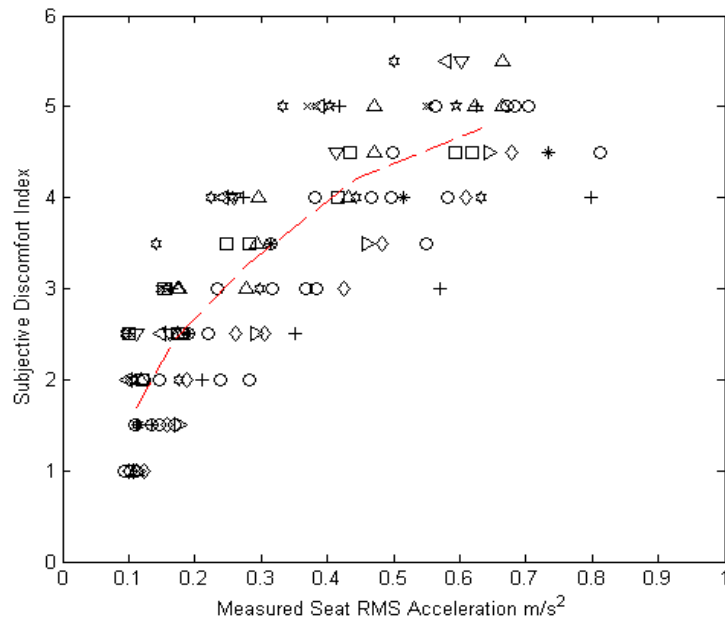


Figure 5.13: Subjective discomfort index with respect to the measured linear RMS acceleration on the seat in pitch mode at 3 Hz for vertical vibration. _ _ _ lines represent the mean of the subjective ratings and measured seat RMS accelerations.

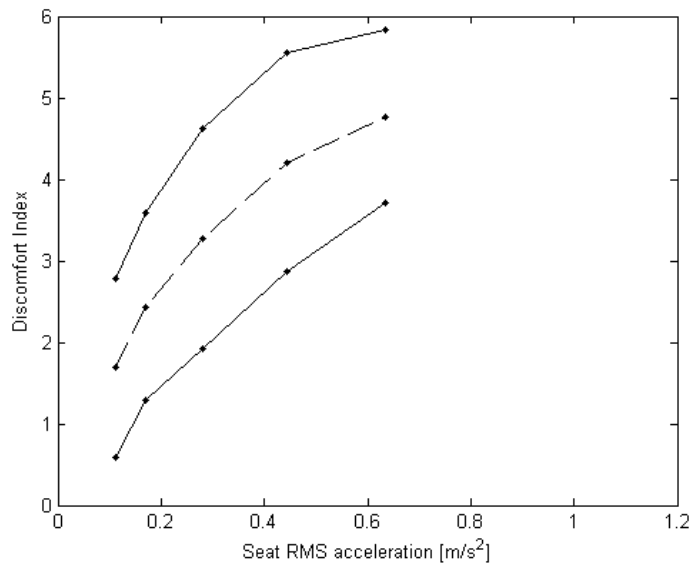


Figure 5.14: Discomfort index variation for 24 participants as a function of seat RMS acceleration as measured during pitch input to the vehicle at excitation frequency 3 Hz. _ _ _ _ mean discomfort index, _ _ _ _ mean discomfort index $\pm 2\sigma$.

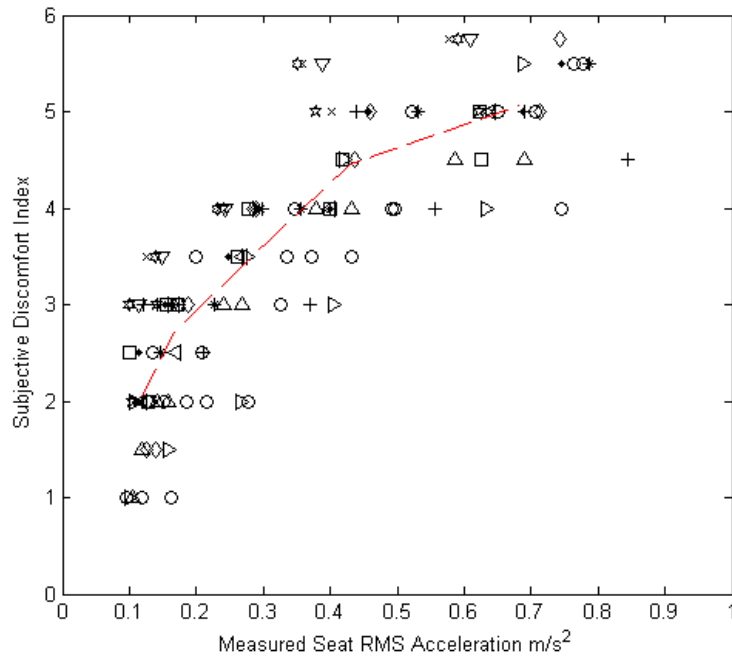


Figure 5.15: Subjective discomfort index with respect to the measured linear RMS acceleration on the seat in pitch mode at 5 Hz for vertical vibration. --- lines represent the mean of the subjective ratings and measured seat RMS accelerations.

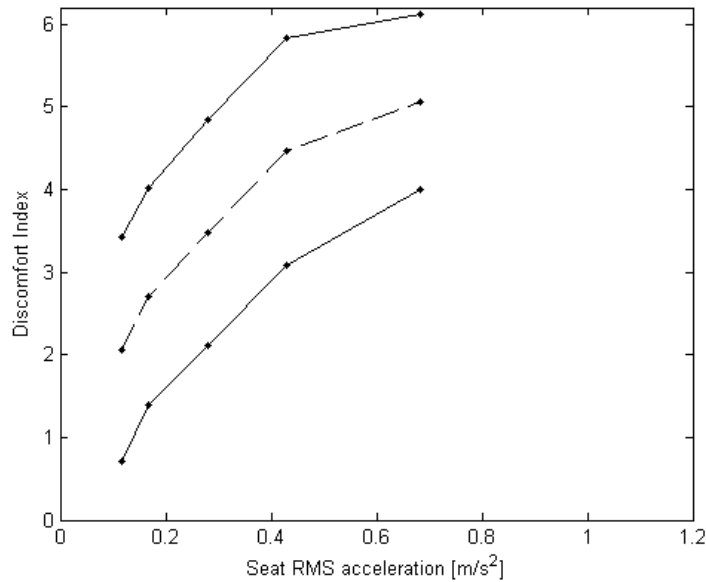


Figure 5.16: Discomfort index variation for 24 participants as a function of seat RMS acceleration as measured during pitch input to the vehicle at excitation frequency 5 Hz. --- mean discomfort index, _____ mean discomfort index $\pm 2\sigma$.

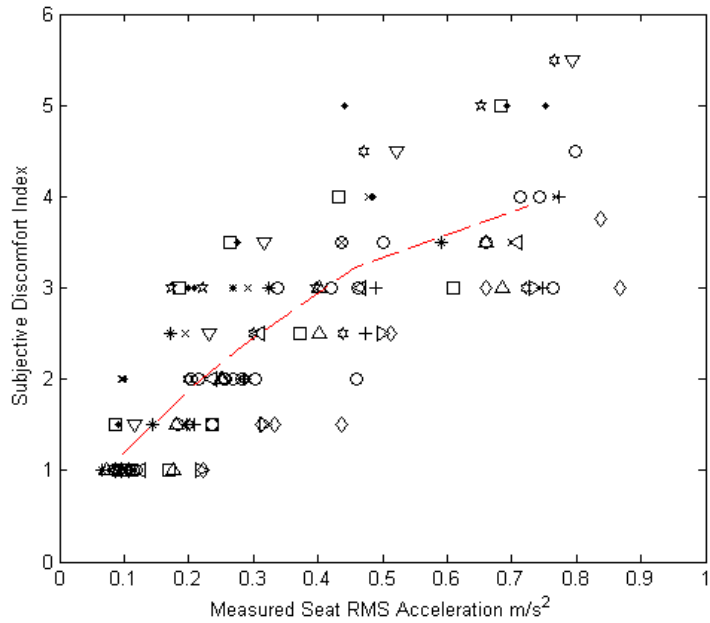


Figure 5.17: Subjective discomfort index with respect to the measured linear RMS acceleration on the seat in pitch mode at 10 Hz for vertical vibration. - - - lines represent the mean of the subjective ratings and measured seat RMS accelerations.

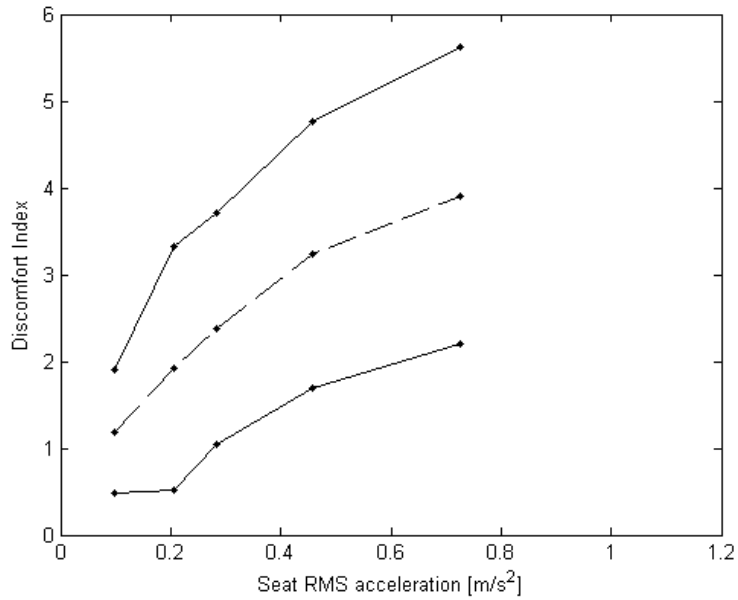


Figure 5.18: Discomfort index variation for 24 participants as a function of seat RMS acceleration as measured during pitch input to the vehicle at excitation frequency 10 Hz. - - - - mean discomfort index, _____ mean discomfort index $\pm 2\sigma$.

Figures 5.19 to 5.21 show the collection of discomfort rating curves measured at different frequencies. In pitch mode (Fig. 19), the frequency levels below 5 Hz show similar vibration behaviour in terms of sensitivity unlike of heave mode (Fig. 5.10). However, the sensitivity decreases in frequency increases between 6 Hz and 10 Hz (Fig. 5.20). The low accelerations show very little difference. For frequencies above 10 Hz (Fig. 5.21), except for 13Hz, very little difference is seen between curves for changing seat accelerations.

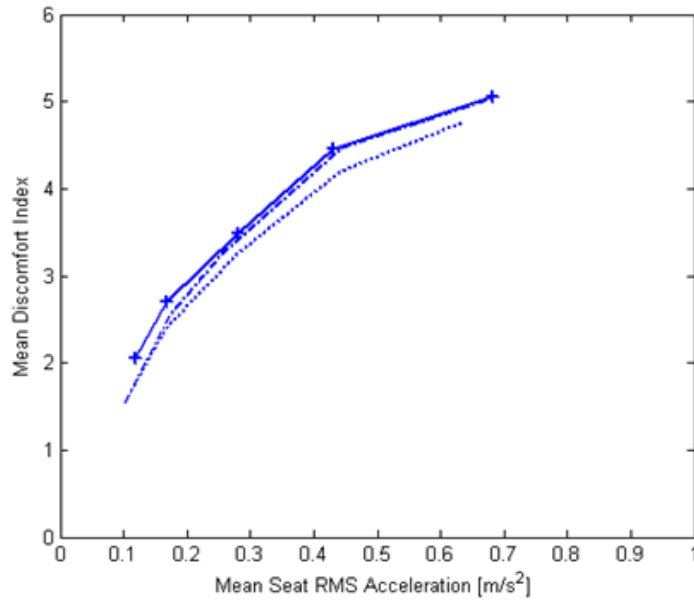


Figure 5.19: Mean discomfort index variation for 24 participants as a function of mean seat RMS acceleration as measured during pitch input to the vehicle at excitation frequency level between 3 Hz - 5 Hz. 3 Hz, -.-.- 4 Hz, —+— 5 Hz.

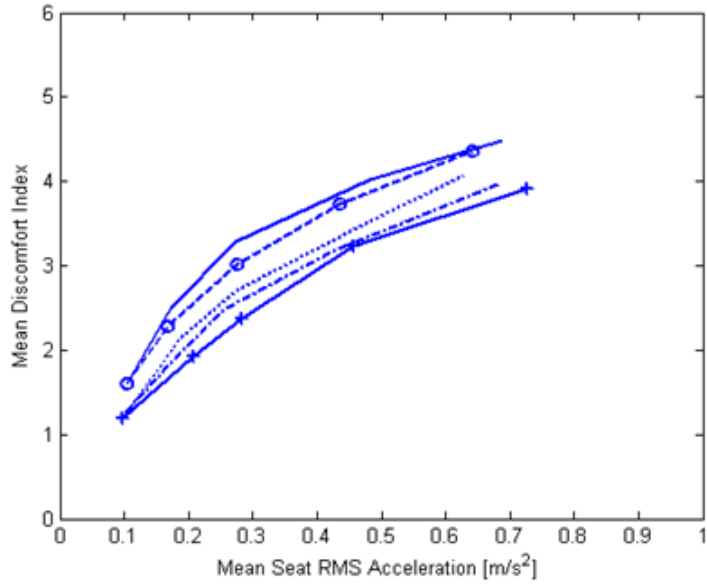


Figure 5.20: Mean discomfort index variation for 24 participants as a function of mean seat RMS acceleration as measured during pitch input to the vehicle at excitation frequency level between 6 Hz - 10 Hz. — 6 Hz, -○- 7 Hz, 8 Hz, -.-.- 9 Hz, —+— 10 Hz.

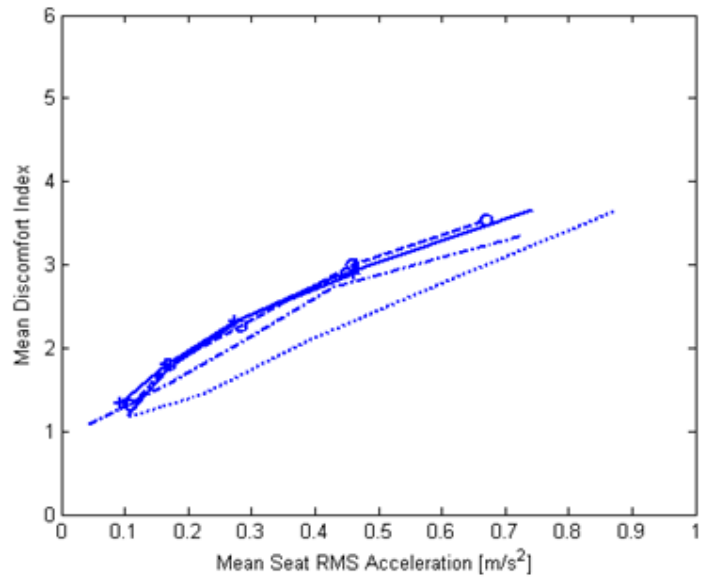


Figure 5.21: Mean discomfort index variation for 24 participants as a function of mean seat RMS acceleration as measured during pitch input to the vehicle at excitation frequency level between 11 Hz - 15 Hz. — 11 Hz, -○- 12 Hz, 13 Hz, -.-.- 14 Hz, —+— 15 Hz.

5.2.3 Analysis of Subjective Discomfort Assessment in Roll Mode

Figures 5.22 and 5.23 show discomfort index variation at 3 Hz roll mode of input. As before in the pitch mode of input, the X axis is shown in terms of equivalent rectilinear motion rather than angular motion. The plots show increased sensitivity to vibration in the input in roll mode as compared with heave mode input for both low and high accelerations; similarly small increase as compared to pitch input. The highly discomfortable perception is reached at much smaller values of seat accelerations. The scatter (Fig.14) is a slightly smaller at low accelerations as compared with high seat accelerations.

Figures 5.24 and 5.25 show results for 5 Hz roll mode input. Relatively, the sensitivity is lower at this frequency compared with a 3 Hz. The scatter is of similar range throughout the acceleration changes.

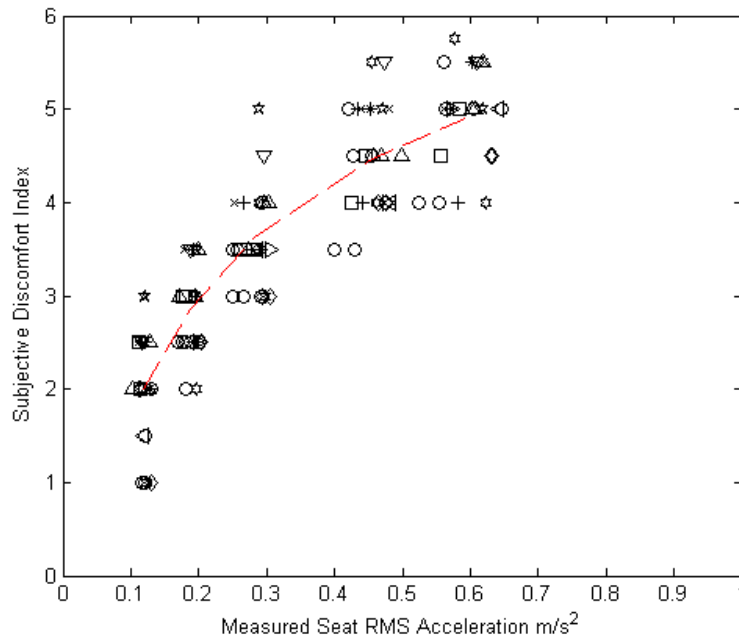


Figure 5.22: Subjective discomfort index with respect to the measured linear RMS acceleration on the seat in roll mode at 3 Hz for vertical vibration. _ _ _ lines represent the mean of the subjective ratings and measured seat RMS accelerations.

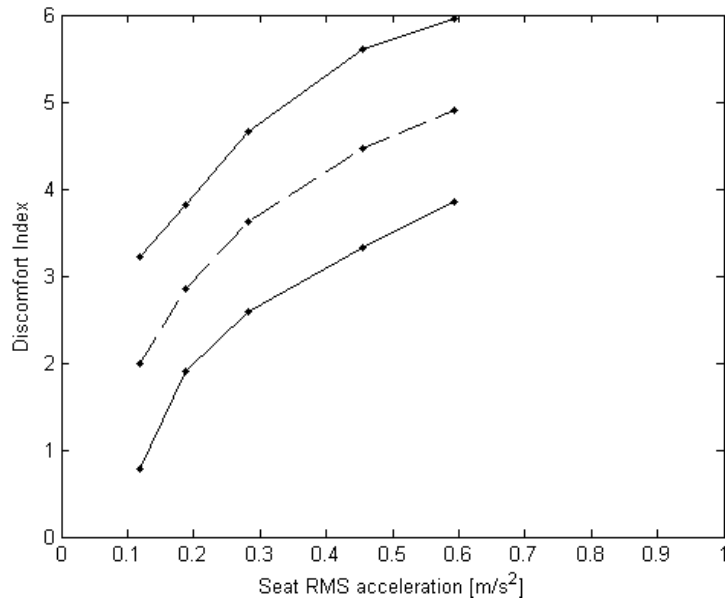


Figure 5.23: Discomfort index variation for 24 participants as a function of seat RMS acceleration as measured on roll input to the vehicle at excitation frequency 3 Hz. — — — — mean discomfort index, _____ mean discomfort index $\pm 2\sigma$.

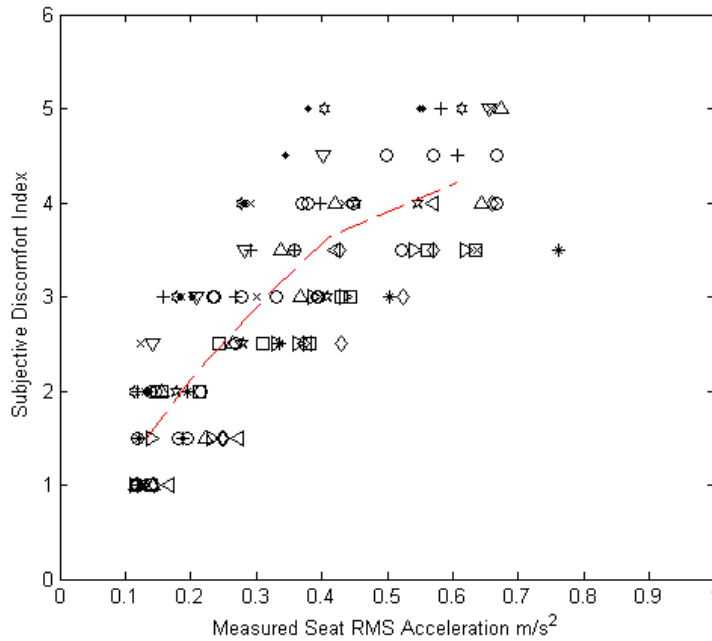


Figure 5.24: Subjective discomfort index with respect to the measured linear RMS acceleration on the seat in roll mode at 5 Hz for vertical vibration. _ _ _ lines represent the mean of the subjective ratings and measured seat RMS accelerations.

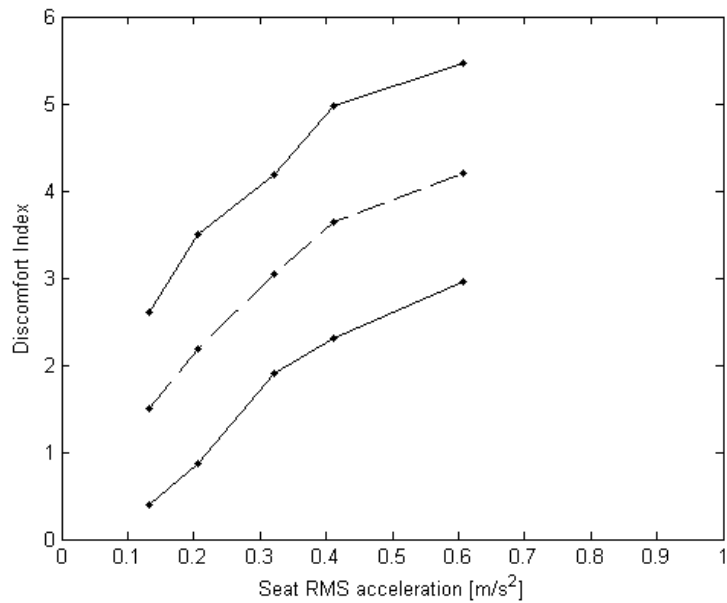


Figure 5.25: Discomfort index variation for 24 participants as a function of seat RMS acceleration as measured during roll input to the vehicle at excitation frequency 5 Hz.
 — — — — mean discomfort index, ———— mean discomfort index $\pm 2\sigma$.

Figures 5.26 to 5.28 shows the collection of discomfort index curves measured at different frequencies for roll mode of input. There is a sudden decrease in sensitivity for 5 Hz (Fig. 5.26) but the sensitivity is of similar level for 3 and 4 Hz. Another feature of the fall in sensitivity at 5 Hz is the decrease of the similar level for all seat accelerations. The frequencies between 6 and 10 Hz (Fig. 5.27) show some variation, an increase in frequency shows a decrease in sensitivity. Very little difference was obtained between curves for the low level vibrations above 10 Hz (except for the 13Hz curve) in pitch mode for varying seat accelerations (Fig. 5.28).

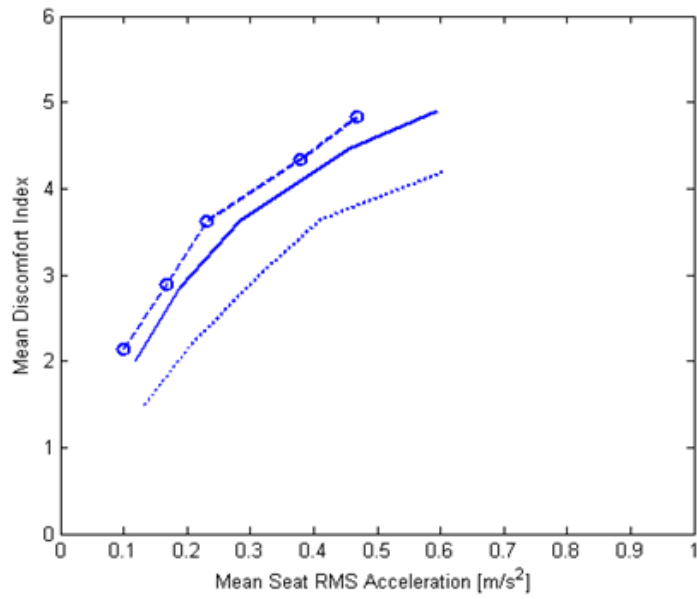


Figure 5.26: Mean discomfort index variation for 24 participants as a function of mean seat RMS acceleration as measured during roll input to the vehicle at excitation frequency level between 3 Hz - 5 Hz. — 3 Hz, -○- 4 Hz, 5 Hz.

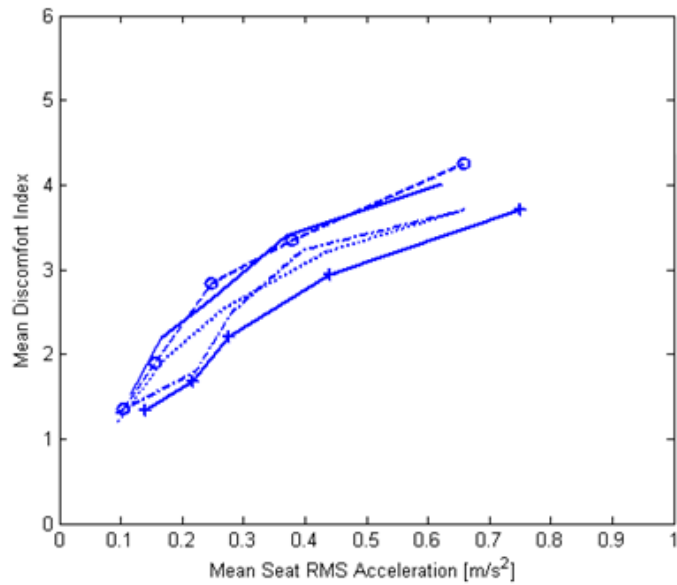


Figure 5.27: Mean discomfort index variation for 24 participants as a function of mean seat RMS acceleration as measured during roll input to the vehicle at excitation frequency level between 6 Hz - 10 Hz. — 6 Hz, -○- 7 Hz, 8 Hz, -·-·- 9 Hz, —+— 10 Hz.

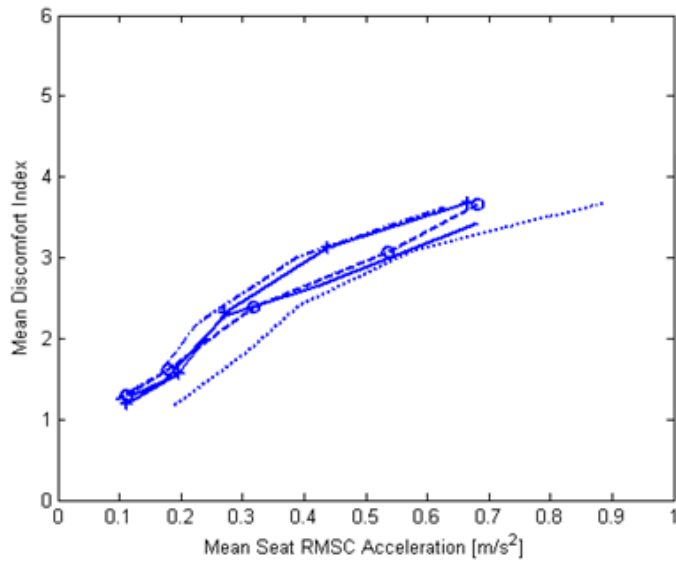


Figure 5.28: Mean discomfort index variation for 24 participants as a function of mean seat RMS acceleration as measured during roll input to the vehicle at excitation frequency level between 11 Hz - 15 Hz. — 11 Hz, - - o - - 12 Hz, 13 Hz, - · - · - 14 Hz, — + — 15 Hz.

5.2.4 Variation of Discomfort Indices as Function of Frequency

In this section the influence of frequency on perception of vibration is analysed; the seat accelerations are held constant. Discomfort curves for the seat acceleration of 0.1 m/s^2 are shown in Figure 5.29. At this vibration level, the variations with changing frequency are small, but definite trends are seen: a) in heave mode input, increased sensitivity at around 5 Hz and 7 Hz, b) in pitch mode input increased sensitivity seen up to 5 Hz and c) in roll mode input increased sensitivity at very low frequencies (below 5 Hz). Similar trend are seen for 0.16 m/s^2 (Fig. 5.30) seat acceleration for pitch and roll mode excitations.

Figure 5.31 shows discomfort curves for 0.25 m/s^2 seat acceleration. Relatively, there is a change in sensitivity to roll and pitch mode input at higher frequencies; these modes of vibrations result in slightly higher sensitivity than the heave mode input. This finding is unlike those from earlier studies (ISO 2631-1). At lower frequencies, below 6 Hz, the relative behaviour is similar but there is a more pronounced perception to low acceleration levels. The discomfort curves for 0.4 m/s^2 acceleration are shown in Figure 5.32. There is a significant difference in the sensitivities for roll and pitch mode inputs as compared to heave mode input at lower frequencies. Roll mode input dominates frequencies below 4 Hz and pitch mode shows increased sensitivities up to 5 Hz. For frequencies between 7 and 10 Hz, the curves appear to converge to a common value of discomfort rating. As the acceleration level increases at 0.63 m/s^2 in Fig. 5.33, the sensitivity increases. At this vibration magnitude level, the sensitivity for the heave mode is seen to be higher than for the pitch and roll modes above 10 Hz. The sensitivity appears to remain relatively constant over the entire frequency range under consideration at 1 m/s^2 vibration magnitude.

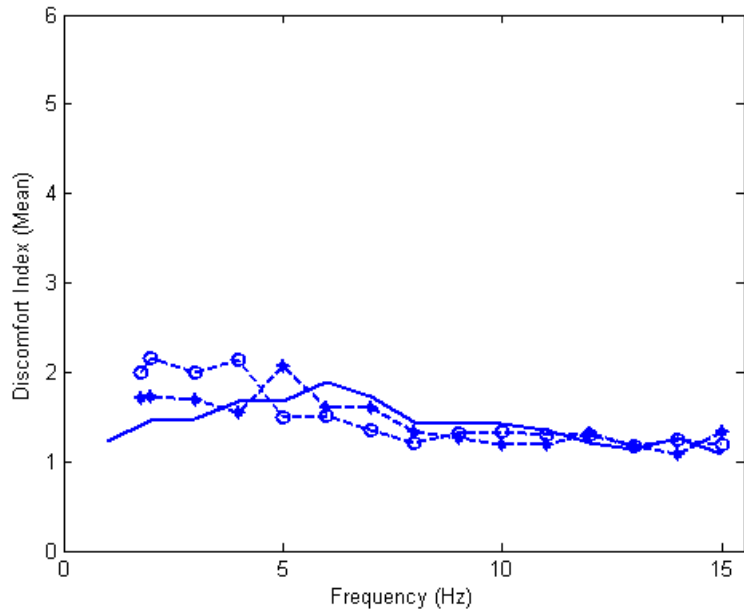


Figure 5.29: Discomfort index level (mean) against to frequency range from 1 Hz to 15 Hz at 0.1 m/s^2 measured seat RMS acceleration for 17 seconds. — heave, -*- pitch, and -*- roll.

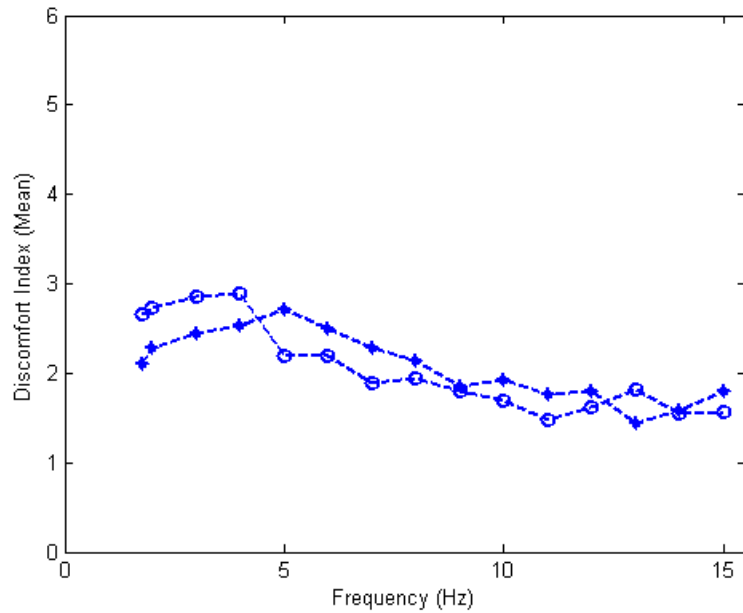


Figure 5.30: Discomfort index level (mean) against to frequency range from 1 Hz to 15 Hz at 0.16 m/s^2 measured seat RMS acceleration for 17 seconds. -*- pitch, and -*- roll.

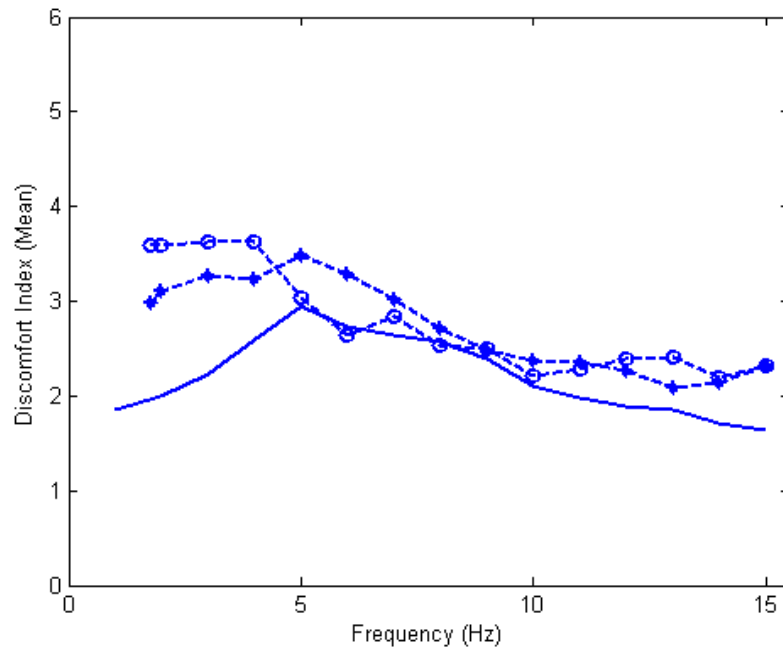


Figure 5.31: Discomfort index level (mean) against to frequency range from 1 Hz to 15 Hz at 0.25 m/s^2 measured seat RMS acceleration for 17 seconds. — heave, -*- pitch, and -*- roll.

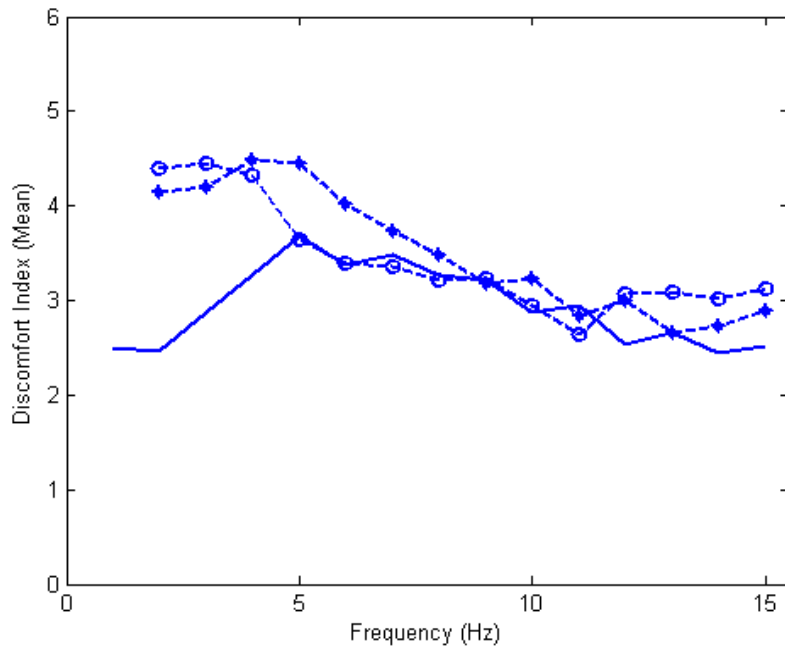


Figure 5.32: Discomfort index level (mean) against to frequency range from 1 Hz to 15 Hz at 0.4 m/s^2 measured seat RMS acceleration for 17 seconds. — heave, -*- pitch, and -*- roll.

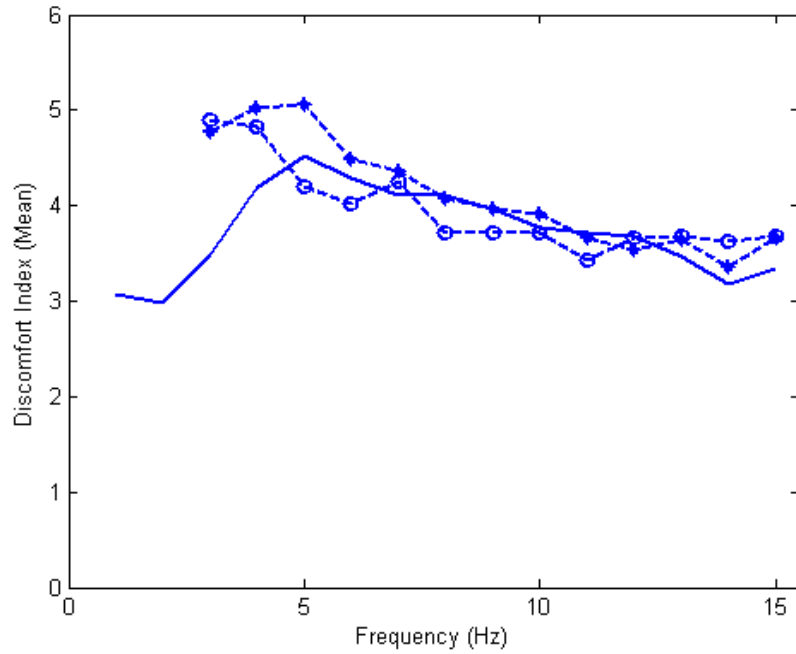


Figure 5.33: Discomfort index level (mean) against to frequency range from 1 Hz to 15 Hz at 0.63 m/s^2 measured seat RMS acceleration for 17 seconds. — heave, —◆— pitch, and —○— roll.

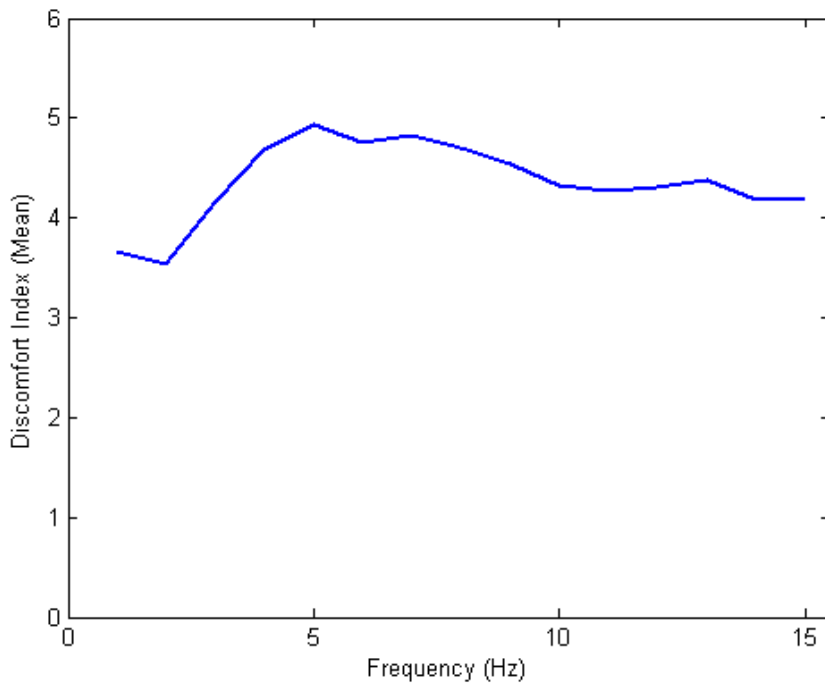


Figure 5.34: Discomfort index level (mean) against to frequency range from 1 Hz to 15 Hz in heave mode at 1 m/s^2 measured seat RMS acceleration for 17 seconds.

5.3 DISCUSSION

Subjective and dynamic responses of twenty-four seated participants, in a car on the four-post rig, exposed to vertical sinusoidal vibration at five magnitudes in the heave, pitch and roll motions were measured. A discomfort metric was developed by using the relationship between RMS seat acceleration and subjective assessment.

The seated human subjects in a car have different sensitivity limits for varying frequencies and magnitudes of vibration. In this study a new experimental method, using a seated human in a car on the four-post rig simulator, was introduced to quantify discomfort in a real environmental condition. The experiments allowed excitation in all possible directions allowing analysis of directional sensitivity and the frequency sensitivity of human response to vibration input.

As expected the human response was very sensitive to low frequency excitation. The seated subjects were found to slightly change the seat response and in turn may affect subjective rating a little bit. However, the variations in seat accelerations due to mass loading by participants were much smaller than the target seat accelerations. The results here may be, to some extent, affected by the type of car tested. The vehicle dynamics could have some influence on the subjective rating because of coupling between various modes of vibration. In this study, human sensitivity level and discomfort index were analyzed and quantified based on a BMW Mini Cooper. Therefore, the human sensitivity level may show differences on different vehicles. This was not scope within this study; however, the developed new experimental method can be applied to different vehicles on the four-post rig to enable comparative data to be obtained.

The main findings for the *in-situ* experimental study; a discomfort metric was developed by quantification of human perception which shows the human threshold level to vibration in heave, pitch and roll motions. As the magnitude of vibration increases the human perception of discomfort initially increases but as the

frequency gets larger then starts to decrease (>10 Hz). Human body is more sensitivity to vibration at around 5-7 Hz. Low level of vibration magnitudes (0.1 m/s^2 , 0.16 m/s^2) were found not uncomfortable or noticeable but not discomfortable than high level of vibration magnitudes (0.23 m/s^2 , 0.4 m/s^2 , 0.63 m/s^2 , 1 m/s^2).

Although not used to analyse the results, the perceived effects of vibration on human body parts were also recorded for all of participants. The participants related their feelings at low frequencies to the response of: a) stomach and head in heave and pitch modes at very large amplitudes and b) back and legs in roll mode. It was pointed out that roll mode was more tolerable than heave and pitch modes. Due to vehicle dynamics above 10 Hz the roll motion appeared to occur in combination with yaw motion, which felt more comfortable for the subjects. This behaviour may be specific to the car under test. Furthermore, general feeling was that at small amplitudes the pitch mode felt uncomfortable. As expected, sensitivity to acceleration decreased with decreasing amplitude and increasing frequency.

CHAPTER 6

MODELLING OF BIODYNAMIC RESPONSE OF THE SEATED HUMAN BODY IN A CAR

6.1 INTRODUCTION

The human body segments (i.e. head, back, legs, and arms, etc.) under the vibration or exposed to the vibration may have dissimilar dynamic influences on the vibration transmitted and eventually the human perceptivity. The knowledge of resonance of human body segments in different frequency ranges is used for biomechanical modelling to predict the movements of human body. The mechanisms of the human body actions are not easy to analyze and also they are not fully understood [2] because the body postures are dissimilar between subjects.

The aim of this chapter is to develop a mathematical model to characterize the dynamic response of a seated human body subject in a car. In the subsequent chapter this model will be combined with experimental results to predict the ride discomfort for a given road input. The direction of vibration, i.e. vertical, horizontal and rotational vibration, may have different influences on the human body; the vibrational energy may enter to human body in different ways. Based on the vibration transmitted, the characteristic of human response to vibration is assessed. The human body is sensitive to vibration input in a bandwidth of 4 Hz to 8 Hz for the vertical vibration and 1 Hz to 2 Hz for the horizontal vibration [2, 93]. However, based on the published studies, there is inadequate information on the human sensitivity in the rotational motion such as roll and pitch.

A vehicle-occupant model (an integrated vehicle-seat-human model) is developed to represent the dynamic behaviour in vertical and rotational directions for human motion in a sitting position. In order to model and analyse an integrated vehicle-seat-human model, seated human body biomechanical

models of varying degree of complexity are considered; the chapter starts with a SDOF model and later several multi-DOF models are considered. The main aim of studying multi-DOF models is to develop a model to analyse and evaluate the human body segments (i.e., head, lower body and upper body). To limit some of the complexities, the vehicle is modelled based on half car behaviour. The following steps are used in building and understanding the models:

- **Biomechanical Modelling:** To predict transmissibility of the human body in the frequency domain using following models.
 - *Single degree-of-freedom model (SDOF):* This model is easy to use, analyse and validate; however, the disadvantage is the limitation of one-directional analysis.
 - *Three degree-of-freedom model (3-DOF):* This model is useful to analyse and validate the response of the individual segments of the human body in either multi-directions or to study dynamics of the seat and human body. The 3-DOF models are specifically used for developing and analysing the seat-to-head transmissibility.
- **An Integrated human-seat-vehicle model:** A 3-DOF model is integrated on the 4-DOF vehicle model which is called 7-DOF model.

The expected results for the integrated model are:

- The biodynamic behaviour of a seated human subject,
- The resonance values of the segments of a seated human subject in a car with given input,
- The influence of vibration transmitted from the road to the vehicle floor and the driver seat in the heave and pitch modes of input.

6.2 BIOMECHANICAL MODELLING

The human body is a complex dynamic system; the dynamic behaviour may vary from one individual to another based on the size, mass, posture, and body conditions [2, 28] (inter-subject and intra-subject variability, see Chapter 2). The lumped parameter models are sufficient to analyse the vibration transmission between the segments of the human body in order to assess the tolerable levels of mechanical vibrations.

The values of the lumped parameters play an important role in determining the reliability of the models. The biomechanical parameters, such as the masses, stiffness and damping coefficients of the human body segments can be found in the literature or in the anthropometric database [94]. Several methods were used to estimate the parameters of human segments using the simulated dummy (for example, Kim *et al.*[33]). These results, however, may not be accurate because of ill-representation of the thorax-abdomen segment of the human body.

Many publications on methods and calculations to obtain parameters, the stiffness coefficient and damping coefficient of the human body segments, of the biomechanical model lack details, except for the early published studies by Coermann [52, 56], Suggs [59], and Mertens [66]. The mean proportions of total human body segmental weights have been assumed from the anthropometric measurement data as 18.2 % or 25 % for the thighs and shanks; 52.4 % or 59% for the trunk, upper arms, forearms, and hands; and 7.5 % or 9% for the head [28, 95]. Moreover, 78 % of the weight of a seated human body is defined as being supported by the seat [95]. The stiffness value range is between 100-300 kN/m for the spine in the lumbar segments of the back and 150-200 kN/m for the chest. The range of values of damping coefficients was determined for a human body model by Mertens [66].

In this chapter, two biomechanical models (SDOF and 3-DOF) are analysed in order to characterize the biodynamic response behaviours of a seated human body subject to the vertical vibration. The analysis of these models will provide the basis for developing of an “integrated human-seat-vehicle model”. The estimation of parameters of the models used is not in the scope of this study. The parameters of human segments used in the models, like the stiffness and damping coefficients, are taken from published results. The dynamic behaviour of the linear N-DOF model exposed to vibration excitation will be analysed based on vibration transmissibility, specifically, the seat-to-head transmissibility (Section 6.2 and 6.3).

6.2.1 Single Degree of Freedom Model

SDOF model consists of a mass-spring-damper system for a seated human body. In modelling, the hip of the human body is directly in contact with the seat surface and therefore only part of the human body mass is considered to move. The SDOF model has input displacements applied on the base where spring and damper are connected. The motion of the SDOF model is described by Newton’s second law (Eq. 6.1).

$$F = m\ddot{x} \tag{6.1}$$

In Figure 6.1, a seat has seat spring (k_{sv}) and damper (c_{sv}) serially connected to the hip having spring (k_v) and damper (c_v). The model was used to study motion in the vertical direction. The input displacement is x_o and x_1 is the displacement of the human body. The parameters of this model are shown in Table 6.1 [28].

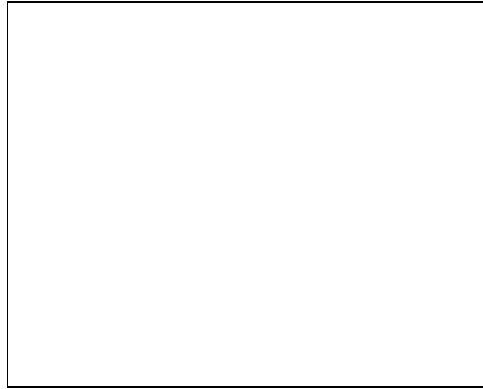


Figure 6.1: A SDOF biomechanical seated human model [28, 56].

| Mass (kg) | Stiffness (kN/m) | Damping (Ns/m) |
|-------------|------------------|----------------|
| $m_1: 56.8$ | $k_v: 75.5$ | $c_v: 3840$ |
| | $k_{sv}: 72.3$ | $c_{sv}: 357$ |

Table 6.1: The parameters for a seated human body SDOF model from Cho and Yoon [28].

In Figure 6.1, as the mass of the seat cushion is neglected, an equivalent model (Fig. 6.2) was developed. The spring (k_1) and damper (c_1) are equivalent parameters. The parameters for the proposed equivalent model are shown in Table 6.2.

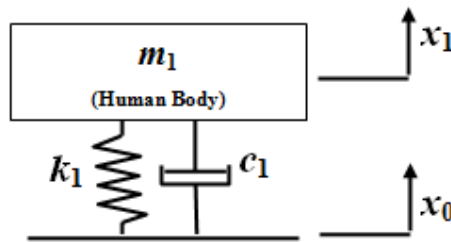


Figure 6.2: The proposed equivalent SDOF model.

| Mass (kg) | Stiffness (N/m) | Damping (Ns/m) |
|-------------|-----------------|----------------|
| $m_1: 56.8$ | $k_1: 36392$ | $c_1: 326.63$ |

Table 6.2: The parameters for the proposed SDOF model.

In the model, input was assumed greater than output, so free body diagrams were shown based on this movement.

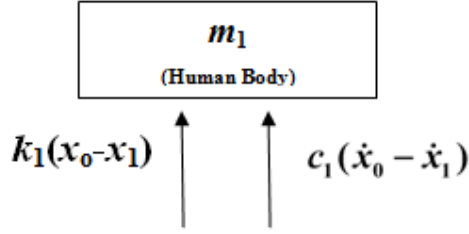


Figure 6.3: Free body diagram for SDOF model.

$$k_1(x_0 - x_1) - c_1(\dot{x}_0 - \dot{x}_1) = m_1\ddot{x}_1 \quad (6.2)$$

Using harmonic input, the frequency response function (Eq. 6.3) relating to the input and the output can be obtained as below;

$$\text{FRF} = \frac{X_1}{X_0} = \frac{\left[1 + jc \frac{\omega}{k}\right]}{\left[1 - \omega^2 \frac{m}{k} + jc \frac{\omega}{k}\right]} = \frac{[1 + j\alpha]}{[1 - r^2 + j\alpha]} \quad (6.3)$$

Where, $r = \frac{\omega}{\omega_n}$, $\omega_n^2 = \frac{k}{m}$, $\alpha = \frac{c\omega}{k}$, r is the frequency ratio, ω_n is the natural frequency and the damping ratio is;

$$\zeta = \frac{c}{2\sqrt{km}} \quad (6.4)$$

From Eq. 6.3, the vibration transmissibility can be shown as:

$$TR = |\text{frf}| \quad (6.5)$$

In this study the SDOF system is simulated and analysed using MATLAB commercial software. The degree-of-freedom models and calculations are my work. In this proposed model, the magnitude of transmissibility is analysed based on the vibration input point such the human hip point and the floor where the seat is mounted.

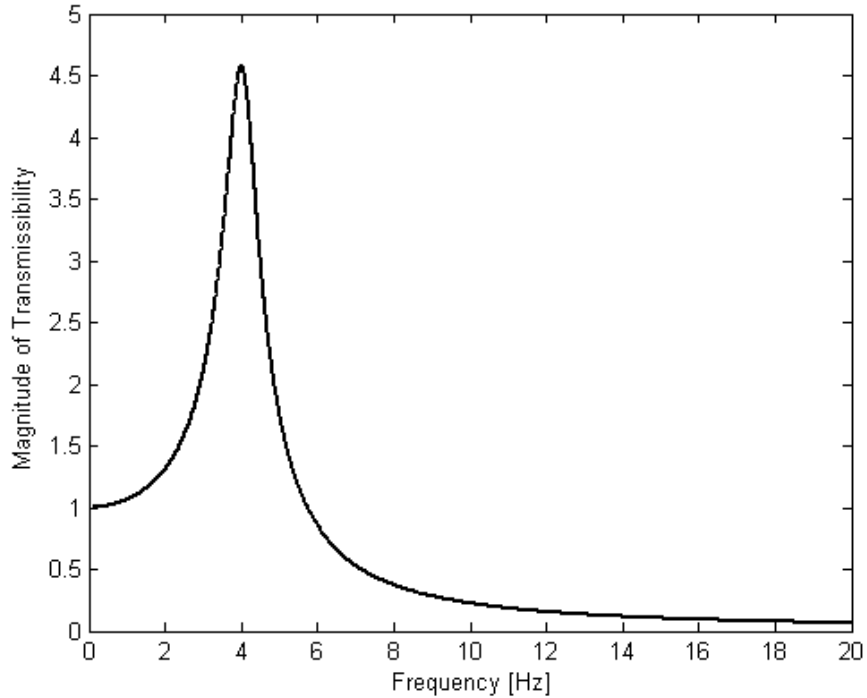


Figure 6.4: Magnitude of transmissibility for a seated human body response with respect to floor input.

Figure 6.4 shows the magnitude of transmissibility between the hip surface and the floor based on the determined parameters. The resonance frequency occurs at 4 Hz, where the transmissibility is 4.57. This peak corresponds to the human body response to vibration in heave mode.

The response behaviour of a seated human body calculated using the SDOF model can be affected by the parameters (the body's mass, stiffness coefficient and damping coefficient) of the model. In order to understand the change in biodynamic response behaviour of a seated human body, the body mass, stiffness and damping coefficient are analysed separately by using the data from literature. The parameter values that have been used by Coermann [56], Wei and Griffin [58], Cho and Yoon [28] vary significantly; it is not clear which of the parameter values serve the purpose best.

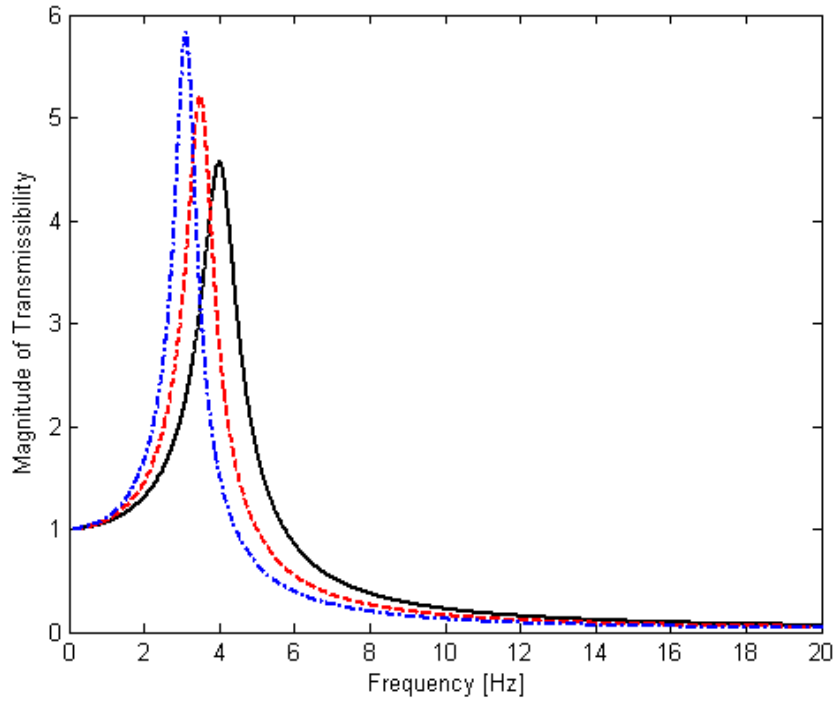


Figure 6.5: Effect of human body's mass for a SDOF model. Three total body masses:
 — 56.8 kg, - - - 75 kg, - · - · - 95 kg.

Figure 6.5 shows the effects of three different total human body masses (56.8 kg, 75 kg, and 90 kg) on the biodynamic response behaviours for a seated human body SDOF model. The increase in the body mass for a fixed stiffness value reduces the natural frequencies; the resonance frequency is reduced as seen from the plot. The damping ratio also gets affected by the change in mass; for a fixed value of damping coefficient decreasing mass results in increasing damping ratio.

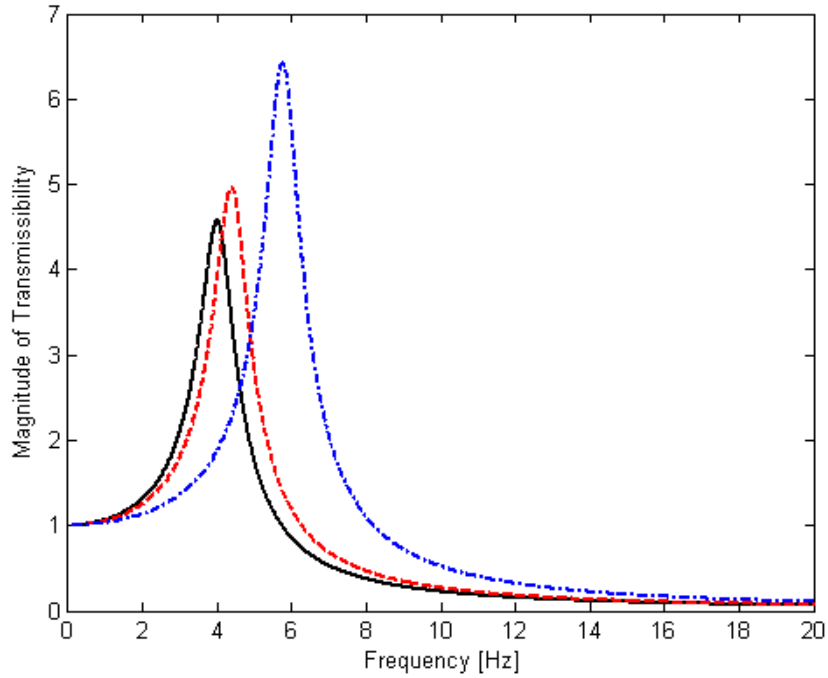


Figure 6.6: Effect of stiffness coefficient for a 56.8 kg seated human body SDOF model. Three total stiffness coefficients: ————— 36932 N/m, - - - - - 44130 N/m, - · - · - 75500N/m.

Three different values of stiffness were analysed to understand the effect of pelvic/hip on the dynamic behaviour of a human body (Fig. 6.6). From these plots, biodynamic response amplitude of a seated human body is found to increase when the pelvic stiffness coefficient increases.

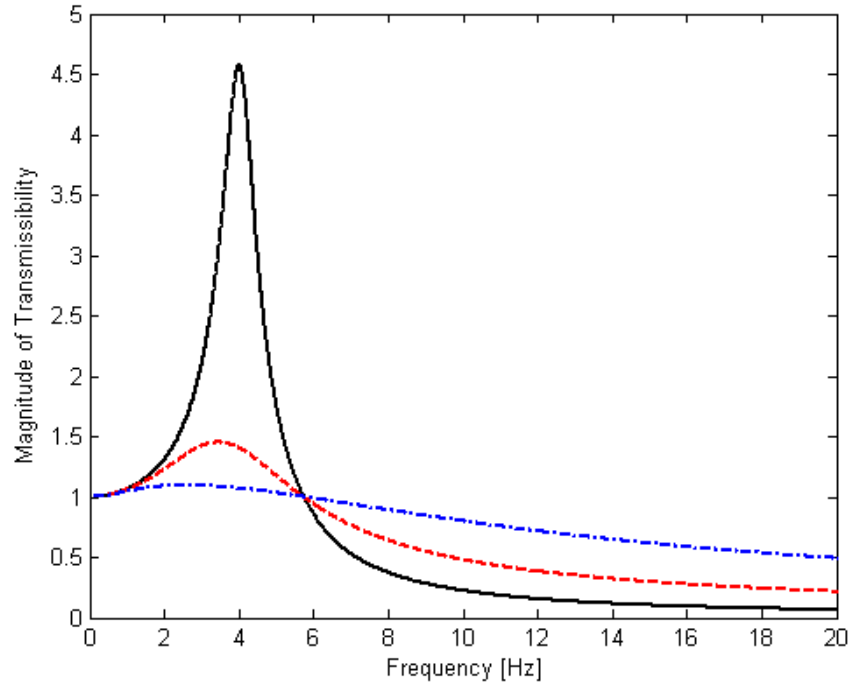


Figure 6.7: Effect of damping coefficient for a 56.8 kg seated human body SDOF model. Three total stiffness coefficients: ————— 326.63Ns/m, - - - - - 1485 Ns/m, - · - · - 3840 Ns/m.

Three different values of damping coefficients were analysed to understand the effect of pelvic/hip on the dynamic behaviour of a human body (Fig. 6.7). As expected, from these plots, the biodynamic response of a seated human body decreases when the pelvic/hip damping coefficient increases.

6.2.2 Three Degree of Freedom Model

The three degree-of-freedom (3-DOF) model consists of three body parts (i.e. lower body, upper body and head) which are interconnected. An anatomical description of a seated human body 3-DOF lumped-parameter model was proposed by Muksian and Nash [60, 61] in order to estimate the damping coefficients of the human body connections (see Chapter 2, Table 2.3). The published studies on a 3-DOF model for a seated human body have not clearly shown the connection between the buttocks and seat. Most of the papers state as *the buttocks in contact with the seat*, and also in this connection the parameters of seat are not given and clearly explained.

Therefore in this study, the proposed 3-DOF model is a simplified version of a 6-DOF (Fig. 6.8) seated human body model. The 6-DOF model consists of a *4-DOF seated human body model* (see Chapter 2, Table 2.5) and a *2-DOF seat model*. The seated human body 4-DOF model was proposed by Boileau and Rakhejas [64]. The four masses represent the human body segments as the head and neck (m_1); the chest and upper torso (m_2); the lower torso (m_3); and the thighs and pelvis (m_4) in contact with the seat (seat cushion and foam).

The seat directly is in contact with the floor because of high stiffness. The damping and stiffness properties for a seated human body are given as the buttocks and thighs by k_4 and c_4 , the lumbar spine by k_3 and c_3 , the thoracic spine by k_2 and c_2 , the cervical spine by k_1 and c_1 . The seat cushion properties are represented as spring constant by k_5 and damping coefficient c_5 . The parameters are shown in Table 6.3.

The parameters of human body segments are taken from Boilea and Rakheja's model [64]. The rigid seat was used in Boilea and Rakheja's model. Therefore, the seat parameters for the simplified and proposed model in Figure 6.8 (cushion stiffness and damping coefficients) are taken from Papalukopoulos and Natsiavas's model [76] and Liang *et al.*'s model [77]. The human body has very high damping, so in the modelling small mass values and large stiffness values

are required. Also, we do not want high frequency. So, in Fig. 6.8, the lumbar spine stiffness (k_3) and damping coefficient (c_3) are neglected because of stiffness. The seat mass is neglected because seat foam is soft, so stiffer than a cushion.

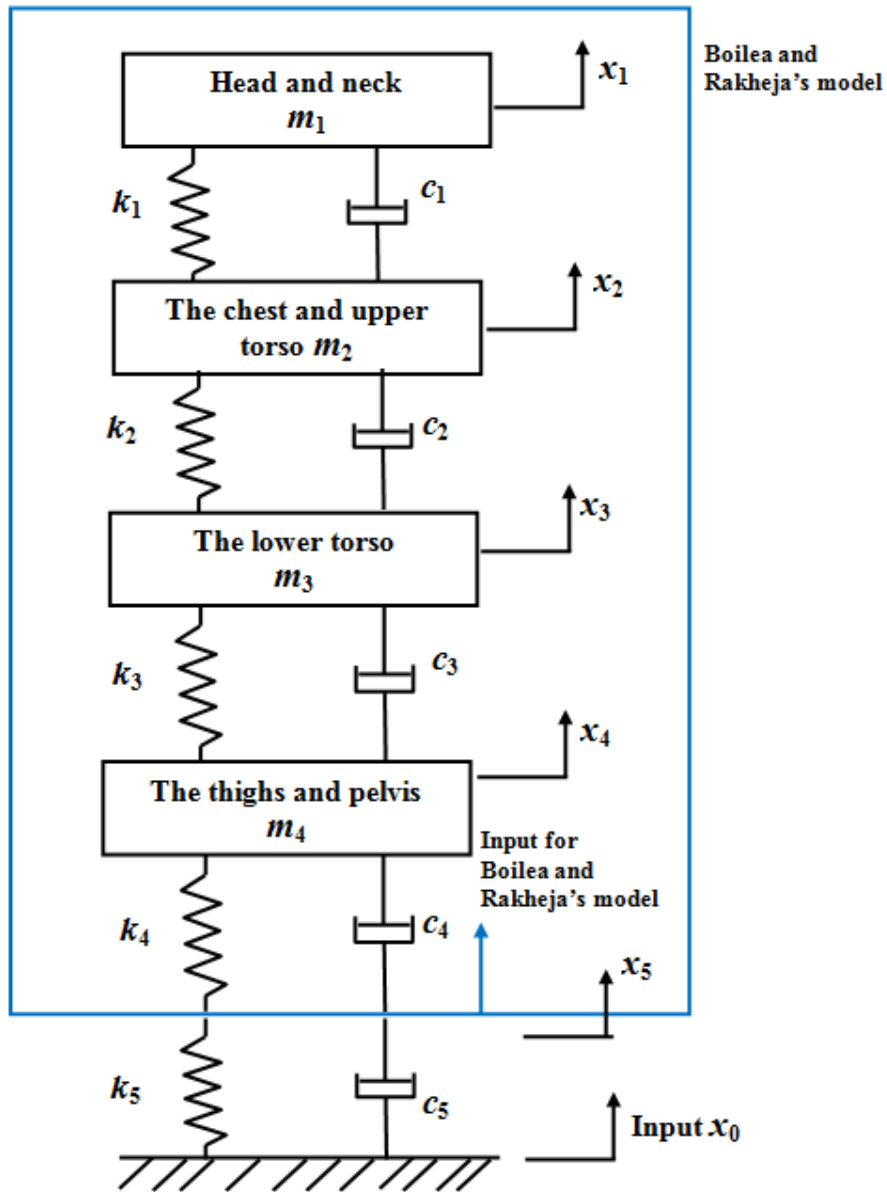


Figure 6.8: Biomechanical 6-DOF model for a seated human body subject.

| Mass (kg) | Stiffness (N/m) | Damping (Ns/m) |
|------------------------|-----------------|----------------|
| $m_1=5.31$ | $k_1= 310000$ | $c_1=400$ |
| $m_2=28.49$ | $k_2=183000$ | $c_2=4750$ |
| $m_3=8.62$ | $k_3=162800$ | $c_3=4585$ |
| $m_4=12.78$ | $k_4=90000$ | $c_4=2064$ |
| Seat mass is neglected | $k_5=200000$ | $c_5=875.6$ |

Table 6.3: The parameters for the 6-DOF model.

The aim of the proposed 3-DOF model (Fig. 6.9) is to analyse the magnitude of transmissibility for human body segments as the seat-to-head and floor-to-lower body in the vertical direction for a seated human body subject without seat back support.

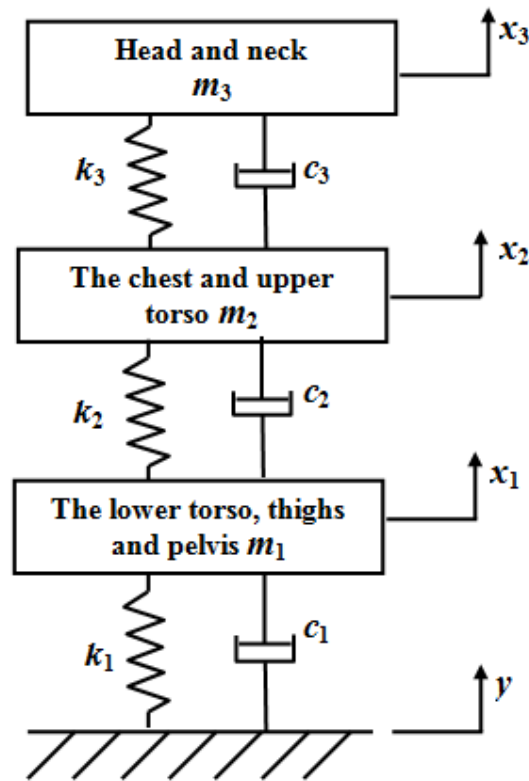


Figure 6.9: The proposed 3-DOF model for a seated human body subject.

The model shown in Figure 6.9 consists of three rigid bodies represented by their masses, interconnected by springs and dampers. The three masses are: the head and neck (m_3), the chest and upper torso (m_2), the lower torso, thighs and pelvis (m_1). The mass of seat, lower legs and the feet is neglected. The stiffness and damping properties are as shown; the lower torso, thighs and pelvis are (k_1) and (c_1), the chest and upper torso are (k_2) and (c_2), and head are (k_3) and (c_3). The parameters of the 3-DOF model for a seated human body without backrest (from the simplification from Figure 6.8 and Table 6.3) are given in Table 6.4. The three generalized coordinates used to describe the motion of the masses are: the head and neck (x_3); the chest and upper torso (x_2); and the lower torso, thighs and pelvis (x_1).

Assuming that the stiffness and damping properties of the model are linear, the mathematical model of the seated human body can be obtained as follows:

$$\begin{aligned}
 m_3 \ddot{x}_3 + k_3 (x_3 - x_2) + c_3 (\dot{x}_3 - \dot{x}_2) &= 0 \\
 m_2 \ddot{x}_2 + k_2 (x_2 - x_1) + c_2 (\dot{x}_2 - \dot{x}_1) - k_3 (x_3 - x_2) - c_3 (\dot{x}_3 - \dot{x}_2) &= 0 \\
 m_1 \ddot{x}_1 - k_2 (x_2 - x_1) - c_2 (\dot{x}_2 - \dot{x}_1) + k_1 x_1 + c_1 \dot{x}_1 &= k_1 y + c_1 \dot{y}
 \end{aligned} \tag{6.6}$$

The equations of motion, Eq. 6.6, for the model can be expressed in matrix form as given below.

$$[\mathbf{M}]\{\ddot{\mathbf{x}}\} + [\mathbf{C}]\{\dot{\mathbf{x}}\} + [\mathbf{K}]\{\mathbf{x}\} = \{\mathbf{f}\} \tag{6.7}$$

Where $[\mathbf{M}]$, $[\mathbf{C}]$, and $[\mathbf{K}]$ are mass, damping, and stiffness matrices respectively. $\{\mathbf{f}\}$ is the force vector.

$$\mathbf{M} = \begin{bmatrix} m_3 & 0 & 0 \\ 0 & m_2 & 0 \\ 0 & 0 & m_1 \end{bmatrix} \quad \mathbf{K} = \begin{bmatrix} k_3 & -k_3 & 0 \\ -k_3 & k_2 + k_3 & -k_2 \\ 0 & -k_2 & k_1 + k_2 \end{bmatrix} \quad \mathbf{C} = \begin{bmatrix} c_3 & -c_3 & 0 \\ -c_3 & c_2 + c_3 & -c_2 \\ 0 & -c_2 & c_1 + c_2 \end{bmatrix}$$

and

$$\{\mathbf{f}\} = \{0 \quad 0 \quad k_1 y + c_1 \dot{y}\}^T$$

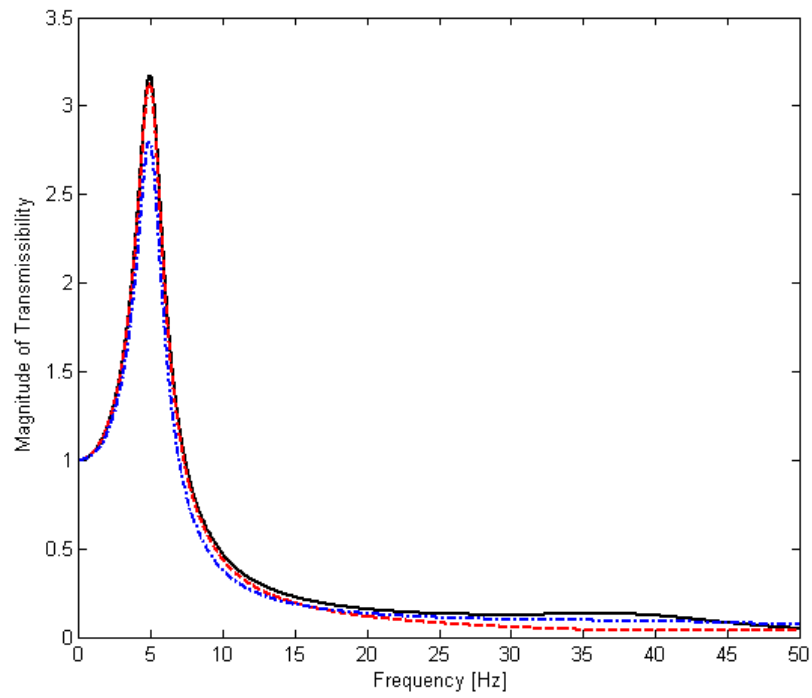
| Mass (kg) | Stiffness (N/m) | Damping (Ns/m) |
|-------------|-----------------|----------------|
| $m_3=5.31$ | $k_3=310000$ | $c_3=400$ |
| $m_2=28.49$ | $k_2=183000$ | $c_2=4750$ |
| $m_1=21.4$ | $k_1=62068.96$ | $c_1=614.79$ |

Table 6.4: The parameters for the proposed 3-DOF model.

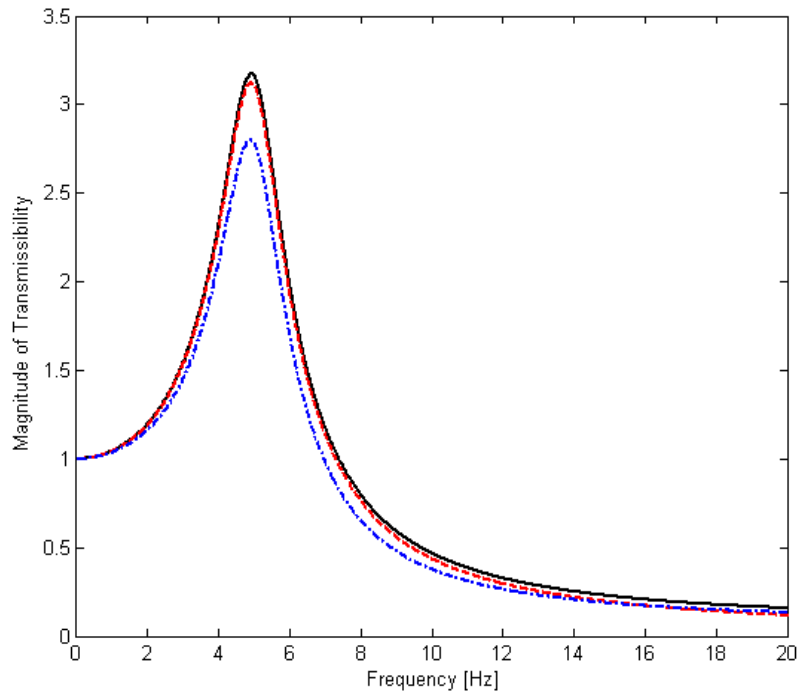
The biodynamic response behaviours for a seated human body with a total mass of 55.2 kg are analysed in 3-DOF model by using the data from Table 6.4.

Figure 6.10 shows the magnitude of transmissibilities for the head, upper torso and lower torso body segments of the 3-DOF seated human body model in the frequency range of 0-50 Hz at floor input. From the plots, a resonance occurs at 4.9 Hz where the transmissibility is 3.17 for head response. For the upper torso response, a resonance occurs at 4.8 Hz where the transmissibility is 3.1. The upper torso and head show similar response behaviour below 9.4 Hz. With the increasing frequency level, the head response increases and the upper torso response decreases. This is because of the dynamics of the connection between the head and upper torso. Also, it might be defined as the resonance frequency of head increases with frequency increased.

As is seen from the plots, the lower torso (thighs, pelvis and buttocks) response is less than the head and upper torso response below around 13 Hz. A resonance occurs at 4.8 Hz where the transmissibility is 2.7 for the lower torso response. Above 14 Hz, the lower torso response increases with the increased frequency level. This might be explained as the lower body is in contact with the seat so the increased transmitted vibration level is directly felt by the lower body segments of the human body.



(a) The frequency is up to 50 Hz.



(b) The frequency is up to 20 Hz.

Figure 6.10: The magnitude of transmissibilities in respect to the floor input for the 3-DOF model. — Head response, - - - Upper torso response, - · - Lower torso response.

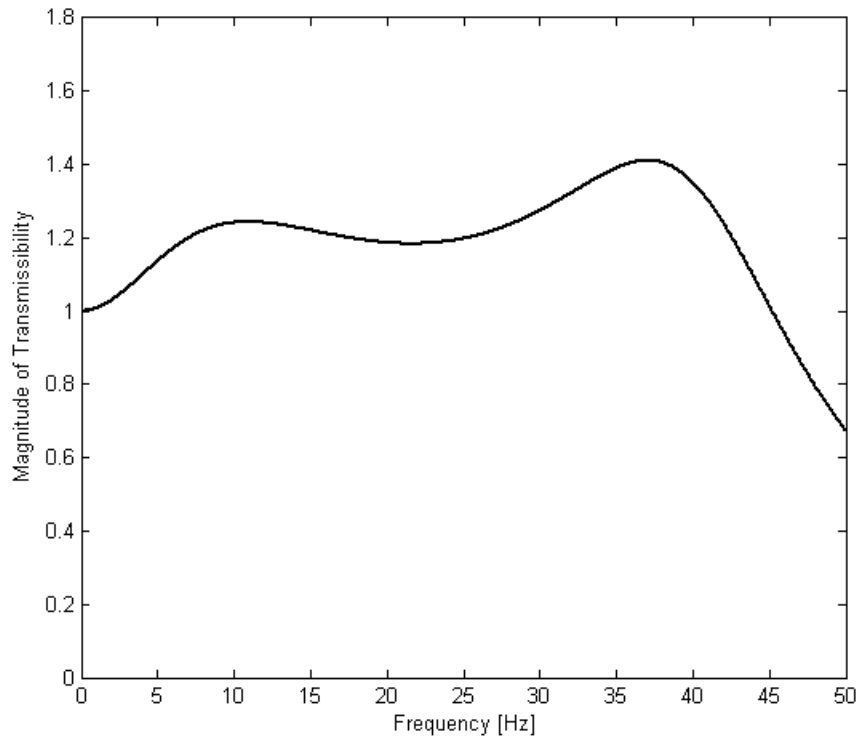


Figure 6.11: The magnitude of transmissibility for head response in respect to the seat input for the 3-DOF model.

Figure 6.11 shows the transmitted vibration magnitude from the seat to the head. Two resonances (peaks) are seen in the plot. A first resonance, which is not clearly a peak, occurs at around 10 Hz, where the transmissibility is 1.2. The second resonance occurs at around 37 Hz where the transmissibility is 1.4. The second peak behaviour may not influence the planned study of this project as the maximum frequency is limited to 15 Hz.

6.2.3 Summary

The single and three degree-of-freedom models were analysed in order to characterize the biodynamic response of a seated human body subject to vertical vibration input. From these models the transmissibility characteristics from the floor to different body segments, i.e. the lower body, upper body and the head, were determined. Also the transmissibility characteristic was defined from the

seat to the head in three degree-of-freedom model. From the SDOF model the natural frequency was found to occur at around 4 Hz based on the parameters [28] determined by Cho and Yoon. Different parameters determined by researchers were compared to evaluate the effect on the resonance behaviour of the human body.

The 3-DOF model was developed and analysed in the vertical direction. The aim of this model is to validate the response of the individual body segments of the human with the dynamics of the seat. From this model, the resonance frequency was found to occur at around 4.9 Hz for the head, 4.8 Hz for the upper torso and 4.8 Hz for the lower torso with the transmissibility 3.17, 3.1, and 2.7 respectively with respect to the floor input.

In this 3-DOF model, many different parameters were analysed to find the best parameter values for characterization of human response behaviour. However, it was very difficult to determine the correct parameters because 3-DOF models have been developed for different purposes by many researchers, and they do not clearly define either the calculation of the parameters or the purposes of the parameters. For example, the models in the literature were not clear on how the lower body was connected to the seat or seat surface. They only defined that '*the lower body was in contact with seat*' which does not clearly show the seat dynamics for a seated human body model.

In this study, a human body model was connected with a seat in order to develop a seated human body model. Each body segment of human body was analyzed with different parameters. The developed 3-DOF model was connected with a 2-DOF seat model. The parameters of human body segments were used by Boileau and Rakheja's proposed model [64]. The seat parameters were used from Liang and Chiang's paper [55] and Papalukopoulos and Natsiavas's model [76].

The proposed 3-DOF model was used to develop an integrated human-seat-vehicle model which is given in the following section. The reason this 3-DOF model is useful that it can analyse in the vertical direction and in multiple

directions. Therefore, it can be integrated with a vehicle model easily to evaluate and analyse the ride quality of a vehicle. This integrated model will help to analyze the human response behaviour in a car which will be closer to reality. Hence, the determined parameter values (Table 6.4) are important for later models. It was not easy to determine the correct parameters. The proposed model, with the parameters determined, provides a reasonable estimate of the transmissibility characteristics.

6.3 INTEGRATED HUMAN-SEAT-VEHICLE MODEL

Vehicle drivers are exposed to whole-body vibration (WBV) based on the road conditions; the vibration is transferred through, the tyres, the suspension system and the seat. The biomechanical models of a seated human body are not adequate to completely characterize the biomechanical human responses with respect to the road input. Alternatively, a vehicle model cannot be used on its own to predict driver vibration response in a car.

In this study, in order to characterize and evaluate the influence of interaction between the vehicle vibration and the seated human on, integrated-human-seat-vehicle model (seven degree-of-freedom model) is developed this restricts the analysis to heave and pitch modes of motion. This model allows the analysis of the human response to vehicle vibration excitation in various motion situations based on the '*cause-effect*' relations. There have not been many published studies on the 'integrated human-seat-vehicle lumped parameter model'.

6.3.1 Seven Degree of Freedom Model

A seven degree-of-freedom (7-DOF) lumped parameter model is developed in order to characterize the biodynamic response behaviour of a seated human body in a car in the heave and pitch modes. This model shown in Figure 6.12 consists of a 3-DOF seated human body model (see Fig. 6.9) and a 4-DOF half car suspension vehicle model (see Chapter 3.4.1 and Fig. 3.4).

Figure 6.12 shows that the sprung mass is allowed to heave and pitch while the unsprung masses, the seat and the human masses are allowed to bounce vertically. If y_3 and θ represent the bounce and pitch displacements of the sprung mass, respectively, then $y'_1 = y_3 + \theta l_r$, $y'_2 = y_3 - \theta l_f$ and $y_0 = y_3 + \theta e_1$ will be the sprung mass displacements at the front and rear suspension connections to the vehicle body, respectively. The distance from the vehicle centre of gravity (C.G.) to the front suspension is l_f , the distance from the vehicle C.G. to the rear suspension is l_r and e_1 is the distance from the vehicle C.G. to the driver seat. In the model, the human hip has contact with the seat surface which in turn is connected by a set of spring k_1 and damper c_1 to the vehicle body. The road input displacements are r_{11} and r_{21} .

The free-body diagrams of the seven degree-of-freedom model and the derivation of equations are given in Appendix D, Section D.1.

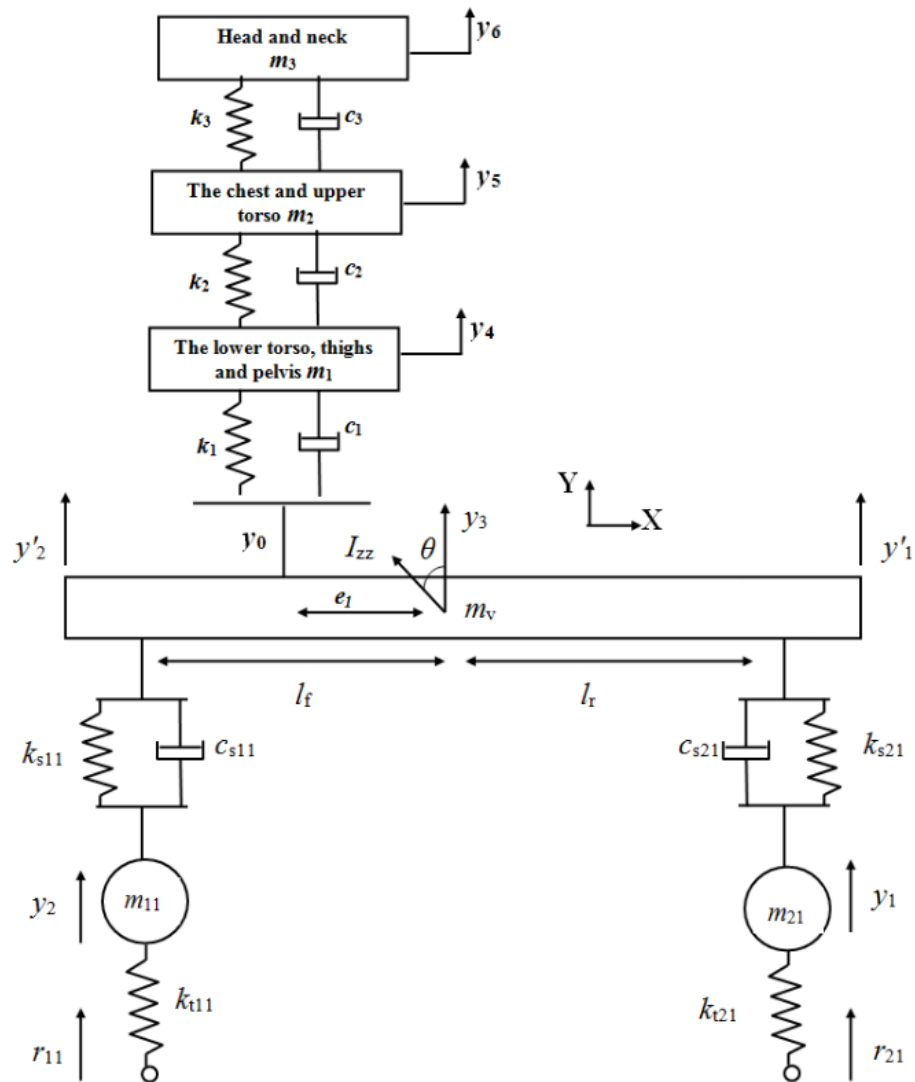


Figure 6.12: A lumped parameter integrated human-seat-vehicle model (7-DOF) model without backrest support in the motion of heave and pitch modes at road input.

Assuming that the stiffness and damping properties of the model are linear, the mathematical model of the integrated human-seat-vehicle model in the vertical and rotational directions can be obtained as follows:

$$\begin{aligned}
m_3\ddot{y}_6 + k_3(y_6 - y_5) + c_3(\dot{y}_6 - \dot{y}_5) &= 0 \\
m_2\ddot{y}_5 + k_2(y_5 - y_4) + c_2(\dot{y}_5 - \dot{y}_4) - k_3(y_6 - y_5) - c_3(\dot{y}_6 - \dot{y}_5) &= 0 \\
m_1\ddot{y}_4 + k_1(y_4 - y_0) + c_1(\dot{y}_4 - \dot{y}_0) - k_2(y_5 - y_4) - c_2(\dot{y}_5 - \dot{y}_4) &= 0 \\
m_v\ddot{y}_3 + k_{s11}(y_2' - y_2) + c_{s11}(\dot{y}_2' - \dot{y}_2) + k_{s21}(y_1' - y_1) + c_{s21}(\dot{y}_1' - \dot{y}_1) - k_1(y_4 - y_0) - c_1(\dot{y}_4 - \dot{y}_0) &= 0 \\
m_{11}\ddot{y}_2 + k_{r11}(y_2) - k_{s11}(y_2' - y_2) - c_{s11}(\dot{y}_2' - \dot{y}_2) &= k_{r11}r_{11} \\
m_{21}\ddot{y}_1 + k_{r21}(y_1) - k_{s21}(y_1' - y_1) - c_{s21}(\dot{y}_1' - \dot{y}_1) &= k_{r21}r_{21} \\
I_{zz}\ddot{\theta} + [k_{s21}(y_1' - y_1) + c_{s21}(\dot{y}_1' - \dot{y}_1)]l_r - [k_{s11}(y_2' - y_2) + c_{s11}(\dot{y}_2' - \dot{y}_2)]l_f \\
- [k_1(y_4 - y_0) + c_1(\dot{y}_4 - \dot{y}_0)]e_1 &= 0
\end{aligned} \tag{6.8}$$

The equations of motion, Eq. 6.8, for the model can be expressed in matrix form as given below

$$[\mathbf{M}]\{\ddot{\mathbf{y}}\} + [\mathbf{C}]\{\dot{\mathbf{y}}\} + [\mathbf{K}]\{\mathbf{y}\} = \{\mathbf{f}\} \tag{6.9}$$

Where $[\mathbf{M}]$, $[\mathbf{C}]$, and $[\mathbf{K}]$ are mass, stiffness and damping matrices respectively. The response $\mathbf{y}(t)$, represents the displacement of the masses. The vectors (Eq. 6.9) $\ddot{\mathbf{y}}$ and $\dot{\mathbf{y}}$ represent the acceleration and velocity respectively of the lumped masses. The input vector is $\{\mathbf{f}\}$. All the matrices and vectors can be further represented as given below:

$$\mathbf{M} = \begin{bmatrix} m_3 & 0 & 0 & 0 & 0 & 0 & 0 \\ 0 & m_2 & 0 & 0 & 0 & 0 & 0 \\ 0 & 0 & m_1 & 0 & 0 & 0 & 0 \\ 0 & 0 & 0 & m_v & 0 & 0 & 0 \\ 0 & 0 & 0 & 0 & m_{11} & 0 & 0 \\ 0 & 0 & 0 & 0 & 0 & m_{21} & 0 \\ 0 & 0 & 0 & 0 & 0 & 0 & I_{zz} \end{bmatrix}$$

$$\mathbf{K} = \begin{bmatrix} k_3 & -k_3 & 0 & 0 & 0 & 0 & 0 \\ -k_3 & k_2 + k_3 & -k_2 & 0 & 0 & 0 & 0 \\ 0 & -k_2 & k_1 + k_2 & -k_1 & 0 & 0 & -k_1 e_1 \\ 0 & 0 & -k_1 & k_{s11} + k_{s21} + k_1 & -k_{s11} & -k_{s21} & -k_{s11} l_f + k_{s21} l_r + k_1 e_1 \\ 0 & 0 & 0 & -k_{s11} & k_{t11} + k_{s11} & 0 & k_{s11} l_f \\ 0 & 0 & 0 & -k_{s21} & 0 & k_{t12} + k_{s21} & -k_{s21} l_r \\ 0 & 0 & -k_1 e_1 & k_{s21} l_r - k_{s11} l_f + k_1 e_1 & k_{s11} l_f & -k_{s21} l_r & k_{s21} l_r^2 + k_{s11} l_f^2 + k_1 e_1^2 \end{bmatrix}$$

$$\mathbf{C} = \begin{bmatrix} c_3 & -c_3 & 0 & 0 & 0 & 0 & 0 \\ -c_3 & c_2 + c_3 & -c_2 & 0 & 0 & 0 & 0 \\ 0 & -c_2 & c_1 + c_2 & -c_1 & 0 & 0 & -c_1 e_1 \\ 0 & 0 & -c_1 & c_{s11} + c_{s21} + c_1 & -c_{s11} & -c_{s21} & -c_{s11} l_f + c_{s21} l_r + c_1 e_1 \\ 0 & 0 & 0 & -c_{s11} & c_{s11} & 0 & c_{s11} l_f \\ 0 & 0 & 0 & -c_{s21} & 0 & c_{s21} & -c_{s21} l_r \\ 0 & 0 & -c_1 e_1 & c_{s21} l_r - c_{s11} l_f + c_1 e_1 & c_{s11} l_f & -c_{s21} l_r & c_{s21} l_r^2 + c_{s11} l_f^2 + c_1 e_1^2 \end{bmatrix}$$

$$\mathbf{y} = \{y_6 \quad y_5 \quad y_4 \quad y_3 \quad y_2 \quad y_1 \quad \theta\}^T \quad \mathbf{f} = \{0 \quad 0 \quad 0 \quad 0 \quad k_{t11} r_{11} \quad k_{t12} r_{12} \quad 0\}^T$$

The parameter values used in this model are listed in Table 6.5. The parameters of human body segments were used from Boileau and Rakheja's [64] proposed model. The seat parameters were used from Liang and Chiang's paper [55] and Papalukopoulos and Natsiavas's model [76]. The vehicle parameters were taken from the measured data of a BMW Mini Cooper.

| Parameter | Value |
|---------------------------------|-----------------------|
| Head mass | 5.31 kg |
| Upper torso mass | 28.49 kg |
| Lower torso mass | 21.4 kg |
| Head stiffness | 310000 N/m |
| Upper torso stiffness | 183000 N/m |
| Lower torso stiffness | 62068.96 N/m |
| Head damping coefficient | 400 Ns/m |
| Upper torso damping coefficient | 4750 Ns/m |
| Lower torso damping coefficient | 614.79 Ns/m |
| Sprung mass | 534 kg |
| Front axle to centre of gravity | 0.871 m |
| Rear axle to centre of gravity | 1.596 m |
| Seat axle to centre of gravity | 0.1 m |
| Front unsprung mass | 33 kg |
| Rear unsprung mass | 36 kg |
| Pitch inertia | 585 kg m ² |
| Front suspension stiffness | 48000 N/m |
| Rear suspension stiffness | 32200 N/m |
| Front damping coefficient | 4500 Ns/m |
| Rear damping coefficient | 1660 Ns/m |
| Front tyre stiffness | 433000 N/m |
| Rear tyre stiffness | 410000 N/m |

Table 6.5: The parameters for the integrated human-seat-vehicle (7-DOF) model.

The seated human body is exposed to whole-body vibration because of the interaction between the vehicle wheels and the road surface. Based on these interactions “through-the-human body” response function is analysed; in this model following transmissibilities for the seated human body subject are investigated: road-to-floor, road-to-seat, road-to-head, floor-to-head and seat-to-head. In order to generate the transmissibility (frequency response function) for seat, human and vehicle; the listed parameters in Table 6.5 are used.

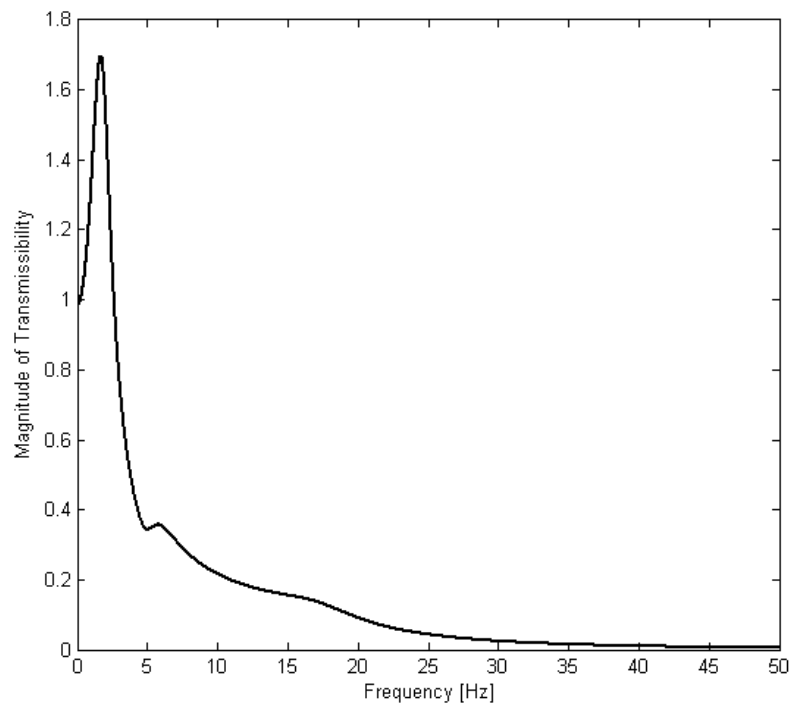
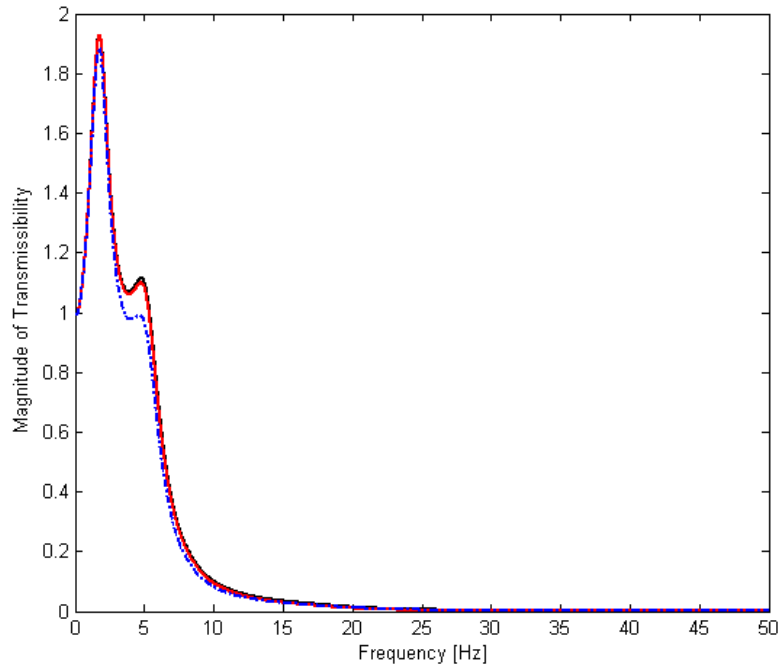
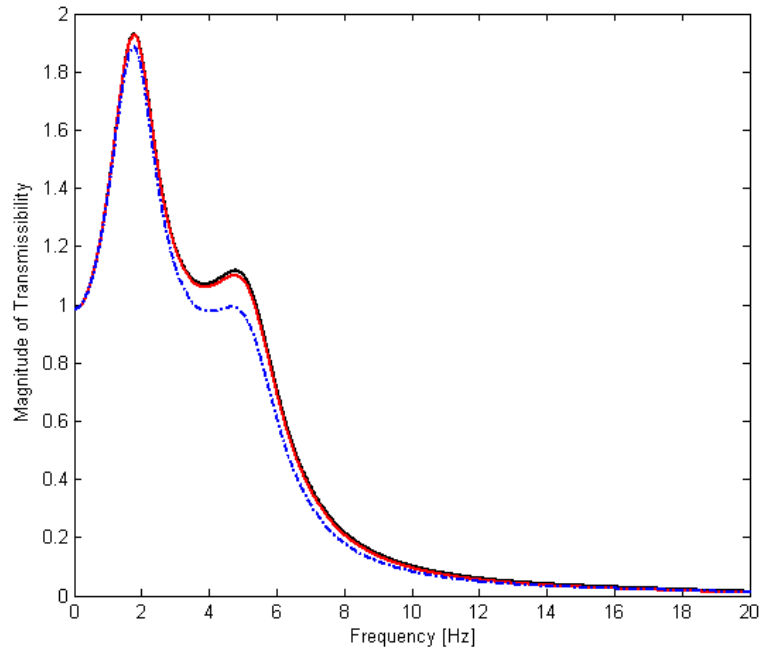


Figure 6.13: The magnitude of transmissibility (vehicle/sprung mass) in heave mode with road input.

Figure 6.13 shows the magnitude of transmissibility for the vehicle sprung mass. Resonance behaviour is clearly seen in the plot. The first peak for the sprung mass occurs at 1.73 Hz where the transmissibility is 1.6. The peak corresponds to the car body heave mode of vibration. There are small variations at around 5.8 Hz and 17 Hz, where the transmissibility is 0.35 and 0.13 respectively. The first variation corresponds to the lower body and seat response to vibration in heave mode. The second variation represents the hub mode of the vehicle.



(a) Frequency is up to 50 Hz.



(b) Frequency is up to 20 Hz.

Figure 6.14: The magnitude of transmissibility in heave mode with road input.

————— Head response, - - - - - Upper torso response, - · - · - Lower torso response.

Figure 6.14 shows the seated human response in heave mode with road input. The first peak occurs at 1.7 Hz, where the transmissibility is 1.9 for car body response. Head, upper and lower torso resonance frequency occur at around 4.8 Hz. The response of the lower body which is supported by the seat is less than the head and upper torso below 12 Hz.

The second small peaks occur at around 4.8 Hz for head, upper torso and lower torso where the transmissibilities are 1.1 (head and upper torso) and 0.9 for lower torso, respectively.

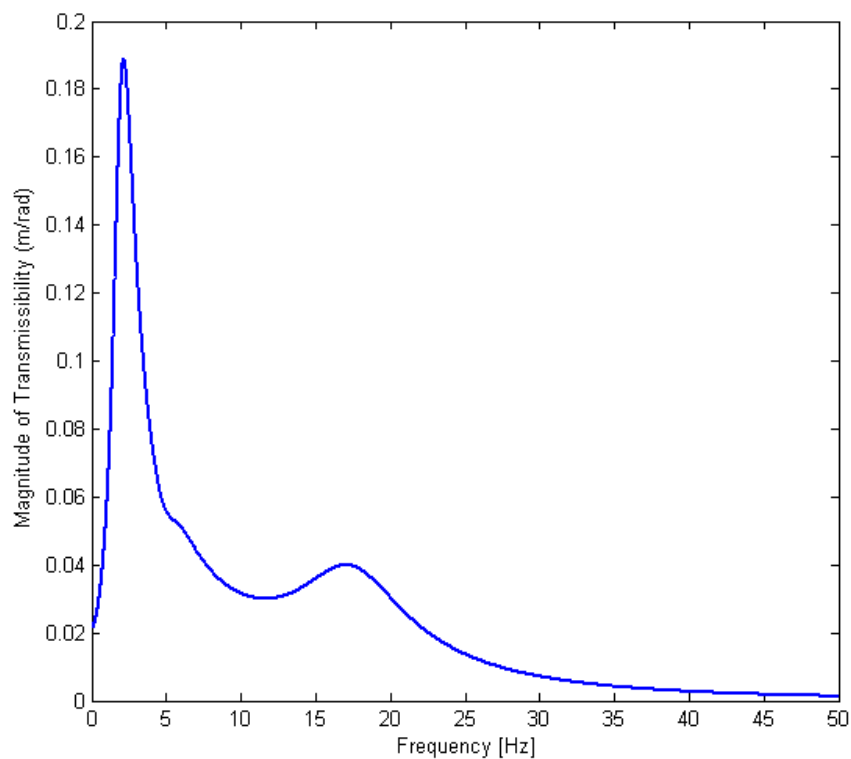


Figure 6.15: The magnitude of transmissibility (vehicle/sprung mass) in pitch mode with road input.

The pitch motion of the vehicle is shown in Figure 6.15. The first peak occurs at 2.2 Hz, where the transmissibility is 0.18 rad/m; the peak corresponds to the car body pitch mode. The second peak occurs at around 17.3 Hz where the transmissibility is 0.03 rad/m; which represents the dominant hub mode (wheel

motion) of the car. A small variation is seen at around 5.5 Hz, where the transmissibility is 0.05 rad/m. This variation represents the seat response in pitch mode.

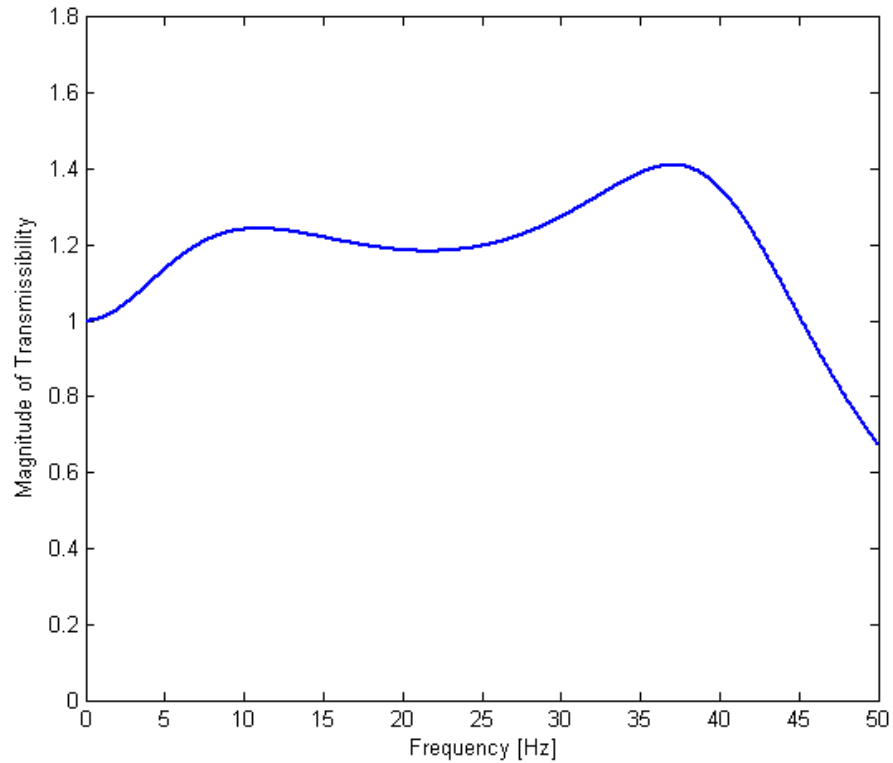


Figure 6.16: The magnitude of transmissibility for head response in respect to the seat input.

Figure 6.16 shows the seat-to-head transmissibility for the seated human response in heave and pitch motions. A variation is seen from the plot at around 10 Hz where the transmissibility is 1.2. The first dominant peak occurs at 37 Hz where the transmissibility is 1.4; this peak corresponds to resonance of the head based on the connection to rest of the body.

6.3.2 Summary

In this section, a 7-DOF integrated human-seat-vehicle model was developed for dynamics of a seated human body subject in a car, where the car is exposed to the vertical and rotational vibrations due to the heave and pitch motions. From the model, the vibration influence on the seated human body segments, i.e. head, lower body and upper body were analysed.

The 7-DOF model demonstrates dynamics of a seated human body subject in a car without backrest support with respect to the road input. The following results were obtained from this model;

- The first resonance frequency is 1.73 Hz for the vehicle body in heave mode.
- The second resonance frequency occurs at 2.2 Hz which is the vehicle pitch mode.
- Wheel hub modes occur around 17 Hz-17.3 Hz.
- Road-to-head and road-to-upper body transmissibilities peak at about 4.8 Hz, where the transmissibility is around 1.1.
- Road-to-lower body transmissibility peaks at about 4.8 Hz where the transmissibility is around 0.9.
- The resonance frequency for seat and lower body occur at 5.5 Hz for pitch mode, at around 4 Hz-6 Hz for heave mode.
- Seat-to-head transmissibility has a peak at about 37 Hz where the transmissibility is around 1.4. The peak corresponds to head resonance.

6.4 DISCUSSION

In this chapter, the biodynamic behaviour of a seated human body in the vehicle was characterized in two parts:

1. The biomechanical lumped parameter SDOF, and 3-DOF models were analysed under the influence of the floor input in the vertical direction.
2. The integrated human-seat-vehicle (7-DOF) model without backrest and headrest was developed. The vibration transmitted to the human body segments and the seat in the motion of heave and pitch modes in the vertical and rotational directions were analysed.

For this model, parameter values from the published papers were used. Based on these parameters, the effect of mass, stiffness coefficient and damping coefficient were analysed and evaluated based on the SDOF model. The following can be concluded from the analysis:

- The parameter values used in the models play an important role in determining the usefulness of the model. The published literature shows no definite value being used by the researchers. The parametric study in this chapter has shown the likely parameter values resulting in reliable response estimates.
- The biomechanical modelling of a seated human body alone may not be sufficient to obtain vehicle discomfort features. Either the floor-to-human body segment transmissibility or seat-to-head transmissibility may not represent the real environmental vibration and its influence on the human body.

- N degree-of-freedom models in multiple directions provide significantly more useful information than the one directional model for analysing the human body segments. However, there is a degree of difficulty in obtaining the parameter values.
- A driver seat in a car has a limited movement because the seat does not move as much as before car body moves. However, the vibration may transfer to the seat in different directions. There is no dominant direction for vibration transferred to and through the seat, so the seat dynamic response may have to be studied using multi directional inputs.

CHAPTER 7

PREDICTIVE MODEL OF HUMAN BODY COMFORT IN A CAR

7.1 INTRODUCTION

The *in-situ* experimental study in Chapter 5 developed a discomfort metric by the measured objective and subjective comfort data in heave, pitch and roll modes. The evaluated results investigate the relation between multi-direction excitation and corresponding response and its influence on discomfort metric. The mathematical models that were developed and explained in Chapter 6 helped to depict human motion in a sitting position and to quantify the biodynamic response of seated human subjects in a car to the vibrational excitation in heave and pitch modes.

In this chapter, a predictive model of human body discomfort in a car is developed combining the transmissibility results and the *in-situ* discomfort curve measurements.

7.2 PREDICTIVE MODEL OF HUMAN BODY DISCOMFORT IN A CAR

A predictive model of the human body is developed in order to characterize the vibration transmission from the road to a seated human body in a car in 3 dimensional analyses in the heave, pitch and roll mode. The model (Figure 7.1) has *10-DOFs* and consists of *a full (7-DOF) vehicle model* and *a 3-DOF seated human body model*. The model has been developed using knowledge of the pitch plane model and the analytical study of integrated models of Chapter 6.

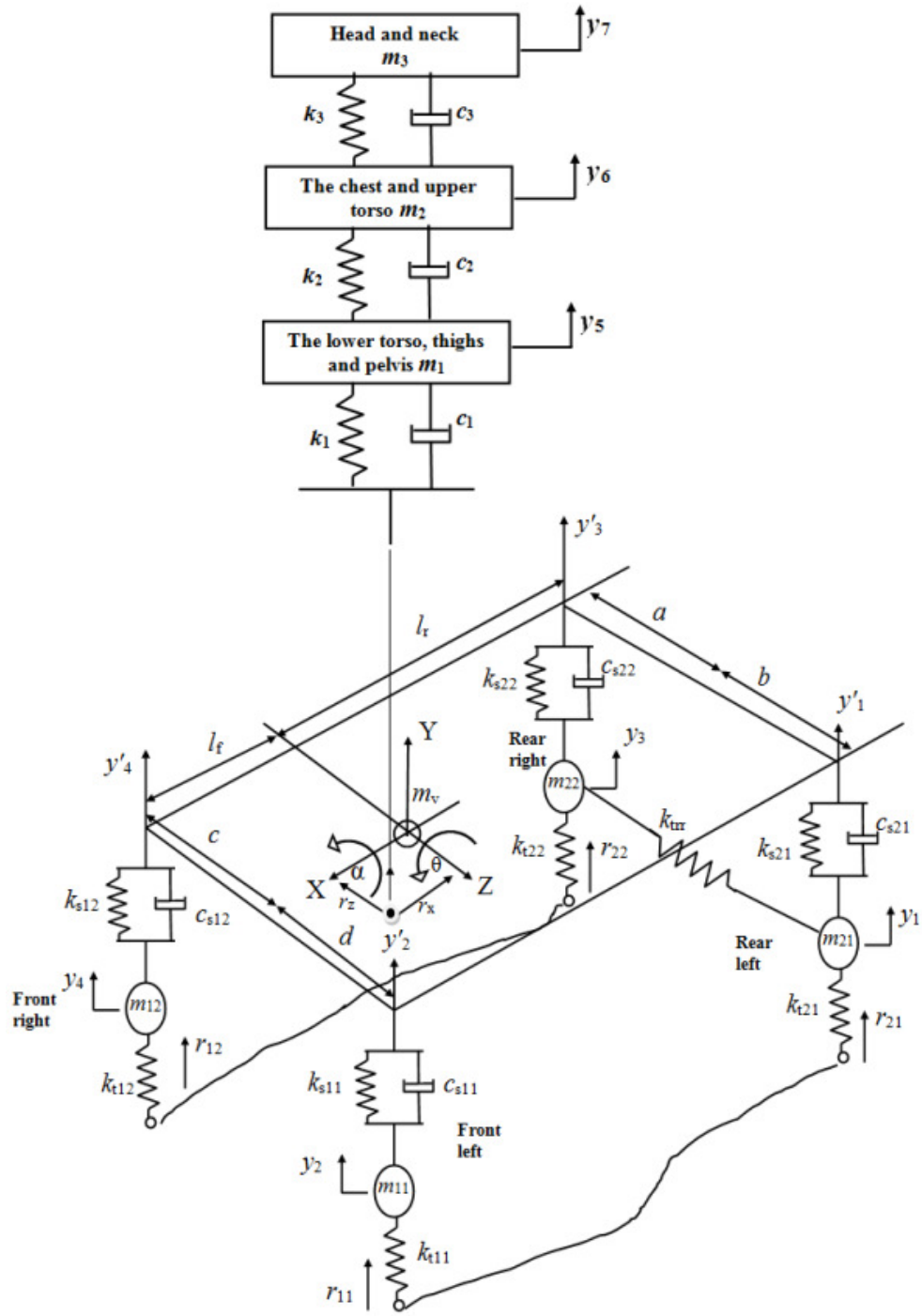


Figure 7.1: A lumped parameter integrated human-seat-vehicle (10-DOF) model without backrest in the motion of heave, pitch and roll modes at road input.

Figure 7.1 shows the lumped parameter integrated human-vehicle model without backrest for the motion in the vertical direction of the sprung mass (car body), which is connected to four unsprung masses (front-left, front-right, rear-left, and rear-right), considering heave, pitch and roll modes. The displacements of unsprung masses in the vertical direction are y_1 , y_2 , y_3 , and y_4 for left rear, left front, right rear and right front respectively. The vertical displacement, pitch angle, and roll angle are y , θ and α respectively. The displacements of the seated human body in the vertical direction are y_5 , y_6 , and y_7 for the lower body which is in contact with the seat, the upper torso and head, respectively.

The seated human body segments are the head and neck (m_3), the chest and upper torso (m_2), the lower torso, thighs and pelvis (m_1). The mass of the seat, lower legs and the feet is neglected. The stiffness and damping properties for the lower torso, thighs and pelvis are (k_1) and (c_1), for the chest and upper torso are (k_2) and (c_2), and for the head are (k_3) and (c_3).

The centre of gravity is assigned at l_f to the front axle and l_r to the rear axle; and d to the right-front tyre, c to the right-front tyre, b to the left-rear tyre, a to the right-rear tyre, respectively. The seat position is allocated with distances r_x and r_z from the centre of gravity. In the model, the parameters of masses are shown as m_3 , m_2 , and m_1 for the human body segments; m_v vehicle body; m_{11} , m_{12} , m_{21} , m_{22} wheel masses; I_{zz} is the sprung mass pitch moment of inertia; I_{xx} is the sprung mass roll moment of inertia; k_{rr} is the roll stiffness. The road input displacements are r_{11} , r_{12} , r_{21} , r_{22} . The driver is located through the lower body contact to the seat which is in turn connected by a spring k_1 and damper c_1 to the vehicle body.

The free-body diagrams of this ten degree-of-freedom model and the derivation of equations are given in Appendix E.

Assuming that the stiffness and damping properties of the model are linear, the mathematical model of the seated human body can be obtained as follows:

$$\begin{aligned}
y_s &= y - r_z \theta + r_x \alpha \\
y'_2 &= y - l_f \theta + d \alpha \\
y'_1 &= y - l_r \theta + b \alpha \\
y'_3 &= y + l_r \theta - a \alpha \\
y'_4 &= y - l_f \theta - c \alpha
\end{aligned} \tag{7.1}$$

$$\begin{aligned}
m_3 \ddot{y}_7 + k_3 (y_7 - y_6) + c_3 (\dot{y}_7 - \dot{y}_6) &= 0 \\
m_2 \ddot{y}_6 + k_2 (y_6 - y_5) + c_2 (\dot{y}_6 - \dot{y}_5) - k_3 (y_7 - y_6) - c_3 (\dot{y}_7 - \dot{y}_6) &= 0 \\
m_1 \ddot{y}_5 + k_1 (y_5 - y_{seat}) + c_1 (\dot{y}_5 - \dot{y}_{seat}) - k_2 (y_6 - y_5) - c_2 (\dot{y}_6 - \dot{y}_5) &= 0 \\
m_{11} \ddot{y}_2 + k_{t11} (y_2) - k_{s11} (y'_2 - y_2) - c_{s11} (\dot{y}'_2 - \dot{y}_2) &= k_{t11} r_{11} \\
m_{21} \ddot{y}_1 + k_{t21} (y_1) - k_{s21} (y'_1 - y_1) - c_{s21} (\dot{y}'_1 - \dot{y}_1) + \left\{ \frac{k_{tr}}{2} (y_1 - y_3) \right\} &= k_{t21} r_{21} \\
m_{12} \ddot{y}_4 + k_{t12} (y_4) - k_{s12} (y'_4 - y_4) - c_{s12} (\dot{y}'_4 - \dot{y}_4) &= k_{t12} r_{12} \\
m_{22} \ddot{y}_3 + k_{t22} (y_3) - k_{s22} (y'_3 - y_3) - c_{s22} (\dot{y}'_3 - \dot{y}_3) - \left\{ \frac{k_{tr}}{2} (y_1 - y_3) \right\} &= k_{t22} r_{22} \\
m_v \ddot{y} + k_{s11} (y'_2 - y_2) + c_{s11} (\dot{y}'_2 - \dot{y}_2) + k_{s21} (y'_1 - y_1) + c_{s21} (\dot{y}'_1 - \dot{y}_1) \\
+ k_{s12} (y'_4 - y_4) + c_{s12} (\dot{y}'_4 - \dot{y}_4) + k_{s22} (y'_3 - y_3) + c_{s22} (\dot{y}'_3 - \dot{y}_3) \\
- k_1 (y_5 - y_{seat}) - c_1 (\dot{y}_5 - \dot{y}_{seat}) &= 0 \\
I_{zz} \ddot{\theta} - \{ k_{s11} (y'_2 - y_2) + c_{s11} (\dot{y}'_2 - \dot{y}_2) \} l_f - \{ k_{s12} (y'_4 - y_4) + c_{s12} (\dot{y}'_4 - \dot{y}_4) \} l_f \\
+ \{ k_{s21} (y'_1 - y_1) + c_{s21} (\dot{y}'_1 - \dot{y}_1) \} l_r + \{ k_{s22} (y'_3 - y_3) + c_{s22} (\dot{y}'_3 - \dot{y}_3) \} l_r \\
+ \{ r_z (k_1 (y_5 - y_{seat}) + c_1 (\dot{y}_5 - \dot{y}_{seat})) \} &= 0 \\
I_{xx} \ddot{\alpha} - \{ k_{s12} (y'_4 - y_4) + c_{s12} (\dot{y}'_4 - \dot{y}_4) \} c + \{ k_{s11} (y'_2 - y_2) + c_{s11} (\dot{y}'_2 - \dot{y}_2) \} d \\
+ \{ k_{s21} (y'_1 - y_1) + c_{s21} (\dot{y}'_1 - \dot{y}_1) \} b - \{ k_{s22} (y'_3 - y_3) + c_{s22} (\dot{y}'_3 - \dot{y}_3) \} a \\
- \{ r_x (k_1 (y_5 - y_{seat}) + c_1 (\dot{y}_5 - \dot{y}_{seat})) \} &= 0
\end{aligned} \tag{7.2}$$

The equation (Eq. 7.2) of motion for the model can be expressed in matrix form as given below

$$[\mathbf{M}]\{\ddot{\mathbf{y}}\} + [\mathbf{C}]\{\dot{\mathbf{y}}\} + [\mathbf{K}]\{\mathbf{y}\} = \{\mathbf{f}\} \quad (7.3)$$

Where $[\mathbf{M}]$, $[\mathbf{C}]$, and $[\mathbf{K}]$ are mass, stiffness and damping matrices respectively. The response $\mathbf{y}(\mathbf{t})$, represents the displacement of the masses. The vectors (Eq. 7.3) $\ddot{\mathbf{y}}$ and $\dot{\mathbf{y}}$ represent the acceleration and velocity respectively of the lumped masses. The input vector is $\{\mathbf{f}\}$. All the matrices and vectors can be further represented as given in below:

$$\mathbf{M} = \begin{bmatrix} m_3 & 0 & 0 & 0 & 0 & 0 & 0 & 0 & 0 & 0 \\ 0 & m_2 & 0 & 0 & 0 & 0 & 0 & 0 & 0 & 0 \\ 0 & 0 & m_1 & 0 & 0 & 0 & 0 & 0 & 0 & 0 \\ 0 & 0 & 0 & m_{11} & 0 & 0 & 0 & 0 & 0 & 0 \\ 0 & 0 & 0 & 0 & m_{21} & 0 & 0 & 0 & 0 & 0 \\ 0 & 0 & 0 & 0 & 0 & m_{12} & 0 & 0 & 0 & 0 \\ 0 & 0 & 0 & 0 & 0 & 0 & m_{22} & 0 & 0 & 0 \\ 0 & 0 & 0 & 0 & 0 & 0 & 0 & m_v & 0 & 0 \\ 0 & 0 & 0 & 0 & 0 & 0 & 0 & 0 & I_{zz} & 0 \\ 0 & 0 & 0 & 0 & 0 & 0 & 0 & 0 & 0 & I_{xx} \end{bmatrix}$$

$$\{\mathbf{y}\} = \{y_7 \quad y_6 \quad y_5 \quad y_2 \quad y_1 \quad y_4 \quad y_3 \quad y \quad \theta \quad \alpha\}^T$$

$$\mathbf{f} = \{0 \quad 0 \quad 0 \quad k_{t11}r_{11} \quad k_{t21}r_{21} \quad k_{t12}r_{12} \quad k_{t22}r_{22} \quad 0 \quad 0 \quad 0\}^T$$

$$\mathbf{K} = \begin{array}{c} \begin{array}{|c|} \hline \begin{array}{ccc} k_3 & -k_3 & 0 \\ -k_3 & k_2 + k_3 & -k_2 \\ 0 & -k_2 & k_2 \end{array} \\ \hline \end{array} \\ \begin{array}{|c|} \hline \begin{array}{c} \uparrow \\ \text{Human model} \\ [0] \end{array} \\ \hline \end{array} \\ \begin{array}{|c|} \hline \begin{array}{c} \leftarrow \\ \text{Vehicle model} \end{array} \\ \hline \end{array} \end{array} \begin{array}{|c|} \hline \begin{array}{c} \downarrow \\ \text{Human-seat interface} \\ [0] \end{array} \\ \hline \end{array} \begin{array}{|c|} \hline \begin{array}{cccccccccccc} 0 & 0 & 0 & 0 & 0 & -k_1 & k_1 r_z & -k_1 r_x \\ \hline \begin{array}{cccccccc} k_{t11} + k_{s11} & 0 & 0 & 0 & -k_{s11} & k_{s11} l_f & -k_{s11} d \\ 0 & K_{55} & 0 & -k_{trr} / 2 & -k_{s21} & -k_{s21} l_r & -k_{s21} b \\ 0 & 0 & k_{t12} + k_{s12} & 0 & -k_{s12} & k_{s12} l_f & k_{s12} c \\ 0 & -k_{trr} / 2 & 0 & K_{77} & -k_{s22} & -k_{s22} l_r & k_{s22} a \\ \hline -k_1 & -k_{s11} & -k_{s21} & -k_{s12} & -k_{s22} & K_{88} & K_{89} & K_{810} \\ k_1 r_z & k_{s11} l_f & -k_{s21} l_r & k_{s12} l_f & -k_{s22} l_r & K_{98} & K_{99} & K_{910} \\ -k_1 r_x & -k_{s11} d & -k_{s21} b & k_{s12} c & k_{s22} a & K_{108} & K_{109} & K_{1010} \end{array} \\ \hline \end{array} \end{array}$$

$$K_{55} = k_{t21} + k_{s21} + k_{trr} / 2$$

$$K_{77} = k_{t22} + k_{s22} + k_{trr} / 2$$

$$K_{88} = k_{s11} + k_{s21} + k_{s12} + k_{s22} + k_1 =$$

$$K_{98} = (-k_{s11} l_f) - (k_{s12} l_f) + (k_{s21} l_r) + (k_{s22} l_r) - (k_1 r_z) = K_{89}$$

$$K_{108} = ((-k_{s12} c) + (k_{s11} d) + (k_{s21} b) - (k_{s22} a) + k_1 r_x) = K_{810}$$

$$K_{99} = k_{s11} l_f^2 + k_{s12} l_f^2 + k_{s21} l_r^2 + k_1 r_z^2 + k_{s22} l_r^2 - k_1 r_x r_z$$

$$K_{109} = k_{s12} l_f c - k_{s11} l_f d + k_{s21} l_r b - k_{s22} l_r a - k_1 r_x r_z = K_{910}$$

$$K_{1010} = k_{s12} c^2 + k_{s11} d^2 + k_{s21} b^2 + k_{s22} a^2 + k_1 r_x^2$$

$$\mathbf{C} = \begin{array}{c} \begin{array}{|c|} \hline \begin{array}{c} \text{Human model} \\ [0] \end{array} \\ \hline \end{array} \begin{array}{|c|} \hline \begin{array}{c} \text{Human-seat interface} \\ [0] \end{array} \\ \hline \end{array} \begin{array}{|c|} \hline \begin{array}{c} \text{Vehicle model} \\ [0] \end{array} \\ \hline \end{array} \end{array} \begin{bmatrix} c_3 & -c_3 & 0 & 0 & 0 & 0 & 0 & 0 & -c_1 & c_1 r_z & -c_1 r_x \\ -c_3 & c_2 + c_3 & -c_2 & 0 & 0 & 0 & 0 & 0 & -c_1 & c_1 r_z & -c_1 r_x \\ 0 & -c_2 & c_2 + c_1 & 0 & 0 & 0 & 0 & 0 & -c_1 & c_1 r_z & -c_1 r_x \\ 0 & 0 & 0 & c_{s11} & 0 & 0 & 0 & -c_{s11} & c_{s11} l_f & -c_{s11} d \\ 0 & 0 & 0 & 0 & c_{s21} & 0 & 0 & -c_{s21} & -c_{s21} l_r & -c_{s21} b \\ 0 & 0 & 0 & 0 & 0 & c_{s12} & 0 & -c_{s12} & c_{s12} l_f & c_{s12} c \\ 0 & 0 & 0 & 0 & 0 & 0 & c_{s22} & -c_{s22} & -c_{s22} l_r & c_{s22} a \\ -c_1 & -c_{s11} & -c_{s21} & -c_{s12} & -c_{s22} & C_{88} & C_{89} & C_{810} & C_{89} & C_{810} \\ c_1 r_z & c_{s11} l_f & -c_{s21} l_r & c_{s12} l_f & -c_{s22} l_r & C_{98} & C_{99} & C_{910} & C_{99} & C_{910} \\ -c_1 r_x & -c_{s11} d & -c_{s21} b & c_{s12} c & c_{s22} a & C_{108} & C_{109} & C_{1010} & C_{109} & C_{1010} \end{bmatrix}$$

$$C_{88} = c_{s11} + c_{s21} + c_{s12} + c_{s22} + c_1$$

$$C_{98} = -c_{s11} l_f - c_{s12} l_f + c_{s21} l_r + c_{s22} l_r - c_1 r_z = C_{89}$$

$$C_{108} = -c_{s12} c + c_{s11} d + c_{s21} b - c_{s22} a + c_1 r_x = C_{810}$$

$$C_{99} = c_{s11} l_f^2 + c_{s12} l_f^2 + c_{s21} l_r^2 + c_1 r_z^2 + c_{s22} l_r^2 - c_1 r_x r_z$$

$$C_{109} = c_{s12} l_f c - c_{s11} l_f d + c_{s21} l_r b - c_{s22} l_r a - c_1 r_x r_z = C_{910}$$

$$C_{1010} = c_{s12} c^2 + c_{s11} d^2 + c_{s21} b^2 + c_{s22} a^2 + c_1 r_x^2$$

7.3 VALIDATION OF PREDICTIVE MODEL

The transmissibilities estimated using the predictive model are compared with measured values. The parameter values used in this predictive 10-DOF model are listed in Table 7.1.

Figure 7.2 shows the road-to-seat transmissibility for measured vibration and the proposed model. The principal resonance occurs at about 2 Hz for both curves, where the transmissibility is 1.7 for proposed model, and 1.6 for experimental study. The peaks correspond to vehicle body bounce frequency. The second resonance for modelling occurs at around 5 Hz, where the transmissibility is 0.87. This peak corresponds to the seat response. At most other frequencies the predictive model results in slightly larger values than the experimental.

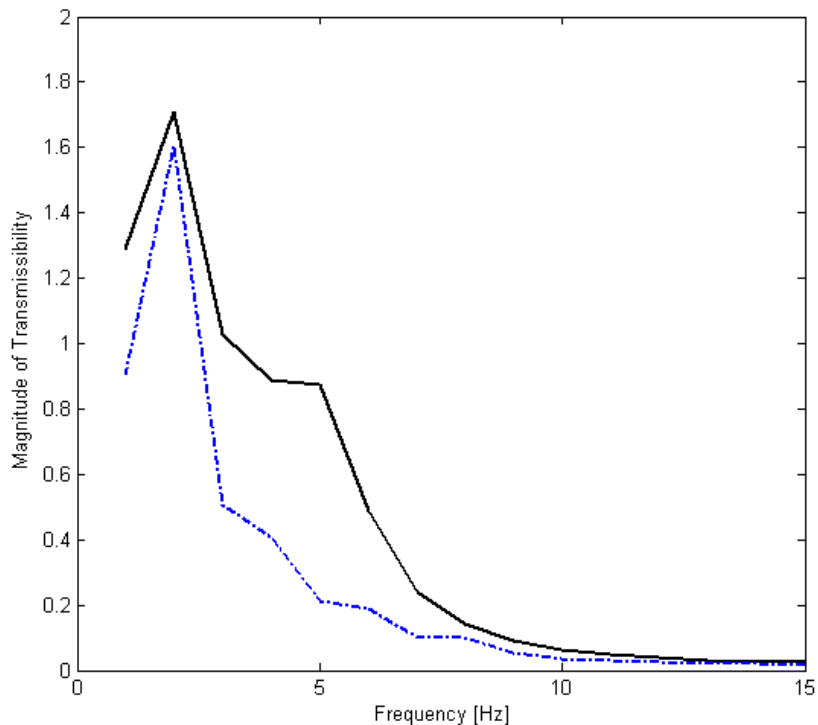


Figure 7.2: Comparison of road-to-seat transmissibility in heave mode. _____ Proposed model, -.-.-.- measured vibration transmissibility for 24 participants at 0.1 m/s² vibration excitation.

| Parameter | Value |
|---------------------------------|------------------------|
| Head mass | 5.31 kg |
| Upper torso mass | 28.49 kg |
| Lower torso mass | 21.4 kg |
| Head stiffness | 310000 N/m |
| Upper torso stiffness | 183000 N/m |
| Lower torso stiffness | 62068.96 N/m |
| Head damping coefficient | 400 Ns/m |
| Upper torso damping coefficient | 4750 Ns/m |
| Lower torso damping coefficient | 614.79 Ns/m |
| Sprung mass | 1068 kg |
| Front axle to centre of gravity | 0.871 m |
| Rear axle to centre of gravity | 1.596 m |
| Front unsprung mass | 33 kg |
| Rear unsprung mass | 36 kg |
| Pitch inertia | 1170 kg m ² |
| Front suspension stiffness | 48000 N/m |
| Rear suspension stiffness | 32200 N/m |
| Front damping coefficient | 4500 Ns/m |
| Rear damping coefficient | 1660 Ns/m |
| Front tyre stiffness | 433000 N/m |
| Rear tyre stiffness | 410000 N/m |
| Rear roll stiffness | 19600 N/m |
| Rear track | 1.465 m |
| Front track | 1.455 m |
| Wheelbase | 2.467 m |

Table 7.1: The parameters for the predictive 10-DOF model.

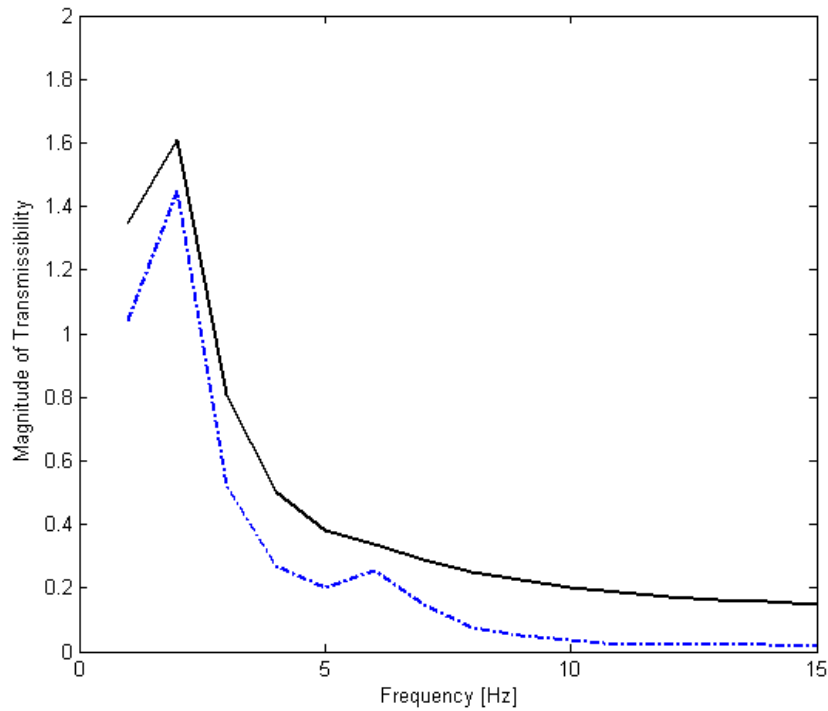


Figure 7.3: Comparison of road-to-floor transmissibility in heave mode. _____ Proposed model, -.-.-.- measured vibration transmissibility for 24 participants at 0.1 m/s² vibration excitation.

Figure 7.3 shows the floor transmissibility in respect of road input for measured vibration and proposed model. The principal resonance occurs at around 2 Hz, where the transmissibility is 1.6 for proposed model and 1.4 for the experimental study. The response of the proposed model is higher than the curve of the experimental study. Small variations occur at around 6 Hz, where the transmissibility is 0.25 for the experimental study. Overall, the frequency responses show similar trends, some smoothing is seen in the predictive model; the damping values may not be accurate enough. The model refinement could involve parameter estimation which is out of the scope of this study. Hence, the predictive model resulting in fairly accurate trends here using published parameters will be used in obtaining discomfort curves.

7.3.1 Prediction of Discomfort Index

Discomfort Index (DCI) curves were obtained by measuring objective responses and relating the responses to subjective assessment of the twenty-four people from the *in-situ* experimental data (see Chapter 3, 4 and 5). The predicted DCI is determined by following the steps below:

- The tyre input displacements are calculated based on the 1 m/s^2 road input on the wheel for the heave motion in the frequency range of 1 Hz to 15 Hz. The input displacements are given by the Eq. 7.4.

$$r_{11}(\omega) = \frac{(2\pi)^2}{\omega^2} \quad (7.4)$$

- The tyre input displacements are calculated based on the 0.63 m/s^2 road input on the wheel for pitch and roll in the frequency range of 3 Hz to 15 Hz. The inputs are phase managed to have either pitch or roll motion input.
- The determined RMS (root-mean-square) acceleration values are matched to discomfort indices (see Chapter 5) for particular frequencies. The resulting discomfort indices are plotted as a function frequency.

The frequencies, seat accelerations and corresponding discomfort index (DCI) values are listed in Table 7.2 for heave mode, Table 7.3 for pitch mode and Table 7.4 for roll mode.

| Frequency (Hz) | Seat Output Acc (m/s ²) | DCI |
|----------------|-------------------------------------|-----|
| 1 | 1.2 | 3.8 |
| 2 | 1.5 | 3.4 |
| 3 | 1.1 | 4.3 |
| 4 | 0.8 | 4.4 |
| 5 | 0.6 | 3.9 |
| 6 | 0.5 | 3.5 |
| 7 | 0.4 | 3.5 |
| 8 | 0.4 | 2.9 |
| 9 | 0.3 | 2.7 |
| 10 | 0.3 | 2.2 |
| 11 | 0.2 | 1.8 |
| 12 | 0.2 | 1.5 |
| 13 | 0.6 | 3.1 |
| 14 | 0.6 | 3.0 |
| 15 | 0.5 | 2.7 |

Table 7.2: Predicted discomfort index with seat output acceleration up to 15 Hz in heave mode.

| Frequency (Hz) | Seat Output Acc (m/s ²) | DCI |
|----------------|-------------------------------------|-----|
| 3 | 0.2 | 2.4 |
| 4 | 0.1 | 1.5 |
| 5 | 0.1 | 1.4 |
| 6 | 0.1 | 1.4 |
| 7 | 0.1 | 1.5 |
| 8 | 0.1 | 0.6 |
| 9 | 0.1 | 1.3 |
| 10 | 0.1 | 1.3 |
| 11 | 0.1 | 1.2 |
| 12 | 0.1 | 0.9 |
| 13 | 0.3 | 2.0 |
| 14 | 0.1 | 1.5 |
| 15 | 0.2 | 2.2 |

Table 7.3: Predicted discomfort index with seat output acceleration up to 15 Hz in pitch mode.

| Frequency (Hz) | Seat Output Acc (m/s ²) | DCI |
|----------------|-------------------------------------|-----|
| 3 | 0.4 | 4.3 |
| 4 | 0.1 | 2.6 |
| 5 | 0.2 | 2.1 |
| 6 | 0.2 | 2.1 |
| 7 | 0.2 | 2.8 |
| 8 | 0.5 | 3.3 |
| 9 | 0.4 | 3.3 |
| 10 | 0.3 | 2.3 |
| 11 | 0.2 | 1.7 |
| 12 | 0.1 | 1.4 |
| 13 | 0.1 | 0.8 |
| 14 | 0.1 | 1.3 |
| 15 | 0.1 | 1.2 |

Table 7.4: Predicted discomfort index with seat output acceleration up to 15 Hz in roll mode.

The predicted discomfort index (DCI) graphs are given in Figure 7.4 for heave mode, Figure 7.5 for pitch mode, and Figure 7.6 for roll mode. The differences of discomfort index for predicted model and experimental study are that the predicted discomfort index was calculated based on constant road input (measurement on a road); the discomfort index defined from the in-situ experimental study was calculated based on driver seat input (measurement on a driver seat).

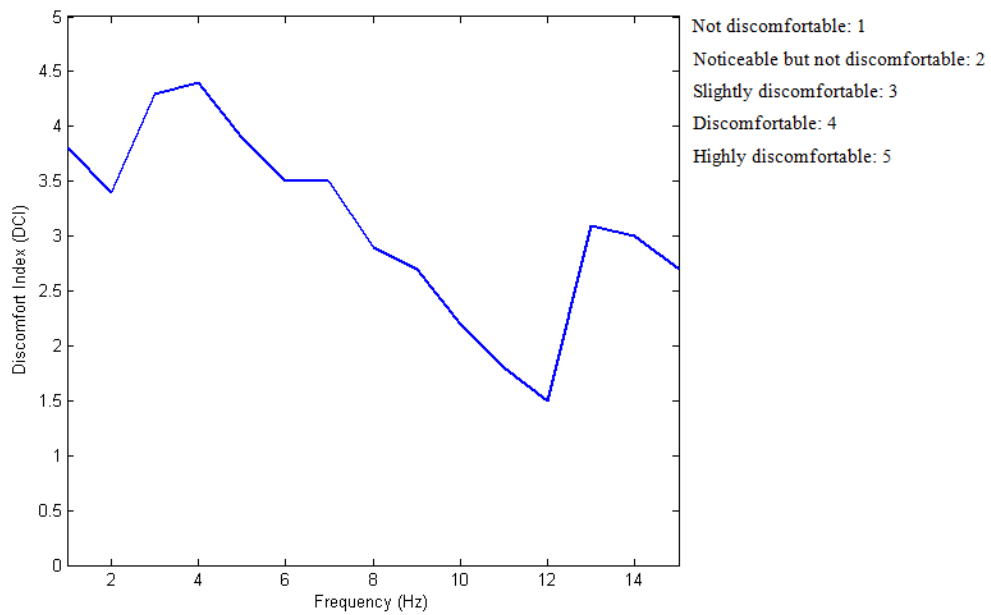


Figure 7.4: Predicted discomfort index for heave mode.

Figure 7.4 shows the predicted discomfort index up to 15 Hz in heave mode. The discomfort rate decreases above 5 Hz until 12 Hz. The highly uncomfortable rate is seen from the plot at around 3 Hz and 4 Hz.

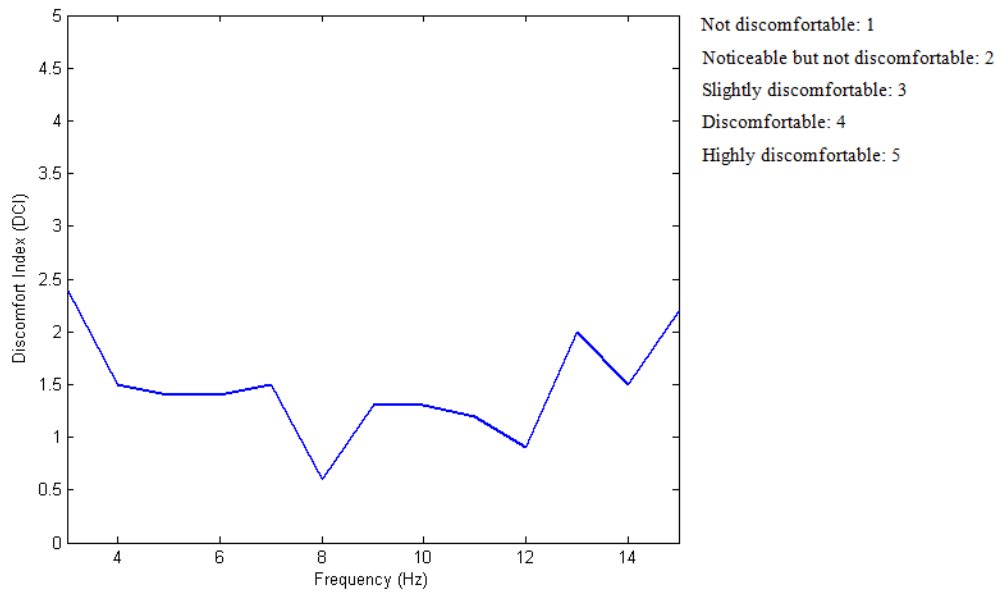


Figure 7.5: Predicted discomfort index for pitch mode.

Figure 7.5 shows the predicted discomfort index in the frequency range of 3 Hz to 15 Hz in pitch mode. From the plot, the discomfort index is seen not above 2.5. In general, the DCI is between noticeable but not uncomfortable and slightly uncomfortable in the frequency range of 15 Hz. The DCI rate decreases at around 8 Hz, 12 Hz and 14 Hz.

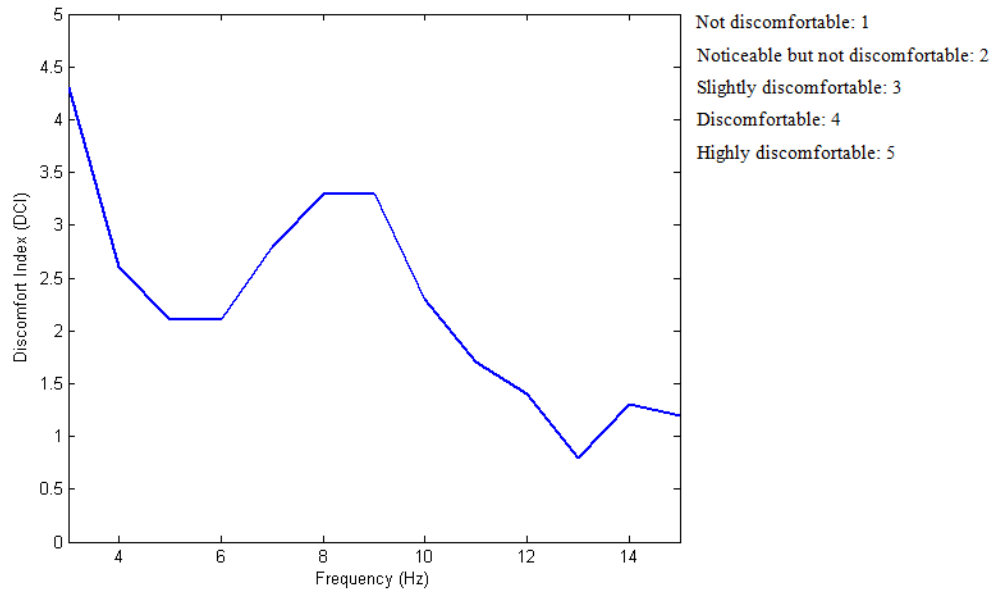


Figure 7.6: Predicted discomfort index for roll mode.

Figure 7.6 shows the predicted discomfort index in the frequency range of 3 Hz to 15 Hz in roll mode. The discomfort rate of the roll motion is higher than pitch mode. From the plot, the DCI decreases between 3 Hz to 5 Hz, 9 Hz to 13 Hz.

7.4 DISCUSSION

In this study, the model of a seated human body in a car was developed. This model has been analysed in terms of vibration transmissibility between the road input and the floor and seat by experimental data from Chapter 4 and 5. The human body parameters are used from Chapter 6.

From the model analysis and validations, the proposed model predicts results that slightly deviate from the experimental data because the possible errors in parameters of the biodynamic human model taken from the published studies. In spite of this, the experimental and predictive models, (Fig. 7.2 and Fig. 7.3) show the similar response behaviours.

The discomfort indices (DCI) were predicted by combining the modelling study and the experimental results for heave, pitch and roll modes. The DCI curves can be very useful in obtaining frequency based information eventually helping to establish design targets. The refined model can be handy in the initial design stages for figuring comfort issues.

CHAPTER 8

CONCLUSIONS

This research is mainly concerned with the study of quantification of a seated human response to vibration and development of a discomfort metric. The *in-situ* new experimental study, using twenty-four seated participants in a car on the four-post rig simulator for the first time, was performed to quantify discomfort in a real environmental condition. The measured acceleration and rated subjective judgement discomfort scale were analysed at every frequency level to develop the discomfort index in heave, pitch and roll mode based on the seat input. A predictive model was developed to analyze the vibration transmitted to the human body segments based on road input. A predictive discomfort metric was developed in terms of vibration transmissibility from the subjective assessment of twenty-four seated participants and the road input calculated. In this research, the following objectives were achieved:

Objective 1: A new experimental protocol, which differs from other published studies, was developed in order to understand the dynamic behaviour of vehicles.

Objective 2: An objective vibration measurement on the occupants in a car was studied to quantify the biodynamic response, human discomfort and perception.

Objective 3: A discomfort index was determined and a discomfort metric was developed using subjective assessment of car passengers.

Objective 4: A mathematical model was developed to represent the dynamics of a vehicle-seat-occupant system to predict discomfort in a car.

Objective 5: The discomfort indices were predicted by combining the modelling study and experimental results for heave pitch and roll modes.

On the basis of the studies conducted in this thesis, the following conclusions are drawn:

In the experimental study:

- Dynamic behaviour of a vehicle was characterized based on ‘cause-effect’ relations in terms of the vehicle resonant modes and the vibration transmitted. From the experimental data, vibration transmitted from road-to-floor, road-to-seat and floor-to-seat were quantified and the influence of vibration on discomfort was evaluated.
- The vehicle resonance frequencies occurred at 1.75 Hz and 13.25 Hz in heave mode; 2 Hz and 12.75 Hz in pitch mode; and 2.25 Hz and 13.75 Hz in roll mode.
- Seat responded well at 9 Hz in heave mode, 10.5 Hz in pitch mode and 11.25 Hz in roll mode.
- A new measurement method was developed and investigated for objective and subjective assessment by using the limitations of vehicle response to vibration from the four-post rig.
- The discomfort index (mean, standard deviation) as a function of seat RMS acceleration was analysed and evaluated to assess the human perception to vibration and human sensitivity for varying input frequency and vibration magnitude.
- The influence of excitation frequency on perception of vibration was analysed based on constant seat acceleration. The findings are :
 - In general, increase in the stimuli results in increased discomfort. The human perception sensitivity varies depending on the input vibration magnitude and frequency. For a given frequency, the discomfort index (mean) increases when vibration magnitude increased. For a given input vibration magnitude, when the frequency increases, the discomfort index (mean) decreases.

In the analytical study:

- Mathematical vehicle dynamic models were studied to predict the characterisation of vehicle response in heave, pitch and roll modes. The undamped natural frequencies from the studied models were calculated:
 - Half (4-DOF) vehicle model: Pitch, 1.87 Hz; heave, 2.21 Hz; front left-hub, 19.22; rear left-hub, 17.65 Hz.
 - Full (7-DOF) vehicle model: Pitch, 1.76 Hz; roll, 2.41 Hz; heave, 2.19. The natural frequencies for each unsprung mass are 19.22 Hz (front left), 18.62 Hz (front right), 17.65 Hz (rear left), and 17.30 Hz (rear right).
- The vibration transmitted and its influences on the whole human body were quantified; and the perceptions were analysed in the experimental study. The resonance behaviour of the human body segments were not measured due to the limited experimental resources.
- In biomechanical modelling, the parameters play an important role in determining the reliability of the models. Therefore, many models with different parameters were analysed from published studies to determine the accurate parameters for the developed models in the study. The measurement and calculation methods of the parameters were not clearly given in the published studies. In spite of this, due to difficulty in experimental measurements and not being in the scope of this study, the parameters of the human body segments (i.e. stiffness and damping coefficient) were used from the published studies.
- The results of analyzed SDOF model:
 - The resonance frequency of the seated human body was observed at 4 Hz in heave mode.
 - The increase in the body mass for a fixed stiffness value reduces the natural frequencies.
 - Biodynamic response amplitude of a seated human body increases when the pelvic stiffness increases.
 - Biodynamic response decreases when the pelvic/hip damping coefficient increases.

- In the 3-DOF model developed, the resonance frequency was observed around 4.9 Hz for the head, 4.8 Hz for the upper torso and 4.8 Hz for the lower torso with respect to the floor input.
- In the developed 7-DOF model, the first and second resonance frequencies were observed at 1.73 Hz and 2.2 Hz for the vehicle in heave and pitch mode respectively. The transmissibility for the lower body occurred at around 4-5 Hz in respect to road input. However, the modelling of the human body segments may not represent the real vibration influences in terms of transmissibility.

In the predictive model:

- To develop a predictive 10-DOF model of a seated human body in a car, a 3-DOF biomechanical seated human model was combined with a 7-DOF full vehicle model.
- The main reason for the full vehicle model being used was to characterize and analyse the vibration transmitted from road to human body in heave, pitch and roll modes.
- The principal resonance frequency for a seat-lower body was observed at around 4.8 Hz for the measured and proposed model in respect to road input.
- In the predictive model, the tyre input displacements were calculated based on road input in heave, pitch and roll.
- The results of transmissibility calculated from the predictive model were compared and analyzed with the subjective assessment data from the *in-situ* experimental study. For both of the models, first resonance frequency for human body occurs at around 4-5 Hz.
- The vibration transmissibility results of the predicted model were compared with the measured data to obtain the discomfort index (DCI) in heave, pitch and roll modes.

- A predictive discomfort index was developed for heave, pitch and roll modes from calculated RMS acceleration and quantified subjective assessment data.
- Based on the predictive discomfort index; below 8 Hz, the perception of vibration is between uncomfortable and highly uncomfortable in heave mode. Pitch and Roll mode are seen slightly more uncomfortable below about 6 Hz. However, roll and pitch mode are less uncomfortable after 7 Hz.
- This model can be handy for initial design of discomfort or comfort with varying degree-of-freedom models or multi-directional complicated models.

8.2 RECOMMENDATIONS FOR FUTURE WORK

In this study, a discomfort metric was developed for a seated human body in a car on the four-post rig. Based on the current study, the following future works are recommended:

- The study of predictive models may be extended to other linear models such as more complicated models to analyse the human body segments in terms of transmissibility. To analyse the human body dynamics and the response of the human body segments, skin-based experimental measurement methods may be developed for parametric study. This study could not be done in the current research because of lack of instrumentation.
- The human head response to vibration is difficult to measure. The participants can be trained and appropriate instrumental set-up developed so that the seat-to-head transmissibility measurements may be carried out to understand the head response.
- The seat dynamics may be analysed by a designer to develop a new seat to reduce the vibration transmitted through the human body.

REFERENCES

- [1] Looze, M.P. de, Vink, P., Koningsveld, E.A. P., Kuijt-Evers, L., & Van Rhijn, J. W. 2010. "Cost-effectiveness of ergonomic interventions in production". *Human Factors and Ergonomics in Manufacturing & Service Industries*, vol. 20, issue. 4, pp.316–323.
- [2] Griffin, M.J. 1990. "Handbook of Human Vibration", Academic Press, London.
- [3] Mansfield, N.J. 2005. "Human Response to Vibration", CRC Press, London.
- [4] Silva, C.W.De. 2007. "Vibration monitoring, testing, and instrumentation", CRC Press, London.
- [5] Cheng, B. and Nakashima, A. 2006. "A review on the effects of frequency of oscillation on motion sickness". Defence R&D Canada Toronto Technical Report. Paper number 229.
- [6] South, T. 2004. "Managing Noise and Vibration at Work". Elsevier Butterworth-Heinemann, Oxford.
- [7] International Standard 2631-1997: "Mechanical Vibration and Shock – Evaluation of human exposure to whole-body vibration".
- [8] Ebe, K. and Griffin, M.J. 2000. "Qualitative models of seat discomfort including static and dynamic factors". *Ergonomics*, vol. 43, pp. 771-790.
- [9] Kyung, G., Nussbaum, M.A., Babski-Reeves, K. 2008. "Driver sitting comfort and discomfort (Part I): Use of subjective ratings in discriminating car seats and correspondence among ratings". *International Journal of Industrial Ergonomics*, vol. 38, pp. 516-252.
- [10] Kolich, M. 2008. "A conceptual framework proposed to formalize the scientific investigation of automobile seat comfort". *Applied Ergonomics*, vol. 39, pp. 15-27.
- [11] Schust, M., Bluther, R., and Seidel. H. 2006. "Examination of perceptions (intensity, seat comfort, effort) and reaction times (brake and accelerator) during low-frequency vibration in x- or y-direction and biaxial (xy-) vibration of driver seats with activated and deactivated suspension". *Journal of Sound and Vibration*, vol. 298, pp. 606-626.

- [12] Sayers, M., 1985. "Development, Implementation, and Application of the Reference Quarter-Car Simulation". ASTM STP, vol. 884, pp. 25-47.
- [13] Wong, J, Y. 2001. "Theory of Ground Vehicles". John Wiley & Sons, Canada.
- [14] Hacaambwa, T.M. and Giacomini J. 2007. "Subjective response to seated fore-and-aft direction whole-body vibration", International Journal of Industrial Ergonomics, vol. 37, pp. 61-72.
- [15] British Standard 6841, 1987: "Guide to measurement and evaluation of human exposure to whole-body mechanical vibration and repeated shock".
- [16] Guglielmino, E. and Siretenau, T. 2008. "Semi-active suspension control". Springer, London.
- [17] Venor, J. 2001. "Vibration simulation and comfort assessment as part of the vehicle design and development process". 1st IMechE Automobile Division Southern Centre Conference, UK.
- [18] Westhuizen, A and Nierker, J.L. 2006. "Verification of seat effective amplitude transmissibility (SEAT) value as a reliable metric to predict dynamic seat comfort". Journal of Sound and Vibration, vol. 2965, pp. 1060-1075.
- [19] Demic, M.S. and Lukic, J.K. 2008. "Human body under two-directional random vibration". Journal of Low Frequency Noise, Vibration and Active Control, vol. 27, pp. 185-201.
- [20] Dynasoft Multimatix. "MX user manual", 2009, MTCA Ltd.
- [21] Fairley, T.E. and Griffin, M.J. 1989. "The apparent mass of the seated human body: Vertical vibration". Journal of Biomechanics, vol. 22, pp. 81-94.
- [22] Jones A.J. and Saunders D.J. 1972. "Equal comfort contours for whole body vertical, pulsed sinusoidal vibration". Journal of Sound and Vibration, vol. 23, pp. 1-14.
- [23] Nierkerk, J.L., Pielemeier, W.J. and Greenberg, J.A. 2003. "The use of seat effective amplitude transmissibility (SEAT) values to predict seat comfort". Journal of Sound and Vibration, vol. 260, pp. 867-888.
- [24] Vanhess, G. and Maes, M. 2002. "Vehicle suspension characterisation by using road simulation on a 4 poster rig". ISMA 1, pp. 63-70.

- [25] International Standard 5982- 2001: “Mechanical Vibration and Shock - Range of Idealized Values to Characterize Seated-Body Biodynamic Response under Vibration”.
- [26] Davis, J.R., Johnson, R., and Stepanek, J. 2008. “Fundamental of Aerospace Medicine”. 4th Edition, Lippincott Williams & Wilkins, USA.
- [27] Silva, C.W. 2002. “Vibration and Shock Handbook”. CRC Press, FL.
- [28] Cho, Y. and Yoon, Y.S.. 2001. “Biomechanical model of human on seat with backrest for evaluating ride quality”. International Journal of Industrial Ergonomics, vol. 27, pp. 331-345.
- [29] Silva, C.W. 1999. “Vibration Fundamentals and Practice”. CRC Press, London.
- [30] Osborne D.J. 1978. “Vibration and passenger comfort: can data from subjects be used to predict passenger comfort?”. Applied Ergonomics, vol. 9.3, pp. 155-161.
- [31] Osborne, D.J. and Boarer, P.A. 1982. “Variability in human response to whole-body vibration the effects of instructions”. Ergonomics, vol. 25, pp. 759-769.
- [32] Osborne, D.J. and Humphreys D.A. 1976. “Individual variability in human response to whole-body vibration”. Ergonomics, vol. 19, pp. 719-726.
- [33] Kim, T.H., Kim, Y.T. and Yoon, Y.S. 2005. “Development of a biomechanical model of the human body in a sitting posture with vibration transmissibility in the vertical direction”. International Journal of Industrial Ergonomics, vol. 35, pp. 817-829.
- [34] Nishiyama, S. and Uesugi. 2000. N. “Research on vibration characteristics between human body and seat, steering wheel, and pedals (Effects of seat position on ride comfort)”. Journal of Sound and Vibration, vol. 236, pp. 1-21.
- [35] Hinz, B., Blüthner, R., Rützel, S., Seidel, H., Wölfel, H.P. 2006. “Apparent mass of seated men-determination with single-and multi-axis excitations at different magnitudes”. Journal of Sound and Vibration, vol. 298, pp. 788–809.
- [36] Kaneko, C., Hagiwara, T., and Maeda, S. 2005. “Evaluation of whole-body vibration by the category judgement method”. Industrial Health, vol. 43, pp. 221-232.
- [37] Directive 2002/44/EC, Official Journal of the European Communities, L 177/13-19.

- [38] Kulakowski, B.T. "Vehicle-Road Interaction", ASTM, 1992 California.
- [39] Happian-Smith, J. 2002. "An Introduction to Modern Vehicle Design". Butterworth-Heinemann, Oxford.
- [40] Hrovat, D. 1988. "Influence of unsprung weight on vehicle ride quality". Journal of Sound and Vibration, vol. 124, pp. 497-516.
- [41] Abduljabbar, Z.S., and El-Madany, M.M. (2000). "Optimal active suspension with preview for a quarter-car model incorporating integral constraint and vibration absorber". International MDP Conference 2000, pp. 95-103.
- [42] Turkyay, S. and Akcay H. 2005. "A study of random vibration characteristics of the quarter-car model". Journal of Sound and Vibration, vol. 282, pp. 111-124.
- [43] Lin, J.S., and Huang, C.J., 2004. "Nonlinear Backstepping Active Suspension Design Applied to a Half-Car Model". Vehicle System Dynamics, vol. 6, pp.373-393.
- [44] Zeyada, Y., El-Beheiry, E., El-Arabi, M. and Karnopp, D. 2000. "Driver modelling using fuzzy logic controls for human-in-loop vehicle simulations". International MDP Conference, pp. 85-94.
- [45] Rakheja, S., Ahmed, A.K.W., Liu, P., and Richard, M.J. 2000. "Dynamic ride properties of a roll-connected vehicle suspension". Current Advances in Mechanical Design and Production, 7th Cairo University International MDP Conference, Cairo, pp. 105-112.
- [46] Zhu, Q. and Ishitobi, M. 2006. "Chaotic vibration of a nonlinear full-vehicle model". International Journal of Solids and Structures, vol. 43, pp. 747-759.
- [47] Yu, L. and Jun, L. 2005. "A study of active suspension based on full DOF vehicle model". Journal of Chongqing Univ. Eng-Ed., vol. 4, pp. 63-66.
- [48] Bouazara, M., Richard, M.J. and Rakheja, S. 2006. "Safety and comfort analysis of a 3-D vehicle model with optimal non-linear active seat suspension". Journal of Terramechanics, vol. 43, pp. 97-118.
- [49] Imine, H., Delanne, Y., M'Sirdi, N.K. 2006. "Road profile input estimation in vehicle dynamics simulation". Vehicle System Dynamics, vol. 44, pp. 285-303.

- [50] Bouazara, M. and Richard, M.J. 2001. "An optimization method designed to improve 3-D vehicle comfort and road holding capability through the use of active and semi-active suspensions". *J. Mech. A/Solids*, vol. 20, pp. 509-520.
- [51] Bonin, G. Cantisani, G. Loprencipe G. and Sbroli M. 2007. "Ride quality evaluation: 8 D.O.F. vehicle model calibration". 4th International SIIV Congress.
- [52] Coermann, R.R. 1960. "The passive dynamic mechanical properties of the human thorax-abdomen system and of the whole body system". *The Journal of Aviation Medicine*, vol. 31, pp. 443-455.
- [53] Rakheja, S., Dong, R.G., Patra, S., Boileau, P.E., Marcotte, P., and Warren, C. 2010. "Biodynamics of the human body under whole-body vibration: Synthesis of the reported data". *International Journal of Industrial Ergonomics*, vol. 40, pp. 710-732.
- [54] Rakheja, S., Stiharu, I., Zhang, H., and Boileau, P.E., 2006. "Seated occupant interactions with seat backrest and pan, and biodynamic responses under vertical vibration". *Journal of Sound and Vibration*, vol. 298, pp. 651-671.
- [55] Liang, C.C. and Chiang, C.F. 2006. "A study on biodynamic models of seated human subjects exposed to vertical vibration". *International Journal of Industrial Ergonomics*, vol. 36, pp. 869-890.
- [56] Coermann, R.R. 1962. "The mechanical impedance of the human body in sitting and standing position at low frequencies". *Human Factor*, pp. 1-27.
- [57] Amirouche, F. (2006). *Fundamentals of Multibody Dynamics*. Birkhauser, Boston.
- [58] Wei, L. and Griffin, M.J. 1998. "The prediction of seat transmissibility from measures of seat impedance". *Journal of Sound and Vibration*, vol. 214, pp. 121-137.
- [59] Suggs, C.W., Abrams, C.F. and Stikeleather, L.F. 1969. "Application of a damped spring-mass human vibration simulator in vibration testing of vehicle seats". *Ergonomics*, vol. 12, pp. 79-90.
- [60] Muksian, R. and Nash, C.D. 1974. "A model for the response of seated humans to sinusoidal displacements of the seat". *Journal of Biomechanics*, vol. 7, pp. 209-215.
- [61] Muksian, R. and Nash, C.D. 1976. "On frequency-dependent damping coefficients in lumped-parameter models of human beings". *Journal of Biomechanics*, vol. 9, pp. 339-342.

- [62] Tewari, V.K. and Prasad, N. 1999. "Three-DOF modelling of tractor seat-operator system". *Journal of Terramechanics*, vol. 36, pp. 207-219.
- [63] Wan, Y. and Schimmels, J.S. 1995. "A simple model that captures the essential dynamics of a seated human exposed to whole body vibration". *Advanced in Bioengineering*, vol. 31, pp. 333-334.
- [64] Boileau, P.E. and Rakheja, S. (1998). "Whole-body biodynamic response characteristics of the seated vehicle driver: Measurement and model development". *International Journal of Industrial Ergonomics*, vol. 22, pp. 449-472.
- [65] Srdjevic, Z., and Cveticanin, L., 2004. "Entropy compromise programming method for parameter identification in the seated driver biomechanical model". *International Journal of Industrial Ergonomics*, vol. 34, pp. 307-318.
- [66] Mertens, H. 1978. "Nonlinear behaviour of sitting humans under increasing gravity". *Aviation Space and Environmental Medicine*, pp. 287-298.
- [67] Kubo, M., Terauchi, F., Aoki, H. and Matsuoka, Y. 2001. "An investigation into a synthetic vibration model for humans: An investigation into a mechanical vibration human model constructed according to the relations between the physical, psychological and physiological reactions of humans exposed to vibration". *International Journal of Industrial Ergonomics*, vol. 27, pp. 219-232.
- [68] Qassem, W., Othman, M.O. and Abdul-Majeed, S. 1994. "The effects of vertical and horizontal vibrations on the human body". *Med. Eng. Physics*, vol. 16, pp. 151-161.
- [69] Qaasem, W. 1996. "Model prediction of vibration effects on human subjects seated on various cushions". *Med. Eng. Physics*, vol. 18, pp. 350-358.
- [70] Qassem, W., Othman, M.O. 1996. "Vibration effects on setting pregnant women- subjects of various masses". *Journal of Biomechanics*, vol. 29, pp. 493-301.
- [71] Liang, C.C. and Chiang, C.F. 2008. "Modeling of a seated human body exposed to vertical vibrations in various automotive postures". *Industrial Health*, vol. 46, pp. 125-137.
- [72] Patil, M.K., Palanicham, M.S. and Ghista, D.N. 1978. "Man-tractor system dynamics: Towards a better suspension system for human ride comfort". *Journal of Biomechanics*, vol. 11, pp. 397-406.

- [73] Patil, M.K., Palanicham, M.S. and Ghista, D.N. 1980. "Response of human body to tractor vibrations and its minimisation by provision of relaxation suspensions to both wheels and seat at the plane of centre of gravity". *Med. & Bio. Eng & Comp.*, vol. 18, pp. 554-562.
- [74] Kumar, A., Mahajan, P., Mohan, D., and Varghese, M., 2001. "Tractor Vibration Severity and Driver Health: a Study from Rural India". *Journal of Agriculture Engineering*, vol. 80, pp. 313-328.
- [75] Gundogdu, O. 2007. "Optimal seat and suspension design for a quarter car with driver model using genetic algorithms". *International Journal of Industrial Ergonomics*, vol. 37, pp. 327-332.
- [76] Papalukopoulos, C. and Natsiavas, S. 2007. "Nonlinear biodynamics of passengers coupled with quarter car models". *Journal of Sound and Vibration*, vol. 304, pp. 50-71.
- [77] Liang, C.C., Chiang, C.F. and Nguyen, T.G. 2007. "Biodynamic responses of seated pregnant subjects exposed to vertical vibrations in driving conditions". *Vehicle System Dynamics*, vol. 45, pp. 1017-1049.
- [78] Sugimoto, T. and Yamazaki, K. 2005. "First results from the JAMA human model project". Japan Automobile Research Institute. Paper number 05-0291, pp. 119-115.
- [79] Lee, K. 2006. "CAD System for Human-Centered Design". *Computer-Aided Design & Applications*, vol. 3, no. 5, pp. 615-628.
- [80] Jazar, R.N. 2008. "Vehicle Dynamics Theory and Application". Springer, NY.
- [81] Gillespie, T.D. 1992. "Fundamental of Vehicle Dynamics", Society of Automotive Engineers, Inc., PA.
- [82] Smith, S.D., Smith, J.A., and Bowden, D.R. 2008. "Transmission characteristics of suspension seats in multi-axis vibration environments". *International Journal of Industrial Ergonomics*, vol. 38, pp. 434-446.
- [83] Pacejka, H.B. 2006. "Tyre and Vehicle Dynamics". Butterworth-Heinemann, Oxford.
- [84] Thite, A., Banvidi, S., Ibicek, T., and Bennett, L. 2011. "Suspension parameter estimation in the frequency domain using a matrix inversion approach". *Vehicle System Dynamics*, vol. 49, issue 12 pp. 1803-1822.
- [85] Dynosoft MX. 2008. "Oxford Brookes Four Post Rig Operating Procedure". Multimatic Technical Centre Europe.

- [86] Vanhees, I.G. and Maes, I.M. 2002. "Vehicle suspension characterisation by using road simulation on a 4 poster test rig". ISMA, vol. I, pp. 63-70.
- [87] Henry, J. J. and Wambold, J.C. 1992. "Vehicle, Tire, Pavement Interface". ASTM, Philadelphia.
- [88] Kolich, M. 2008. "A conceptual framework proposed to formalize the scientific investigation of automobile seat comfort". Applied Ergonomics, vol. 39, pp. 15-27.
- [89] Jones, A.J. and Saunders, D.J. 1972. "Equal comfort contours for whole body vertical, pulsed sinusoidal vibration". Journal of Sound and Vibration, vol. 23 (1), pp. 1-14.
- [90] Maeda, S. 2005. "Necessary research for standardization of subjective scaling of whole-body vibration". Industrial Health, vol. 43, pp.390-401.
- [91] Maeda, S., Mansfield, N.J. and Shibata, N. 2008. "Evaluation of subjective responses to whole-body vibration exposure: Effect of frequency content". International Journal of Industrial Ergonomics, vol. 38, pp. 509-515.
- [92] Ibicek, T., and Thite, A. 2010. "Quantification of human comfort in a vehicle using a four-post rig excitation". Journal of Low Frequency Noise, Vibration and Active Control, vol. 31, no. 1.
- [93] Fukai, H., Tomita, Y., Mitsukura, Y., Watai, H., Tashiro, K., and Murakami, K. 2009. "Proposal of ride comfort evaluation method Using the EEG". 5th International Conference on Intelligent Computing, ICIC, pp. 824-833.
- [94] Srdevic, Z. and Cveticanin, L. 2004. "Entropy comprise programming method for parameter identification in the seated driver biomechanical model". International Journal of Industrial Ergonomics, vol. 34, pp. 307-318.
- [95] Abdeen, M.A.M and Abbas, W. 2010. "Analytical investigation and numeric prediction for biodynamic response of the seated human body". Journal of American Science, vol. 6 (11), pp. 289-239.

APPENDIX A

A.1 FULL VEHICLE MODELS

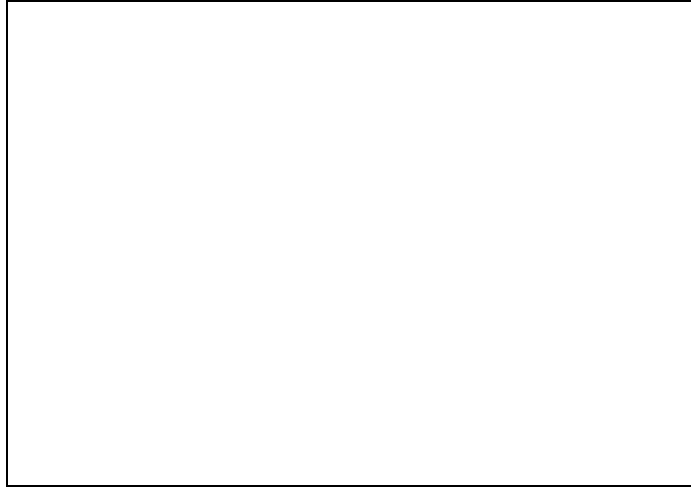


Figure A.1: Nonlinear full vehicle model [46].



Figure A.2: Full vehicle model [48].

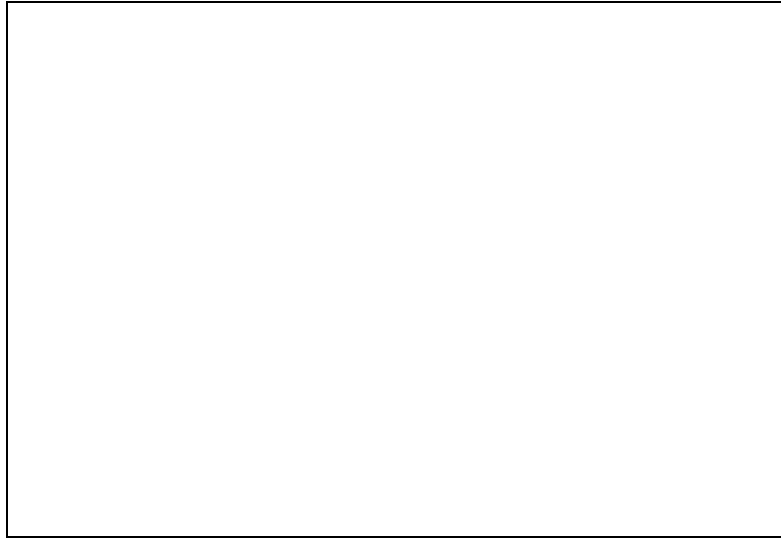


Figure A.3: Eight-DOF full vehicle model [51].

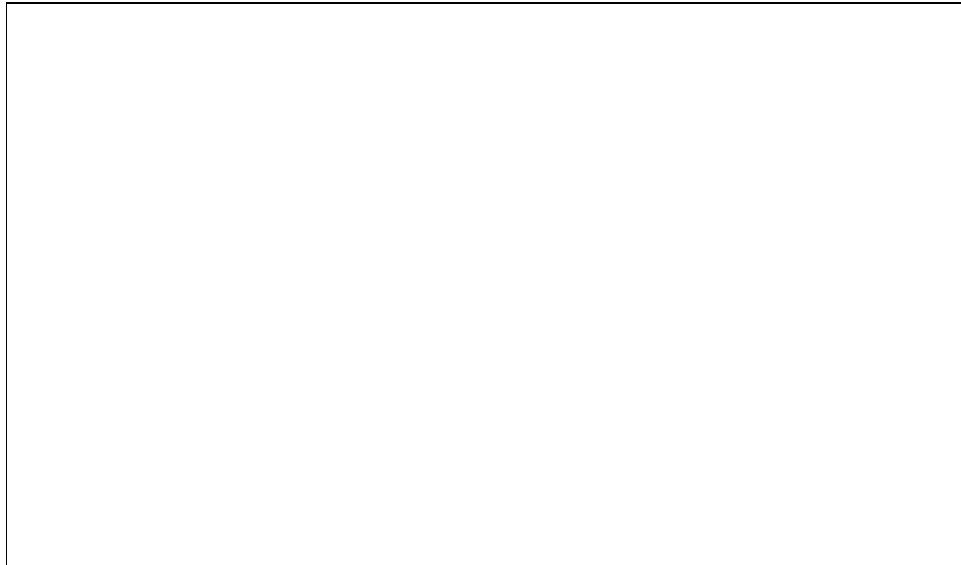


Figure A.4: Eight-DOF full vehicle model [47].

A.2 MULTI DEGREE-OF-FREEDOM LUMPED PARAMETER MODELS

| Authors & Remarks | Biomechanical parameters | | | Schematic of Model |
|--|--|---|--|--------------------|
| | Mass (kg) | Damping (Ns/m) | Stiffness (N/m) | |
| Merten's 5-DOF non-linear model of the upright sitting body in the vertical direction [66]. | $m_1=10$ $m_2=10$ $m_4=15$ $m_6=22$ $m_7=7$ Mtotal: 69 | Damping coefficient ranging 500-4000 | $100 < k_3 < 300$ $150 < k_5 < 200$ | |

Table A.1: Five-DOF lumped-parameter models of seated human subjects.

| Authors & Remarks | Biomechanical parameters | | | Schematic of Model |
|---|---|--|--|--------------------|
| | Mass (kg) | Damping (Ns/m) | Stiffness (N/m) | |
| <p>Muksian and Nash's 6-DOF non-linear model in the vertical direction [55, 60].</p> <p>*: Damping force between two related masses= Damping coefficient [rel.velocity+(rel.velocity)³].</p> <p>‡: Spring force between two related masses= Spring constant [rel. displacement +(rel.displacement)³].</p> <p>Patil's 7-DOF non-linear model [55].</p> | <p>$m_1=27.230$</p> <p>$m_2=5.921$</p> <p>$m_3=0.455$</p> <p>$m_4=1.362$</p> <p>$m_5=32.762$</p> <p>$m_6=6.820$</p> <p>$m_7=5.450$</p> <p>Mtotal: 80</p> <p>$m_1=27.230$</p> | <p>$c_1= -$</p> <p>$c_2=292.0^*$</p> <p>$c_3=292.0^*$</p> <p>$c_4=292.0^*$</p> <p>$c_5=292.0^*$</p> <p>$c_{56}=3580.0^*$</p> <p>$c_6=3580.0$</p> <p>$c_7=3580.0$</p> <p>$c_1=371.0$</p> | <p>$k_1= -$</p> <p>$k_2=877.0^\ddagger$</p> <p>$k_3=877.0^\ddagger$</p> <p>$k_4=877.0^\ddagger$</p> <p>$k_5=877.0^\ddagger$</p> <p>$k_{56}=52600.0^\ddagger$</p> <p>$k_6=52600.0$</p> <p>$k_7=52600.0$</p> <p>$k_1=25500.0$</p> | |

Table A. 2: Six and Seven-DOF lumped-parameter models of seated human subjects.

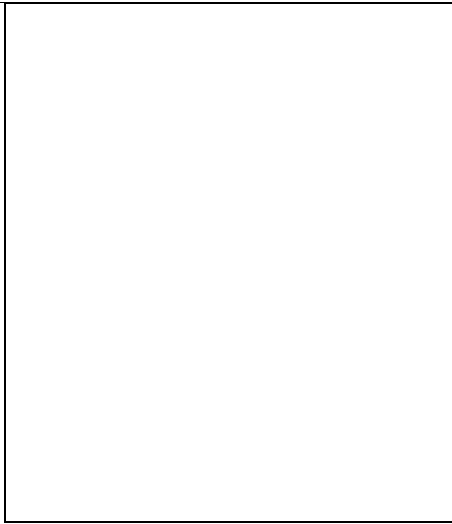
| Authors & Remarks | Biomechanical parameters | | | Schematic of Model |
|--|--|---------------------------|-----------------------|--|
| | Mass (kg) Inertia (kgm ²) | Damping (Ns/m) | Stiffness (kN/m) | |
| Cho and Yoon's 9-DOF linear biomechanical model of a seated human in the vertical and rotational direction. The lower part and the upper part of body were supported by the hip cushion and backrest cushion respectively [28]. | $m_1=15.3\pm 2.5$ | $c_{v1}=29.4\pm 14.4$ | $k_{v1}=72.0\pm 25.3$ |  |
| | $m_2=36.0\pm 6.0$ | $c_{h1}=447\pm 167.1$ | $k_{h1}=46.3\pm 10.9$ | |
| | $m_3=5.5\pm 0.9$ | $c_{v2}=0.4\pm 0.8$ | $k_{v2}=2.3\pm 0.8$ | |
| | $I_1=0.90\pm 0.20 \text{ kgm}^2$ | $c_{h2}=446\pm 165.4$ | $k_{h2}=20.2\pm 7.1$ | |
| | $I_2=1.10\pm 0.25 \text{ kgm}^2$ | $c_{t1}=380.6\pm 77.5$ | $k_{t1}=17.2\pm 4.6$ | |
| | $I_3=0.03\pm 0.00 \text{ kgm}^2$ | $c_{t2}=182.1\pm 40.1$ | $k_{t2}=25.0\pm 18.4$ | |
| | | $c_{r1}=2576.5\pm 1006.4$ | $k_{r1}=0$ | |
| | $c_{r2}=1.3\pm 1.7$ | $k_{r2}=0.1\pm 0.0$ | | |

Table A. 3: Nine-DOF lumped-parameter models.

| Authors & Remarks | Biomechanical parameters | | | Schematic of Model |
|--|---|--------------------------------------|---------------------------------------|--------------------|
| | Mass (kg) Inertia (kgm ²) | Damping (Ns/m) | Stiffness (Unit X 10N/m) | |
| Kubo's 9-DOF model in the vertical and rotational direction. It was assumed that parts of the human body would only swing back and forth as well as moves up and down [67]. | | 5 Hz Real Part | 5 Hz Real Part | |
| | | <i>c</i> ₁ = 754.1 | <i>k</i> ₁ = 1261.7 | |
| | | <i>c</i> ₂ = 469.8 | <i>k</i> ₂ = 452.2 | |
| | | <i>c</i> ₃ = 168.0 | <i>k</i> ₃ = 457.6 | |
| | | <i>c</i> ₄ = 181.2 | <i>k</i> ₄ = 665.7 | |
| | | <i>c</i> ₅ = 457.8 | <i>k</i> ₅ = 948.5 | |
| | | <i>c</i> ₆ = 256.9 | <i>k</i> ₆ = 338.0 | |
| | <i>c</i> ₇ = 182.8 | <i>k</i> ₇ = 239.5 | | |

Table A. 4: A masses-spring-dampers system of Nine-DOF model.

| Authors & Remarks | Biomechanical parameters | | | Schematic of Model |
|--|--|--------------------|---------------------|--------------------|
| | Mass (kg) Inertia (kgm ²) | Damping (kNs/m) | Stiffness (kN/m) | |
| Kim's 10-DOF (Multi) model for vertical, pitch and fore-aft motions [33]. | $m_1=20.3$ | $c_1=0.061$ | $k_1=6.40$ | |
| | $m_2=11.0$ | $c_2=1.79$ | $k_2=0.299$ | |
| | $m_3=19.87$ | $c_3=0.066$ | $k_3=113.7$ | |
| | $m_4=7.25$ | $c_4=0.079$ | $k_4=1.93$ | |
| | $m_5=12.9$ | $c_5=0.197$ | $k_5=18.37$ | |
| | $m_6= -$ | $c_6=0.154$ | $k_6=23.55$ | |
| | $I_1=1.16$ | $c_{h1}=0.014$ | $k_{h1}=0.614$ | |
| | $I_2=0.680$ | $c_{v1}=8.01$ | $k_{v1}=16.71$ | |
| | $I_3=1.53$ | $c_{h2}=0.015$ | $k_{h2}=0.905$ | |
| | $I_4=0.402$ | $c_{v2}=0.047$ | $k_{v2}=121.3$ | |
| | | $c_{r1}=0.030$ | $k_{r1}=0.162$ | |
| | Mtotal: 71.32 | $c_{r2}=0.724$ | $k_{r2}=0.328$ | |
| | | $c_{r3}=0.340$ | $k_{r3}=0.915$ | |
| | $c_{r6}=00.104$ | $k_{r6}=0.220$ | | |

Table A. 5: Multi 10-DOF model.

| Authors & Remarks | Biomechanical parameters | | | Schematic of Model |
|---|--|---|--|--------------------|
| | Mass (kg) | Damping (Ns/m) | Stiffness (N/m) | |
| Qassem's 11-DOF linear model of the upright sitting body in the vertical direction [55, 68]. | $m_1=27.23$ $m_2=5.906$ $m_3=0.454$ $m_4=1.326$ $m_5=32.697$ $m_6=5.470$ $m_7=5.297$ $m_8=2.002$ $m_9=4.806$ $m_{10}=1.084$ $m_{11}=5.445$ | $c_1=370.8$ $c_2=292.3$ $c_3=292.3$ $c_4=292.3$ $c_{54}=292.3$ $c_{59}=3581.6$ $c_6=3581.6$ $c_7=3581.6$ $c_8=3581.6$ $c_9=3581.6$ $c_{10}=3581.6$ $c_{11}=3581.6$ | $k_1=25016$ $k_2=877$ $k_3=877$ $k_4=877$ $k_{59}=877$ $k_{54}=52621$ $k_6=67542$ $k_7=67542$ $k_8=52621$ $k_9=52621$ $k_{10}=52621$ $k_{11}=52621$ | |

Table A. 6: Eleven-DOF lumped-parameter model.

| Authors & Remarks | Biomechanical parameters | | | Schematic of Model |
|---|---|---|--|--------------------|
| | Mass (kg) Inertia (kgm ²) | Damping (Ns/m and Nms/rad) | Stiffness (N/m and Nm/rad) | |
| <p>Liang and Chiang's 14-DOF model of a seated human body exposed to vertical vibrations in various automotive postures [71].</p> <p>*2: value for normal sitting posture without backrest support;</p> <p>*3: value for sitting posture with vertical or inclined backrest.</p> | <p>$m_1=20.3$</p> <p>$m_2=11.0$</p> <p>$m_3=19.87$</p> <p>$m_4=7.25$</p> <p>$m_5=12.9$</p> <p>$I_1=1.160$</p> <p>$I_2=0.680$</p> <p>$I_3=1.530$</p> <p>$I_4=0.402$</p> | <p>$c_1=14.0$</p> <p>$c_2=61.0$</p> <p>$c_3=1500.0$</p> <p>$c_4=266.0$</p> <p>$c_{h3}=334.5$</p> <p>$c_{h4}=266.0$</p> <p>$c_{v1}=8,010.0$</p> <p>$c_{v2}=47.0$</p> <p>$c_{h1}=14.0$</p> <p>$c_{h2}=15.0$</p> <p>$c_{v3}=154.0$</p> <p>$c_{v5}=0.4$</p> <p>$c_{R1}=104.0$</p> <p>$c_{R2}=30.0$</p> <p>$c_{R3}=724.0$</p> <p>$c_{R4}=34.0$</p> | <p>$k_1=72,000$</p> <p>$k_2=2,300$</p> <p>$k_3=46,300$</p> <p>$k_4=20,200$</p> <p>$k_{h3}=17,200$</p> <p>$k_{h5}=25,000$</p> <p>$k_{v1}=16,710$</p> <p>$k_{v2}=$</p> <p>$151,625^{*2}$</p> <p>$212,275^{*3}$</p> <p>$k_{h1}=614$</p> <p>$k_{h2}=905$</p> <p>$k_{v3}=2,300$</p> <p>$k_{v5}=18,370$</p> <p>$k_{R1}=22.0$</p> <p>$k_{R2}=162.0$</p> <p>$k_{R3}=328.0$</p> <p>$k_{R4}=915.0$</p> | |

Table A. 7: Fourteen-DOF model.

APPENDIX B

B.1 ANALOG ACCELEROMETER MODULE

Figure B.1: a) SD Silicon Design 2210 Model Accelerometers.

Figure B.1: b) SD Silicon Design 2210 Model Accelerometers.

Figure B.1: c) SD Silicon Design 2210 Model Accelerometers.

B.2 INDEPENDENT PURELY COMFORT STUDY-CONTROL OF INPUT

| Frequency (Hz) | Input Amp (mm) | *Linear Transmissibility | Frequency (Hz) | Input Amp (mm) | *Linear Transmissibility |
|----------------|----------------|--------------------------|----------------|----------------|--------------------------|
| 0.25 | 50 | 0.9864 | 10.25 | 1.25 | 0.1633 |
| 0.5 | 25 | 1.014 | 10.5 | 1.2 | 0.1532 |
| 0.75 | 17.5 | 1.0749 | 10.75 | 1.2 | 0.1437 |
| 1 | 13 | 1.2125 | 11 | 1.15 | 0.1379 |
| 1.25 | 10 | 1.3837 | 11.25 | 1.15 | 0.1518 |
| 1.5 | 8.5 | 1.5163 | 11.5 | 1.1 | 0.1575 |
| 1.75 | 7.5 | 1.5531 | 11.75 | 1.1 | 0.158 |
| 2 | 6.5 | 1.5071 | 12 | 1.05 | 0.1642 |
| 2.25 | 5.5 | 1.4057 | 12.25 | 1.05 | 0.2024 |
| 2.5 | 5 | 1.2857 | 12.5 | 1.05 | 0.272 |
| 2.75 | 4.5 | 1.16 | 12.75 | 1 | 0.343 |
| 3 | 4.25 | 1.0437 | 13 | 1 | 0.3764 |
| 3.25 | 4 | 0.9358 | 13.25 | 0.95 | 0.3795 |
| 3.5 | 3.7 | 0.8268 | 13.5 | 0.95 | 0.3707 |
| 3.75 | 3.5 | 0.7387 | 13.75 | 0.95 | 0.3527 |
| 4 | 3.25 | 0.6636 | 14 | 0.9 | 0.3381 |
| 4.25 | 3.1 | 0.6 | 14.25 | 0.9 | 0.321 |
| 4.5 | 2.95 | 0.5448 | 14.5 | 0.875 | 0.3063 |
| 4.75 | 2.8 | 0.4988 | 14.75 | 0.875 | 0.2909 |
| 5 | 2.65 | 0.4592 | 15 | 0.85 | 0.2791 |
| 5.25 | 2.5 | 0.4261 | 15.25 | 0.85 | 0.2676 |
| 5.5 | 2.45 | 0.3998 | 15.5 | 0.825 | 0.2599 |
| 5.75 | 2.3 | 0.3686 | 15.75 | 0.8 | 0.2534 |
| 6 | 2.25 | 0.3431 | 16 | 0.8 | 0.2447 |
| 6.25 | 2.1 | 0.3189 | 16.25 | 0.8 | 0.2348 |
| 6.5 | 2 | 0.3006 | 16.5 | 0.775 | 0.226 |
| 6.75 | 1.95 | 0.2841 | 16.75 | 0.775 | 0.2273 |
| 7 | 1.9 | 0.2658 | 17 | 0.75 | 0.2297 |
| 7.25 | 1.85 | 0.2513 | 17.25 | 0.75 | 0.2334 |
| 7.5 | 1.75 | 0.2405 | 17.5 | 0.75 | 0.2327 |
| 7.75 | 1.65 | 0.2302 | 17.75 | 0.725 | 0.2308 |
| 8 | 1.6 | 0.2272 | 18 | 0.73 | 0.2299 |
| 8.25 | 1.55 | 0.2287 | 18.25 | 0.73 | 0.2278 |
| 8.5 | 1.5 | 0.2298 | 18.5 | 0.7 | 0.2217 |
| 8.75 | 1.45 | 0.2278 | 18.75 | 0.685 | 0.2162 |
| 9 | 1.4 | 0.2223 | 19 | 0.685 | 0.2104 |
| 9.25 | 1.4 | 0.2152 | 19.25 | 0.675 | 0.2042 |
| 9.5 | 1.35 | 0.2063 | 19.5 | 0.65 | 0.1982 |
| 9.75 | 1.3 | 0.1948 | 19.75 | 0.65 | 0.1919 |
| 10 | 1.3 | 0.1742 | 20 | 0.65 | 0.1859 |

Table B.1: Pad to Floor linear transmissibility measurement variables:

The frequency range is from 0.25 Hz to 20 Hz; 10 seconds duration time; 80 mm/s constant peak velocity; 75 mm displacement position. Linear Transmissibility, shown as *, is calculated by the average of pad accelerations to floor accelerations.

APPENDIX C
JOURNAL ACCEPTANCE LETTER

*Journal of Low Frequency Noise, Vibration
and Active Control*

Editor: Dr W Tempest
Associate Editor: Dr H G Leventhall

Multi-Science Publishing Company Ltd, 5 Wates Way, Brentwood, Essex CM15 9TB, U.K.

23 January 2012

Dr Anand Thite
Dept of Mechanical Engineering
and Mathematical Sciences
Faculty of Technology, design and Environment
University of Oxford Brookes
Weatley Campus
Wheatley
OXFORD
OX33 1HX

Our ref WT/ST/ITM/5


Dear Dr Thite

'Quantification of human comfort in a vehicle using a four-post rig excitation' by T Ibicek, & A Thite

I thank you for the revised manuscript of the above paper, I plan to include this in Vol 31 No 1 of the journal, due out in about three month's time.

With best wishes

Yours sincerely


W Tempest, Editor.

Quantification of human discomfort in a vehicle using a four-post rig excitation

T Ibicek and A N Thite

Department of Mechanical Engineering and Mathematical Sciences, Oxford
Brookes University, Wheatley Campus, Wheatley, Oxford OX33 1HX, UK

Corresponding author:

A N Thite

Department of Mechanical Engineering and Mathematical Sciences
Faculty of Technology, Design and Environment
Oxford Brookes University
Wheatley Campus, Oxford
OX33 1HX

Email: athite@brookes.ac.uk

Tel: 01865484320

Total number of pages: 29

Tables: 3

Figures: 9

Abstract

The ride comfort of a vehicle is a vital aspect determining competitiveness of vehicles. The comfort is intricately related to feeling of discomfort due to vibrations. The discomfort depends on various dynamic aspects of the suspension-seat and surrounding system. In industry, the discomfort due to vibration is assessed by road testing on various surfaces; these road tests may not be accurately repeatable. Discomfort, in general, can be assessed by measurements based on a shaker table and seat combination. These results when used for “in vehicle situations” may not accurately indicate the level of human discomfort in a vehicle. In view of this, to quantify seated human discomfort in a vehicle, measurements were performed using a four-post rig simulator; the setup allows controlled *in-situ* experiments to be conducted. A group of six subjects were exposed to sinusoidal vibration at five magnitudes in vertical direction for heave, roll and pitch motion. The objective is to develop a discomfort metric which could be used to compare vehicles. The preliminary results show varying significance of roll, pitch and heave motion. The results, however, confirm nonlinear variation of perception as a function of physical stimulus. The test setup can be used to study the effects of complex road inputs and eventually may contribute towards reduced reliance on the road tests.

APPENDIX D

D.1 SEVEN DEGREE-OF-FREEDOM MODEL

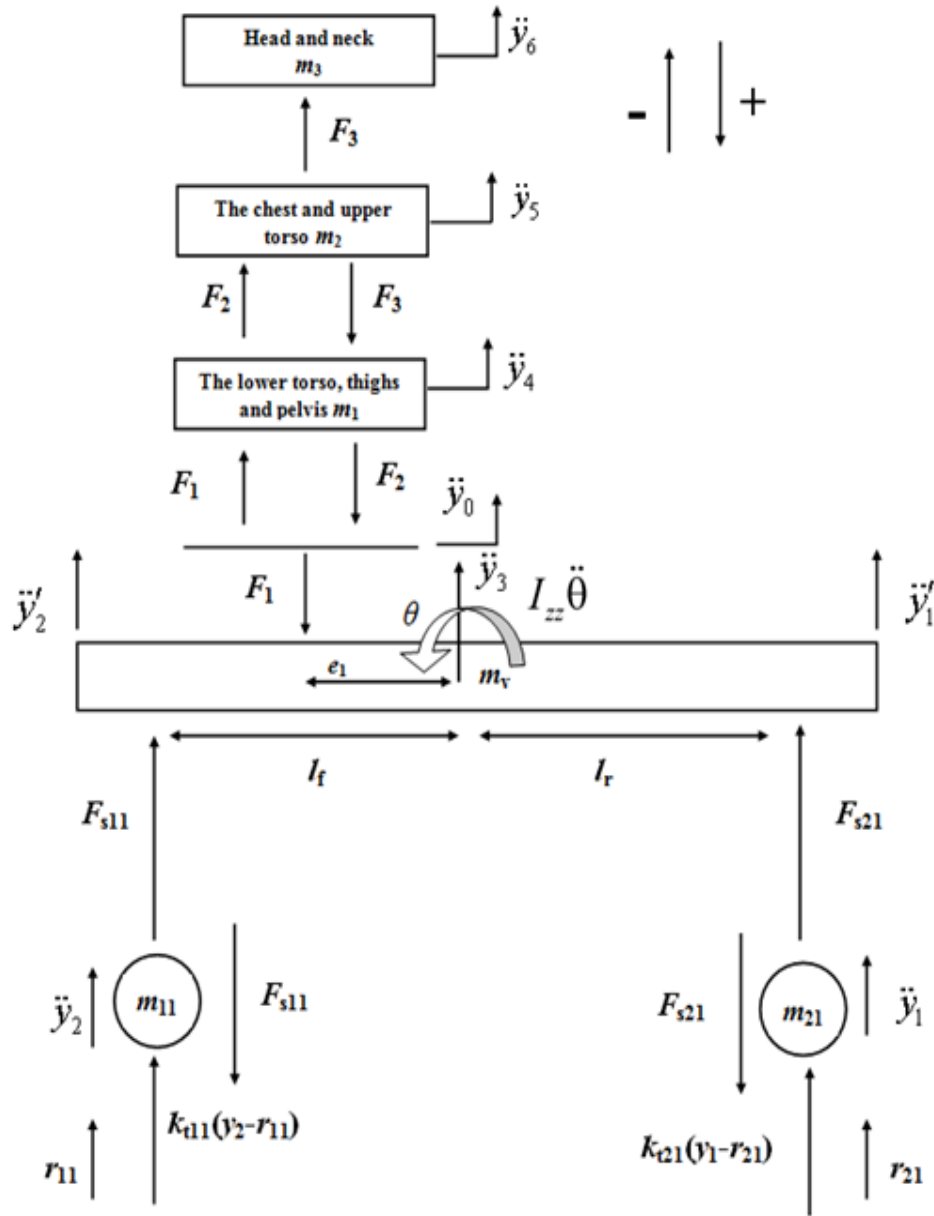


Figure D.1: Free-body diagrams for 7-DOF integrated human-seat-vehicle model.

Derivation of 7-DOF model equations

$$y_1' = y_3 + \theta l_r \quad (\text{D.1})$$

$$y_2' = y_3 - \theta l_f \quad (\text{D.2})$$

$$y_0 = y_3 + \theta e_1 \quad (\text{D.3})$$

$$F_3 = k_3(y_6 - y_5) + c_3(\dot{y}_6 - \dot{y}_5) \quad (\text{D.4})$$

$$F_2 = k_2(y_5 - y_4) + c_2(\dot{y}_5 - \dot{y}_4) \quad (\text{D.5})$$

$$F_1 = k_1(y_4 - y_0) + c_1(\dot{y}_4 - \dot{y}_0) \quad (\text{D.6})$$

$$F_{s11} = k_{s11}(y_2' - y_2) + c_{s11}(\dot{y}_2' - \dot{y}_2) \quad (\text{D.7})$$

$$F_{s21} = k_{s21}(y_1' - y_1) + c_{s21}(\dot{y}_1' - \dot{y}_1) \quad (\text{D.8})$$

$$m_3 \ddot{y}_6 = -F_3 \quad (\text{D.9})$$

$$m_2 \ddot{y}_5 = -F_2 + F_3 \quad (\text{D.10})$$

$$m_1 \ddot{y}_4 = -F_1 + F_2 \quad (\text{D.11})$$

$$m_v \ddot{y}_3 = -F_{s11} - F_{s21} + F_1 \quad (\text{D.12})$$

$$m_{t11} \ddot{y}_2 = F_{s11} - k_{t11}(y_2 - r_{t11}) \quad (\text{D.13})$$

$$m_{t21} \ddot{y}_1 = F_{s21} - k_{t21}(y_1 - r_{t21}) \quad (\text{D.14})$$

$$I_{zz} \ddot{\theta} = -l_r F_{s21} + l_f F_{s11} + e_1 F_1 \quad (\text{D.15})$$

APPENDIX E

E.1 TEN DEGREE-OF-FREEDOM PREDICTIVE MODEL

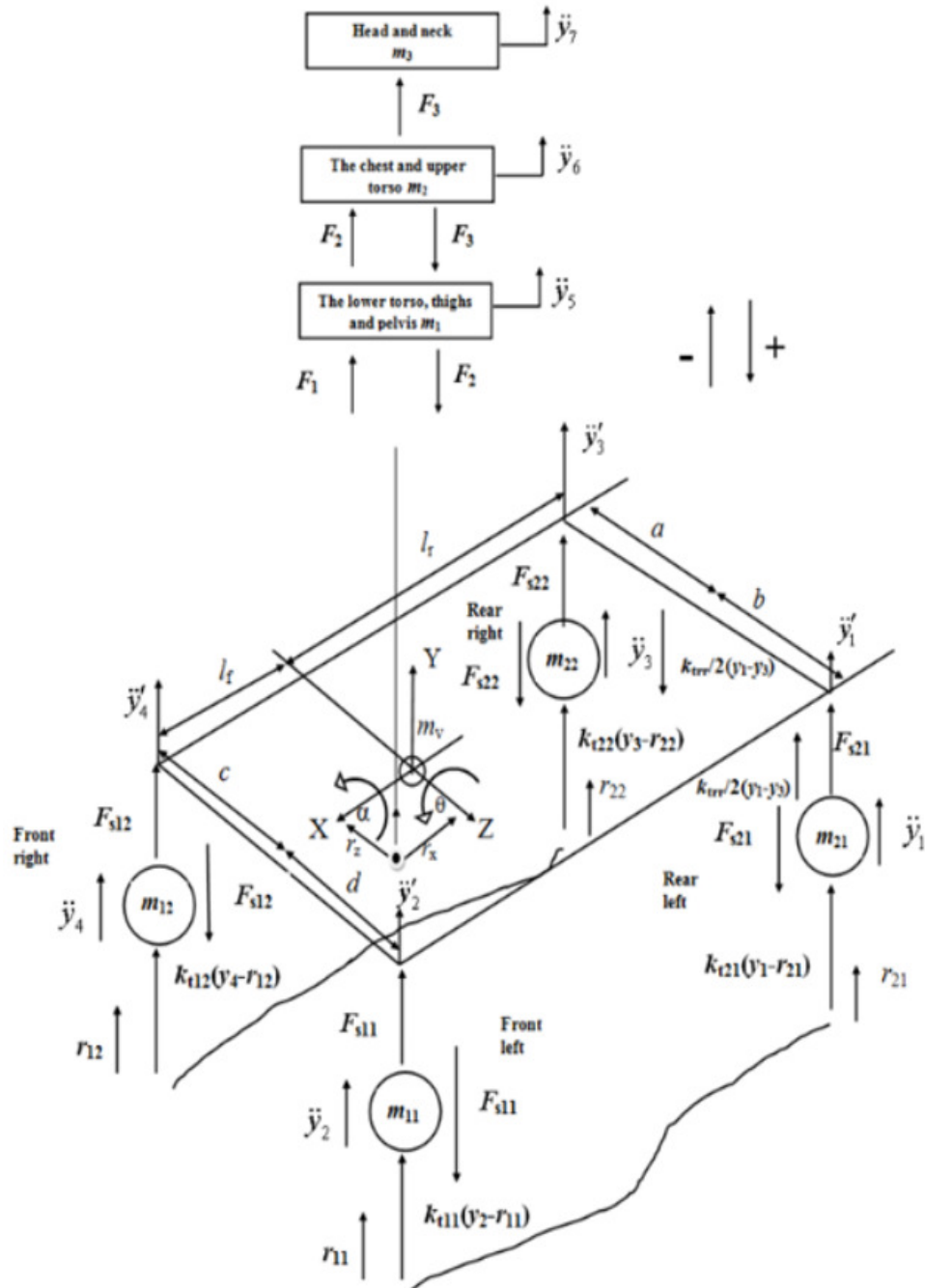


Figure E.1: Free-body diagrams for 10-DOF integrated human-seat-vehicle model.

Derivation of 10-DOF model equations

$$y_s = y - r_z \theta + r_x \alpha \quad (\text{E.1})$$

$$y'_2 = y - l_f \theta + d \alpha \quad (\text{E.2})$$

$$y'_1 = y - l_r \theta + b \alpha \quad (\text{E.3})$$

$$y'_3 = y + l_r \theta - a \alpha \quad (\text{E.4})$$

$$y'_4 = y - l_f \theta - c \alpha \quad (\text{E.5})$$

$$F_3 = k_3(y_7 - y_6) + c_3(\dot{y}_7 - \dot{y}_6) \quad (\text{E.6})$$

$$F_2 = k_2(y_6 - y_5) + c_2(\dot{y}_6 - \dot{y}_5) \quad (\text{E.7})$$

$$F_1 = k_1(y_5 - y_{seat}) + c_1(\dot{y}_5 - \dot{y}_{seat}) \quad (\text{E.8})$$

$$F_{s11} = k_{s11}(y'_2 - y_2) + c_{s11}(\dot{y}'_2 - \dot{y}_2) \quad (\text{E.9})$$

$$F_{s21} = k_{s21}(y'_1 - y_1) + c_{s21}(\dot{y}'_1 - \dot{y}_1) \quad (\text{E.10})$$

$$F_{s12} = k_{s12}(y'_4 - y_4) + c_{s12}(\dot{y}'_4 - \dot{y}_4) \quad (\text{E.11})$$

$$F_{s22} = k_{s22}(y'_3 - y_3) + c_{s22}(\dot{y}'_3 - \dot{y}_3) \quad (\text{E.12})$$

$$m_3 \ddot{y}_7 = -F_3 \quad (\text{E.13})$$

$$m_2 \ddot{y}_6 = -F_2 + F_3 \quad (\text{E.14})$$

$$m_1 \ddot{y}_5 = -F_1 + F_2 \quad (\text{E.15})$$

$$m_{t11} \ddot{y}_2 = F_{s11} - k_{t11}(y_2 - r_{t1}) \quad (\text{E.16})$$

$$m_{21} \ddot{y}_1 = -k_{t21}(y_1 - r_{21}) + F_{s21} - \left\{ \frac{k_{tr}}{2}(y_1 - y_3) \right\} \quad (\text{E.17})$$

$$m_{12} \ddot{y}_4 = -k_{t12}(y_4 - r_{12}) + F_{s12} \quad (\text{E.18})$$

$$m_{22} \ddot{y}_3 = -k_{t22}(y_3 - r_{22}) + F_{s22} + \left\{ \frac{k_{tr}}{2}(y_1 - y_3) \right\} \quad (\text{E.19})$$

$$m_v \ddot{y} = -F_{s11} - F_{s21} - F_{s12} - F_{s22} + F_1 \quad (\text{E.20})$$

$$I_{zz} \ddot{\theta} = l_f F_{s11} + l_f F_{s12} - l_r F_{s21} - l_r F_{s22} - r_z F_1 \quad (\text{E.21})$$

$$I_{xx} \ddot{\alpha} = c F_{s12} - d F_{s11} - b F_{s21} + a F_{s22} + r_x F_1 \quad (\text{E.22})$$